The Role of Cofactors, Replication, and
Intranucleosomal UASp Elements
in Chromatin Remodeling
at Yeast *PHO* Promoters

Franziska Ertel
München

Juni 2010

Eingereicht am 02.06.2010

Mündliche Prüfung am 16.07.2010

1. Gutachter: Prof. Peter Becker

2. Gutachter: Prof. Dirk Eick

3. Gutachter: Prof. Charles David

4. Gutachter: Prof. Kirsten Jung

5. Gutachter: Prof. Böttger

6. Gutachter: Prof. Leonhardt

Ehrenwörtliche Versicherung

Ich versichere hiermit ehrenwörtlich, dass die vorgelegte Dissertation von mir selbständig und ohne unerlaubte Hilfe angefertigt wurde.

München, den ....
(Franziska Ertel)

Erklärung

Hiermit erkläre ich, dass ich mich nicht anderweitig einer Doktorprüfung ohne Erfolg unterzogen habe.

München, den ....
                                                    (Franziska Ertel)

Acknowledgements

Table of contents

Summary

The *PHO5* promoter in *S. cerevisiae* represents a classical model to analyze the role of chromatin in gene regulation. The transition between the chromatin states at the *PHO5* promoter, from the positioned nucleosomes under repressing conditions to the nucleosome-free region under inducing conditions, served as a paradigm in chromatin biology. Its study led to the discovery of many chromatin related features that turned out to be relevant on a global level. Until today the mechanism that leads to the chromatin transition from the repressed to the induced state and eventually to *PHO5* activation is not completely elucidated. To address this question we set out to reconstitute this process *in vitro*. A yeast extract-based *in vitro* system assembled properly positioned nucleosomes corresponding to the repressed state *in vivo*. Addition of the transactivator Pho4 generated an extensive hypersensitive site that was very similar to the induced *PHO5* promoter chromatin *in vivo*. Importantly, this remodeling was energy-dependent which very likely points to the involvement of ATP-dependent chromatin remodelers. Still, remodeling *in vitro* was not as complete as *in vivo*. In contrast to *PHO5*, the co-regulated *PHO8* and *PHO84* promoters showed less or no chromatin remodeling in this *in vitro* system. This indicates that something is still missing in the reaction. As the *in vitro* conditions are still suboptimal, we wondered why we could remodel the *PHO5* but not the *PHO8* and *PHO84* promoter chromatin. Only the *PHO5* promoter harbors an intranucleosomal high-affinity Pho4 binding site (UASp) whereas the other two promoters have freely accessible high-affinity UASp sites in the linker regions. The intranucleosomal Pho4 binding site might lead to a competition between Pho4 binding and nucleosome re-formation during chromatin remodeling. We analyzed the importance of such binding competition for the efficiency of promoter opening by testing *PHO5* UASp mutants *in vivo*. We deleted the intranucleosomal high-affinity site and introduced new high-affinity linker binding sites. The intranucleosomal location of the UASp element was critical, but not essential, for complete remodeling of *PHO5* promoter chromatin *in vivo*. We conclude that the competition between Pho4 and histones for DNA binding has an important and so far unrecognized supporting role in the mechanism of *PHO5* promoter chromatin remodeling *in vivo*.

As *PHO5* promoter induction is a slow process that usually involves several rounds of replication under physiological induction conditions, such a binding competition may be affected during replication. On the one hand, replication could help chromatin remodeling creating a window of opportunity by displacing histones from the DNA and enabling transcription factor binding. On the other hand, replication could lead to reassembly of repressive chromatin and hinder Pho4 binding. Monitoring kinetics of histone H3 loss at the *PHO5* promoter by ChIP, we observed slower promoter opening in replicating than in non-replicating cells. This suggested reassembly of promoter chromatin during replication. We confirmed this using synchronized yeast cells and demonstrated histone reassembly at the promoter during S phase by ChIP. So replication counteracts chromatin remodeling at the *PHO5* promoter, apparently because histone reassembly after the replication fork is faster than Pho4 binding.

Zusammenfassung

Der *PHO5* Promotor in *Saccharomyces cerevisiae* ist ein typisches Beispiel für die Genregulierung durch Chromatin. Im reprimiertem Zustand gibt es vier positionierte Nukleosomen am *PHO5* Promoter. Diese werden im Zuge der Genaktivierung remoduliert und führen zu einer Promotorregion ohne Nukleosomen. Mit diesem Übergang zwischen beiden Chromatinzuständen stellt der *PHO5* Promotor ein exzellentes Modellsystem dar, das zur Entdeckung vieler Faktoren in der Chromatinforschung führte, die allgemeine Gültigkeit erlangten. Trotz ausführlicher Studien ist der molekulare Mechanismus, der vom reprimierten zum induzierten *PHO5* Promotorchromatin führt, nicht geklärt. Mit Hilfe eines *in vitro* Rekonstitutionssystems sollte diese Fragestellung beantwortet werden. In diesem *in vitro* System konnten durch die Zugabe von Hefeextrakt zu Salzdialysechromatin die Nukleosomen am *PHO5* Promotor so positioniert werden, dass sie dem reprimiertem Zustand *in vivo* sehr ähnlich waren. Die Zugabe des Transaktivators Pho4 führte zu einer ausgeprägten hypersensitiven Region, die ein Merkmal des induzierten *PHO5* Promotorchromatins *in vivo* darstellt. Diese Nukleosomen-Remodulierung war energieabhängig und deutet daher höchstwahrscheinlich auf eine Beteiligung von Chromatin-Remodulierungsmaschinen hin. Die Nukleosomen des *PHO5* Promotors wurden *in vitro* jedoch nicht so vollständig remoduliert wie *in vivo*, und das gleiche *in vitro* System löste bei den ko-regulierten *PHO8* und *PHO84* Promotoren wenig oder gar keine Änderung in der Nukleosomenstruktur aus. Dies deutet darauf hin, dass das *in vitro* System noch unvollständig und verbesserungsfähig ist. Wir stellten uns die Frage, warum sich *PHO5*, aber nicht *PHO8* und *PHO84* Promotorchromatin *in vitro* remodulieren lässt. Im Gegensatz zum *PHO5* Promotor, der eine intranukleosomale hochaffine Pho4 Bindungsstelle (UASp) besitzt, haben die beiden anderen Promotoren frei zugängliche hochaffine UASp Elemente in Linkerregionen. Diese intranukleosomale Pho4 Bindungsstelle könnte zu einer Kompetition zwischen Bindung von Pho4 und Assemblierung eines Nukleosoms während der Chromatin-Remodulierung führen. Um die Bedeutung dieser Kompetition für die Effizienz der Promotoröffnung zu klären, wurden *PHO5* UASp Mutanten *in vivo* untersucht. Bei den Mutanten wurde die intranukleosomale hochaffine Pho4 Bindungsstelle entfernt und zusätzliche hochaffine UASp Elemente in Linkerregionen eingeführt. Wir zeigen, dass die intranukleosomale Position der UASp Elemente entscheidend jedoch nicht essentiell ist, um eine vollständige Remodulierung aller Nukleosomen des *PHO5* Promotors *in vivo* zu erreichen. Daher ist die Kompetition zwischen Pho4 und Histonen um die DNA-Bindung ein wichtiger und bislang unerkannter unterstützender Faktor für die *PHO5* Promotorchromatin-Remodulierung *in vivo*.

Der *PHO5* Promotor wird relativ langsam induziert und benötigt einige Replikationszyklen bis zur maximalen Induktion. Es ist daher möglich, dass die Kompetition zwischen Pho4 und Histonen während der Replikation beeinflusst wird. Einerseits könnte Replikation während der Chromatin-Remodulierung unterstützend wirken und dabei helfen Histon-DNA-Kontakte zu lösen und dadurch die Bindung von Pho4 ermöglichen. Es ist jedoch auch vorstellbar, dass Replikation die Reassemblierung von Chromatin fördert und somit Pho4-Bindung erschwert. Es wurde mit Hilfe von ChIP-

Kinetiken die Besetzung der Promotorregion mit Histon H3 untersucht. Dabei konnte festgestellt werden, dass die Öffnung des *PHO5* Promotors durch Replikation behindert wird, also Zellen ohne Replikation die Promotorregion schneller remodulierten. Dies deutet darauf hin, dass sich die Nukleosomen des Promotors während der Replikation wieder neu assemblieren. In der Tat zeigte eine ChIP-Kinetik von synchronisierten Hefezellen eine Erhöhung der Histondichte während der S-Phase. Anscheinend beruht die hemmende Wirkung der Replikation auf die Chromatin-Remodulierung am *PHO5* Promotor darin, dass die Nukleosomen-Assemblierung nach der Replikationsgabel schneller ist als die Bindung von Pho4.

1   Introduction

1.1   Chromatin

1.1.1   Organization

As DNA is an extensive polyanion inter- and intramolecular repulsive forces have to be antagonized by positive counter-charges to allow packaging of the several mega-base pair long DNA molecules into the confined space of the nucleus. Basic histone proteins provide positively charged residues that contact the DNA backbone phosphate. The histones, two copies of each histone protein H2A, H2B, H3 and H4, form a disc shaped octamer that can organize 146 bp DNA, when wrapped around in 1.7 left handed superhelical turns. Fourteen contacts are formed between histones and DNA (Luger et al. 1997). This structure represents the nucleosome core particle, the basic unit of the DNA-protein structure chromatin and a very stable entity due to the multiple interaction points.
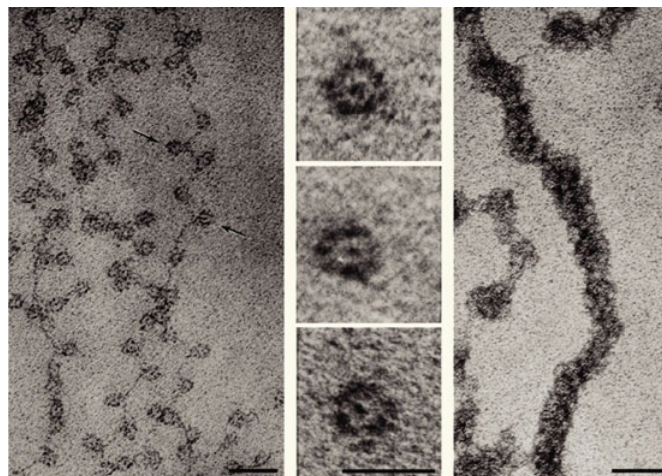
Fig. 1 Electron micrographs of chromatin. Left: 10 nm fiber as beads-on-a-string structure, size marker: 30 nm, arrows highlight nucleosome core particles. Middle: mononucleosomes from nuclease-digested chromatin, size marker: 10 nm. Right: 30 nm higher-order fiber, size marker: 50 nm (taken from (Olins and Olins 2003)).

Histones have three functional domains: the histone fold domain and the N- and C-terminal tails. The first organizes the nucleosome core, whereas the N-terminal tail interacts with linker DNA and neighboring nucleosomes thereby influencing higher order structures (Nemeth and Langst 2004). Nucleosomes are connected by linker DNA that can range from 10 to 60 bp. Electron microscopy uncovered that nucleosomal arrays exist in a beads-on-a-string structure of 10 nm diameter at low salt concentrations representing a 5-10 fold compaction and the primary level of chromatin condensation. Formation of the 30 nm fiber represents the second level of compaction. Two different models of 30 nm fiber folding and organization have been proposed. The solenoid model describes a one-start helix

in which the sequential nucleosomes wrap around a central axis, whereas the two-start helix model favors a zigzag arrangement of nucleosomes (Schalch et al. 2005; Robinson et al. 2006; Robinson and Rhodes 2006). Histone-histone interactions and incorporation of linker histones compact the 30 nm fiber 50 fold (Horn and Peterson 2002; Felsenfeld and Groudine 2003). Further compaction beyond the 30 nm fiber is not well understood but folding at the tertiary level probably involves additional non-histone nucleosomal binding proteins to finally build the mitotic chromosome with fiber diameters of 1.5 μm (**Fig. 1**, **Fig. 2**) (Luger and Hansen 2005; Tremethick 2007).

| double stranded DNA | 1st level of compaction beads-on-a-string | 2nd level of compaction 30 nm fibre | 3rd level of compaction mitotic chromosome and nuclear context |
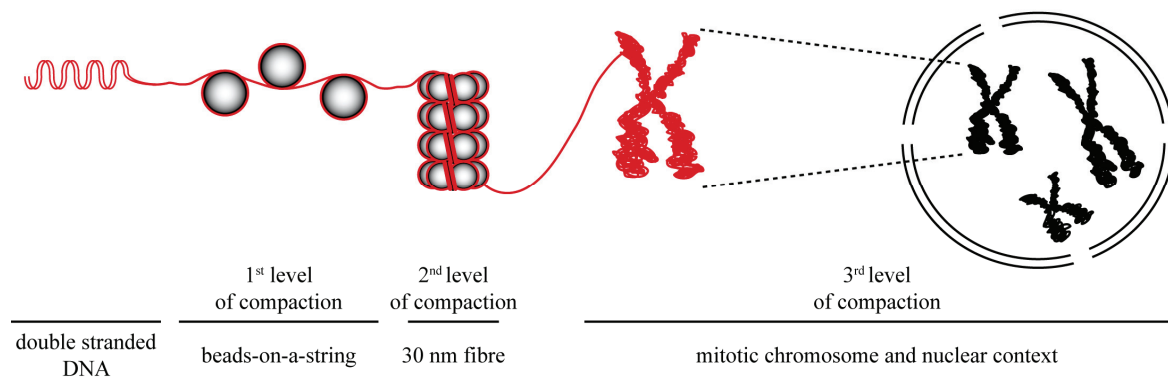
Fig. 2 Compaction levels of genetic material. Double helix of DNA with a diameter of 2 nm is wrapped into nucleosomes, known as the beads-on-a-string fiber with 10 nm diameter. Further compaction involves the 30 nm fiber and the mitotic chromosome (adapted from (Babu et al. 2008)).

Initially, distinct chromatin types were distinguished *in vivo* on the basis of their degrees of compaction, visible by light microscopy. Chromatin in the nucleus is present either as heterochromatin, a compact structure that stays condensed during interphase and is transcriptionally mostly inactive, or euchromatin, that decondenses during interphase and is prone to transcriptional activation (Luger and Hansen 2005; Bassett et al. 2009). Chromosomes occupy distinct compartments in the nucleus. These chromosome territories are, for example, implicated in the transcriptional status of genes. Often, gene-rich portions of chromosomes that show less condensation are positioned at the border of the territory and expand into interchromatin compartments. These almost chromatin-free spaces between the chromosome territories contain factors for fundamental processes in gene regulation (Cremer and Cremer 2001; Cremer et al. 2006; Cremer and Cremer 2010).

Nucleosomal DNA is less accessible to transcription factor binding than linker DNA. Accordingly, positioned nucleosomes regulate the availability of included DNA elements (Venter et al. 1994), e.g., origins of replication (Simpson 1990). Therefore, chromatin is not only a structure to package the genome into the nucleus, it is also the basal level when it comes to the regulation of genome functions like gene expression, DNA replication, recombination of chromosomes or DNA damage repair (Ehrenhofer-Murray 2004). Mechanisms like posttranslational modifications of histones (PTMs), exchange of histone variants and ATP-dependent remodeling transform chromatin into a dynamic substrate that switches between restrictive compaction and easy accessibility.

1.1.2 Posttranslational modifications and histone variants

Chromatin is altered by histone modifications that influence the structure of the nucleosome and render it more instable or stable, and can even establish binding platforms that are recognized by regulatory factors (Felsenfeld and Groudine 2003). The flexible N-terminal tails are the major target of chromatin modifications because they are easily accessible and protrude from the nucleosome. Histone tails make contacts to various substrates including the underlying DNA that participates in nucleosome formation, neighboring nucleosomes and DNA, and chromatin associated factors. Setting of PTMs includes acetylation of lysines, methylation of arginines and lysines and phosphorylation of serines and threonines (Kouzarides 2007). Dedicated enzymes such as histone acetyltransferases (HATs, in yeast for example: Gcn5, Esa1, Sas2 and Rtt109), histone deacetylases (HDACs, in yeast for example: Rpd3, Sir2, Hda1, Hos1, Hos2, Hos3), histone methyltransferases (HMTs, in yeast for example: Set1, Set2) and histone demetylases (HDMs) control the setting of these modifications (Kurdistani and Grunstein 2003; Bonisch et al. 2008). Acetylation of histones influences processes like nucleosome assembly, chromatin condensation and folding, heterochromatin silencing and gene transcription. Nucleosome assembly coupled to DNA replication involves the deposition of newly synthesized and acetylated histones onto DNA which are subsequently deacetylated. An example is H3K56ac that is observed in S phase on newly synthesized histones but is deacetylated rapidly after incorporation into chromatin. Acetylation is also implicated in regulating chromatin de-condensation as it loosens the chromatin structure by neutralizing the basic charge of the lysine, which disrupts electrostatic interactions formed between the histones and phosphate groups of the DNA. Heterochromatic gene silencing in yeast occurs at rDNA loci (repetitive ribosomal DNA), mating type loci and telomeric regions and is characterized mainly by unacetylated nucleosomes. Telomeric heterochromatin, for example, is silenced by initial binding of the Sir silencing complex to telomere ends followed by heterochromatic spreading that depends on the HDAC Sir2 (silent information regulator). Uncontrolled spreading of heterochromatic regions into euchromatin is prevented by acetylation of subtelomeric regions by the action of the HATs Esa1 and Sas2. Acetylation probably also supports transcription. An example is the Gcn5 containing complex SAGA that is recruited to UAS elements in promoter regions. Acetylated chromatin at promoters leads to the binding of transcription factors and remodeling complexes (Shahbazian and Grunstein 2007). Not only acetylation of histones is linked to particular processes in chromatin regulation, but other PTMs are also implicated. This led to the hypothesis of the "histone code" that proposes the combination of diverse modifications of the histone tails to be recognized by specific effector molecules which modify gene regulation. In addition to the genetic code this would enhance the possible levels of regulating gene expression (Jenuwein and Allis 2001; Turner 2002).

Nucleosomes are no stable entities that are constantly bound to DNA. Genome-wide studies of replication-independent histone turnover observed a dynamic equilibrium of nucleosome assembly and disassembly for H3 and H2B especially at promoter regions (Dion et al. 2007; Jamai et al. 2007; Rufiange et al. 2007).

In the context of histone turnover, histone variants add to the diversity by displacing canonical core histones. This leads to changes in the structure of the nucleosome or alters recognition sites for interacting factors. Higher eukaryotes express variants of the core histones H2A, H2B, H3 and the linker histone H1 (Hake and Allis 2006; Bonisch et al. 2008). Budding yeast encodes two variants, the centromer-localized H3 variant Cse4 and the H2A variant Htz1. Htz1 is found at promoters, at borders to heterochromatin and probably marks the sites of RNA polymerase II initiation (Rando and Chang 2009).

1.1.3 Chromatin remodeling machines

Nucleosome remodeling factors are the basis for the dynamic regulation of chromatin. They use energy from ATP hydrolysis to weaken histone-DNA contacts. This influences the nucleosomal structure by introducing nucleosome movement along DNA (sliding), exchange or removal of H2A-H2B dimers or eviction of entire nucleosomes (**Fig. 3**) (Becker and Horz 2002; Eberharter and Becker 2004; Flaus et al. 2006; Clapier and Cairns 2009). Nucleosome remodeling complexes are differentiated by their functions but are also characterized by common properties including an affinity for the nucleosome, domains for recognizing covalent histone modifications, an ATPase subunit, domains that regulate the ATPase subunit and proteins for the interaction with other factors (Clapier and Cairns 2009). All remodelers contain an ATPase of the SNF2 helicase family and some associate with additional factors in multiprotein complexes (Eberharter and Becker 2004). There are four different chromatin remodeling families according to their ATPase subunit, each specialized to perform distinctive tasks (**Table 1**).
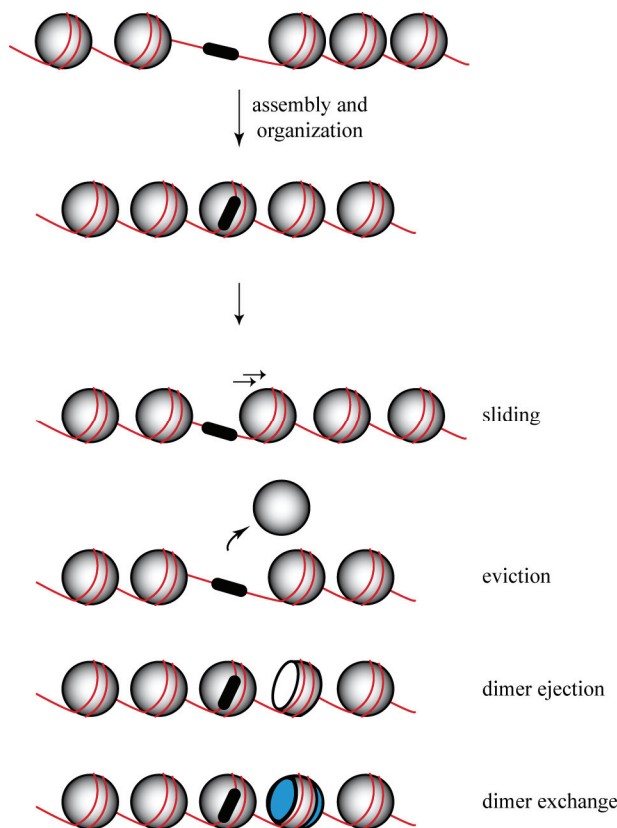
Fig. 3 Nucleosome dynamics. From top to bottom: Chromatin remodelers assemble and organize nucleosomal arrays resulting in even spaced nucleosomes, move or eject whole nucleosomes which expose occluded factor binding sites (black box), eject dimers or reconstruct nucleosomes by incorporating histone variants (adapted from (Cairns 2007; Clapier and Cairns 2009)).

The first remodeler to be discovered was SWI/SNF (switching defective/sucrose nonfermenting). It was discovered through yeast mutants defective for switching of the mating type (SWI) or for growth on the carbon source sucrose (SNF). The eleven subunit complex contains the ATPase subunit Swi2 (=Snf2) (Peterson and Herskowitz 1992; Sudarsanam and Winston 2000) and was the founding member of the SWI/SNF subfamily. ATPases of this subfamily contain a bromodomain motif that interacts with acetylated histone residues (Clapier and Cairns 2009). A second complex related to SWI/SNF is RSC, an essential complex for cell growth with the ATPase subunit Sth1. SWI/SNF subfamily remodelers slide or eject nucleosomes and render DNA more accessible (Lorch et al. 1999). Studies on SWI/SNF and RSC revealed that they function both in activation and repression of certain genes (Sudarsanam and Winston 2000; Eberharter and Becker 2004; Gangaraju and Bartholomew 2007; Clapier and Cairns 2009).

Remodelers of the ISWI (imitation switch) family are most closely related to the SWI/SNF remodelers. Their ATPase subunit was named Imitation SWItch (ISWI) because it resembled the ATPase Swi2. The mechanism of remodeling by ISWI complexes was extensively studied (Tsukiyama and Wu 1995; Varga-Weisz et al. 1997; Corona et al. 1999; Eberharter et al. 2001). These remodelers carry characteristic C-terminal SANT and SLIDE domains which mediate interaction with histones and DNA. The complexes assemble and organize chromatin for an equal spacing of DNA between the nucleosomes and are known to repress transcription (Gangaraju and Bartholomew 2007; Clapier and Cairns 2009; Racki et al. 2009).

The CHD (chromodomain, helicase, DNA binding) subfamily contains characteristic chromodomains that interact with methyl-groups or nucleic acids (Akhtar et al. 2000; Bouazoune et al. 2002). Chd1 does not assemble with any other subunits in yeast but is found as a component of SAGA and SLIK complexes (Pray-Grant et al. 2005). It relocates nucleosomes and is involved in transcriptional elongation as well as in repression (Gangaraju and Bartholomew 2007; Marfella and Imbalzano 2007; Clapier and Cairns 2009).

INO80 (inositol requiring 80) remodelers represent the fourth subfamily including the SWR1 (Swi/snf related) complex. They carry a characteristic split ATPase domain and contain Rvb-like subunits. These multisubunit complexes support transcriptional activation and DNA repair. A special ability of SWR1 is to alter the composition of nucleosomes. SWR1 replaces H2A-H2B dimers with Htz1-H2B dimers within the nucleosome in cooperation with the two Htz1 chaperones Nap1 and Chz1 that probably deliver the variant to the remodeler (Bao and Shen 2007; Gangaraju and Bartholomew 2007; Luk et al. 2007; Clapier and Cairns 2009) (**Table 1**).

SWI/SNF

Family and composition	Yeast		Fly		Human	
Complex	SWI/SNF	RSC	BAP	PBAP	BAF	PBAF
ATPase	Swi2/Snf2	Sth1	BRM/Brahma		hBRM or BRG1	BRG1
Noncatalytic homologous subunits	Swi1/Adr6		OSA/eyelid		BAF250/hOSA1	
				Polybromo		BAF180
				BAP170		BAF200
	Swi3	Rsc8/Swh3	MOR/BAP155		BAF155, BAF170	
	Swp73	Rsc6	BAP60		BAF60a or b or c	
	Snf5	Sfh1	SNR1/BAP45		hSNF5/BAF47/INI1	
			BAP111/dalao		BAF57	
	Arp7, Arp9		BAP55 or BAP47		BAF53a or b	
			Actin		β-actin	
Unique	a	b				

ISWI

Family and composition	Yeast			Fly			Human		
Complex	ISW1a	ISW1b	ISW2	NURF	CHRAC	ACF	NURF	CHRAC	ACF
ATPase	Isw1		Isw2	ISWI			SNF2L	SNF2H [c]	
Noncatalytic homologous subunits			Itc1	NURF301	ACF1		BPTF	hACF1/WCRF180	
					CHRAC14			hCHRAC17	
					CHRAC16			hCHRAC15	
				NURF55/p55			RbAp46 or 48		
Unique	Ioc3	Ioc2, Ioc4		NURF38					

CHD

Family and composition	Yeast	Fly		Human	
Complex	CHD1	CHD1	Mi-2/NuRD	CHD1	NuRD
ATPase	Chd1	dCHD1	dMi-2	CHD1	Mi-2α/CHD3, Mi-2β/CHD4
Noncatalytic homologous subunits			dMBD2/3		MBD3
			dMTA		MTA1,2,3
			dRPD3		HDAC1,2
			p55		RbAp46 or 48
			p66/68		p66α,β
Unique					DOC-1?

INO80

Family and composition	Yeast		Fly		Human		
Complex	INO80	SWR1	Pho-dINO80	Tip60	INO80	SRCAP	TRRAP/Tip60
ATPase	Ino80	Swr1	dIno80	Domino	hIno80	SRCAP	p400
Noncatalytic homologous subunits	Rvb1,2		Reptin, Pontin		RUVBL1,2/Tip49a,b		
	Arp5,8	Arp6	dArp5,8	BAP55	BAF53a		
	Arp4, Actin1		dActin1	Actin87E	Arp5,8	Arp6	Actin
	Taf14	Yaf9		dGAS41		GAS41	
	Ies2,6				hIes2,6		
		Swc4/Eaf2		dDMAP1		DMAP1	
		Swc2/Vps72		dYL-1		YL-1	
		Bdf1		dBrd8			Brd8/TRC/p120
		H2AZ,H2B		H2Av,H2B		H2AZ,H2B	
		Swc6/Vps71				ZnF-HIT1	
				dTra1			TRRAP
				dTip60			Tip60
				dMRG15			MRG15
							MRGX
				dEaf6			FLJ11730
				dMRGBP			MRGBP
				E(Pc)			EPC1, EPC-like
				dING3			ING3
Unique	Ies1,Ies3-5,Nhp10	Swc3,5,7	Pho		d		

[a] Swp82, Taf14, Snf6, Snf11.
[b] Rsc1 or Rsc2, Rsc3-5, 7, 9, 10, 30, Htl1, Ldb7, Rtt102.
[c] In addition, SNF2H associates respectively with Tip5, RSF1, and WSTF to form **NoRC**, **RSF**, and **WICH** remodelers.
[d] Amida, NFRKB, MCRS1, UCH37, FLJ90652, FLJ20309.

Table 1 Subfamilies of remodelers and composition. Chromatin remodeling subfamilies are grouped according to their ATPase subunits (taken from (Clapier and Cairns 2009)).

1.1.4 Replication

Replication of the eukaryotic genome leads to the exact duplication of the genetic material. During this process the chromatin structure has to be copied to both daughter strands to maintain the epigenetic information beyond the DNA sequence (Groth 2009). But how the heritable chromatin structure is propagated through the cell cycle is poorly understood. To elucidate epigenetic inheritance several questions are addressed: Which parts of the parental structure of chromatin are inherited upon disassembly of the nucleosomes? How are the parental structures distributed upon reassembly at both daughter strands and how is this information duplicated (Francis 2009; Probst et al. 2009)?

1.1.4.1 Nucleosome disassembly

Parental nucleosomes are disrupted upon replication fork passage by dissociation of the octamer into two H2A-H2B dimers and a (H3-H4)$_2$ tetramer (**Fig. 4**) (Corpet and Almouzni 2009; Probst et al. 2009). It is still unclear which chaperones mediate this disassembly and if chromatin remodeling machines are involved as experimental setups are not able to differentiate between the tightly regulated processes of dis- and reassembly during replication (Ransom et al. 2010).
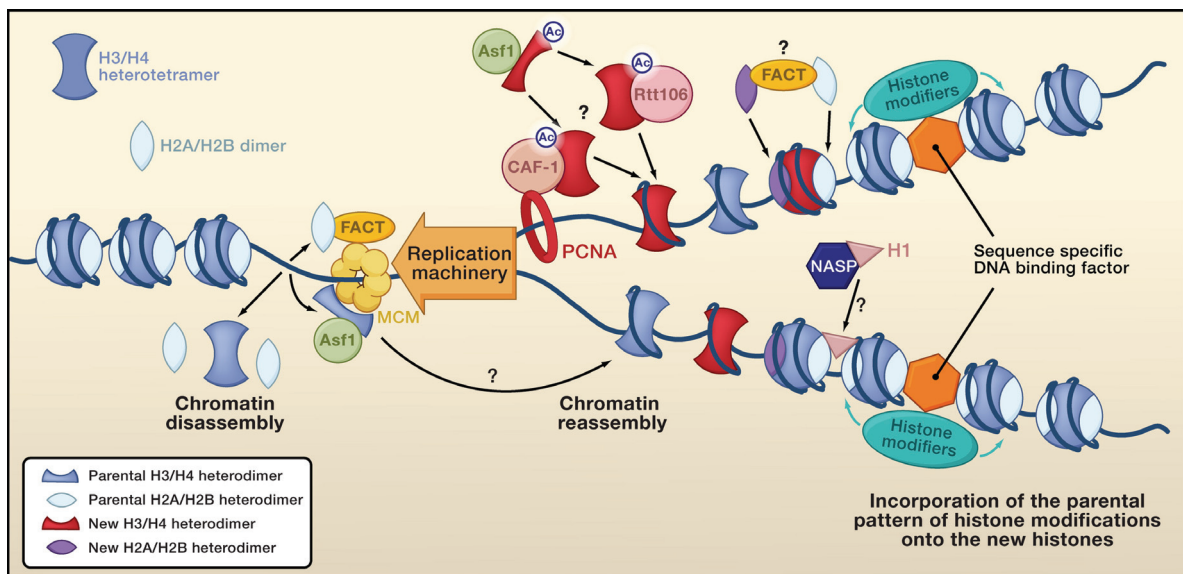
Fig. 4 Chromatin disassembly and reassembly during replication. Possible histone and histone chaperone interactions during passage of the replication fork are shown, for details see text (taken from (Ransom et al. 2010)).

The H2A-H2B chaperone FACT (facilitates chromatin transcription) is part of the replication machinery as it was found to interact with MCM proteins (minichromosome maintenance) and localized to origins of replication (Wittmeyer and Formosa 1997; Tan et al. 2006; Ransom et al. 2010). A further H2A-H2B chaperone possibly involved in disassembly is Nap1 (nucleosome assembly protein 1) that interacts with the H2A-H2B dimer in co-immunoprecipitation studies (Ito et al. 1996). Interestingly, Nap1 also interacts with the remodeler RSC to disassemble nucleosomes *in vitro* (Lorch et al. 2006). The histone chaperone Asf1 (antisilencing function) is thought to remove the H3-H4 tetramer

from the DNA. Although the crystal structure of Asf1 strongly argues for H3-H4 dimer binding that physically inhibits the formation of the H3/H4 tetramer (English et al. 2006). Asf1 was shown to interact with the PCNA loader RFC (replication factor C) and the MCM proteins. Deletion of Asf1 influences DNA unwinding (Groth et al. 2007a; Ransom et al. 2010). In addition to chaperones, the Ino80 remodeling enzyme is also recruited to sites of replication during S phase. It was shown to be required for progression of the replication fork and stabilization of the replisome (Papamichos-Chronakis and Peterson 2008), which could be linked to the RuvB-like DNA helicases, subunits of the Ino80 complex.

1.1.4.2 Nucleosome reassembly

After the passage of the replication fork nucleosomes are reassembled onto the two daughter strands (**Fig. 4**). Nucleosomes that are deposited consist of recycled parental histones and newly synthesized histones. The distribution of both along the leading and lagging strand is still not clear. There are three models for the distribution of histones after DNA replication. The first model postulates a random distribution of parental and newly synthesized histones onto both daughter strands. To maintain the modifications, neighboring nucleosomes would act as blueprint to copy the marks onto the new histones. An alternative is the semi-conservative histone distribution that suggests an even assembly of parental H3-H4 dimers onto the DNA strands that are completed by newly synthesized H3-H4 dimers which adopt the parental marks directly from the `hemimodified´ nucleosome. The third model favors an asymmetric segregation that deposits parental and new histones each on a different daughter strand. To copy histone modification interstrand crosstalk would have to occur (Probst et al. 2009).

Newly synthesized H3-H4 dimers do not form into tetramers prior to deposition and are incorporated after DNA replication (Verreault et al. 1996). Interaction with PCNA probably targets the chaperone Asf1 loaded with newly synthesized H3-H4 dimers (English et al. 2006) to replication sites where it presents H3K56 to the HAT Rtt109 for acetylation as prerequisite for incorporation by CAF1 (chromatin assembly factor) onto newly replicated DNA (De Koning et al. 2007). H3-H4 tetramer assembly onto the DNA is followed by H2A-H2B dimer incorporation on both sides of the tetramer. It is not known if Nap1 and/or FACT complete this task after replication (Groth 2009).

Histone chaperones deposit histones in a rather random manner, creating order-less nucleosomal arrays that require subsequently remodeling enzymes for the nucleosome to reach the characteristic position on the DNA (Ransom et al. 2010). A proposed model is described for the chromatin remodeler WSTF-SNF2h (Williams syndrome transcription factor) which interacts with PCNA and targets SNF2h to sites of replication and might remodel chromatin to render it more open after passage of the replication fork. The authors suggest a window of opportunity upon remodeling for the binding of factors that mediate the re-establishment of epigenetic marks to the newly formed chromatin structure (Poot et al. 2005). ATP-dependent remodelers therefore adopt an important role in transmitting epigenetic memory and chromatin maturation (Falbo and Shen 2006).

1.1.5   What defines a promoter

Transcription of eukaryotic protein-coding genes depends on the recruitment of RNA polymerase II to the initiation site. DNA elements within the promoter mediate this recruitment. Multiple processes like chromatin de-condensation at the locus, remodeling of nucleosomes, PTMs of histones and binding of transcription factors act as prerequisite for activation (Levine and Tjian 2003; Smale and Kadonaga 2003). Upon activation of the promoter, general transcription factors, RNA polymerase II and Mediator assemble into a complex to initiate transcription (Boeger et al. 2005). With regard to chromatin structure, two opposing promoter architectures are described that correspond to constitutive and highly regulated genes and are termed open and covered promoter, respectively (Tirosh and Barkai 2008; Cairns 2009). Most promoters contain features of both promoter types but the concept helps clarify how we think about promoter organization.

Constitutive genes have open promoters in a way that they contain a nucleosome depleted region (NDR) upstream of the transcriptional start site (TSS) and thus facilitate the binding of transcription factors. Poly (dA:dT) stretches in the NDR disfavor nucleosome formation as these DNA sequences resist bending (Segal and Widom 2009). The NDR often also contains binding sites for transactivators. Additional features are nucleosomes -1 and +1 at the boundaries of the NDR; one of them often incorporates the H2A variant Htz1 that is thought to help transcriptional activation (Raisner et al. 2005).

The covered promoter structure is found at inducible genes. The repressed state of a promoter is represented by positioned nucleosomes relative to the TSS, which also occlude binding sites for transcriptional activators. Contrary to open promoters, nucleosomes and transcription factors compete for binding to regulatory DNA elements which makes gene activation at such promoters more dependent on remodeling machines and chromatin modifying enzymes. To start the initial activation of this region there is usually at least one binding site along the promoter that is not covered by a nucleosome but resides in a linker region. Furthermore, covered promoters are more likely to contain a TATA-box that is also often masked by a nucleosome (Cairns 2009). A typical example of a covered promoter is the yeast *PHO5* promoter with an accessible Pho4 binding site in a linker region, and another Pho4 site that, together with the TATA box, is occluded by a nucleosome (Almer et al. 1986).

1.2   The *PHO* system in *Saccharomyces cerevisiae*

The cell`s ability to maintain nutrients, such as inorganic phosphate, at a constant internal level is established by control of uptake and consumption. The *PHO* (phosphatase) pathway monitors the level of inorganic phosphate inside the cell. If changes in availability occur the *PHO* pathway triggers immediate reactions by regulating the transcriptional status of *PHO* responsive genes. Yeast cells starved for phosphate activate the *PHO* signaling transduction pathway. Using this *PHO* pathway, the cell regulates phosphate availability that is important for the biosynthesis of cellular components like nucleic acids, proteins, lipids, sugars and phosphometabolites. The signals lead in the end to the bind-

ing of the transactivator protein Pho4 to its cognate binding sites, the UASp elements (upstream acti-vating sequence phosphate), within promoter regions.

Many genes of the *PHO* regulon encode phosphatases that supply the cells with inorganic phosphate. There are two different kinds of phosphatases: acid phosphatases and alkaline phosphatases. Acid phosphatases are found in the periplasm and are optimized for the acidic conditions outside the cell whereas alkaline phosphatases are located in the vacuole. Limiting phosphate in the medium leads to an increased production of secreted acid phosphatase by the genes *PHO5*, *PHO10* and *PHO11* (Svaren and Horz 1997) while most phosphatase is produced from the *PHO5* gene. The alkaline phosphatase is encoded by *PHO8*. An additional class of PHO proteins are phosphate transporters that regulate the uptake of phosphate into the cell and are encoded by several genes, among them the most regulated *PHO84* gene (Wykoff et al. 2007).

1.2.1   Signal transduction

The *PHO* genes in yeast are one of the best studied model systems of eukaryotic gene regulation through chromatin. The promoters of the *PHO5*, *PHO8* and *PHO84* genes that are studied in our group all show a highly ordered chromatin structure under repressive conditions. Upon induction, all three display major changes of the chromatin structure at their promoters. Induction of these three *PHO* genes and the accompanying changes at the chromatin level absolutely depend on the helix-loop-helix protein Pho4.
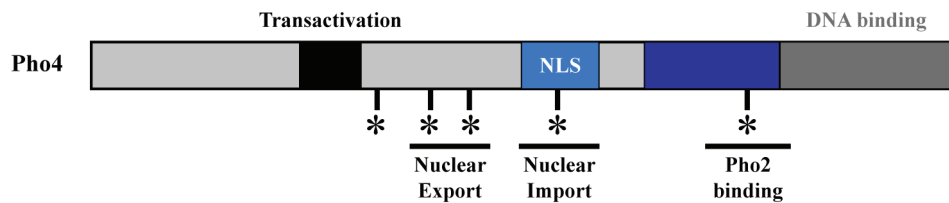
Fig. 5 The transactivator Pho4. The protein comprises a transactivation domain (in black), a DNA binding domain (in grey) and harbors specific serine residues that can be modified by phosphorylation and thereby activate nuclear export, and inhibit nuclear import and interaction with the transcription factor Pho2 (adapted from Springer et al. 2003).

Pho4 can be phosphorylated at several sites which determine its interaction potential with a set of different proteins (**Fig. 5**) (Ogawa and Oshima 1990; Komeili and O'Shea 1999; Springer et al. 2003). During conditions of abundant phosphate Pho80 and Pho85, a cyclin/cyclin dependent kinase complex, phosphorylate Pho4 at multiple serine residues (Kaffman et al. 1994). Phosphorylation of two serine residues leads to an active export into the cytoplasm by the export receptor Msn5. Simultaneously, a different phosphorylated serine prevents re-import into the nucleus (Kaffman et al. 1998a; Kaffman et al. 1998b). Moreover, the modification of a fourth site inhibits interaction with the homeobox protein Pho2, a binding helper for Pho4 (Fascher et al. 1990), thereby turning off the expression of the phosphate responsive genes (Komeili and O'Shea 1999).
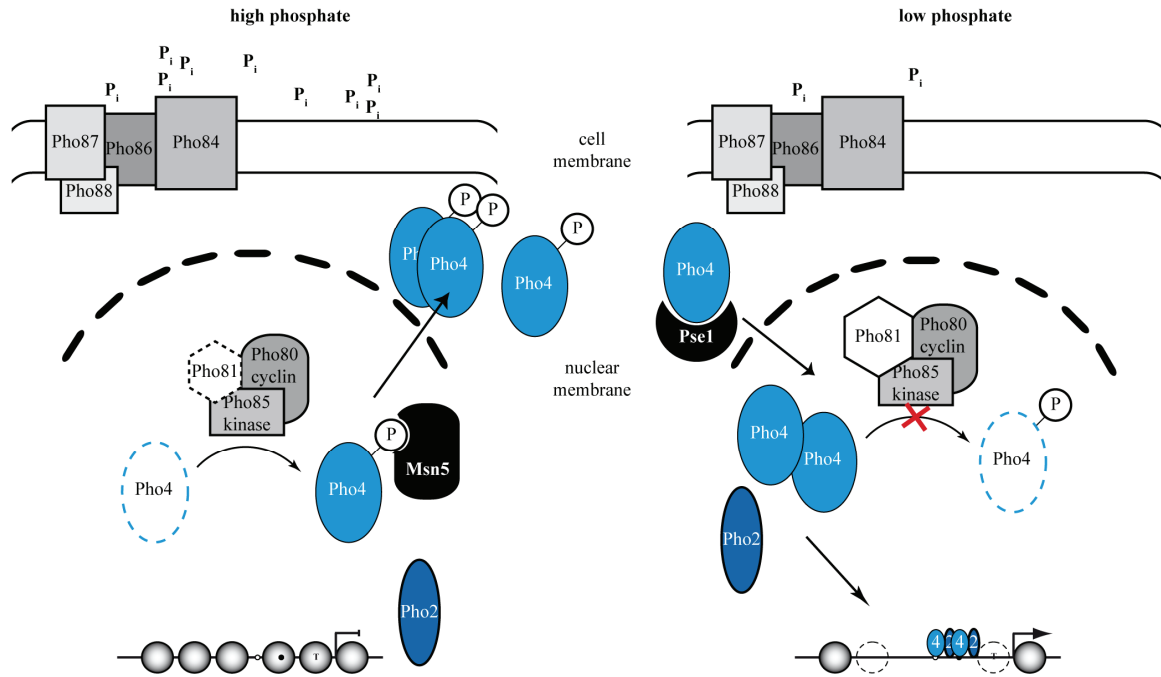
Fig. 6 Signal transduction pathway regulating the expression of phosphate responsive genes. High phosphate conditions lead to the export of Pho4 from the nucleus into the cytoplasm, the *PHO* promoter stays repressed, the *PHO5* promoter region is assembled with nucleosomes. Phosphate depletion induces import of Pho4 into the nucleus and subsequent binding to the promoter region which activates transcription, the *PHO5* promoter is depleted of nucleosomes (adapted from Oshima 1997 and Gregory et al. 2000).

Phosphate starvation activates the CDK inhibitor Pho81 that is constitutively associated with Pho80/Pho85 but inhibits the activity of the kinase only during phosphate limitation. Kinase inactivation is dependent on the small-molecule ligand inositol heptakisposphate (IP$_7$). IP$_7$ induces additional interaction of Pho81 with Pho80/Pho85 which prevents Pho4 to access the active site of the kinase (Lee et al. 2008). Pho4 in its unphosphorylated state is recognized by the importin factor Pse1, imported into the nucleus and triggers transcription of the *PHO* genes (**Fig. 6**) (Kaffman et al. 1998b).

Importantly, the *PHO* system monitors the intracellular phosphate levels. Therefore, maximal induction of the *PHO* genes is a rather slow process that requires several rounds of replication in phosphate-free medium to delete intracellular phosphate pools.

1.2.2   Chromatin structure

The repressed *PHO5* promoter chromatin consists of four positioned nucleosomes (-1 to -4, **Fig. 7**A). A short 60 bp hypersensitive site, sHS2, resides between nucleosome -2 and -3 and harbors binding sites for the transcription factors Pho4 (UASp1) and Pho2. A second binding site for Pho4 (UASp2) and Pho2 is covered by nucleosome -2 in the repressed state. Also the TATA-box is located beneath nucleosome -1 (Almer et al. 1986). *PHO5* is induced by the cooperative binding of Pho4 and Pho2. The promoter nucleosomes undergo a considerable chromatin transition from the repressed to the activated state.

A   *PHO5* **promoter region**

B   *PHO8* **promoter region**

C   *PHO84* **promoter region**
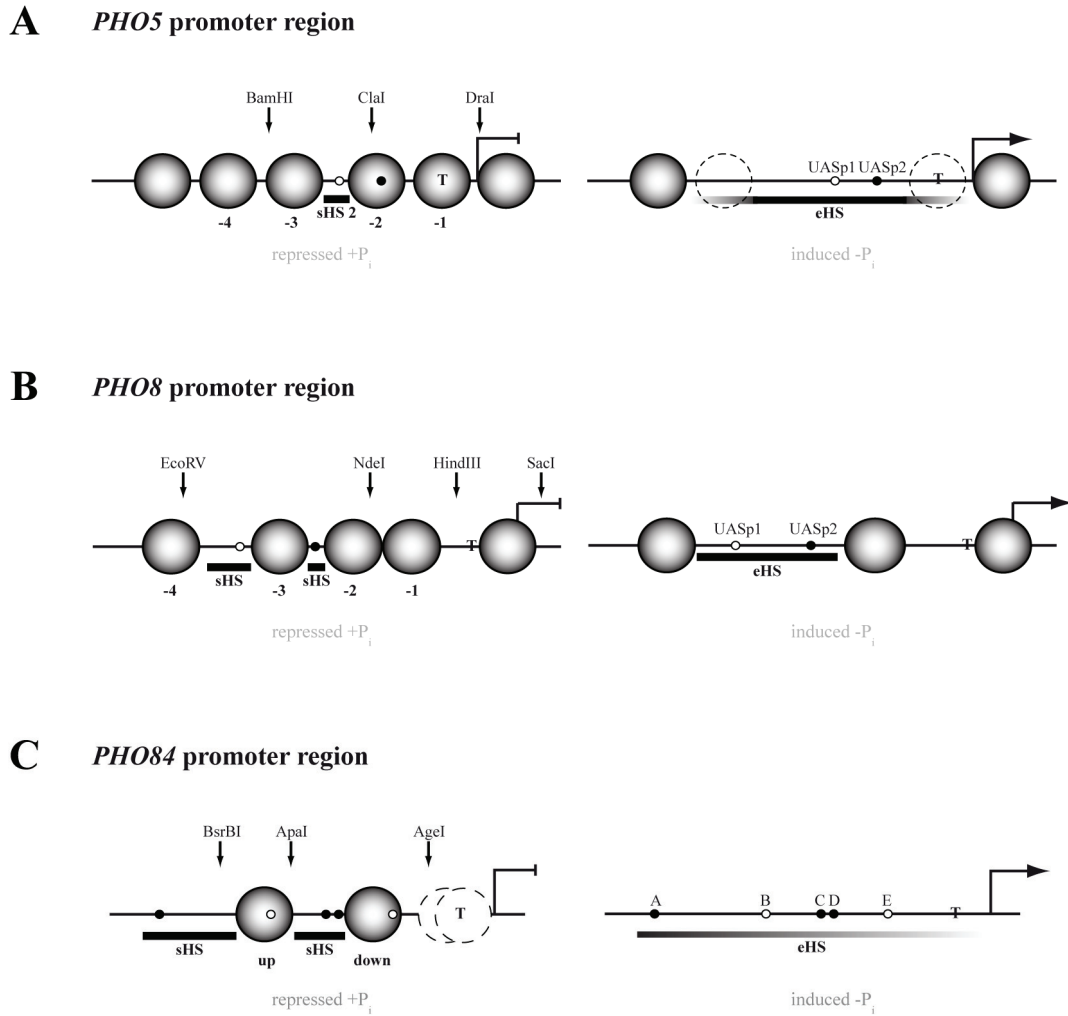
Fig. 7 Nucleosomal organization of model promoters at repressing (+P$_i$) and inducing (-P$_i$) conditions. Large circles represent positioned nucleosomes. Nucleosomes are numbered relative to the ATG (*PHO5* and *PHO8*) or labeled with "up" and "down" (*PHO84*) relative to the sHS. Stippled circles represent partial remodeling of a nucleosome (*PHO5*, -P$_i$) or unclear positioning (*PHO84*, +P$_i$). Bold horizontal bars stand for short (sHS) and extensive (eHS) DNaseI hypersensitive sites and fading indicates less hypersensitivity. High-affinity sites are indicated by small filled circles and low-affinity sites by small open circles. Position of the TATA box (T), the ATG (broken blunt and broken pointed arrow for repressed and induced state, respectively) and the restriction sites used for marker fragments are included. Nucleosome positions are drawn to scale and width of one nucleosome corresponds to 150 bp.

In the activated state, the promoter nucleosomes upstream and downstream of the short hypersensitive site become remodeled and the entire promoter region of approximately 600 bp becomes accessible (Almer et al. 1986). During chromatin remodeling hyperacetylation of the promoter nucleosomes takes place, followed by the eviction of histones from the promoter region in *trans* (Reinke and Horz 2003; Boeger et al. 2004; Korber et al. 2004). Chromatin opening and disruption of three out of four nucleosomes occurs in an all or nothing fashion and was described as a chromatin microdomain that is uniformly remodeled upon action of Pho4 (Svaren and Horz 1997). This may suggest that the nucleosomes are structurally linked and that the disruption is cooperative.

Another well studied *PHO* promoter is the *PHO8* promoter. *PHO5* and *PHO8* share the same signal transduction pathway and are regulated by the same transactivator Pho4. The *PHO8* promoter

shows a characteristic pattern of three short hypersensitive sites and positioned nucleosomes (**Fig. 7**B). It contains two Pho4 binding sites, UASp1 and UASp2, which are located in hypersensitive regions and are therefore constitutively accessible. Upon induction, not all *PHO8* promoter nucleosomes become fully remodeled. Remodeling gives rise to a large hypersensitive site of 300 bp, but the region upstream of the *PHO8* TATA box (nucleosome -1 and -2) stays protected and still harbors a nucleosome. The extent of remodeling at the *PHO8* promoter is therefore less than at the *PHO5* promoter. Activation of *PHO8* is only partially dependent on Pho2. There are no binding sites described at the promoter region, but Pho2 influences promoter remodeling by enhancing the activation potential of Pho4 (Munsterkotter et al. 2000).

The promoter of the gene that encodes the main high-affinity phosphate transporter Pho84 harbors two well positioned nucleosomes ("up" and "down") and one region of ambiguous nucleosome organization in the vicinity of the TATA-box. A short hypersensitive site (sHS) of about 150 bp is flanked by the upstream and downstream nucleosomes and contains two high-affinity Pho4 binding sites (UASpC and UASpD). Two additional low-affinity Pho4 binding sites (UASpB and UASpE) are covered by the two positioned nucleosomes. Upon induction the nucleosomes are remodeled generating a very extensive hypersensitive site of about 500 bp (**Fig. 7**C) (Wippo et al. 2009).

1.2.3   Cofactor requirements for promoter chromatin remodeling at the *PHO5* and *PHO8* promoters

1.2.3.1 Transactivators

The transactivator Pho4 belongs to the helix-loop-helix family of proteins that bind to a cognate site containing a six bp E-box (CACGTG) (Venter et al. 1994) and is absolutely essential for the opening of the *PHO5* and *PHO8* promoters (Fascher et al. 1990). TATA-box deletion mutants are still able to remodel the promoter chromatin with no effect on kinetics (Barbaric et al. 2007; Uhler et al. 2007) or final levels of transcription (Fascher et al. 1993), which argues for the chromatin transitions as a prerequisite for transcription to occur. The deletion of the activation domain of Pho4 results in a truncated protein that consists only of the DNA binding domain. This domain by itself is not sufficient to activate nucleosome disruption *in vivo*, not even after overexpression. Consequently, the acidic activation domain is involved in the process of disruption of the promoter nucleosomes upon activation (Svaren et al. 1994).

The homeodomain protein Pho2 is also involved in chromatin remodeling at the *PHO5* promoter. Pho2 helps Pho4 in binding to its recognition site and enhances transcriptional activation (Barbaric et al. 1996; Barbaric et al. 1998). There are two binding sites for Pho2 along the *PHO5* promoter; none was detected at the *PHO8* promoter. Nonetheless, Pho2 increases the transactivation potential of Pho4 at the *PHO8* promoter (Barbaric et al. 1996; Munsterkotter et al. 2000). Whereas Pho2 acts as a pleiotropic activator not only in regulating genes of the phosphatase family but also at *HIS4*, *TRP4*, *HO* and

certain *ADE* genes, the action of Pho4 is restricted to the *PHO* genes (Barbaric et al. 1992; Barbaric et al. 1996). Overexpression of *PHO4* in a deletion mutant of *pho2* can compensate for the loss and induce *PHO5* but *PHO2* cannot make up for loss of *pho4* (Fascher et al. 1990).

1.2.3.2 ATP dependent remodeling machines

Data from the Hörz lab showed that *PHO5* promoter chromatin remodeling was independent of replication (Schmid et al. 1992). Chromatin remodeling factors with a role in *PHO5* chromatin transition upon induction were analyzed. 17 Snf2 type helicases are encoded in the yeast genome (Flaus et al. 2006). Two of these enzymes, Sth1 and Mot1, are encoded by essential genes (Davis et al. 1992; Cairns et al. 1996) and therefore complicate studying these enzymes *in vivo*. The remaining remodeler ATPase genes (*SNF2, ISW1, ISW2, CHD1, IRC5, SWR1, INO80, FUN30, RAD54, RDH54, RAD5, RAD16, ULS1, IRC20,* and *RAD26*) were deleted and their effect on remodeling *PHO5* promoter chromatin was tested. It turned out that only Swi/Snf (Gaudreau et al. 1997; Neef and Kladde 2003; Barbaric et al. 2007) and Ino80 (Steger et al. 2003; Barbaric et al. 2007) play a role in opening the *PHO5* promoter. Both mutants had an effect on *PHO5* induction as the opening showed a clear kinetic delay in the two strains. Despite this kinetic delay, there was no influence on the final chromatin structure or final transcription levels (Neef and Kladde 2003; Barbaric et al. 2007). Interestingly, even the induced nucleosomal pattern of the double mutant *snf2 ino80* was indistinguishable from wild type, but still showed a strong delay in the opening kinetics. This indicates that both enzymes are dispensable for remodeling because alternative pathways exist to compensate for their loss (Barbaric et al. 2007). The histone variant Htz1 shows some enrichment at the *PHO5* promoter chromatin (Albert et al. 2007). A possible role might involve priming of the promoter for opening or resetting the nucleosomal structure after induction. As deletion of *swr1* did not influence promoter induction and also *htz1* deletion had no effect (Barbaric et al. 2007), it seems that Htz1 is not important for remodeling *PHO5* promoter structure. There is no mutation known that would keep the *PHO5* promoter from being remodeled and fully induced, except mutations that influence the activity and binding of Pho4 (Fascher et al. 1990; Nourani et al. 2004). So either there is no dedicated remodeler for *PHO5* activation or this remodeling enzyme is essential for cell viability, like for example the remodeling complex RSC.

In contrast to the *PHO5* promoter, the *PHO8* promoter does not show the same redundancy of chromatin remodeling enzymes regarding promoter chromatin opening. There is also a delay in *PHO8* promoter remodeling in *ino80* mutants but *PHO8* strictly depends on the ATPase activity of the SWI/SNF remodeling complex (Gregory et al. 1999b).

1.2.3.3 Histone chaperones

As remodeling at the *PHO5* and probably also at the *PHO8* promoter leads to histone eviction in *trans* (Boeger et al. 2004; Korber et al. 2004), histone chaperones were the most likely candidates as histone accepting cofactors. Mutants of the H3/H4-binding chaperones Asf1 (Sutton et al. 2001; Adkins et al. 2004; Mousson et al. 2007), of the HIR complex, involved in replication-independent

nucleosome assembly, and of the CAF complex, involved in replication-dependent assembly (Gaillard et al. 1996; Verreault et al. 1996) were tested for their role in *PHO5* and *PHO8* chromatin remodeling. Among the *hir1*, *hir2*, *hir3*, *cac1* and *asf1* mutants, only the *asf1* mutant exhibited an effect. Asf1 enhances the rate of histone eviction at both promoters but loss of Asf1 does not affect the final level of chromatin remodeling (Korber et al. 2006). Spt6, an essential H3-H4 chaperone mediates the reassembly of the *PHO5* and *PHO8* promoter nucleosomes and with it also the transcriptional repression of both promoters (Adkins and Tyler 2006). In addition, the histone chaperone Nap1 is also involved in *PHO5* regulation as it associates with chromatin and reassembles nucleosomes during transcription elongation (Del Rosario and Pemberton 2008).

1.2.3.4 Histone acetyltransferases

One prominent member of the HAT enzymes, Gcn5, is a catalytic subunit of at least two protein complexes, Ada and SAGA (Grant et al. 1997). It was demonstrated that the rate of *PHO5* activation is slower in a *gcn5* strain but does not affect final transcription levels (Barbaric et al. 2001). During induction of *PHO5*, histones along the promoter are transiently hyperacetylated, followed by the loss of histones from this region (Boeger et al. 2003; Reinke and Horz 2003). As SAGA is recruited to the *PHO5* promoter under inducing conditions (Barbaric et al. 2003) this can explain the delay in chromatin remodeling in the absence of Gcn5. Elucidating the role of Gcn5 in *PHO5* promoter chromatin remodeling, suboptimal activation conditions using a deletion of the gene for the negative regulator Pho80 enable promoter activation in the presence of phosphate but activate the gene only to 30-50% compared to phosphate depletion conditions. Under these conditions, deletion of Gcn5 led to a randomized nucleosomal pattern along the promoter and reduced activity which points to a direct role of Gcn5 in chromatin remodeling (Gregory et al. 1998b) whereas maximal *PHO5* activation can compensate for the loss of *gcn5*. The double mutants *snf2 gcn5* and *ino80 gcn5* showed a synthetic delay and were even slower in *PHO5* chromatin opening but did not affect final opening (Barbaric et al. 2007). *PHO8* promoter remodeling is much more severely affected by a deletion of Gcn5 HAT activity and results in only partially localized remodeling around UASp2 even under maximal induction conditions and shows impaired induction (Gregory et al. 1999b). SAGA establishes a hyperacetylation peak over the *PHO8* promoter nucleosomes which are subjected to subsequent remodeling. As this hyperacetylation is observed prior to SWI/SNF action it probably presents a prerequisite for nucleosome remodeling (Reinke et al. 2001).

Another HAT complex, NuA4, containing the H4 acetylase Esa1 also regulates histone acetylation levels at the *PHO5* promoter. It was shown that Pho4 binding to the *PHO5* promoter did not happen until Pho2 recruitment of NuA4 and H4 acetylation was completed. This suggests a priming of the promoter region by H4 acetylation for subsequent binding of Pho4. Loss of H4 acetylation caused defects in *PHO5* chromatin opening but could be compensated by overexpression of *PHO4* (Vogelauer et al. 2000; Nourani et al. 2004).

Asf1 probably does not only act as histone acceptor but has a further function that involves the HAT Rtt109. Rtt109 acetylates H3K56 and essentially requires Asf1. *PHO5* promoter induction is delayed in an *rtt109* mutant and equally so in an *asf1* mutant (Williams et al. 2008; Wippo et al. 2009). A double mutant showed no synthetic effect which suggests that both work in the same pathway and that they mediate histone eviction through H3K56ac.

1.2.4   Replication and influence of the cell cycle

A long standing question in the chromatin field was if remodeling of chromatin needs the process of replication during which nucleosomes are assembled onto newly synthesized DNA. This question was addressed using an elegant approach by replacing the *PHO80* gene, coding for the negative regulator of *PHO5*, with a temperature-sensitive allele. This way *PHO5* could be activated by a temperature up-shift even at high phosphate concentrations which enabled a direct comparison of promoter induction kinetics in replicating and non-replicating yeast cells. At the *PHO5* promoter it was shown that nucleosome disruption is independent of replication, passage through S phase was not required (Schmid et al. 1992).

Recently it was shown that *PHO5* is also activated during mitosis in response to cell cycle-dependent variations of intracellular phosphate and that mitotic activation strongly depends on SWI/SNF and Gcn5 (Neef and Kladde 2003). In addition, two sequence-specific activators, apart from Pho4 and Pho2, were discovered to bind the *PHO5* promoter region, Mcm1 and Fkh2, to induce the gene in late M/G1 phase. Mcm1, involved in cell cycle control and gene activation in G2/M phase, was found to be essential for mitotic induction of *PHO5* whereas Fkh2 was less important. The results link mitotic cell cycle progression and cellular phosphate control (Pondugula et al. 2009).

The open question is if replication has an effect on the promoter opening kinetics.

1.2.5   *In vitro* chromatin assemblies

The molecular mechanism underlying the changes in the nucleosomal *PHO5* and *PHO8* promoter structure upon induction is still not fully understood from *in vivo* studies. Therefore it is reasonable to develop an *in vitro* chromatin reconstitution and remodeling assay to gain more insight into the mechanism of remodeling the *PHO5*, *PHO8* and *PHO84* promoter chromatin. Using such a biochemical system would allow the dissection of the remodeling process and identification of involved cofactors by titrating individual factors and arranging the order of addition. There are not many *in vitro* systems that would allow chromatin remodeling with templates that correspond to physiological conditions. That´s why earlier studies using chromatin *in vitro* assemblies made use of templates with strong nucleosome positioning sequences like the naturally occurring 5 S rDNA (Shimamura et al. 1988) or non-natural DNA arrays containing the 601 nucleosome positioning sequence (Lowary and Widom 1998; Maier et al. 2008) to elucidate chromatin structure and function. So far only few promoters are used in chromatin assembly *in vitro* systems that have the potential to recapitulate mechanisms known to af-

fect these nucleosomal sites *in vivo* and further investigate so far unknown variables. Among them are the *Drosophila* hsp26 promoter regulated by GAGA factor and HSF (heat shock factor) (Sandaltzopoulos et al. 1995; Wall et al. 1995), the HIV-1 promoter (Sheridan et al. 1995; Pazin et al. 1996), the PEPCK promoter (Phosphoenolpyruvate carboxykinase) (Li et al. 2010) and also the *PHO5* and MMTV (mouse mammary tumor virus) promoter.

The MMTV promoter has been a model system to analyze transcription activation by steroid hormone receptors. Integrated into the genome it is organized into a characteristic chromatin structure that modulates transcription factor access and activation. Hormone treatment stimulates transcription by changes in activator binding and nucleosomal structure (Truss et al. 1995). Reconstitution of the MMTV promoter into chromatin *in vitro* recapitulated *in vivo* remodeling events and extended the knowledge on regulation. This includes, for example, the finding of transient glucocorticoid or progesterone receptor (GR or PR, respectively) binding during activation (Fletcher et al. 2000; Rayasam et al. 2005) and the elucidation of sequential events like GR binding to chromatin which directly recruits a remodeling activity and thereby enables the binding of transcription factors accompanied by simultaneous loss of the GR (Fletcher et al. 2002). *In vitro* studies also demonstrated the importance of the central HREs 2 and 3 (hormone response element) in PR- and NF1- (nuclear factor 1) dependent transcriptional activation of the MMTV promoter (Vicent et al. 2010).

There were previous attempts to reconstitute *PHO5* promoter chromatin remodeling *in vitro* in other labs. Minichromosomes bearing the *PHO5* locus were isolated from cells *ex vivo* and showed to have an intact chromatin structure. Remodeling was initiated by addition of Pho4, Pho2, ATP and nuclear extract *in vitro* which led to smeared MNase ladders but not to the proper induced pattern as seen by occurrence of the hypersensitive site. Reconstitution assays of *PHO5* chromatin with purified histones and extract also failed to produce templates with positioned nucleosomes (Haswell and O'Shea 1999). A different approach used *de novo in vitro* assembly of the *PHO5* locus. Laybourn and colleges reconstituted chromatin templates with recombinant yeast core histones and the histone chaperone Nap1 and claimed that positioning of the repressed promoter pattern was determined by the DNA sequence alone. They further described Pho4, ATP and nuclear extract induced remodeling and even transcription (Terrell et al. 2002). But the chromatin patterns showed Pho4 binding and nucleosome occupancy at UASp2 at the same time, which contradicts *in vivo* data (Venter et al. 1994). Both approaches were not followed up any further. A third approach made use of R recombinase that excised the *PHO5* promoter from its chromosomal locus in the cell. Minicircles were isolated after conversion by recombination to a circular template. A drawback in this system were the relative small amounts of isolated material (Griesenbeck et al. 2003). Still, comparing associated factors of affinity purified minicircles of repressed and induced cells may allow for the identification of induction specific factors in the future.

The Korber lab established a different *de novo* assembly *in vitro* approach which used yeast extract with additional exogenous histones and energy. In contrast to the Nap1 chaperone mediated as-

sembly, the yeast extract system provides enzymatic activity that is sufficient to deposit histones to their *in vivo* nucleosome positions. This system showed that the chromatin structure of the repressed *PHO5* promoter is not generated by or reliant on active processes like transcription, replication or higher order chromatin structures (Korber and Horz 2004). It was shown to work for the *PHO8* (Hertel et al. 2005) and for the *PHO84* promoters (Wippo et al. 2009) as well. Using this *in vitro* assembly system, titration of histone concentrations led to the finding of different intrinsic stabilities of positioned nucleosomes at all three promoters and showed that they correlate with the degree of cofactor requirement for chromatin remodeling *in vivo* (Hertel et al. 2005; Wippo et al. 2009).

1.3 Goals of this study

1.3.1 *In vitro* reconstitution of promoter chromatin remodeling at the *PHO* promoters

In this study several questions are addressed: Can *PHO5* and *PHO8* promoter chromatin remodeling be reconstituted *in vitro*? If remodeling *in vitro* can be accomplished, the necessary factors should be identified, addressing also their direct role during chromatin remodeling. The factors could comprise all chromatin related cofactors like transactivating proteins, chromatin remodelers, chaperones, enzymes for setting or removing PTMs and also ATP. If remodeling machines are involved, the question would arise if all remodelers are involved or only the members of a certain class, e.g., the Swi/Snf type remodelers but not the ISWI type remodelers. Is there initial sliding prior to histone eviction and what is the histone acceptor in the system? Is the activation domain of Pho4 needed only for the recruitment to increase the local concentration of cofactors? It could also be possible to dissect the sequence of events that lead from repressed to induced promoter chromatin. *In vitro* reactions are analyzed using limited DNaseI digest and indirect end-labeling to visualize the positions of promoter nucleosomes, and restriction enzyme digestion to monitor the accessibility of the DNA.

1.3.2 The role of replication during *PHO5* and *PHO8* promoter remodeling

The Hörz lab showed many years ago that *PHO5* promoter chromatin opens and re-closes in the absence of replication (Schmid et al. 1992). Nevertheless, this study only addressed the question if replication was essential and not if it had any role during the induction process. After all, replication does happen during physiological induction of the *PHO* system because even in phosphate-free medium the cell still has to replicate two to three rounds to use up intracellular phosphate pools. It could be that replication during *PHO5* promoter opening either reassembles repressive chromatin over the promoter region or enhances the displacement of nucleosomes. In the first case replication would be a hindrance and in the latter case a help for promoter opening.

To compare chromatin opening kinetics of replicating and non-replicating yeast cells, induction conditions have to be changed. *PHO5* promoter activation can be accomplished by either starving the cells for phosphate or deletion of genes that code for a negative regulator, such as *PHO80*. Using a

temperature sensitive *pho80* allele allows activation of *PHO5* and circumvents the need for replication to deplete phosphate pools. Using the temperature sensitive *pho80* allele, we compare promoter opening kinetics in the presence or absence of replication. As a measure of chromatin remodeling at the promoter we use ChIP (chromatin immunoprecipitation) which monitors histone loss. ChIP is reliably fast for kinetic measurements as cross-linking with formaldehyde instantly preserves the chromatin state. Cells are blocked from replicating by depleting the medium of uracil.

The study of cofactor mutants that exhibit a kinetic delay in *PHO5* induction will be a further interesting point to address with the same assay. Either the delay is still measurable in the absence of replication which would indicate a rather general role of the cofactor in *PHO5* opening or it is lost compared to wild type induction kinetics which would hint at a role in overcoming the hindrance that is established by replication. A prime candidate for this is Ino80 that is known to affect *PHO5* induction and was recently linked to stabilize the replisome during replication (Papamichos-Chronakis and Peterson 2008).

In the context of replication during *PHO5* promoter induction we also check if the *PHO5* promoter in its open state becomes transiently reassembled into nucleosomes during replication or if it stays open all the time. This experiment could address the question of epigenetic memory, i.e. if a defined chromatin state is inherited. For this we synchronize *pho80* cells and monitor the histone occupancy over the *PHO5* promoter during the cell cycle by ChIP. Will a transient peak of histone occupancy appear during S phase over the otherwise histone depleted *PHO5* promoter? If so, replication may represent a hindrance for promoter chromatin remodeling. Which cofactors are necessary to either keep the chromatin open or reassemble it during S phase and re-open it again?

2   Materials and Methods

2.1   Materials

2.1.1   Chemicals

Unless stated otherwise, all common chemicals were purchased in analytical grade from Merck.

AcetylCoA	Sigma
Agarose SeaKem$^{®}$ ME	Biozym
Amino acids	Sigma and Merck
Ampicillin	Roth
Aprotinin	Sigma
ATP	Sigma
α-^{32}P-dCTP	Hartmann Analytics
Bacto Agar	Becton Dickinson
Bacto Peptone	Becton Dickinson
Bacto Tryptone	Becton Dickinson
Bacto Yeast extract	Becton Dickinson, Difco
Bacto Yeast nitrogen base w/o aa	Becton Dickinson, Difco
Barrier food wrap	Saran
Benzamidine	Sigma
Bradford Reagent	BioRad
Bromphenolblue	Merck
BSA 98% pure	Sigma
BSA, purified	NEB
β-Mercaptoethanol	Sigma
Chloramphenicol	Roth
Chloroform	Merck
Complete protease inhibitors, EDTA-free	Roche
Coomassie	Serva
Creatine phosphate	Sigma
DMSO	Sigma
dNTP mix	NEB
DTT	Roth
EDTA	Sigma
EGTA	Sigma
EtBr	Roth
Ficoll	Sigma
Formaldehyde	Sigma
Glycogen	Roche
Guanidinium HCl	Sigma
[^{3}H] acetyl CoA	Amersham

Hepes	Roth
Hydroxylapatite	BioRad
Hydroxyurea	Sigma
IPTG	Roche
Isoamylalcohol	Merck
Laboratory film	Parafilm
Leupeptin	Sigma
NaClO$_4$	Merck
NPP	Fluka
Nocodazole	Sigma
Nonidet P40 (Igepal CA-630)	Sigma
Orange G	Sigma
Pepstatin	Sigma
Phenol for DNA separation	Sigma
PEG 4000	Roth
PMSF	Sigma
Propidium iodide	Sigma
Rotiphorese Acrylamid-Bisacrylamid-mix	Roth
SDS	Serva
Spermidine	Fluka
Spermin	Fluka
Sytox green	Molecular probes
TEMED	Roth
TSA	Sigma
Tris	Invitrogen
Triton X-100	Sigma
Tween 20	Sigma
Zymolyase 100 T	MP Biomedicals

2.1.2 Enzymes

Antarctic Phosphatase	NEB
Apyrase	NEB
DNaseI	Roche
Creatine Kinase	Roche
MNase	Sigma
Pfu turbo polymerase	Stratagene, Agilent
Phusion polymerase	Finnzymes, NEB
Proteinase K	Roche
Restriction endonucleases	NEB and Roche
RNase A	Roche
Taq DNA Polymerase	NEB
T4 DNA Ligase	NEB

2.1.3 Others

2-Log DNA Ladder (0.1–10.0 kb)	NEB
100 bp DNA Ladder	NEB
Gel Extraction Kit	Qiagen

Dialysis membrane Spectra/Por, 3.5 kDa	Roth
Enliten Luciferase reagent	Promega
FACS tubes	Becton Dickinson
Filter tips	Molecular Bioproducts
Fuji medical X-ray film	Fuji
Glas beads, 0.45-0.5	Braun Biotech International
MaXtract	Qiagen
Microsep Centrifugal Concentrators	Pall Corporation
Miracloth	Merck
Ni^{2+}-NTA agarose	Qiagen
Nylon Transfer membrane, Biodyne B 0.45 μm	Pall Corporation
QiaQuick purification kit	Qiagen
P81 paper filter	Whatman
PCR Purification Kit	Qiagen
Plasmid Maxi, Midi, Mini Kit	Qiagen
Prime-It II Random Primer Labeling Kit	Stratagene
Protein G Sepharose 4 Fast Flow	GE Healthcare
QuickChange kit	Stratagene
Quick spin columns (Sephadex G-50)	Roche
Siliconised reaction tubes, 1.5 ml	Biozym
Whatman 3MM Blotting Paper	Whatman

2.2   Standard methods

The standard methods were done according to standard protocols (Sambrook et al. 1989). This included measuring protein concentration, agarose gel electrophoresis, cloning, SDS PAGE and subsequent staining with coomassie or silver stain, western blotting, precipitating DNA using ethanol or isopropanol, making competent *E.coli* cells, transformation of *E.coli* and plasmid preparation using alkaline lysis.

2.3   *Saccharomyces cerevisiae* strains

Strain	Genotype	Reference source
AH2341	MAT**a** *ura3(Δ:ApaI to NcoI)::YIP-Var.31 his3 leu2-3, 112 pho5 pho3 gal4*::TRP1	(Ertinger 1998)
BY4741	*MATahis3Δ1 leu2Δ0 met15Δ0 ura3Δ0*	(Brachmann et al. 1998)
CY337	*MATaura3-52 lys2-801 ade2-101 leu2-Δ1 his3-Δ200*	C. Peterson
CY338	CY337 *pho4*::URA3	lab
CY339	CY337 *pho5*::URA3	(Wippo et al. 2009)
CY407	CY337 *snf2*::HIS3	C. Peterson
CY337 EB1615	see below	lab
CY337 EB1615 +2μ	CY337 EB1615 pP4-70leu	this work
CY337 EB1615 *pho80*	CY337 EB1615 *pho80*::URA3	this work

CY337 EB1626	see below	lab
CY337 EB1626 +2μ	CY337 EB1626 pP4-70leu	this work
CY337 EB1500	see below	lab
CY337 FE1600	see below	this work
CY341	CY337 *pho5* (ΔUASp2)	lab
CY341 +2μ	CY341 pP4-70leu	lab
CY337 UASp2-5	see below	lab
CY337 UASp2-5 +2μ	CY337 UASp2-5 pP4-70ura	lab
CY337 UASp2-8	see below	lab
CY337 UASp2-8 +2μ	CY337 UASp2-8 pP4-70ura	lab
CY380	CY337 *pho80*::*URA3*	lab
CY390	CY380 *bar1*::*HIS3*	lab
YDL39	MAT**a** *trp1-1 ura3-1 his3-11, 15 leu2-3, 112 ade2-1 can 1-100, cdc7-4*	A. Verreault
YDL39 *pho80*	YDL39 *pho80*::*LEU2*	this work
YS18	MATα, *his3*-11 *his3*-15 *leu2*-3 *leu2*-112 can^R *ura3*Δ5	(Sengstag and Hinnen 1987)
YS22	YS18 *pho4::ura3Δ5*	(Barbaric et al. 1998)
YS27	see below	lab
YS44	YS18 *pho80^{ts}*	(Schmid et al. 1992)
YS70	YS18 *PHO5* UAS elements inverted	(Venter et al. 1994)

The strain YS27 carries null mutations in *pho4* and *pho2* (Sengstag and Hinnen 1988; Barbaric et al. 1998) and was additionally deleted in *cbf1* with the disruption plasmid pMF33 (Mellor et al. 1990) to yield strain YS27 *cbf1::URA3*. Strains CY337 EB1615, CY337 EB1626, and CY337 EB1500 carry the H1, H2, and H4 *PHO5* promoter mutants, respectively, as in Lam et al. (Lam et al. 2008) and were generated by transformation of CY337 with the PflMI linearized pRS306-based plasmids EB1615, EB1626, and EB1500, kindly provided by Erin O'Shea (**Fig. 36**). Strain CY337 FE1600 (H5) carries a mutant version of EB1615, where the CACGTGG sequence in sHS2 was changed back to UASp1 E Box CACGTTT and a CACGTGG sequence was introduced close to the BstEII site as described in **Fig. 36**. The BstEII site is a proxy for the position of the linker between nucleosome –1 and -2 (Almer et al. 1986; Boeger et al. 2003). Both mutations were generated using the QuickChange kit and the primers UASp1fwd: 5'-attaaattagcacgttttcgcatagaacgcaac-3', UASp1rev: 5'-gttgcgttctatgcgaaaacgtgctaatttaat-3', Bst-UASfwd: 5'-tatcaaattggtcacgtggcttggcaaggcatatac-3', Bst-UASrev: 5'-gtatatgccttgccaagccacgtgaccaatttgata-3' and EB1615 as template. Strain CY339 *ura3* was derived from CY339 after selection on FOA containing media and confirmed for uracil auxotrophy. Strain CY341 is derived from CY337 and described in **Fig. 36**. Plasmid pCB-UASp2-5 Δ2 was derived from pCB(*LEU2*) (Korber and Horz 2004) and carries the BamHI-ClaI fragment of the *PHO5* promoter region of strain YS70 and the ClaI-Bsu36I fragment of pCB-ΔUASp2 where the CACGTG sequence of UASp2 in plasmid pCB(*LEU2*) was replaced by the AAGCTT HindIII site (Venter et al.

1994). Plasmid pCB-UASp2-8 Δ2 was also derived from pCB(*LEU2*) and carries the ApaI-PmlI fragment of the PCR product using the primers 5'-TGGCTGGATAAATGGGCCCC-3' and 5'-ATCGCTGCACGTGGCCCGACGTAGATGACCCTTTTGTGCAGACAAAGAAAAAGCGC-3' with pCB(*LEU2*) as template, and the PmlI-Bsu36I fragment of the PCR product using the primers 5'-TCGGGCCACGTGCAGCGATCGAACGCAACTGCACAATGC-3'   and   5'-GTCGACATCGGCTAGTTTGC-3' with pCB-ΔUASp2 as template. The plasmid for overexpression of *PHO4* was YEpP4 (Svaren et al. 1994). The expression plasmid for the Gal4 DNA-binding domain, YCpGal4(1-147), carries a *CEN* element, a *HIS3* marker, was derived from pRJR266 (L. Gaudreau), has the Gal4-construct under the control of the *GAL4* promoter and terminator and is described in ref. Ertinger 1998.

2.4   Media for growing *S. cerevisiae*

Yeast strains were grown as described (Korber et al. 2006; Barbaric et al. 2007), i.e. under repressive conditions (high phosphate) in YPD with 0.1 g/l adenine and 1 g/l KH_2PO_4, or in yeast nitrogen base selection medium supplemented with the required amino acids for plasmid-bearing strains, and in corresponding synthetic phosphate-free medium for induction (no phosphate).

2.4.1   YPDA medium

1% (w/v) yeast extract, 2% (w/v) peptone, 2% (w/v) glucose, 100 mg/l adenine, 1 g/l KH_2PO_4

2.4.2   YNB minimal medium

6.7 g/l yeast nitrogen base w/o amino acids, 2% (w/v) glucose, 1.6 mg/l amino acid drop-out mix (2 g adenine, 2 g alanine, 2 g arginine, 2 g asparagine, 2 g aspartate, 2 g cysteine, 2 g glutamine, 2 g glutamate, 2 g glycine, 2 g meso-inositol, 2 g isoleucine, 2 g lysine, 2 g methionine, 2 g p-aminobenzoic acid, 2 g phenylalanine, 2 g proline, 2 g serine, 2 g threonine, 2 g tryptophane, 2 g tyrosine, 2 g valine, 2 g histidine, 2 g uracil, 2 g leucine)

2.4.3   Phosphate-free minimal medium

2 g/l asparagine; 500 mg/l $MgSO_4$ x H_2O; 100 mg/l NaCl; 100 mg/l $CaCl_2$ x 2 H_2O; 2 mg/l Inositol; 500 μg/l H_3BO_3; 40 μg/l $CuSO_4$ x H_2O; 100 mg/l KJ; 200 μg/l Fe(III)Cl_3 x 6 H_2O; 400 mg/l $MnSO_4$ x H_2O; 200 μg/l $(NH_4)_6Mo_7O_{27}$ x 4 H_2O; 200 mg/l $ZnSO_4$ x 7 H_2O; 200 μg/l riboflavin; 200 μg/l p-aminobenzoeic acid; 2 μg/l biotin; 2 μg/l folic acid; 400 μg/l nicotin acid; 400 μg/l pyridoxin-HCl; 400 μg/l thiaminchlorid; 13.4 mM KCl; 50 mM natriumcitrate pH 5.0, 2% (w/v) glucose; 1.6 g/l amino acid drop-out mix

2.5 Induction of *PHO* genes

2.5.1 Phosphate starvation

To activate the *PHO* genes, logarithmically growing yeast cells were washed twice in water to get rid of the phosphate containing medium and resuspended in pre-warmed phosphate-free medium for the indicated times.

2.5.2 Growth of replicating and non-replicating cells

YS44 cells were grown logarithmically at 24°C in YPDA. To inhibit replication cells were resuspended in YNB without uracil (dilution: 1 OD_{600}/ml) and incubated for 2 h at 24°C. A parallel culture with replicating cells was grown in YNB with uracil at 24°C. Both cultures were shifted to the restrictive temperature of 37°C by resuspending the cells in pre-warmed 37°C medium with or without uracil, respectively. Inactivation of *pho80* by a temperature up-shift started *PHO* induction. Samples for the ChIP kinetic were taken at several time points (2.11).

2.6 General yeast methods

2.6.1 Transformation of *S. cerevisiae* cells

10 ml logarithmically growing yeast cells of an OD_{600} of 2-3 ($1OD_{600}$ = $1.5x10^7$ cells/ml, photometer: Zeiss, M4 QIII 95067) were washed in 50 ml TE pH 7.4, pelleted and resuspended in TE to reach the concentration of 30 OD cells/ml. Half of the cells were treated with sterile 500 µl 0.2 M LiAc and incubated in a 50 ml tube in a 30°C water bath for 1 h under constant shaking. 100 µl of this cell suspension were transferred into an eppendorf tube that contained 30 µl of DNA (1-2 µg plasmid DNA or 10 µg PCR/restriction fragment DNA) and were incubated for 30 min at 30°C without agitation. 130 µl 60% PEG 4000 were added to the suspension and vortexed rigorously followed by incubation for 1 h at 30°C. The heat shock was applied to the cells for 10 min at 42°C in a water bath. The cells were centrifuged for 1 min at 4000 rpm in a table top centrifuge and washed with 1 ml dH_2O. Washed and pelleted cells were resuspended in a small volume of dH_2O and plated onto an YNB plate selective for the corresponding marker.

2.6.2 DNA isolation from *S. cerevisiae*

1-2 ml YPDA- or 3 ml minimal medium-grown stationary cells were pelleted in a table top centrifuge and washed with an equal volume of dH_2O. The cells were resuspended in 250 µl sorbitol/phosphate buffer (0.9 M sorbitol, 50 mM $Na-P_i$ pH 7.5, 140 mM ß-mercaptoethanol). OD_{600} was measured and 10 µl zymolyase 100 T (freshly made, stock 20 mg/ml in H_2O) were added to the cells for 40 min at 37°C. OD_{600} was measured again and compared to the previous optical density. Lysis of

cells should be least 70-90%. 50 µl proteinase K (20 mg/ml in 10 mM Tris-HCl, pH 8.0), 60 µl 0.2 M EDTA and 44 µl 20% SDS were added and the reaction tube was inverted 4-6 times and subsequently incubated for 30 min at 37°C. 1M $NaClO_4$ was added. For phenol extraction 1 volume of phenol (DNA phenol, equilibrated to pH 7.5-8.0) was added to the sample and vortexed hard. 1 volume of chloroform/isoamylalcohol (96%/4%) was added, vortexed and centrifuged at full speed at room temperature for 5 min (Eppendorf 5415 D). The supernatant was transferred into a fresh tube and treated with 1 volume of chloroform/isoamylalcohol and was vortexed and centrifuged. The supernatant was ethanol precipitated by adding 2.5 volumes of 100% ethanol to the sample and incubating it 10 min on ice. Centrifugation with 20.000 x g at 4°C (Eppendorf 5417R) for 20 min resulted in a precipitated DNA visible as white pellet. This was washed with 70% ethanol, air dried and resuspended in 300 µl TE pH 8.0. 15 µl RNase A (10 mg/ml in 5 mM Tris/HCl, pH 7.5) were added to the sample for 1 h at 37°C followed by ethanol precipitation. The DNA was resuspended in 100 µl TE.

2.7   Extract and protein preparation

2.7.1   Yeast whole cell extract

Yeast whole cell extract was prepared as previously described (Hertel et al. 2005; Wippo et al. 2009), but from strain YS27 *cbf1::URA3* and with Tris-HCl instead of Hepes-KOH in the extraction buffer. Briefly, logarithmically growing yeast cells were grown to an optical density at 600 nm of 2 to 4, harvested, and washed with ice-cold extraction buffer (0.2 M Tris-HCl, pH 7.5, 10 mM $MgSO_4$, 20% glycerol, 1 mM EDTA, 390 mM $(NH_4)_2SO_4$, 1 mM DTT, and 1x Complete protease inhibitor without EDTA). The pellet was shock frozen and cells lysed by grinding in liquid nitrogen using an electric mortar (Retsch, RM100). After slow thawing and clearing by centrifugation, proteins were precipitated with 337 mg/ml $(NH_4)_2SO_4$, resuspended in dialysis buffer (20 mM Hepes-KOH, pH 7.5, 20% glycerol, 50 mM NaCl, 1 mM EGTA, 5 mM DTT, and Complete protease inhibitor without EDTA) and dialyzed three times for 30 min against the same buffer. Aliquots of the extract were frozen in liquid nitrogen and stored at -80°C.

2.7.2   Yeast nuclei

Yeast nuclei were prepared as described (Almer et al. 1986; Gregory et al. 1999a). Yeast cells were either grown in medium containing phosphate (YPDA or YNB) or in phosphate-free medium, corresponding to repressed or induced conditions, respectively. Cells were grown to an OD_{600} of 2-4, harvested and washed once with ice-cold water. The weight of the cell pellet was determined. The pellet was resuspended in 2 volumes of pre-incubation buffer (0.7 M ß-mercaptoethanol, 2 mM EDTA) and incubated in a shaking 30°C water bath for 30 min. The pelleted cells were washed in 1 M sorbitol and resuspended in 5 ml 1 M sorbitol, 5 mM ß-mercaptoethanol per gram wet weight. The OD_{600} was measured and spheroblasts were generated by adding zymolyase 100T to a final concentra-

tion of 2%. Cells were incubated for 30 min at 30°C in a shaking water bath. Lysis efficiency was calculated as in 2.6.2. and should be at least 60%. The spheroblasts were washed once in 1 M sorbitol, lysed by resuspending in a hypotonic buffer (18% ficoll, 20 mM KH_2PO_4, 1 mM $MgCl_2$, 0.25 mM EGTA, 0.25 mM EDTA, pH 6.8). The nuclei were pelleted and aliquots frozen and stored at -80°C.

2.7.3 Yeast histone octamers

Expression and purification of recombinant yeast histones was done as described (Luger et al. 1999). Expression plasmids for each histone were a gift of Xuetong Shen (MD Anderson Cancer Center, Texas). Briefly, recombinant histones were expressed in BL21 DE3 pLys. Histone containing inclusion bodies were unfolded in urea buffer (7 M urea, 20 mM sodiumacetate pH 5.2, 200 mM NaCl, and 1 mM EDTA, 5 mM ß-mercaptoethanol) and purified by ion exchange chromatography (SP sepharose, Amersham Bioscience). The eluted histones were dialyzed against water, lyophilized and stored at -80°C. Octamer reconstitution was done dissolving each histone in unfolding buffer (7 M guanidinium HCl, 20 mM Tris pH 7.5, 10 mM DTT) in a final concentration of 2 mg/ml and mixing the four histones in equimolar ratios. After dialysis against refolding buffer (2 M NaCl, 10 mM Tris pH 7.5, 1 mM EDTA, 5 mM ß-mercaptoethanol), aggregates were removed by centrifugation. The supernatant was concentrated by ultrafiltration (centricons, 30 KDa cut off) and purified over a Superdex200 gel filtration column. Fractions were analyzed on an 18% SDS-PAGE gel and fractions with stochiometric amounts of the four core histones were pooled and concentrated. One volume 98% glycerol was added and the recombinant histone octamers were stored at -20°C. Due to some inconsistencies in the purification, recombinant yeast octamers from Barbara Dirac-Svejstrup (group of Jesper Svejstrup, Cancer Research UK London Research Institute, UK) were used (**Fig. 8**, lanes 4-6).
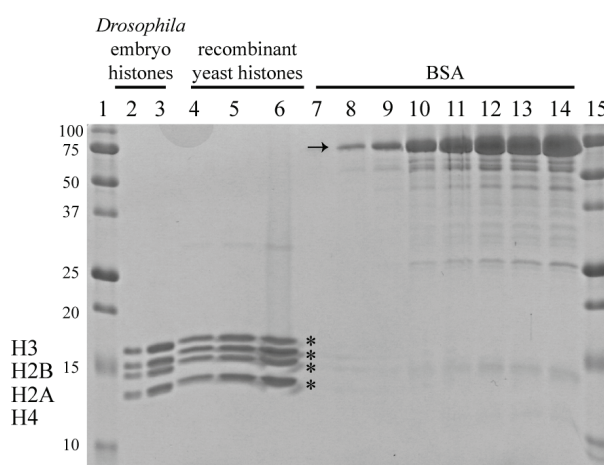
Fig. 8 Purified *Drosophila* embryo histones and recombinant yeast histones. Coomassie gel showing the different purified histone preparations (each asterisk points to one of the core histones): 2 and 6 µl (lanes 2 and 3, respectively) of a 1:20 dilution of *Drosophila* embryo histones were loaded and 1, 2 and 6 µl (lanes 4-6) undiluted recombinant yeast histones were loaded. Increasing concentration of BSA (arrow, 0.1, 0.5, 1, 2.5, 4, 6, 8, 10 µg, lanes 7-14) were loaded to compare the concentration of the histone preparations. Lanes 1 and 15 show protein marker bands (Dual Color, BioRad) with the indicated size in kDa.

2.7.4 *Drosophila* embryo histone octamers

Native *Drosophila* embryo histone octamers were purified as described (Simon and Felsenfeld 1979). Approximately 50 g of 0-12 h *Drosophila* embryos were collected, washed with water and dechorionated in bleach for 3 min. The washed embryos were resuspended in lysis buffer (15 mM Hepes-KOH pH 7.5, 10 mM KCl, 5 mM $MgCl_2$, 0.05 mM EDTA, 0.25 mM EGTA, 10% glycerol, 1 mM DTT, 0.2 mM PMSF and 1x Complete protease inhibitor without EDTA), homogenized six times at 1000 rpm (Yamamoto homogenisator) at 4°C. The homogenized embryos were filtered through miracloth and centrifuged resulting in three layers: a solid pellet, a soft and light layer on top of the pellet containing the nuclei, the supernatant. Nuclei were resuspended in sucrose buffer (15 mM Hepes-KOH pH 7.5, 10 mM KCl, 5 mM $MgCl_2$, 0.05 mM EDTA, 0.25 mM EGTA, 1.2% sucrose, 1 mM DTT, 0.2 mM PMSF), transferred to new tubes, centrifuged, washed once more in sucrose buffer, and resuspended in sucrose buffer. $CaCl_2$ was added to a final concentration of 3 mM and protease inhibitors aprotinin, pepstatin and leupeptin were added. The nuclei were digested with 200 U/µl MNase for 10 min at 26°C. The reaction was stopped with 10 mM EDTA. After centrifugation the pellet was resuspended in TE pH 7.6 including 1 mM DTT and 0.2 mM PMSF and lysed by rotation for 30–45 min in the cold room. After lysis the nuclei were centrifuged and the supernatant containing the soluble nuclear proteins was withdrawn. The salt concentration was adjusted to 0.63 M KCl and the histones were loaded onto equilibrated hydroxylapatite. Mononucleosomes were allowed to bind to the hydroxylapatite by rotation for 60 min at 4°C. The column was washed with 0.63 M KCl, 100 mM K-PO_4 pH 7.2 and loaded onto a FPLC column. The histone octamers were eluted with a salt gradient between 0.63 and 2 M KCl. Eluted fractions were analyzed with an 18% SDS-PAGE gel. Fractions containing the histone octamer were pooled and concentrated (Centricon, 30 KDa cut off) (**Fig. 8**, lanes 2-3). Glycerol concentration was adjusted to 50% and supplemented with 1x Complete protease inhibitor without EDTA. Octamers were stored at -20°C.

2.7.5 Recombinant Pho4, Pho4ΔAD, Pho2

Expression and purification of recombinant Pho4 and Pho2 was previously described (Barbaric et al. 1996). A BbrPI/NcoI fragment of the *PHO4* locus was cloned into pET21d (Stratagene), which was cut with EagI, blunt ended and cut with NcoI. This adds ten amino acids to the C-terminus of Pho4 (AALE(H)$_6$), the last six being the histidine tag. The pET21d-based Pho2 expression plasmid was a kind gift from D. Stillman (University of Utah School of Medicine, Salt Lake City). The *PHO4*-SPA6 mutation (Springer et al. 2003) was introduced into the pET21d-PHO4 expression plasmid by transfer of a 280 bp SfuI/ClaI restriction fragment from plasmid EB1043 (kind gift of E. O'Shea (Harvard University, Cambridge)). *E. coli* strain BL21 DE3 pLysS (Stratagene) was transformed with constructs of Pho4-SPA6, Pho4 wild type, Pho2 or Pho4 ΔAD and grown at 37°C (*PHO4* expression) or 28-30°C (*PHO2* expression) in logarithmic phase in LB medium with chloramphenicol (34 µg/ml) and ampicillin (300 µg/ml). For induction, the culture was treated with 1 mM IPTG and incubated for 3 h. The

cells were harvested, washed and resuspended in sonication buffer (50 mM NaH_2PO_4 pH 8.0, 300 mM NaCl). Complete protease inhibitor without EDTA and 0.1% NP-40 were added. Cells were lysed by a freeze-thaw cycle (liquid nitrogen) and sonication (50% amplitude, ultrasonic homogenizer SONO-PULS 2200 equipped with sonotrode MS73, Bandelin Electronic, Berlin, Germany; four separate 20 sec bursts, > 1 min cooling on ice between the pulses). The cell lysate was cleared by centrifugation (12,000 rpm, SS34, Sorvall, 4°C, 30 min) and the supernatant applied in batch to 1 ml of Ni^{2+}-NTA agarose (equilibrated in sonication buffer). After incubation for 1 h with agitation in the cold room, the resin was washed twice in batch with ice-cold sonication buffer, transferred into a column and washed with 100 ml sonication buffer, 60 mM imidazole pH 8.0 and 1x Complete protease inhibitor without EDTA. Pho4-6xHis or Pho2-6xHis was eluted from the column with 10 ml sonication buffer, 1 M imidazole pH 8.0 and 1x Complete protease inhibitor without EDTA.
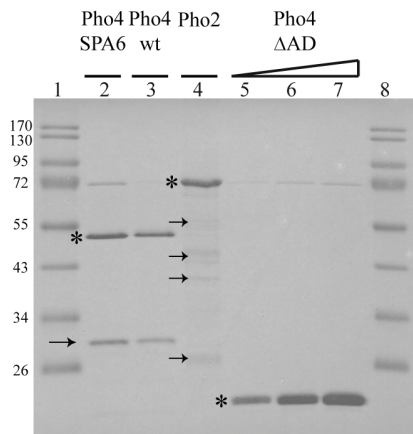
Fig. 9 Purified proteins. Coomassie gel showing the different purified transcription factors. For Pho4-SPA6 (mutated phosphorylation site to ensure interaction with Pho2), Pho4 wild type (wt) and Pho2 (lanes 2-4), 2 µl of each preparation were loaded on the gel. For Pho4 ΔAD (without activation domain) 2, 4 and 6 µl were loaded (lanes 5-7). Lanes 1 and 8 show protein marker bands (peqGOLD protein marker IV, peqlab) with the indicated size in kDa. Running size (asterisk) does not correspond to calculated mass of proteins. Pho4-SPA6 and Pho4 wt have a calculated mass of 34 kDa but runs at 50 kDa, Pho2 has calculated mass of 63 kDa but runs at 90 kDa and Pho4 ΔAD has calculated mass of 23 kDa. Degradation products of Pho4-SPA6, Pho4 wt and Pho2 are marked with an arrow.

Fractions were tested by SDS-PAGE and coomassie staining for the band of proper size (**Fig. 9**). Positive fractions were pooled and dialyzed (MWCO 6,000-8,000 Da) overnight at 4°C against 20 mM Tris-HCl pH 8.0, 100 mM NaCl, 10% glycerol, 0.5 mM DTT, 0.5 mM EDTA, and 0.2 mM PMSF, 1 mM benzamidine.

2.8 *In vitro* chromatin assembly

2.8.1 DNA templates

The DNA templates for all salt gradient dialysis chromatin reconstitution reactions were circular, supercoiled pUC19-based plasmids, where the multiple cloning site contained the *PHO5*, *PHO8* or *PHO84* open reading frame plus upstream regions as follows. Plasmid pUC19-PHO5 was generated by inserting the 3149 bp HindIII-PstI fragment of the *PHO5* locus into pUC19. Plasmid pUC19-PHO8 was prepared by ligating a 3.5 kb PCR product, generated using the primers 5'-CCATGTGCATAGGATCCGGACGTTTGCCATAGTGTTG-3' and 5'-CAGTCAGACGCTGCAGGGGAGAGTTAGATAGGATCAGT-3' and genomic DNA from strain BY4741 as template, via PstI and BamHI into pUC19. Plasmid pUC19-PHO84 (Wippo et al. 2009)

was prepared by ligating a 3.5 kb PCR product, generated using the primers 5'-CCGGAATTCTCGAGTCATGATTTGGAACAGCTCC-3' and 5'-CGCGGATCCGCAGAGAGATGTGAGGAAAT-3' and genomic DNA from strain BY4741 as template, via EcoRI and BamHI into pUC19. Primers for site directed mutagenesis (using Stratagene QuickChange mutagenesis) for UASpB high affinity, i.e, CACGTT to CACGTG, were: 5'-CAGTATTACG<u>CACGTG</u>GGTGCTGTTATAGGC-3' and 5'- GCCTATAACAGCACC-CACGTGCGTAATACTG-3' and used the template pCB84a-l resulting in plasmid pCB84-Bhi. QuickChange mutagenesis of plasmid pP8apain with primers 5'-GTAATCCTAATTTGAGCTCTACACAATACCA<u>CACGTG</u>GGTTAACAGCTACTGCA-3' and 5'-TGCAGTAGCTGTTAACCCACGTGTGGTATTGTGTAGAGCTCAAATTAGGATTAC-3' resulted in pP8apain intra high. Two different plasmids were always combined at equimolar ratio in all *in vitro* assembly reactions.

2.8.2 Salt gradient dialysis assembly

Salt gradient dialysis was performed as described (Langst et al. 1999). A typical assembly reaction contained 10 µg supercoiled plasmid DNA (Qiagen preparation), 20 µg BSA, and variable amounts *Drosophila* histone octamers or recombinant *Saccharomyces cerevisiae* octamers in 100 µl high-salt buffer (10 mM Tris-HCl, pH 7.6, 2 M NaCl, 1 mM EDTA, 1 mM β-mercaptoethanol, 0.05% Igepal). A good assembly degree of salt gradient dialysis chromatin is determined by a serial titration of histones to DNA. The relative amount of histones to DNA that gives a clear repressed promoter pattern with the standard shifting reaction (2.8.3) defines the optimal assembly degree and is defined as 1. This amount of histones corresponds to 11µl of a 1:5 dilution (in 0.1 M KCl) in 100 µl assembly reaction with our histone preparation. This was dialyzed for 15 h at room temperature while slowly diluting 300 ml of high-salt buffer with 3 l of low-salt buffer (same as high-salt buffer, but with 50 mM NaCl) using a peristaltic pump. A final dialysis step versus 1 l low-salt buffer ensured a final NaCl concentration of 50 mM. The chromatin could be stored at 4°C for several months without affecting its chromatin structure.

2.8.3 Nucleosome shifting and remodeling reaction (adding yeast extract and remodeling factors to pre-assembled chromatin)

A 100 µl shifting reaction mixture contained 1 µg DNA in total, either pUC19-PHO5 and -PHO8 or pUC19-PHO84 and -PHO8 in equimolar amounts, preassembled into chromatin by salt gradient dialysis. The reaction was incubated with or without yeast extract (~250 µg protein, judged from coomassie stained gel lanes in comparison to protein standard) and with or without a regenerative energy system (3 mM ATP, 4.5 mM MgCl$_2$, 30 mM creatine phosphate and 50 ng/µl creatine kinase) in assembly buffer (20 mM Hepes-KOH pH 7.5, 10% glycerol, 80 mM KCl, 0.5 mM EGTA, 2.5 mM DTT) for 2 h at 30°C. If called for, Pho4 and/or Pho2 was added to 3 µg/100 µl (Pho4-SPA6), 3.4

μg/100 μl (wt Pho4), and 4.2 μg/100 μl (Pho2), respectively. Gcn5 and acetylCoA could also be added to the reaction. Preparations of the chromatin remodeling complexes RSC and SWI/SNF were kind gifts from Tom Owen-Hughes (University of Dundee, Dundee). The amounts added to the shifting reactions were sufficient to remodel the equivalent chromatin mass of mononucleosomal templates (T. Owen-Hughes, pers. communication). ATP was depleted from reconstitution reactions by a factor of at least 10^{-6} by adding apyrase to a concentration of 3-4 U/100 μl and incubating for 30 min at 30°C.

2.9   Chromatin analysis

2.9.1   Strategy of DNaseI and restriction enzyme digestion and subsequent indirect end-labeling
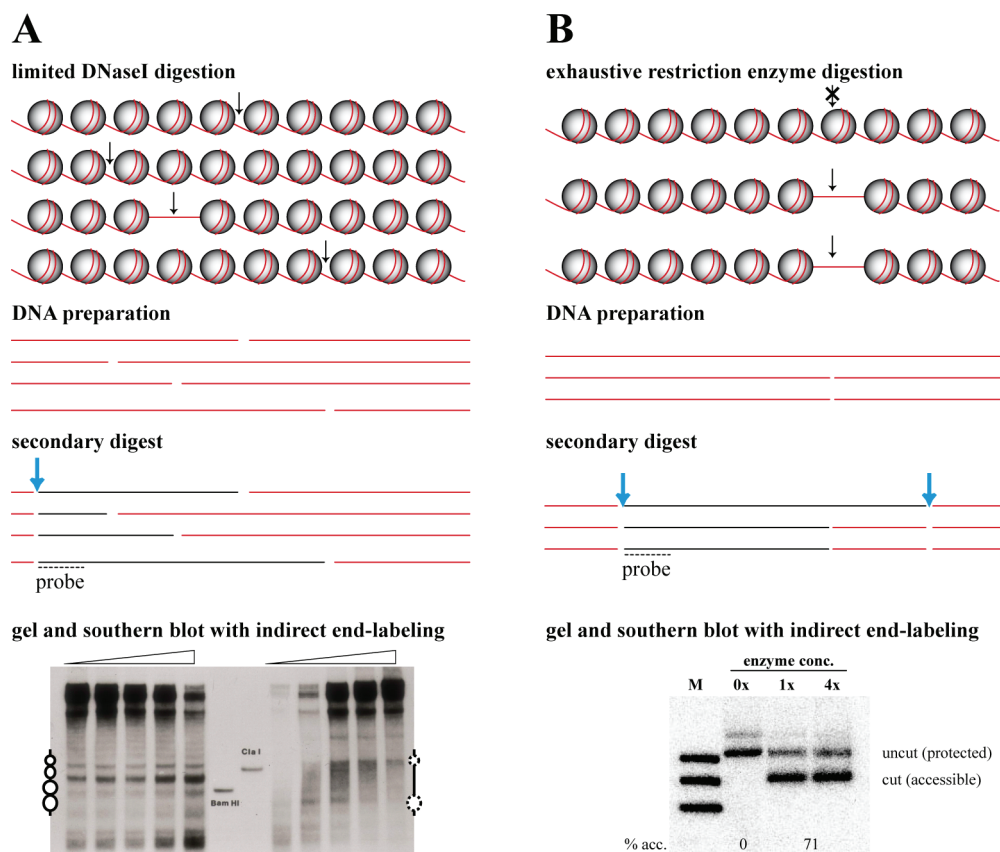
Fig. 10 Strategies to analyze nucleosomal occupancy. (A) Limited DNaseI digestion leads to one cut in the region of interest followed by DNA purification and secondary digest (blue arrow points to the restriction site). The DNA samples are separated on an agarose gel and blotted onto a membrane. Nucleosome positions are visualized by labeling the DNA with a radioactive probe (stippled line). DNA that was accessible to DNaseI digestion appears as hypersensitive sites. Nucleosomes that protected DNA from digestion are represented by spaces in-between. The southern blot shows the *PHO5* promoter with four positioned nucleosomes in the repressed (left) and in the induced state (right). (B) Exhaustive restriction enzyme digestion determines accessibility of DNA at a particular site. Secondary digest with restriction nucleases that cut up- and downstream of the region of interest (blue arrows) leads to detection of two fragment sizes after hybridization of the southern blot to a radioactive probe. PhosphoImager analysis allows the quantification of DNA accessibility that is represented by the ratio of accessible to protected DNA fragment (adapted from Reinke and Hörz 2004).

DNA accessibility of chromatin can be analyzed by DNaseI or restriction enzyme digestion (**Fig. 10**) (Reinke and Horz 2004). Limited or partial digestion of chromatin with DNaseI yields approximately one cut in the region of interest. An indirect end-labeling step ensures that the nuclease cut is mapped relative to a defined point represented by a restriction site in the DNA sequence. Different DNA fragment lengths represent the typical organization of nucleosome positions in the analyzed region visualized by southern blotting and hybridization with a radioactive probe. This method is therefore used to map nucleosome positions. To measure DNA accessibility of a particular site in chromatin quantitatively, two restriction enzyme concentrations are used to ensure exhaustive digestion. Secondary digest includes restriction with enzymes that frame the region of interest and lead after hybridization with an appropriate probe to the detection of two fragments. The larger fragment reflects protection of the DNA, and the smaller one accessibility. Using PhosphorImager analysis of the southern blot the ratio of both fragments and therefore the relative accessibility can be determined.

2.9.2 DNaseI digestion of *in vitro* assembled chromatin

DNaseI indirect end-labeling was performed in analogy to Almer et al. 1986. 10 μl aliquots of a reconstitution reaction were mixed with an equal volume of digestion buffer (20 mM Hepes-KOH pH 7.5, 12% glycerol, 4 mM $MgCl_2$, 5.5 mM $CaCl_2$, 2.5 mM DTT, 80 mM NaCl, 0.1 mg/ml BSA) containing DNaseI at concentrations in the range of 0.02-0.1 U/ml (salt gradient dialysis chromatin) or 2-15 U/ml (salt gradient dialysis chromatin with extract) and incubated at room temperature for 5 min. In all DNaseI mapping experiments chromatin samples were digested with a range of DNaseI concentrations. However, due to space limitations only one lane or a few representative lanes are shown in some figures. The digestion reactions were stopped by adding 4 μl of STOP buffer (10 mM EDTA, 4% SDS), and the DNA was purified by digestion with proteinase K and ethanol precipitation. The DNA was resuspended in TE buffer (10 mM Tris pH 8.0, 1 mM EDTA) followed by a secondary digest with ApaI (Roche) for the *PHO5* promoter or BglII (NEB) for the *PHO8* promoter, including pP8apain intra high, or SspI (NEB) for the *PHO84* promoter and HindIII (NEB) for pCB84 Bhi.

2.9.3 Restriction nuclease digestion of *in vitro* assembled chromatin

Aliquots of chromatin reconstitution reactions were apyrase treated prior to restriction enzyme digestions, to remove the ATP. 2 μl aliquots of an apyrase treated reconstitution reaction were mixed with 15 μl of RE digestion buffer (20 mM Hepes-KOH pH 7.5, 4.5 mM $MgCl_2$, 2.5 mM DTT, 80 mM NaCl, 0.5 mM EGTA) and digested with two different enzyme concentrations for the restriction enzyme (ClaI for the *PHO5* promoter (Roche)). The reactions were stopped by adding 4 μl STOP buffer (2.9.2). DNA purification, secondary cleavage (HaeIII for the *PHO5* promoter), blotting and hybridization were as in 2.9.2.

2.9.4   DNaseI and restriction nuclease digestion of yeast nuclei

The preparation of yeast nuclei and chromatin analysis by restriction nucleases and DNaseI digestion with indirect end-labeling were as described (Almer et al. 1986; Gregory et al. 1998a; Gregory et al. 1999a). Shortly, nuclei were washed and resuspended in DNaseI buffer (15 mM Tris pH 7.5, 75 mM NaCl, 3 mM MgCl$_2$, 0.05 mM CaCl$_2$, 1 mM ß-mercaptoethanol) for DNaseI digestion or in 1 x SSTEEM buffer (0.15 mM spermin, 0.5 mM spermidin, 10 mM Tris pH 7.4, 0.2 mM EDTA, 0.2 mM EGTA, 10 mM MgCl$_2$, 5 mM ß-mercaptoethanol, 50 mM NaCl) for restriction enzyme digestion. The nuclei were digested with a range of DNaseI concentrations for 20 min at 37°C or with 2 different restriction enzyme concentrations (onefold and fourfold) for 30 min at 37°C and stopped with 0.5% SDS, 4 mM EDTA, 50 mM Tris-HCl pH 8.8. 300–600 µg proteinase K were added for 30 min at 37°C. DNA extraction was done using phenol/chloroform, followed by ethanol precipitation. The DNA was resuspended in TE and RNA was digested by adding RNase A to a final concentration of 8% and incubation for 1 h at 37°C followed by ethanol precipitation. For the chromosomal *PHO5* locus, ApaI (DNaseI analysis) or HaeIII (restriction enzyme analysis), for the variant 31 *PHO5* locus in strain AH2341 HindIII (DNaseI analysis) or HindIII/SalI (restriction enzyme analysis), for the *PHO8* locus BglII and for the *PHO84* locus SspI were used for secondary cleavage. For the *PHO5* locus on plasmids pCB-UASp2-5 Δ2 and pCB-UASp2-8 Δ2 secondary cleavage was with NciI.

2.9.5   Southern Blot

Southern blotting was used to transfer DNA from agarose gels to a nylon membrane. The DNA fragments were resolved on a 1.5% agarose gel. The DNA in the gel was denatured for 20 min in denaturing buffer (0.5 M NaOH, 1.5 M NaCl) and laid on top of two wet Whatman papers with each end of the paper soaking in 20 x SSC (6 M NaCl, 600 mM Na-citrate). The blotting membrane was laid on top of the gel (exclude air bubbles) followed by three Whatman papers all equilibrated in 20 x SSC. A stack of dry tissues on top of this setup ensured capillary transfer during overnight blotting. The membrane was baked for 2 h at 80°C and then washed in 3 x SSC (900 mM NaCl, 90 mM Na-citrate) for 30 min at 68°C and in 3 x SSC and 1 x Denhardt (0.5% SDS, 1 mM EDTA, 0.02% BSA, 0.02% PVP-40, 0.02% ficoll) for 2 h at 68°C. The membrane was pre-hybridized in 2 x SSC, 1 x Denhardt with carrier DNA (salmon sperm) for 1 h at 68°C. Hybridization was done overnight adding half of a radioactively labeled probe (see 2.9.6). The blot was washed 3 x 30 min in 2 x SSC and 1 x Denhardt at 68°C.

To analyze the blotting membrane with a second or third probe, the membrane was stripped for the first probe by washing three times in 0.4 M NaOH for 30 min at 45-50°C. This was followed by neutralization of the membrane two times in 0.1 x SSC, 0.1% SDS for 15 min at 45-50°C.

2.9.6   Labeling of probes and analysis of southern blots

Hybridization probes were PCR products corresponding to the following genomic regions:

probe-DNaseI-*PHO5*:	bases -760 to -1296 from the ATG of the *PHO5* ORF,
probe-RE-*PHO5*:	bases -276 to -537 upstream of the *PHO5* gene,
probe-*PHO8*:	bases +78 to +568 from the ATG of the *PHO8* ORF,
probe-*PHO84*:	bases -1083 to -1428 from the ATG of the *PHO84* gene,
probe *PHO5*-plasmid:	bases 172 to 379 of pBR322,
probe pCB84 Bhi or variant 31:	pBR322 HindIII/BamHI (Fascher et al. 1993).

Probes were labeled with α-^{32}P-dCTP using the kit PrimeIt II according to the manufacturer´s protocol.

Blots were exposed to x-ray films using intensifier screens (DuPont, Lightening Plus) and scanned in CMYK modus (MikroTek ScanMaker i900). Scan images were imported in Adobe Photoshop CS2 and the total image was further manipulated by conversion into grayscale format and linear level adjustment. Sometimes parts of the image were rearranged as indicated in the figures and figure legends. Quantification of restriction enzyme accessibility assays was done using a PhosphorImager (Fuji FLA3000, AIDA^{TM} software version 3.52.046).

2.9.7   Luciferase ATP-assay

ATP concentrations were measured using the Enliten Luciferase reagent and a Luminometer (Lumat, Berchtold) according to manufacturer's directions. As this assay is very sensitive and not linear anymore if oversaturated, samples were usually diluted by a factor of 10,000 to 100,000 with water.

2.9.8   Histone acetyltransferase (HAT) filter binding assay using Gcn5 and chromatin templates

The filter binding HAT assay was done as previously described (Imhof and Wolffe 1999) with the following changes. Comparable histone amounts of *Drosophila* histone octamers or salt gradient dialysis chromatin were incubated with or without recombinant Gcn5 and 0.5 µl [^{3}H] acetyl CoA (3.6 Ci/mmol) in a total volume of 14 µl for 1 h at 30°C. Half of the reaction was stopped by adding 1 µl 100 mM acetic acid. In order to assess the effects of HATs and histone deacetylases endogenous to the yeast extract, the second half of the reaction was incubated with 44 µl of 20 mM Hepes-KOH pH 7.5, 10% glycerol, 80 mM KCl, 0.5 mM EGTA, 2.5 mM DTT, 3 mM ATP, 4.5 mM MgCl$_2$, 30 mM creatine phosphate and 50 ng/µl creatine kinase, yeast extract, Pho4 (3.4 µg/100µl) and Pho2 (4.2 µg/100µl), 50 mM trichostatin-A for 2 h at 30°C and quenched with 1 µl 100 mM acetic acid. Each reaction was spotted onto a 1.5 cm x 1.5 cm P81 paper filter (Merck), washed three times for 5 min at room temperature in 50 mM sodium carbonate pH 9.2, air dried, and quantificated in a scintillation counter (LS1801, Beckman).

2.9.9   Acid phosphatase activity

Acid phosphatase activity was measured as described (Haguenauer-Tsapis and Hinnen 1984). Logarithmically growing yeast cells in YPDA or YNB medium were used for non-inducing conditions ($+P_i$), and incubation in medium without phosphate ($-P_i$) for standard overnight induction (12-18 h). Cells of the desired physiological state (2-4 OD for uninduced cells ($+P_i$) and 0.2-0.5 OD for overnight induced cells ($-P_i$)) were centrifuged 3 min at 4,000 rpm. The cell pellet was washed with water (room temperature), resuspended in 0.1 M NaAc buffer pH 3.6, and OD_{600} was measured. The samples and the 20 mM NPP (4-nitrophenyl phosphate disodium salt hexahydrate) solution were pre-incubated in a shaking water bath at 30 °C for at least 10 min. The reaction was started by the addition of 1 ml 20 mM NPP solution to 1 ml of each sample and 1 ml of the NaAc buffer used as reference. Each reaction was stopped after exactly 10 min with 500 µl 1 M NaOH. Samples were centrifuged 2 min at 4,000 rpm (Eppendorff 5180 R) and the A_{410} of the supernatant was measured against the reference. The acid phosphatase activity was calculated according to this formula:

$$(1000 * A_{410}) / (OD_{600} * V_{sample} (1 \text{ ml}) * 10 \text{ min}) = \text{acid phosphatase units}$$

2.10 Chromatin purification

2.10.1 Separation of chromatin populations in sucrose gradients

50 µg of DNA after salt gradient dialysis assembly into chromatin (equimolar amounts of pUC19-PHO5 and -PHO8 in 500 µl) was prepared as previously described (2.8.2). 400 ng DNA packaged in chromatin was taken as input control and stored on ice. The rest of the chromatin was dialyzed against polyethylene glycol (6000) until the volume was reduced to 150 µl. 700 ng of chromatinized plasmid were put aside as second input control. The concentrated chromatin was loaded onto an 11 ml 15% - 40% sucrose gradient (Gradient Master^TM, BIOCOMP) in low-salt dialysis buffer (2.8.2) and centrifuged for 16 h at 30,000 rpm, 4°C (Beckman ultracentrifuge, rotor SW41 Ti, polyallomer centrifuge tubes 14 x 89 mm, Beckman). 500 µl fractions were collected in tubes containing 100 µg BSA using a syringe Micro-Fractionator (Brandel). 400 µl were stored at 4°C. The 100 µl aliquots were treated with 4% SDS and 0.1 M EDTA, digested with 140 µg proteinase K for 3 h at 37°C and precipitated with ethanol. The DNA content was analyzed photometrically (NanoDrop® Spectrophotometer ND-1000, Peqlab) and by agarose gel electrophoresis in order to choose representative fractions of the sucrose gradient containing chromatin. The corresponding 400 µl chromatin samples were dialyzed against low-salt dialysis buffer and concentrated with PEG to counteract the volume increase during dialysis. 1.5 µg chromatinized plasmid of the selected fractions and the two input controls were used for shifting nucleosome positions *in vitro* and afterwards analyzed by DNaseI indirect end-labeling.

2.10.2 Separation of chromatin populations by differential MgCl₂-precipitation

Chromatin reconstituted by salt gradient dialysis with or without extract treatment and/or addition of Pho4 was precipitated stepwise by successive additions of $MgCl_2$ (0.2, 1, 2.5, 6, 8, 10, 15 mM final concentration), always using the supernatant of the preceding precipitation reaction. After each $MgCl_2$-addition the sample was incubated on ice for 15 min and centrifuged for 15 min at 13,000 rpm (15,800 rcf) and 4°C in a table top centrifuge (Eppendorf 5415D). This resulted in a precipitated chromatin fraction in the pellet and a soluble chromatin fraction in the supernatant. The precipitated chromatin fractions were resuspended in low-salt dialysis buffer (2.8.2) or in assembly buffer (2.8.3). An aliquot of each solubilized chromatin pellet was analyzed for DNA content (NanoDrop® and agarose gel electrophoresis). In case of salt gradient dialysis chromatin as starting material, the chromatin fractions were subjected to nucleosome position shifting using yeast extract and energy and analyzed by DNaseI indirect end-labeling before and after this extract treatment. In case of salt gradient dialysis chromatin that was treated with extract and Pho4 prior to the gradient fractionation, the fractions were analyzed directly by DNaseI indirect end-labeling.

2.11 Chromatin immunoprecipitation

2.11.1 Basics
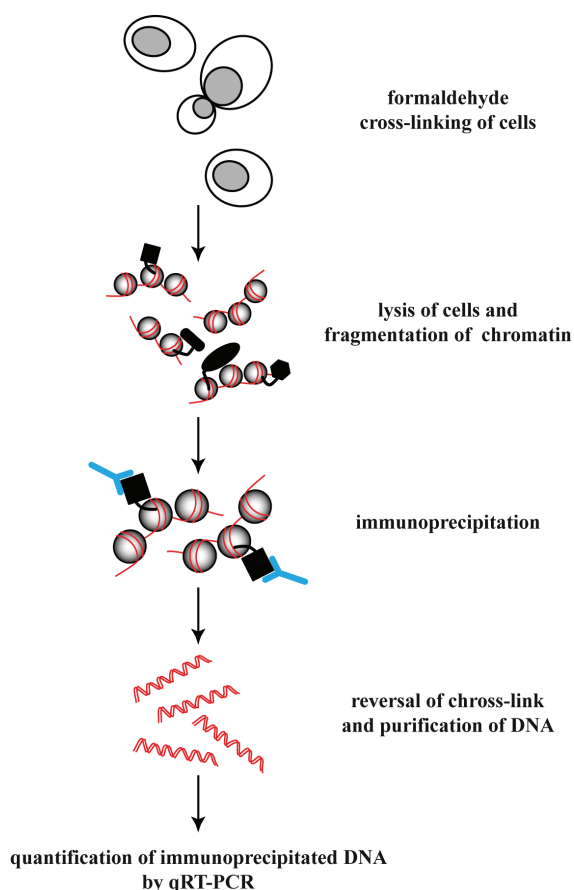
The chromatin immunoprecipitation (ChIP) technique is used to study the association of proteins to a specific genomic region *in vivo* (**Fig. 11**). Proteins that are in close contact to chromatin are cross-linked to DNA by adding formaldehyde, which easily penetrates the membrane, to whole cells. The cells are lysed by vortexing with glass beads. Subsequent sonication leads to the fragmentation of chromatin. The cell lysate is treated with an antibody against the protein of interest.

Fig. 11 Principle of chromatin immunoprecipitation. Whole cells are cross-linked with formaldehyde. Proteins in close proximity to DNA are cross-linked (black shapes). The cells are subsequently lysed and the chromatin is fragmented. Treatment with an antibody (blue) against the protein of interest enables immunoprecipitation and enrichment of the specific locus. Cross-links are reversed and DNA is purified before the immunoprecipitated DNA can be quantified with qRT-PCR (adapted from (Hecht and Grunstein 1999)).

Immunoprecipitation is followed by the reversal of cross-links, purification of the immunoprecipitated DNA and analysis with quantitative RT-PCR using primers and probes of the genomic region of interest. If the immunoprecipitated protein was fixed to the genomic region there is a relative enrichment of IP-DNA to input DNA. An important aspect of the analysis is the normalization to input DNA and control loci that should not respond to the applied experimental setup (like changing phosphate conditions). Control regions are often silenced genomic regions like telomeric heterochromatin. In this study, two control loci were used: the telomere and the actin ORF that should both be inert to changes in phosphate levels that are applied in the study of *PHO* genes. Amplicons that are used in this study were designed by Tim Luckenbach (LMU Munich).

2.11.2 Primer sequences and antibodies

Genomic region	forward and reverse primer and probe (5´-3´)
PHO5 UASp2	GAATAGGCAATCTCTAAATGAATCGA
	GAAAACAGGGACCAGAATCATAAATT
	ACCTTGGCACTCACACGTGGGACTAGC
PHO8	TGCGCCTATTGTTGCTAGCA
	AGTCGGCAAAAGGGTCATCTAC
	ATCGCTGCACGTGGCCCGA
PHO84	GAAAAACACCCGTTCCTCTCACT
	CCCACGTGCTGGAAATAACAC
	CCCGATGCCAATTTAATAGTTCCACGTG
Actin	TGGATTCCGGTGATGGTGTT
	TCAAAATGGCGTGAGGTAGAGA
	CTCACGTCGTTCCAATTTACGCTGGTTT
Telomere	TCCGAACGCTATTCCAGAAAGT
	CCATAATGCCTCCTATATTTAGCCTTT
	TCCAGCCGCTTGTTAACTCTCCGACA

A histone H3 antibody (abcam, ab1791) was used for the ChIP assays which recognized the C-terminal domain of the histone.

2.11.3 Cross-linking yeast cells with formaldehyde and fragmentation of DNA

50 OD cells per sample were collected and cross-linked using 1% formaldehyde final concentration for 20 min at room temperature with little agitation. The cross-linking was stopped by adding glycine to a final concentration of 125 mM for 5 min at room temperature. The cells were pelleted at 4°C and washed twice with equal volume of ice-cold 0.9% NaCl, frozen in liquid nitrogen and stored at -80°C. The cells were resuspended in 8 µl HEG150 buffer (150 mM NaCl, 50 mM Hepes pH 7.6, 10% glycerol, 1% Triton X-100, 1x Complete protease inhibitors) per 1 OD cells and transferred to a

siliconized Eppendorf tube. The cells were lysed by adding an equal volume of glass beads and shaking the tube for 1 h in an Eppendorf shaker at 4°C. The cell lysate was collected by puncturing a hole in the bottom of each tube and brief centrifugation into a fresh tube. The chromatin was sheared by sonication using the bioruptor (Bioruptor® diagenode) with 3 x 30 sec intervals at the highest intensity and in-between cooling in an ice-cold water bath. This fragmentation resulted in a DNA length of around 500 bp. The samples were centrifuged for 10 min at full speed and 4°C to remove cell debris.

2.11.4 Immunoprecipitation

The supernatant representing the whole cell extract (WCE) was transferred to a fresh tube. The clear WCE was pre-cleared with 25 µl Protein G sepharose beads for 1-2 h at 4 °C at constant rotation. In parallel, Protein G beads were blocked with 10% BSA and 0.5 µg/µl salmon sperm DNA in HEG150 buffer for 1-2 h at 4°C with rotation. A 20 µl aliquot of pre-cleared WCE was stored at -20°C as Input DNA. Immunoprecipitation was done by incubating 100-200 µl pre-cleared WCE with an appropriate amount of anti H3 C-terminal antibody and 25 µl of blocked Protein G beads overnight at 4°C at constant rotation. The next day the beads were pelleted and the supernatant aspirated. Beads were washed twice with HEG150, twice with LiCl (10 mM Tris-Cl 8.0, 250 mM LiCl, 0.1% NP-40, 1 mM EDTA) and once with TE (10 mM Tris-Cl, 1 mM EDTA, pH 8.0) using 1 ml each and rotating the tubes at room temperature for 5 min. Following the TE wash step the beads were resuspended in 100 µl TES (50 mM Tris-Cl, 10 mM EDTA, 1% SDS, pH 8.0) and incubated for 15 min at 65°C with agitation. After centrifugation the supernatant was transferred into a fresh tube and the beads were treated again with 100 µl TES and the following steps were repeated. The supernatant of each reaction was pooled resulting in 200 µl reaction volume. The volume of the 20 µl input WCE was adjusted to 200 µl with TES and the immunoprecipitation reactions and the input control were subjected to reverse cross-linking at 65°C overnight.

2.11.5 DNA purification

All samples were treated with RNase A using a final concentration of 0.5 mg/ml for 30 min at 37°C. Subsequently, each sample was treated with 1 mg/ml proteinase K and 10 µg glycogen in TE buffer in a volume of 200 µl for 2 h and 37°C. The samples were extracted with 1 volume (400 µl) of phenol and 1 volume of chloroform/isoamyl alcohol by vortexing for 3 min and centrifugating for 5 min at 14,000 rpm (Eppendorf 5417 R). Using high density MaXtract columns for phase separation allowed precise recovery of the aqueous phase and was important for the reproducibility of DNA yield. The extraction was repeated with 400 µl of chloroform/isoamyl alcohol and the high density MaXtract columns. The supernatant was transferred into a new tube. The DNA was precipitated with 40 µl LITE (5 M LiCl, 50 mM Tris-Cl 8.0) and 1ml 100% ethanol. The reaction was incubated for 10 min on ice and centrifuged for 30 min at 14,000 rpm at 4°C. The pellet was washed with 70% ethanol,

dried and resuspended in 100 µl TE pH 8.0. The DNA was purified with a QiaQuick purification kit, eluted with 100 µl elution buffer and stored at -20°C.

2.11.6 DNA quantification using TaqMan®-PCR

To quantify the immunoprecipitated (IP) and the input DNA, real-time PCR 96-well optical reaction plates (Applied Biosystems) were used. A PCR reaction of 25 µl included the following: 1.25 µl probe (5 µM, MWG), 4.75 µl each of the forward and reverse primer (10 µM each, MWG), 12.5 µl 2xTaqMan Universal PCR Mastermix (Applied Biosystems), IP-DNA (1:10 dilution) ad 25 µl with ddH₂O. PCR reactions were pipetted in duplicates or triplicates for each sample and for each biological condition. At least one control locus amplicon was used. The PCR reaction was performed according to the manufacturer´s protocol (1 x 50°C 2 min, 1 x 95°C 10 min, 40 x 95°C 15 sec, 60°C 1 min). DNA amplification and quantification was done using the ABI PRISM 7000 Sequence Detection System and the corresponding software.

2.11.7 Analyzing the quantitative PCR raw data

Quantitative real time-PCR (qRT-PCR) uses the quantitative relationship between the amount of DNA at the beginning of the reaction and the amount of PCR product in the exponential phase of the PCR. During the PCR reaction fluorescent signal from the Taqman probes accumulates, which indicates the generation of PCR product (**Fig. 12**). The threshold is set in the exponential phase of the amplification curve. The Ct value (cycle-threshold value) represents the PCR cycle number at which the threshold is reached. A small amount of DNA at the beginning of the reaction will reach the threshold later and result in higher Ct values whereas a high amount of DNA shows lower Ct values.
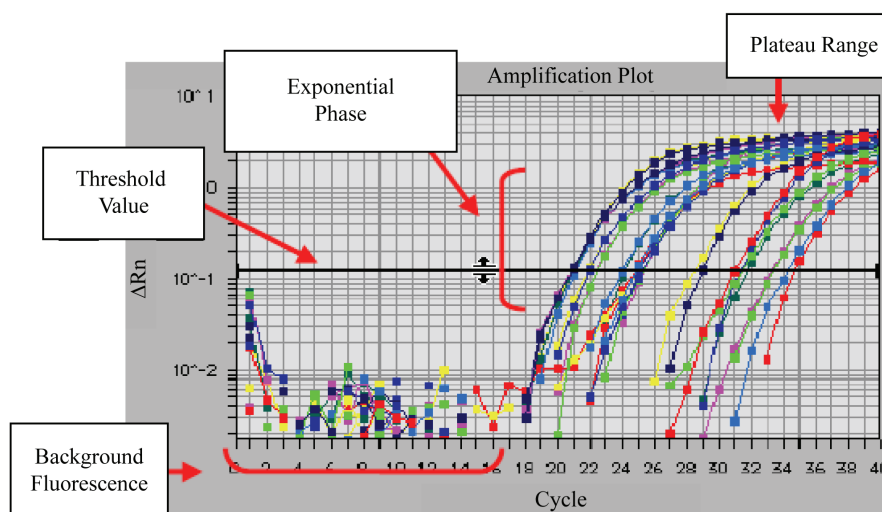
Fig. 12 Characteristics of an amplification plot. The cycle number of the PCR is plotted against fluorescent intensity. Fluorescent signal at the beginning of the qPCR is detected as background signal. When the qPCR is in the exponential phase the threshold defines the point for Ct value determination. Eventually the PCR enters in the plateau range where the fluorescent signal does not change with increasing cycle number anymore, the system becomes saturated (modified from: Data Analysis on the ABI PRISM_ 7700 Sequence Detection System: Setting Baselines and Thresholds).

2.11.7.1   The relative ChIP signal

The standard curves were made for each amplicon using input DNA (non-immunoprecipitated DNA) to control that the PCR product would accumulate exponentially and to control for amplicon (probe and primer) efficiencies. The standard curve was generated from a serial dilution of input DNA (1:5, 1:50, 1:500, 1:5,000, and 1:50,000). Each dilution led to a distinct Ct value that corresponded to the amount of input DNA. The logarithm of the input DNA dilutions were plotted versus the corresponding Ct values which gives a linear relationship. The plot yielded the intercept of the standard curve with the Y-axis and the slope; both were used for data analysis of the IP-DNA (**Fig. 13**). From the average of the triplicate Ct values of the IP-DNA, the relative amount of IP-DNA was determined using the standard curve (intercept and slope) of the corresponding amplicon which could be further normalized to a control locus.
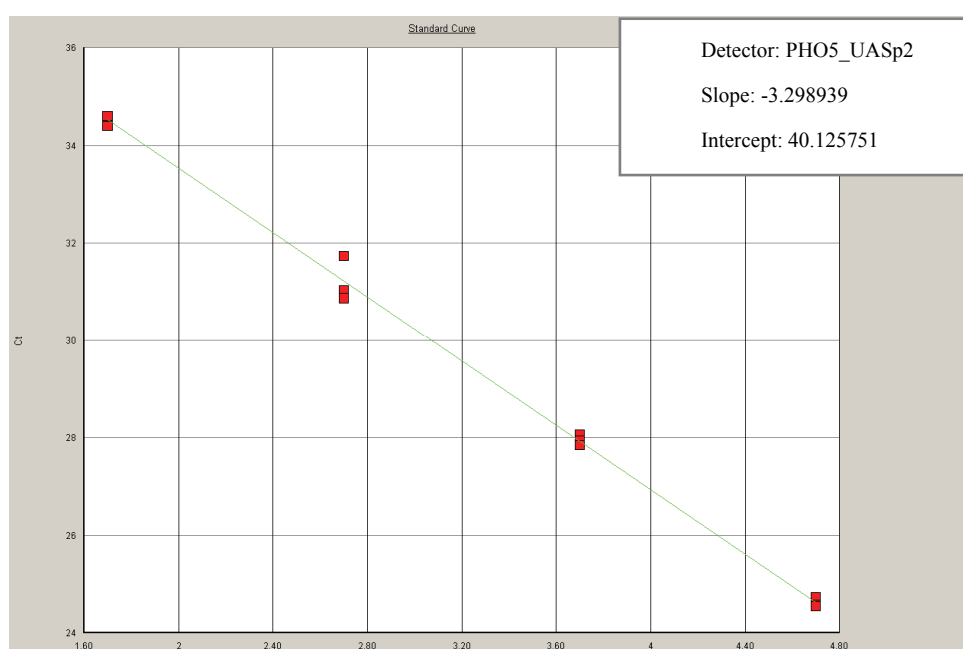
Fig. 13 Characteristic standard curve. Standard curve with four different dilutions of input DNA analyzed by qRT-PCR. Each dilution was pipetted in triplicates. For each input DNA the logarithm of the dilution is plotted versus the corresponding Ct value which gives the standard curve. Each standard curve is defined by the slope and the intercept with the Y axis (marked in upper right corner). Both criteria are used to quantify the immuno-precipitated DNA. Image is taken from a ChIP experiment that was analyzed with the ABI PRISM software.

In contrast to normalization to one standard curve that was generated for each amplicon with purified genomic DNA, we also used the approach of preparing an input DNA sample for each biological condition in parallel to the IP-DNA. Both the IP and the parallel input DNA were analyzed by calculating the average of the Ct values (per duplicate or triplicate) and determining the relative DNA amount using the standard curve for the respective amplicon. The ratio of IP over input ChIP signal gave the read out "% input". This could be further normalized to the % input signal of a control locus, but only if the control locus does not show biological effects. With this approach there is the concern that purification of the DNA (ChIP protocol 2.11.3, 2.11.4 and 2.11.5) might lead to different yields for input versus IP-DNA, which would severely confound the analysis. However, using the MaXtract

column for phenol purification increased the precision of DNA purification sufficiently. Nonetheless, we always included a control locus as internal control.

In general, Ct values should be lower than 30 to ensure good linearity of the amplification plot. Higher Ct values may be ok if the triplicates show no large variation. Ct values definitely have to be within the standard curve.

2.12 Synchronization and flow cytometry analysis of yeast cells

2.12.1 Synchronizing yeast cells with hydroxyurea

For G1/S phase arrest hydroxyurea treatment was used. Yeast cells were grown logarithmically at 30°C for several days. Before synchronization 0.7 OD cells were fixed in ethanol for FACS analysis (see chapter 2.12.3) and 50 OD cells were cross-linked for ChIP analysis, both representing the cell cycle stage of a mixed population of cells. Hydroxyurea was added to the yeast cell culture to a final concentration of 0.2 M followed by incubation for two rounds of duplication. FACS and ChIP samples were taken from the arrested cells as described before. The cell cycle block was released by washing the cells twice with pre-warmed water and resuspending the cells in pre-warmed medium. From the release on FACS and ChIP samples were taken every 15 min to track the different stages during progression through the cell cycle. FACS and ChIP (see chapter 2.11) samples were processed as described.

2.12.2 Synchronizing yeast cells with nocodazole and $cdc7^{ts}$

The $cdc7^{ts}$ mutant had first to be synchronized prior to the G1/S arrest by $cdc7^{ts}$ to avoid premature firing of the early origins, something likely to happen if only the $cdc7^{ts}$ mutation would be used for synchronization. The yeast cells carrying the $cdc7^{ts}$ mutation were grown logarithmically for several days at the permissive temperature of 24°C. For G2/M phase arrest nocodazole was added to a final concentration of 15 µg/ml for 2 h. Nocodazole was removed from the medium by washing the cells twice with pre-warmed water. The cells were resuspended in 24°C warm medium. After 15 min growth at 24°C the cells were resuspended in medium pre-heated to the restrictive temperature of 38°C. G1/S arrest was achieved after 3 h incubation at 38°C. FACS and ChIP samples were taken at indicated time points. Resuspending the cells back in 24°C medium allowed the progression into the cell cycle. Release was monitored by collecting FACS and ChIP samples every 15 min.

2.12.3 Flow cytometry analysis of the cell cycle

FACS samples were taken to monitor cell cycle progression and synchrony of the cell population. For FACS analysis 0.7 OD_{600} cells were harvested and fixed by adding 1 ml 70% ethanol followed by rigorous vortexing and at least 1 h incubation in the cold room with gentle rotation. Fixed cells were

washed once with room temperature 50 mM Tris-HCl pH 7.5 and incubated with 400 µg/ml RNase A in Tris-HCl buffer at 37°C overnight after brief sonication (Branson Digital Sonifier 250-D, 4 x 0.5 sec on and 0.5 sec off, 10% amplitude). Afterwards cells were resuspended in Tris-HCl buffer containing 1 mg/ml proteinase K and incubated at 50°C for 30 min. The cells were resuspended in 500 µl 50 mM Tris-HCl pH 7.5. This way the samples could be stored for several weeks at 4°C. For DNA staining for the FACS analysis, 100 µl of the cells kept in Tris-HCl buffer were added to 1 ml sytox green staining solution (1 mM stock in DMSO) to a final concentration of 1 µM (Haase and Reed 2002). Prior to FACS analysis the cells were sonicated a second time as before. FACS analysis was done using a BD Bioscience FACSCanto. 10,000 cells were counted and the raw data were analyzed and histograms plotted using FlowJo software.
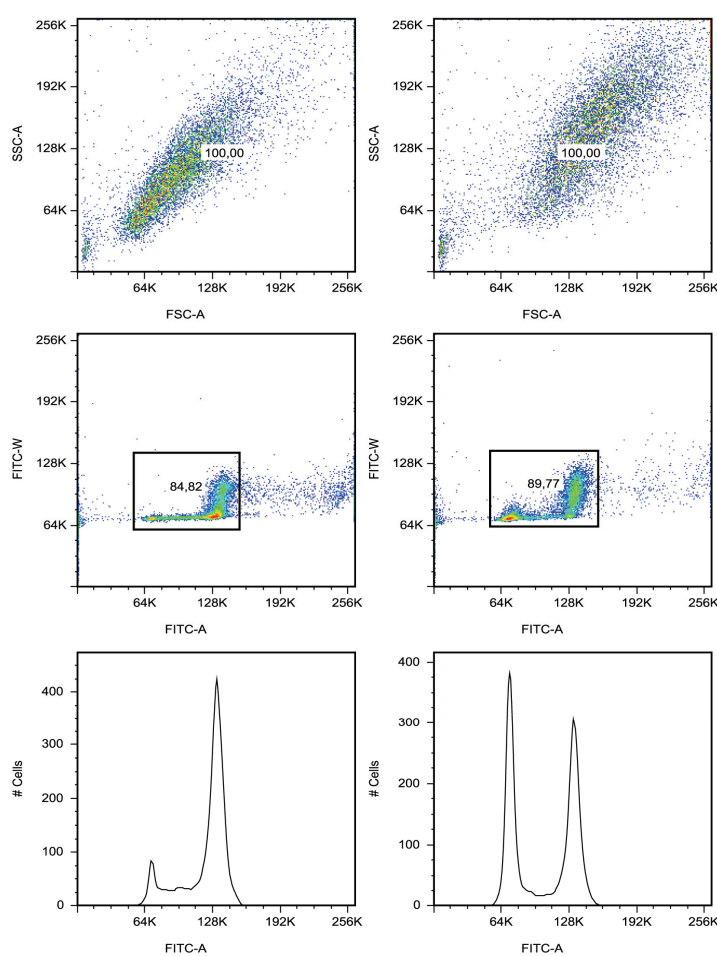
Fig. 14 Typical FACS profiles of yeast cells. Yeast cells stained with sytox green and analyzed on a BD Bioscience FACSCanto. Data evaluation was done using FlowJo software. Two examples are shown each with a dot plot of forward versus side scatter, a dot plot of fluorescence signal versus cell number and a histogram.

Using flow cytometry the number of cells with a certain content of stained DNA is analyzed. This is accomplished by measuring cellular and fluorescent properties of single cells. Using the FlowJo software to analyze the flow cytometry data an initial graph displays a forward (FSC-A) and side (SSC-A) scatter plot (**Fig. 14**). The forward scatter indicates the cell size and the side scatter the granularity of the cells. In a single parameter histogram the relative fluorescence (FITC-A) is plotted against the number of events (cells). If a whole population of cells is analyzed subcellular debris or unimportant cell populations are left out of the analysis by gating. The population within the gate is then plotted separately and can be displayed with a histogram plot of fluorescent signal versus cell number. The analysis of all FACS profiles shown in the results section included gating of the cell population.

3 Results

3.1 Remodeling chromatin at the *PHO5* and *PHO8* promoters *in vitro*

3.1.1 *De novo* positioning of nucleosomes at the *PHO5* promoter

In vitro studies showed *de novo* positioning of nucleosomes along the *PHO5* promoter using a yeast extract *in vitro* assembly system (**Fig. 15**, courtesy of Philipp Korber) (Korber and Horz 2004). With this system, *Drosophila* embryo histone octamers could be assembled onto a supercoiled plasmid harboring the *PHO5* sequence upon addition of yeast whole cell extract and an energy regenerating system (**Fig. 15**, lanes 1-3).
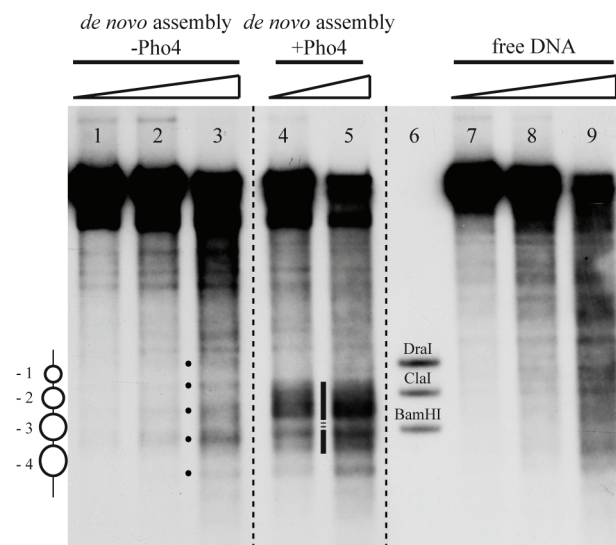
Fig. 15 Pho4-induced generation of a hypersensitive site at the *PHO5* promoter during *de novo* assembly *in vitro*. DNaseI indirect end-labeling analysis of the *PHO5* promoter region in chromatin assembled *de novo* with yeast extract *in vitro* with or without the addition of exogenous Pho4, and in free DNA. The schematic on the left denotes positioned nucleosomes as in the schematic of the *PHO5* promoter in **Fig. 7**A. Black dots in-between lanes 2 and 3 mark the bands corresponding to the linker regions between the positioned nucleosomes. The vertical bar in-between lanes 4 and 5 highlights the hypersensitive region generated by the addition of Pho4. The stippled region interrupting the vertical bar points to a region of maintained protection from DNaseI. Ramps on top of the lanes stand for increasing DNaseI concentrations. Marker fragments were generated by double digests of DraI, ClaI and BamHI each with ApaI. Stippled lines in-between lanes show where lanes from the same blot image were moved next to each other using Adobe Photoshop CS2.

Parallel experiments supplementing this assembly system with the transcription factor Pho4 led to the generation of a hypersensitive site (**Fig. 15**, lanes 4-5), resembling the remodeled *PHO5* promoter pattern. Both nucleosomal patterns differed clearly from the free DNA control (**Fig. 15**, lanes 7-9). In these *de novo* assemblies all factors involved (Pho4, octamers, yeast extract and plasmid DNA) were incubated together so Pho4 was present from the start of chromatin assembly. In theory, this

provided an opportunity for Pho4 to bind to its recognition site before the formation of nucleosome -2 could take place. Accordingly, the observed hypersensitive site might display the prevention of forming this nucleosome, rather than Pho4-initiated remodeling of pre-assembled chromatin. An altered version of the chromatin assembly protocol was developed to elucidate the potential of Pho4 to remodel chromatin *in vitro*.

3.1.2 The *in vitro* remodeling assay

We assembled *Drosophila* embryo octamers (see **Fig. 8**) onto a supercoiled plasmid bearing the *PHO5* locus via salt gradient dialysis (2.8.2). At 2 M salt of the initial salt gradient dialysis buffer conditions octamers are present in a stable conformation. Slow dilution to 50 mM salt disrupts the octamers and leads first to the assembly of H3/H4 tetramers along the DNA, which is completed by the subsequent incorporation of H2A/H2B dimers.
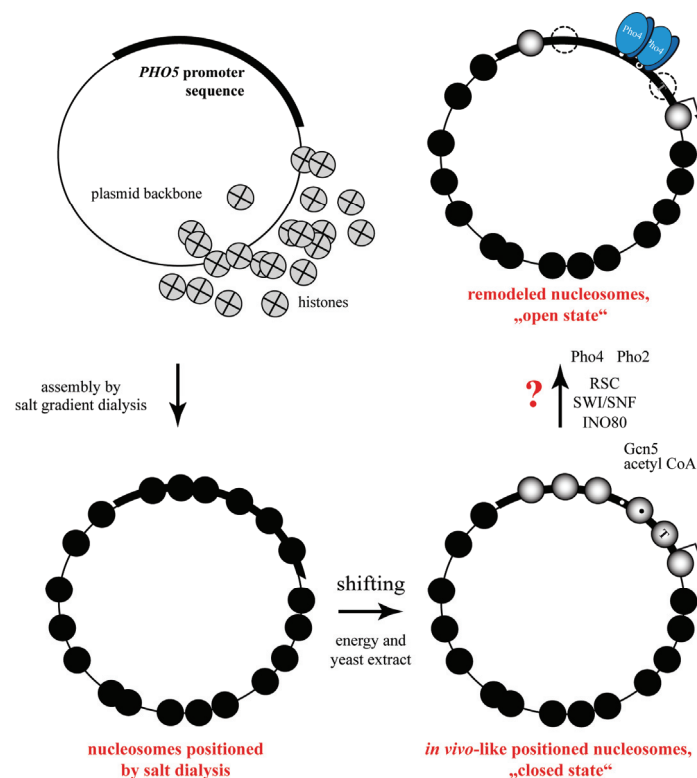
Fig. 16 Scheme of *in vitro* reconstitution of *PHO5* promoter chromatin. Plasmid harboring the *PHO5* sequence was reconstituted with histones by salt gradient dialysis. Nucleosomes were assembled onto the plasmid but did not adopt *in vivo*-like positions. Upon addition of yeast extract and energy the promoter nucleosomes were shifted to their *in vivo*-like positions also called the "closed state" or nucleosome positioning corresponding to the repressed state. Remodeling the promoter chromatin template by supplementation with cofactors led to remodeled nucleosomes or the "open state".

Preparing a large batch of salt gradient dialysis chromatin allowed side-by-side comparisons because the chromatin could be stored over longer periods and experiments were performed using the same starting material. During salt gradient dialysis the nucleosomes assembled onto the plasmid but did not adopt *in vivo*-like positions at the *PHO5* promoter. A standard "*in vitro* shifting reaction" was

performed by adding yeast whole cell extract and an energy regenerating system to chromatin reconstituted by salt gradient dialysis leading to *in vivo*-like positioned nucleosomes as in the repressed state (**Fig. 16**) (Hertel et al. 2005). As addition of yeast whole cell extract *in vitro* did not induce remodeling of the promoter nucleosomes into a hypersensitive site corresponding to the induced state *in vivo*, we were able to test the effects of additional purified cofactors and could directly analyze their impact on remodeling. Promoter nucleosomes were remodeled (2.8.3) by addition of the transactivators Pho4 and Pho2 (**Fig. 9**). Additionally, the remodeling system could be supplemented with remodeling machines like RSC, SWI/SNF and INO80 or the HAT Gcn5 or cofactors like acetyl CoA to test their effect on promoter chromatin remodeling.

3.1.3   Pho4- and energy-dependent remodeling of pre-assembled positioned nucleosomes into a hypersensitive site *in vitro* at the *PHO5* but not at the *PHO8* promoter

Shifting salt gradient dialysis chromatin with yeast extract and an energy regenerating system (**Fig. 16**) established *PHO5* promoter chromatin resembling the repressed state (**Fig. 17**A, lanes 1-2) (Hertel et al. 2005). As Pho4 shuttles between the nucleus and the cytoplasm depending on its phosphorylation status and as the chromatin assembly system uses yeast whole cell extract, it might have been possible that cytosolic Pho4 was able to induce chromatin remodeling at the *PHO5* promoter *in vitro*. Since we wanted to recapitulate the chromatin remodeling mechanism from the repressed promoter state onwards, i.e. assemble the positioned nucleosomes in the repressed state, we used yeast extracts from a *pho4 pho2 cbf1* triple mutant (Hertel et al. 2005). This way factors known to bind at the *PHO5* promoter region were excluded. Later experiments could show that this preventive measure was unnecessary as wild type extracts assembled the repressed promoter state as well (C. Wippo, data not shown). Presumably, the yeast whole cell extract has a very low concentration of endogenous Pho4.

We tested if adding recombinant Pho4 to such chromatin with properly pre-positioned nucleosomes led to a more open chromatin organization as in the *de novo* chromatin assembly experiment. Indeed, we observed a prominent hypersensitive site reaching from the -2 into the -4 nucleosome (**Fig. 17**A, lanes 6-8). This pattern differed clearly from the positioned nucleosomes without Pho4 (compare **Fig. 17**A, lanes 1-2 and lanes 6-8) and was similar to the above described remodeled region in *de novo* assemblies. Therefore Pho4 was able to trigger remodeling of already positioned nucleosomes *in vitro*. The hypersensitive site was not observed when ATP was removed from the reaction by incubation with apyrase prior to the addition of Pho4 (**Fig. 17**A, lanes 3-4). This argued on the one hand for a transcription factor-induced hypersensitivity that is not just due to Pho4 binding and on the other hand for the activity of ATP-dependent chromatin remodeling factors that are present in the yeast extract.

In addition to Pho4, a second transcription factor, Pho2, is known to play a role in activation of the *PHO5* promoter *in vivo*. The phosphorylation sites of Pho4 not only influence the nuclear import

and export but can also prevent interaction with Pho2 *in vivo* (Komeili and O'Shea 1999). As it is known that the cooperative interaction of both transcription factors is important for Pho4 binding and transactivation (Barbaric et al. 1998), we wanted to increase the remodeling potential in our *in vitro* assembly reaction by adding Pho2 as well. We had to make sure that both transcription factors would be able to interact with each other. Considering that the yeast whole cell extract might contain kinases that would be able to phosphorylate Pho4, the Pho4 mutant Pho4-SPA6 was used. Pho4-SPA6 cannot be phosphorylated at the site which mediates the interaction with Pho2 (**Fig. 5**) (Springer et al. 2003). Nevertheless, this turned out to be dispensable as further experiments generated very similar hypersensitive sites using either wild type Pho4 or Pho4-SPA6 (compare **Fig. 18**A, lanes 6-7 with Pho4 wt vs. **Fig. 28**A, lane 9 with Pho4-SPA6). Thus the word Pho4 is used for wild type and mutant Pho4 in the remainder of the thesis.
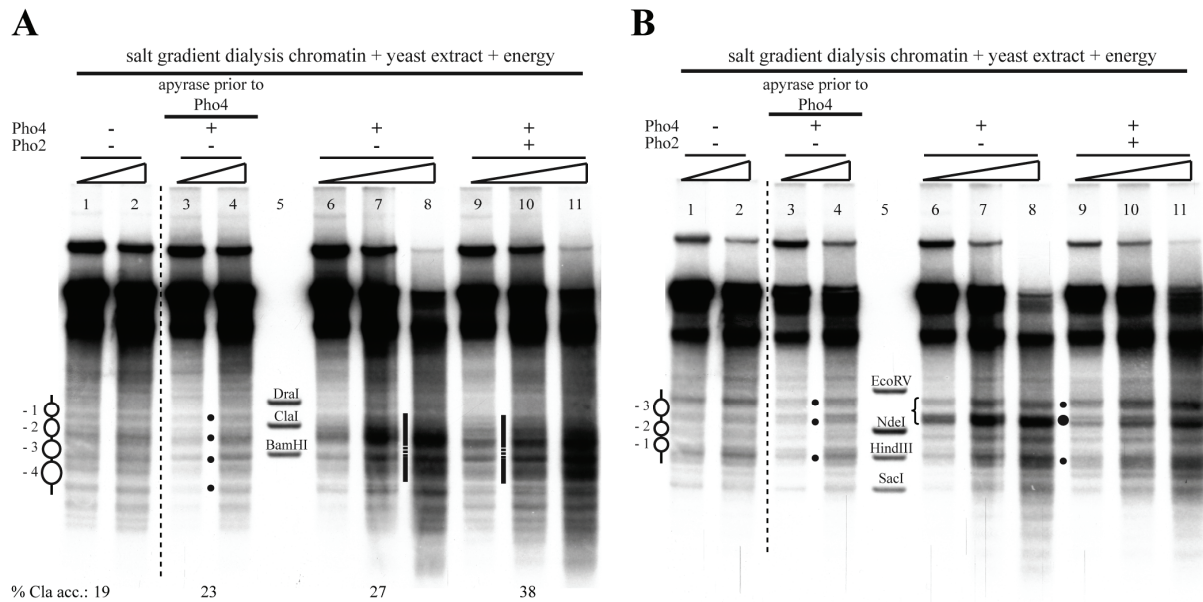
Fig. 17 Pho4- and energy-dependent remodeling of pre-positioned nucleosomes at the *PHO5*, but hardly any Pho4-induced chromatin remodeling at the *PHO8* promoter *in vitro*. (A) DNaseI indirect end-labeling analysis of the chromatin structure at the *PHO5* promoter. Chromatin was treated as indicated after pre-assembly by salt gradient dialysis and incubation with yeast extract in the presence of energy. The schematic on the left shows positioned nucleosomes and is analogous to the schematic of the *PHO5* promoter in **Fig. 7**A. Black dots in-between lanes highlight the bands corresponding to the linker regions between the positioned nucleosomes. Vertical bars in-between lanes mark the hypersensitive region generated by the addition of Pho4, or Pho4 and Pho2, respectively. The stippled region interrupting the vertical bar stands for an area that is protected from DNaseI. Ramps on top of the lanes designate increasing DNaseI concentrations. Marker fragments were generated by double digests of DraI, ClaI and BamHI each with ApaI. All samples were electrophoresed alongside in the same gel. Stippled lines in-between lanes show where lanes were moved next to each other using Adobe Photoshop CS2. Values below the gel correspond to % ClaI-accessibility. (B) Same blot as in panel A but rehybridized for the *PHO8* promoter region. Schematic on the left denotes nucleosomes as in the schematic of the *PHO8* promoter in **Fig. 7**B. Dots in-between lanes mark the hypersensitive domains characteristic for the *PHO8* promoter chromatin pattern of the repressed state. Larger dots mark the increased sensitivity of the region corresponding to the UASp2 Pho4 binding site. Bracket indicates the hypersensitive region that occurs upon induction *in vivo*. Ramps on top of the lanes stand for increasing DNaseI concentrations. Marker fragments were generated by double digests of EcoRV, NdeI, HindIII and SacI each with BglII.

Pho2 was added to the remodeling reaction *in vitro* in almost stochiometric amounts (0.7:1) relative to Pho4. This resulted in a nearly unchanged DNaseI nucleosomal pattern (**Fig. 17**A, lanes 9-11) which indicated that Pho2 addition makes no difference.

A second method to analyze remodeling of *PHO5* promoter chromatin is the restriction enzyme digest with ClaI. The recognition sequence of ClaI is covered by nucleosome -2 in the repressed state and is accessible in the remodeled state of *PHO5* promoter chromatin (**Fig. 7**A). As the digestion with ClaI is done exhaustively, in contrast to digesting the chromatin with limiting amounts of DNaseI and indirect end-labeling, this method gives quantitative information about the degree of remodeling of the total population of chromatin templates (Almer et al. 1986; Gregory et al. 1999a). Earlier *in vivo* experiments showed a 10-20% ClaI-accessibility at the repressed and 70-90% ClaI-accessibility at the induced *PHO5* promoter (Almer et al. 1986). The *in vitro* chromatin preparations that were analyzed by DNaseI digest were also subjected to the ClaI-accessibility assay (**Fig. 17**A, below the blot). There was a significant increase in ClaI-accessibility from 19% of the closed *PHO5* promoter pattern (**Fig. 17**A, lanes 1-2) to 27% of chromatin treated with Pho4 (**Fig. 17**A, lanes 6-8) in the presence of energy. Adding Pho4 together with Pho2 led to an even higher ClaI-accessibility value of 38% (**Fig. 17**A, lanes 9-11). Addition of Pho4 after energy depletion did not change the ClaI-accessibility considerably (23%, **Fig. 17**A, lanes 3-4). Taken together, the occurrence of the DNaseI hypersensitive site and the significant increase in ClaI-accessibility pointed to an activator- and energy-dependent remodeling of pre-positioned nucleosomes at the *PHO5* promoter *in vitro*.

During salt gradient dialysis, two different plasmids were used in equimolar amounts in the same dialysis tube. One contained the *PHO5* and the other the *PHO8* locus. This way it was possible to compare the various chromatin states at these two different promoters simultaneously. The membrane showing the DNaseI indirect end-labeling pattern of the *PHO5* promoter just had to be stripped from the *PHO5* promoter probe and re-hybridized with the *PHO8* promoter probe.

The *PHO8* promoter chromatin could also be properly assembled by the addition of yeast extract and an energy regenerating system (**Fig. 17**B, lanes 1-2) as previously shown (Hertel et al. 2005). The same nucleosomal pattern was observed when the *in vitro* system was depleted of energy before Pho4 addition (**Fig. 17**B, lanes 3-4). *In vivo* it is known that the distinct positions of the nucleosomes at the uninduced *PHO8* promoter give rise to a hypersensitive site upon induction (Barbaric et al. 1992). We wondered if the addition of recombinant Pho4 to our *in vitro* assembly system would generate this hypersensitive site as well. However, addition of the transcription factor in the presence of energy caused only an increase in the intensity of the band corresponding to the position of UASp2 (**Fig. 17**B, lanes 6-7, larger dot). This suggested that Pho4 recognized its binding site and caused at the same time some increase in hypersensitivity between nucleosomes -2 and -3. There was no hypersensitivity detected that would correspond to the region highlighted by the bracket (**Fig. 17**B, lane 6), which indicates the region that is subject to remodeling at the induced *PHO8* promoter *in vivo*. Supplementing the *in vitro* reaction with Pho2 did not change the nucleosomal pattern that was already generated by

Pho4 only (**Fig. 17**B, lanes 9-11). This was expected as Pho2 does not have binding sites along the *PHO8* promoter. The *PHO8* promoter chromatin data stand in striking contrast to the *in vitro* remodeling data of the *PHO5* promoter, arguing that the remodeling power at the *PHO8* promoter was much lower than observed *in vivo*.

3.1.4   Pho4-induced remodeling at the *PHO5* promoter *in vitro* resembled the pattern observed *in vivo*

We compared the similarity of the *in vivo PHO5* promoter pattern of uninduced (+P$_i$) and induced (-P$_i$) cells with our *in vitro* generated chromatin states (**Fig. 18**A). The nucleosomal pattern of the repressed state was similar (**Fig. 18**A, lanes 1-2) to the one we obtained *in vitro* with chromatin that was energy-depleted before Pho4 addition and therefore corresponded to the closed *PHO5* promoter (**Fig. 18**A, lanes 3-4, compare also to the schematic on the left). Induced *in vivo* cells showed a hypersensitive site from the -2 to the -4 nucleosome (**Fig. 18**A, lanes 8-9). The same area was affected in the *in vitro* pattern after addition of Pho4 (**Fig. 18**A, lanes 6-7), i.e. the upper and lower boundary of the hypersensitive part in the lanes were the same.
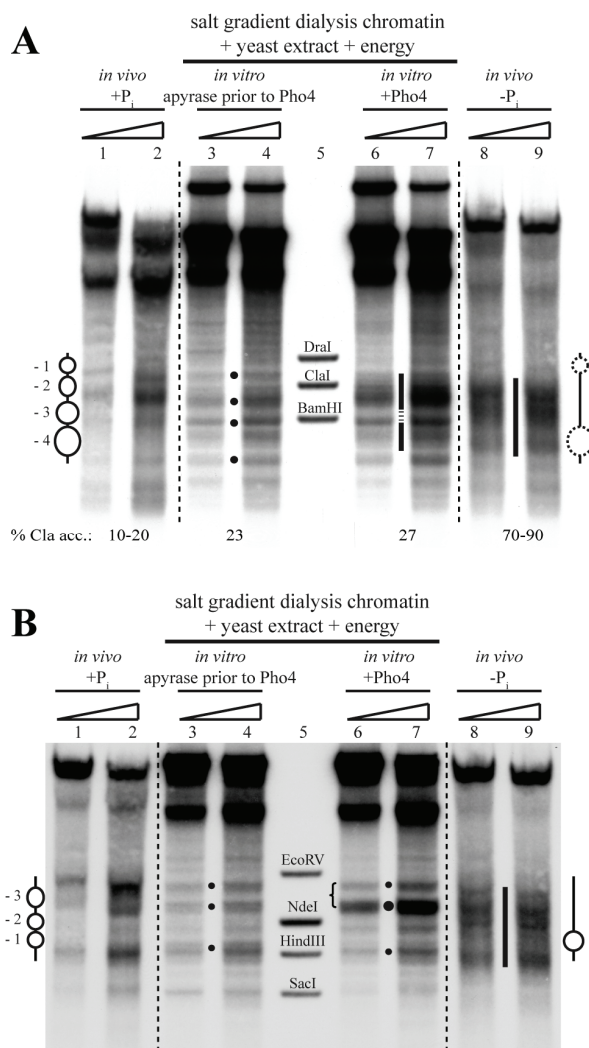
Fig. 18 Pho4-induced remodeling at the *PHO5* promoter *in vitro* was similar to, but less extensive than *in vivo*. *PHO8* promoter remodeling *in vitro* did not resemble the *in vivo* situation. (A) Reproduction as in **Fig. 17**A but with *in vivo* samples from wild type strain CY337 corresponding to the repressed (+P$_i$) and induced (-P$_i$) state of the *PHO5* promoter electrophoresed alongside to *in vitro* samples. Vertical bars highlight the *in vitro* hypersensitive region that is interrupted by a short stippled stretch at a position of DNA protection that is fully accessible in the induced state *in vivo*. See **Fig. 17**A for description of dots, bars, ramps, marker bands and ClaI-accessibility values. (B) Same blot as in panel A but re-hybridized for the *PHO8* promoter. See **Fig. 17**B for description of dots, bracket and marker bands. Schematics on the right show the remodeled *PHO5* and *PHO8* promoters (**Fig. 7**A and B).

However, the *in vitro* pattern showed more distinct bands within the hypersensitive region and a protected part above the BamHI marker band (stippled region in vertical bar) which differed from the rather homogeneous hypersensitive site *in vivo*. On the one hand this could imply that the *in vitro* remodeling reaction was not totally like *in vivo* and on the other hand that the nucleosomal pattern reflected chromatin subpopulations of differently remodeled states.

As mentioned above, ClaI restriction enzyme accessibility was measured to quantitatively compare the remodeling efficiency of *in vivo* and *in vitro* chromatin. The ClaI-accessibility of the closed *PHO5* promoter chromatin *in vitro* of 23% was very similar to the 10–20% ClaI-accessibility of uninduced *in vivo* cells. The significantly higher ClaI-accessibility upon addition of Pho4 of 27% (or 38% upon addition of Pho4 and Pho2, **Fig. 17**A) did not reach the *in vivo* ClaI-accessibility of 70-90%.

Side by side comparison of the closed nucleosomal pattern of the *PHO8* promoter *in vivo* (**Fig. 18**B, lanes 1-2) and *in vitro* (**Fig. 18**B, lanes 3-4) showed the identical and typical arrangement of the three nucleosomes in both cases. But *in vitro* addition of Pho4 and energy did not lead to a pattern that resembled the induced *PHO8* promoter *in vivo* (**Fig. 18**B, lanes 6-7 and 8-9). As noted above (**Fig. 17**B), it resembled the closed pattern almost as if no Pho4 had been added, besides a slight increase in the hypersensitive site in the DNaseI pattern matching the UASp2 Pho4 binding site (**Fig. 18**B, lanes 8-9).

All in all, *in vitro* activator- and energy-dependent remodeling at the *PHO5* promoter induced hypersensitivity in the same area as *in vivo*, resulting in higher ClaI-accessibility, but less extensively. Surprisingly, remodeling of *PHO8* promoter chromatin was not achieved *in vitro* by Pho4 addition.

3.2   Factors that could have improved remodeling

3.2.1   Supplementing the yeast extract with remodelers

Was remodeling *in vitro* less efficient because remodeling activities were limiting in the yeast whole cell extract? We used our *in vitro* assembly system to assess the role of remodeling complexes.

We added yeast extract and energy to salt gradient dialysis chromatin for 2 h and then added Pho4 and Pho2 for another hour. The remodeling extent of this standard reaction was compared to reactions that were supplemented with RSC or SWI/SNF or both chromatin remodeling complexes during the incubation with Pho4 and Pho2 (**Fig. 19**A). Both remodelers were good candidates as SWI/SNF has an important role in *PHO5* promoter chromatin remodeling *in vivo* (Neef and Kladde 2003; Barbaric et al. 2007), and RSC, with the essential ATPase Sth1 is known to disassemble nucleosomes with the help of chaperones (Cairns et al. 1996; Lorch et al. 2006).

The DNaseI hypersensitive region at the *PHO5* promoter after Pho4 and Pho2 addition (**Fig. 19**B, lanes 1-3) was similar, although it appeared lighter in this particular blot compared to the one seen in **Fig. 17**A, and the ClaI-accessibility of 50% was comparatively high. Its extent did not change significantly upon addition of RSC or SWI/SNF (**Fig. 19**B, lanes 5-7 and lanes 9-11) or both complexes together (**Fig. 19**A, lanes 13-15). Substituting the reaction with exogenous RSC did slightly increase the ClaI-accessibility from 50% to 55-57% (**Fig. 19**B, below the blot). No effect was observed when complementing the yeast extract with SWI/SNF only; the ClaI-accessibility remained constant at 49% (**Fig. 19**B, below the blot).

At the *PHO8* promoter there was no additional effect upon addition of the remodelers (**Fig. 19**C). This was rather unexpected, since *PHO8* is strictly Snf2-dependent *in vivo* (Gregory et al. 1999b).
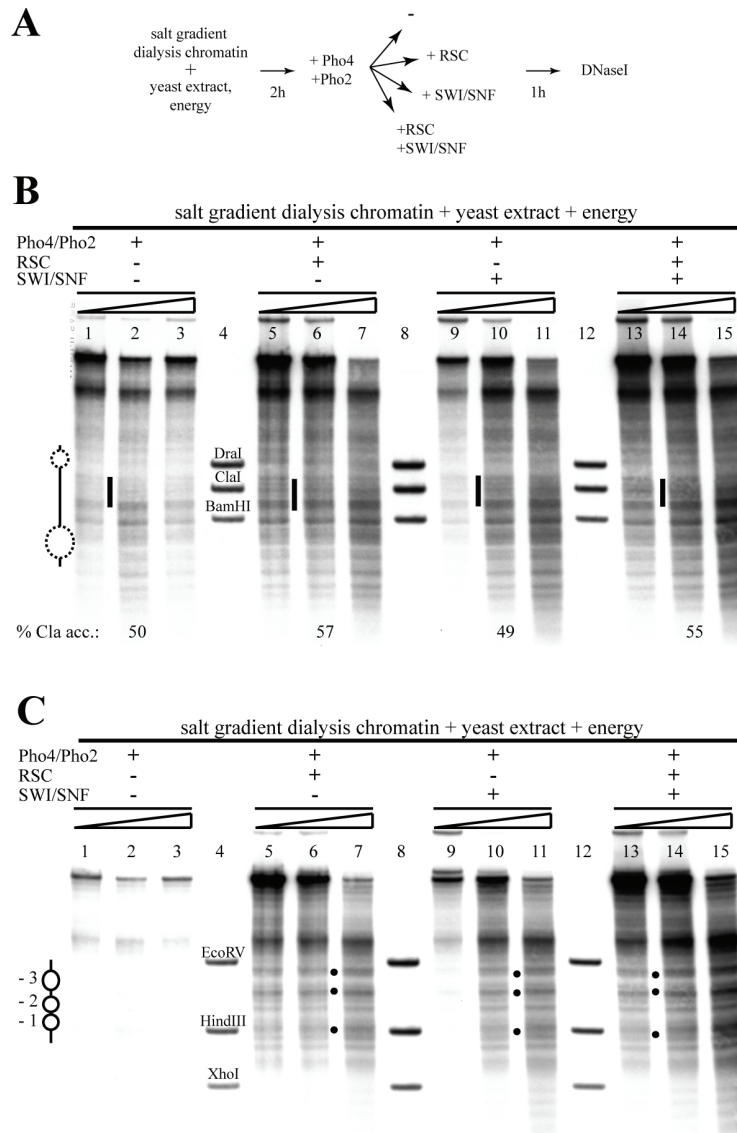
Fig. 19 The extent of remodeling was not significantly affected by supplementing the yeast extract with chromatin remodeling enzymes *in vitro*. (A) Experimental scheme: salt gradient dialysis chromatin was incubated with yeast extract and energy for 2 h. In addition to Pho4 and Pho2, RSC, SWI/SNF, both or no remodeler was added to the reaction. (B) DNaseI indirect end-labeling analysis of the chromatin structure at the *PHO5* promoter. Chromatin was treated as indicated after pre-assembly by salt gradient dialysis and incubation with yeast extract in the presence of energy. The vertical bars highlight the hypersensitive region generated by the addition of the different factors. See **Fig. 17**A for description of ramps, marker bands and ClaI-accessibility values. (C) Same blot as in panel B but re-hybridized for the *PHO8* promoter region. See **Fig. 17**B for description of dots and ramps. Marker fragments were generated by double digests of EcoRV, HindIII and XhoI each with BglII.

Taken together, complementing the yeast extract with the remodeling complexes RSC and SWI/SNF did not increase the remodeling extent at both promoters as judged by DNaseI digestion and indirect end-labeling. RSC caused a modest increase in ClaI-accessibility at the *PHO5* promoter whe-

reas SWI/SNF could not trigger *PHO8* promoter remodeling although it is known to be essential for *PHO8* promoter chromatin remodeling *in vivo*.

3.2.2 *PHO5* promoter chromatin remodeling was enhanced if Pho4 was added together with the yeast extract

The standard *in vitro* shifting reaction re-localized the nucleosomes of salt gradient dialysis chromatin to positions of the repressed state of the *PHO5* and *PHO8* promoters (3.1.2 and 3.1.3). So far, the transcription factors were added after this nucleosome shift to the closed promoter pattern. We asked if the extent of remodeling would increase in the *in vitro* system by adding the transcription factors simultaneously with the extract and energy to the salt dialysis chromatin template. This way a potential binding competition between Pho4 and nucleosome -2 could take place.
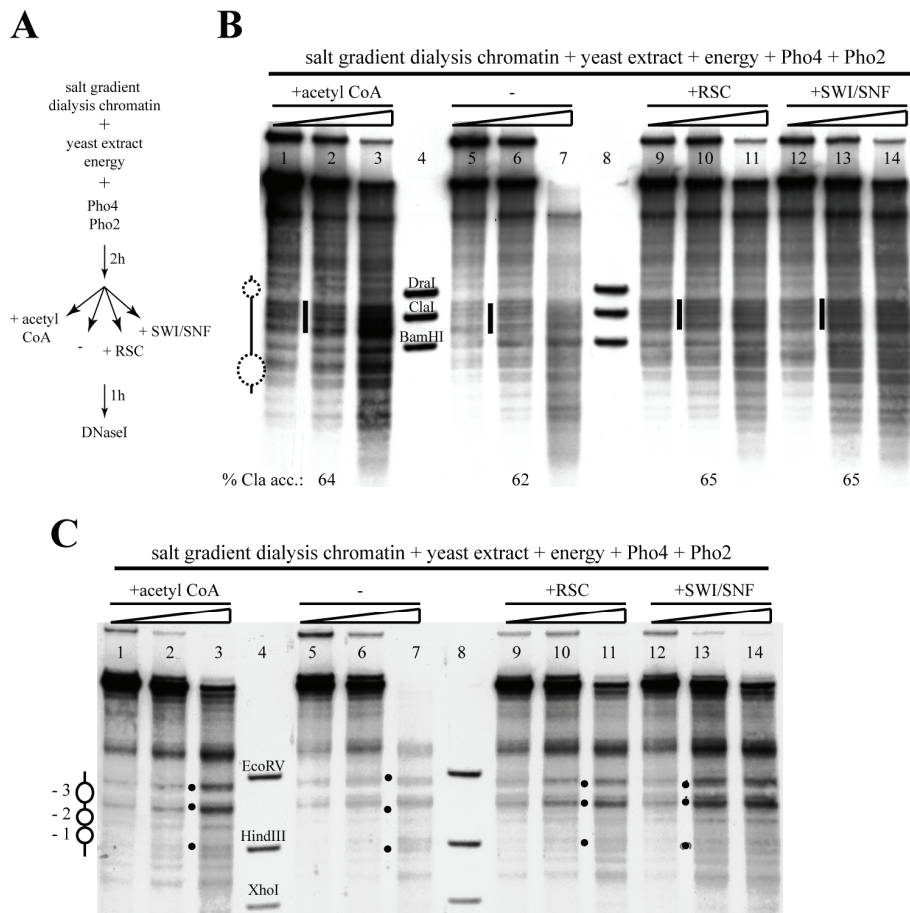
Fig. 20 *In vitro* nucleosome remodeling was slightly enhanced by changing the order of addition of the transcription factors. (A) Experimental scheme: salt gradient dialysis chromatin was incubated with yeast extract, energy, Pho4 and Pho2 for 2 h. Subsequently acetyl CoA (40mM), RSC or SWI/SNF were added to the reaction. (B) DNaseI indirect end-labeling analysis of the chromatin structure at the *PHO5* promoter. Chromatin was treated as indicated after pre-assembly by salt gradient dialysis and incubation with yeast extract, energy, Pho4 and Pho2. The vertical bars highlight the hypersensitive region. See Fig. 17A for description of ramps, marker bands and ClaI-accessibility values. (C) Same blot as in panel B but re-hybridized for the *PHO8* promoter region. See **Fig. 17**B for description of dots and ramps. Marker fragments were generated by double digests of EcoRV, HindIII and XhoI each with BglII.

Salt gradient dialysis chromatin was incubated at the same time with yeast extract, energy, Pho4 and Pho2 (**Fig. 20**A). A similar hypersensitive site at the *PHO5* promoter was observed as before but the region did not enlarge (**Fig. 20**B, lanes 5-7). Surprisingly, the accessibility of the ClaI site became significantly higher and started at 62% for chromatin treated with extract, energy and transcription factors at the same time. This almost resembled the *in vivo* situation of induced cells (70-90%). The extent of remodeling also in this experimental scheme was not further enhanced by the addition of acetyl CoA, RSC or SWI/SNF and showed only slightly higher ClaI-accessibility values of around 65% (**Fig. 20**B).

In contrast, *PHO8* promoter chromatin did not respond with increased remodeling to any of the above mentioned treatments using acetyl CoA, RSC or SWI/SNF (**Fig. 20**C).

Obviously, there was an enhancing effect on *PHO5* promoter chromatin remodeling when the transcription factors participated right from the start in the *in vitro* remodeling reaction, prior to positioning the nucleosomes into the closed pattern. This speaks for binding of Pho4/Pho2 to UASp2 which prevents this region to be occupied by nucleosome -2. The transcription factors prevailed in the binding competition and inhibited nucleosomal occupancy in contrast to the previous remodeling reactions in which Pho4/Pho2 had to open or remodel the -2 nucleosome that had already been positioned by the yeast extract. In contrast, *PHO8* promoter chromatin remodeling was not affected probably due to the fact that it has no intranucleosomal binding site for Pho4.

3.2.3 Effects of acetyl CoA

Histone acetylation is important for the mechanism that leads to *PHO5* and *PHO8* promoter chromatin remodeling   (Gregory et al. 1998b; Barbaric et al. 2001; Nourani et al. 2004; Williams et al. 2008; Wippo et al. 2009). Therefore we tested the impact of acetylation on remodeling *in vitro* by adding exogenous acetyl CoA and Gcn5. To control to which degree the histones incorporated in the salt gradient dialysis chromatin could be acetylated, we performed a histone acetyltransferase filter binding assay.

Equal histone amounts of octamers or salt gradient dialysis chromatin were incubated for 30 min with or without recombinant Gcn5 and tritium labeled acetyl CoA. Yeast extract was titrated into the system at the same time to estimate the effect of HATs and HDACs from the extract. Octamers were easily acetylated by Gcn5 whereas salt gradient dialysis chromatin was acetylated to a lesser extent, although clearly above background (compare **Fig. 21**, columns 1-3). Adding yeast extract to chromatin without Gcn5 increased acetylation (**Fig. 21**, column 4) speaking for HAT activity in the extract. Combining chromatin, Gcn5 and increasing amounts of yeast extract resulted in a higher acetylation level at lower and decreasing levels with increasing concentrations of yeast extract (**Fig. 21**, columns 4-8) arguing for either HAT inhibiting and/or HDAC activities in the extract.
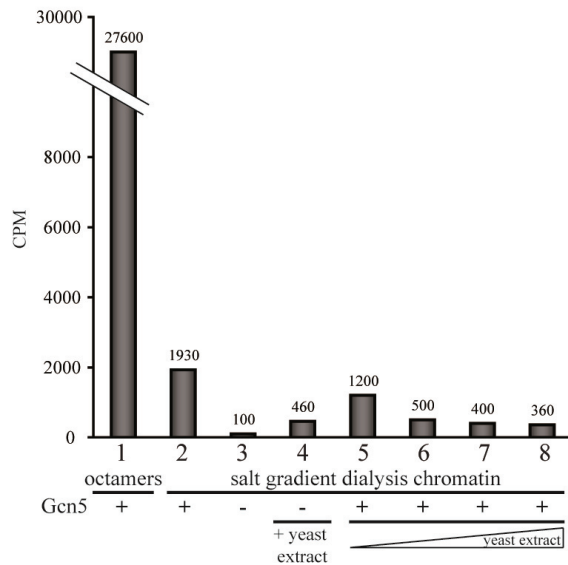
Fig. 21 Salt gradient dialysis chromatin is acetylated by Gcn5 *in vitro*. Histone acetyltransferase (HAT) assay using similar histone amounts of *Drosophila* embryo octamers or salt gradient dialysis chromatin. The substrates were incubated with [^{3}H] acetyl CoA and with or without Gcn5 and/or yeast extract (column 4: 6μl yeast extract, columns 5-8: 3, 6, 8, 36 μl yeast extract, respectively).

We tested how acetylation levels of histones or salt gradient dialysis chromatin pre-incubated with Gcn5 and acetyl CoA were affected under conditions of a standard *in vitro* assembly and shifting reaction. Octamers or chromatin and tritium labeled acetyl CoA were incubated in the presence or absence of Gcn5 for 1 h. Half of the reaction was quenched and the other half was treated with yeast extract, energy, Pho4, Pho2 and the HDAC inhibitor trichostatin-A (TSA) for 2 h.
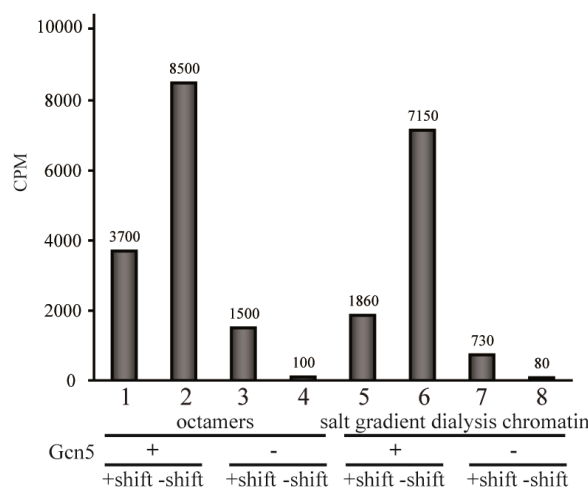
Fig. 22 Acetylation of histones in the context of a complete *in vitro* remodeling reaction. HAT assay as described in **Fig. 21** but using an up-scaled amount of ingredients to directly compare this assay to the *in vitro* remodeling assays described before. Chromatin, extract, energy and transcription factor amounts were the same as in all other *in vitro* shifting and remodeling reactions. Similar histone amounts of *Drosophila* embryo octamers or salt gradient dialysis chromatin, incubated with [^{3}H] acetyl CoA and with or without Gcn5 and with or without (+/- shift) the nucleosome shifting buffer containing energy, an energy regenerating system, yeast extract, Pho4, Pho2 and trichostatin-A (HDAC inhibitor) (**Fig. 21**).

Acetylation levels were always higher when Gcn5 was included (**Fig. 22**, compare columns 1-2 vs. 3-4 and 5-6 vs. 7-8), although factors in the yeast extract alone were able to acetylate octamers as well as chromatin (**Fig. 22**, compare columns 3-4, 7-8). Octamers and chromatin showed a higher acetylation level without the yeast extract and energy regenerating system (**Fig. 22**, columns 1-2, 5-6).

All in all we confirmed increased histone acetylation by Gcn5 and activities endogenous to the extract via incorporation of labeled acetyl groups. We saw that octamers were a better substrate for acetylation by Gcn5 than chromatin which was already observed before (Eberharter et al. 1998). This is probably due to the fact, that chromatin is already neatly packed and the histone tails are not that accessible as in the case of the histone octamers. The yeast extract had a HAT activity of its own but higher amounts led to a decrease in acetylation levels. This could be due to counteracting HDACs in the extract or high amounts of proteins in the extract occluding the substrate and therefore diminishing the detection of acetylation.

With the knowledge that factors in the yeast extract were able to acetylate the histones of salt gradient dialysis chromatin we wondered if this acetylation would increase the remodeling in our *in vitro* system. A standard remodeling assay was performed with or without acetyl CoA. The DNaseI pattern of both the *PHO5* and the *PHO8* promoter showed no significant difference between acetyl CoA treated or untreated chromatin (**Fig. 23**A and B, lanes 2-4 and 5-7). The hypersensitive site at the *PHO5* promoter maybe seemed somewhat more pronounced, but the ClaI restriction values were rather unchanged with 41% versus 42% accessibility (**Fig. 23**A, below the blot).
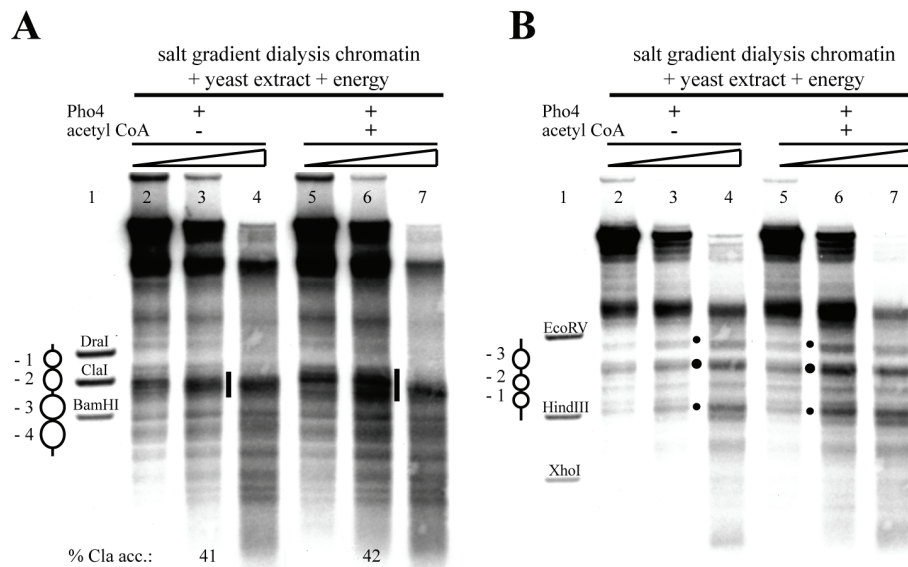
Fig. 23 Addition of acetyl CoA did not increase the extent of the hypersensitive region *in vitro*. (A) DNaseI indirect end-labeling analysis of the *PHO5* promoter region in chromatin after pre-assembly by salt gradient dialysis and incubation with yeast extract in the presence of energy and subsequent addition of Pho4 without (lanes 2-4) or with 40 µM acetyl CoA (lanes 5-7). See **Fig. 17**A for description of ramps, marker bands and ClaI-accessibility values. (B) Same blot as in panel A but re-hybridized for the *PHO8* promoter region. See **Fig. 17**B for description of dots and ramps. Marker fragments were generated by double digests of EcoRV, HindIII and XhoI each with BglII.

As mere addition of acetyl CoA did not significantly increase Pho4-induced remodeling (**Fig. 23**), the *in vitro* assembly protocol was altered to include a pre-incubation step of salt gradient dialysis chromatin with Gcn5 and acetyl CoA. Parallel control reactions contained no Gcn5 or acetyl CoA. Chromatin of a higher assembly degree (relative amount histones to DNA = 1.2:1) than normal was used to check the remodeling power on tightly packed chromatin (see assembly degree in 2.8.2).

The pre-incubation step was followed by a standard shifting reaction. After 2 h the system was supplemented with or without Pho4 and Pho2 and 1 h later Ino80 or ACF1 was added to selected reactions. For unknown reasons, the closed *PHO5* promoter pattern was less clear in this particular experiment (**Fig. 24**A, lanes 4-5) and the hypersensitive region generated by addition of the transcription factors was less extensive as also reflected in only 29% ClaI-accessibility, probably due to the higher assembly degree (**Fig. 24**A, lanes 2-3). Pre-incubation with Gcn5 and acetyl CoA resulted in similar hypersensitivity (**Fig. 24**A, lanes 6-7), maybe a bit less pronounced without acetyl CoA (**Fig. 24**A, lane 8-9). Additional Ino80 or ACF had no effect (**Fig. 24**A, lanes 10-11, 13-14, and 15-16). Accor-

dingly, ClaI-accessibility values were around 30% in all cases where Pho4/Pho2 was included (**Fig. 24**A, below the blot).
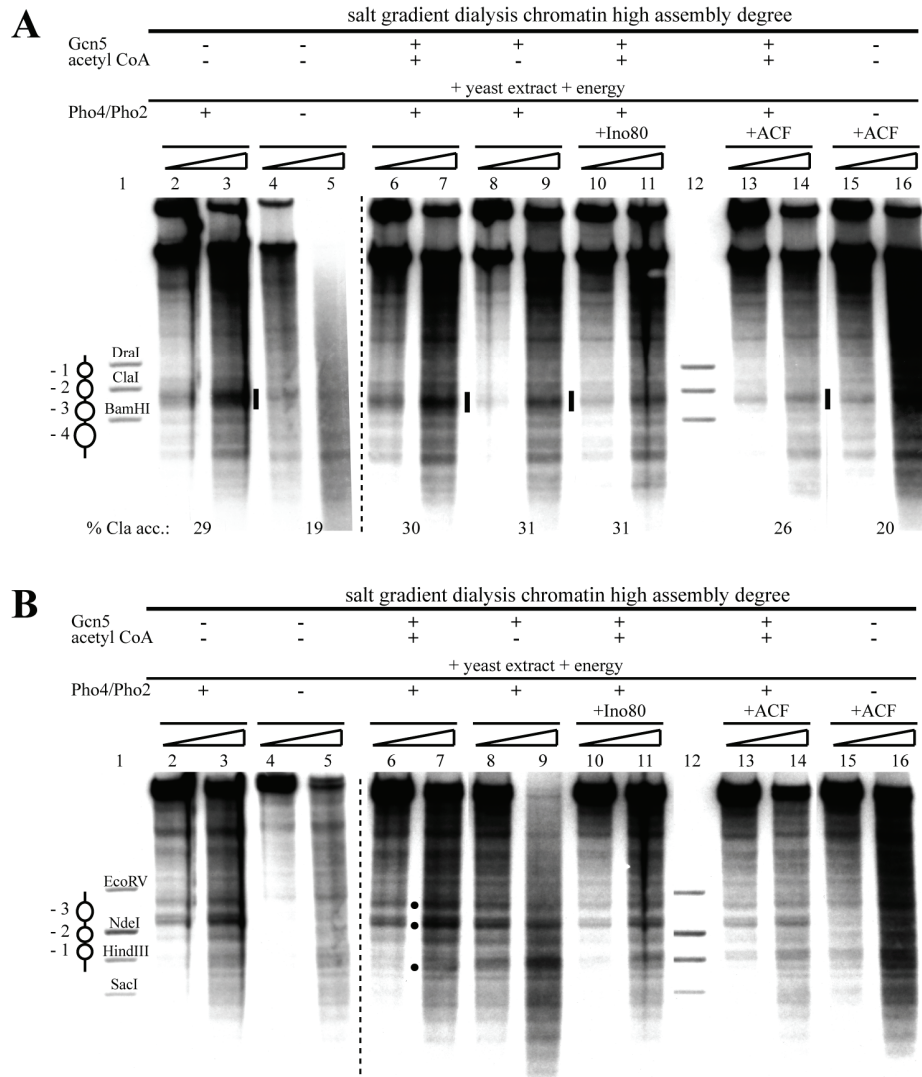
Fig. 24 Gcn5-dependent acetylation of *in vitro* chromatin could not extend the hypersensitive site at the *PHO5* and *PHO8* promoters. (A) DNaseI indirect end-labeling analysis of the *PHO5* promoter region in chromatin treated as indicated. Salt gradient dialysis chromatin of a high assembly degree was pre-incubated with or without Gnc5 and 40 µM acetyl CoA, respectively. Yeast extract in the presence of energy with or without Pho4 and Pho2 was added to the chromatin. The remodeling complexes Ino80 (lanes 10-11) and ACF (lanes 13-16) were added later to the reaction. The amount of ACF (kind gift from A. Eberharter, group of Peter Becker) and Ino80 (kind gift from S. Fenn, group of Karl-Peter Hopfner) that was added to the reaction was sufficient to remodel the equivalent chromatin mass of mononucleosomes. See **Fig. 17**A for description of ramps, marker bands and ClaI-accessibility values. (B) Same blot as in panel A but re-hybridized for the *PHO8* promoter region. See **Fig. 17**B for description of dots, ramps and marker bands.

The described experiments had no influence on remodeling of the *PHO8* promoter chromatin (**Fig. 24**B).

Although we could show that *in vitro* chromatin was acetylated by Gcn5 or by the yeast extract, we were not able to increase the extent of remodeling by supplementing the yeast extract with acetyl CoA or by pre-incubating the chromatin with acetyl CoA and Gcn5.

3.2.4 Influence of competitor DNA

In vitro assays analyzing nucleosome dissociation from DNA made additional use of so called acceptor or nonspecific competitor DNA (Workman and Kingston 1992). The negatively charged DNA is used to capture histones with loosened contacts to DNA due to remodeling activity to be newly deposited and reformed into nucleosomes.
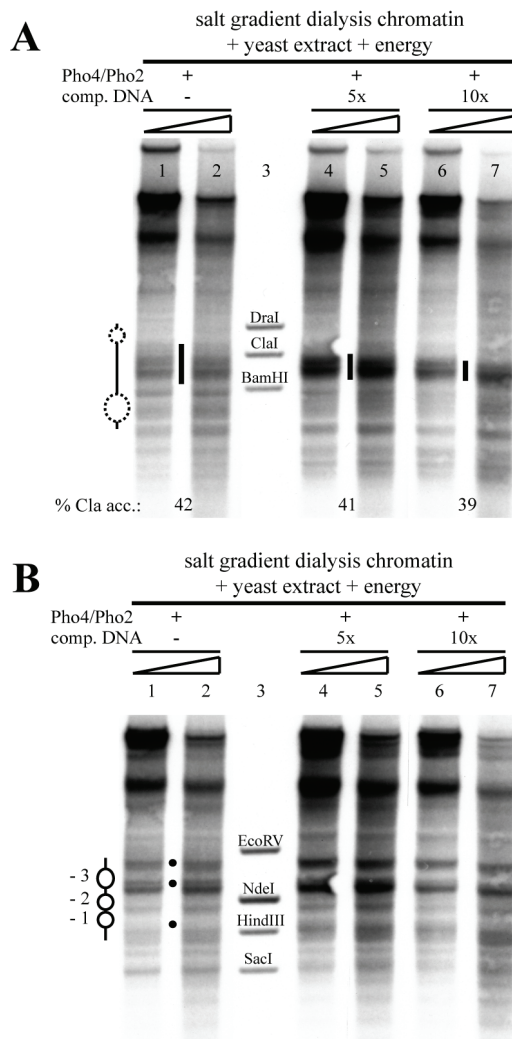
Fig. 25 Addition of competitor DNA did not result in a more extensive hypersensitive site at both promoters. (A) DNaseI indirect end-labeling analysis of the *PHO5* promoter region in chromatin treated as indicated after pre-assembly by salt gradient dialysis and incubation with yeast extract in the presence of energy. Pho4 and Pho2 without or with five and ten fold mass excess of salmon sperm DNA over chromatinized plasmid DNA were added to the reactions. See **Fig. 17**A for description of ramps, marker bands and ClaI-accessibility values. (B) Same blot as in panel A but re-hybridized for the *PHO8* promoter region. See **Fig. 17**B for description of dots, ramps and marker bands.

As we know that remodeling of *PHO5* and probably also of *PHO8* promoter chromatin proceeds by histone eviction in *trans* (Boeger et al. 2003; Reinke and Horz 2003; Boeger et al. 2004; Korber et al. 2004) and involves the histone chaperone Asf1 (Adkins et al. 2004; Korber et al. 2006), we tested the possibility that remodeling *in vitro* was limited by the capacity of histone acceptors in the extract. We titrated a five and ten fold mass excess of nonspecific DNA over chromatinized DNA into the standard remodeling reaction including Pho4 and Pho2 (**Fig. 25**). The intensity of the hypersensitive site at the *PHO5* promoter (**Fig. 25**A, lanes 1-2) increased with five times acceptor DNA but the affected region was smaller (**Fig. 25**A, lanes 4-5). Ten times competitor DNA reduced the hypersensitivity even further (**Fig. 25**A, lanes 6-7). The ClaI-accessibility was constant around 41% (**Fig. 25**A, below the blot). As addition of excess naked DNA is used to stop *in vitro* remodeling reactions by competing away remodeling activities (Langst and Becker 2001) it was possible that addition of competitor DNA abolished the remodeling power of our *in vitro* remodeling assay. Further, high amounts of unspecific DNA may have competed Pho4/Pho2 away from their specific binding sites. However, all this seemed not to be a problem, as Pho4 addition still yielded a clear hypersensitive site at the *PHO5* promoter and remodeling at the *PHO8* promoter showed the same increase in intensity upon addition of competitor DNA as without (**Fig. 25**B).

3.2.5 Use of different histone sources

The previously described experiments were all performed using endogenous histones from *Drosophila* embryos, and the results resembled the *in vivo* situation remarkably well. But this heterologous and *ex vivo* source of histones might limit remodeling *in vitro*, e.g., by pre-existing modifications that could impair the recognition by factors from the yeast extract. An example is H4K20 dimethylation that was mapped in *Drosophila* embryo histones and is a modification not found in yeast (Bonaldi et al. 2004). Although histones are conserved from yeast to human, these histones could also have altered interaction interfaces for binding factors. The histone H3 amino acid sequence, for example, differs slightly between yeast and *Drosophila* (Garcia et al. 2007).
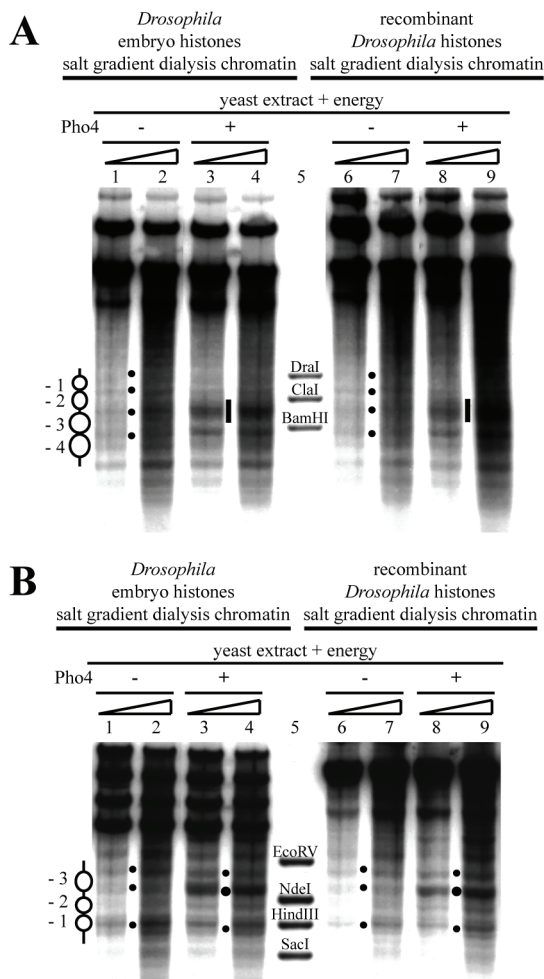
Fig. 26 Comparing endogenous and recombinant *Drosophila* histones in salt gradient dialysis chromatin did not result in different remodeling *in vitro*. (A) DNaseI indirect end-labeling analysis of the *PHO5* promoter region in chromatin treated as indicated after pre-assembly by salt gradient dialysis and incubation with yeast extract in the presence of energy. Salt gradient dialysis was performed using endogenous or recombinant *Drosophila* histones. See **Fig. 17**A for description of ramps and marker bands. (B) Same blot as in panel A but re-hybridized for the *PHO8* promoter region. See **Fig. 17**B for description of dots, ramps and marker bands.

To control for inhibiting modifications, we used recombinant *Drosophila* histones for chromatin reconstitution and compared the nucleosomal patterns of both promoters with chromatin made from *Drosophila* embryo histones (**Fig. 26**). The standard *in vitro* shifting reaction yielded the same closed nucleosomal pattern with both chromatin preparations (**Fig. 26**, lanes 1-2 and 6-7) and addition of Pho4 gave the already observed hypersensitive site (**Fig. 26**, lanes 3-4 and 8-9).

As recombinant yeast histones (**Fig. 8**) control both for modifications as well as for the concern of heterology, we repeated the experiments with recombinant yeast histones. In contrast to *Drosophila* embryo histones, the yeast histones were much more difficult to handle, i.e. it was difficult to obtain good DNaseI patterns of the closed *PHO5* promoter (**Fig. 27**A, lanes 1-2). This was reflected in 41% ClaI-accessibility that was much higher than the 19-23% observed before with *Drosophila* embryo histones (**Fig. 18**). Such difficulties in reconstituting yeast octamers into chromatin *in vitro* were observed by other groups as well (personal communication: Tom Owen-Hughes (University of Dundee, Dundee), Craig Peterson (University of Massachusetts Medical School, Worcester)). Nonetheless, the Pho4-induced hypersensitive site was very

similar as obtained with *Drosophila* embryo histones (**Fig. 27**A, lanes 4-5). Additional acetyl CoA (**Fig. 27**, lanes 7-8), acetyl CoA and RSC (**Fig. 27**, lanes 9-11), or even the combination of adding acetyl CoA, RSC and SWI/SNF (**Fig. 27**, lanes 13-15) did not make much of a difference. ClaI-accessibility reached up to 70% upon Pho4 addition (**Fig. 27**A, below the blot). However, it already started with 41% so it is not meaningful to equal this extent of remodeling to that seen *in vivo*.
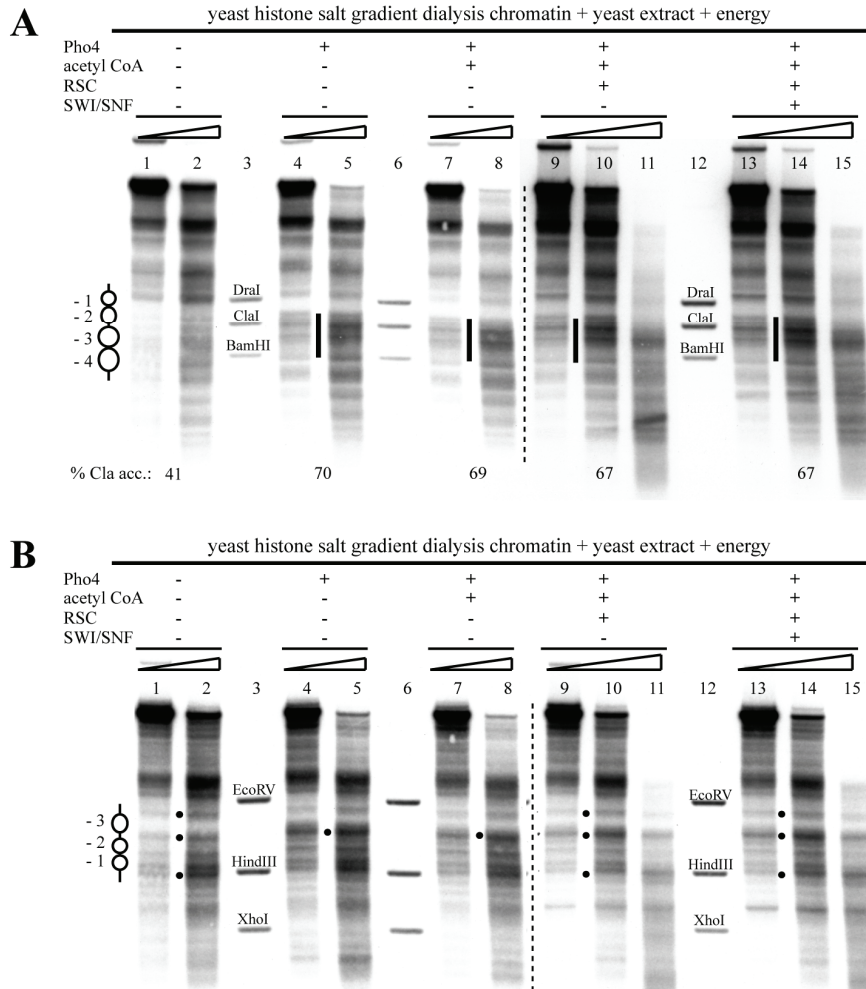
Fig. 27 Remodeling extent at the *PHO5* and *PHO8* promoters was not increased using recombinant *Saccharomyces cerevisiae* octamers in chromatin assembly. (A) DNaseI indirect end-labeling analysis of the *PHO5* promoter region in chromatin treated as indicated after pre-assembly by salt gradient dialysis and incubation with yeast extract in the presence of energy. Salt gradient dialysis was performed using recombinant *Saccharomyces cerevisiae* octamers. See **Fig. 17**A for description of ramps, marker bands and ClaI-accessibility values. (B) Same blot as in panel A but re-hybridized for the *PHO8* promoter region. See **Fig. 17**B for description of dots and ramps. Marker fragments were generated by double digests of EcoRV, HindIII and XhoI each with BglII.

The *PHO8* promoter showed similar nucleosomal patterns as in previous experiments with *Drosophila* embryo histones (**Fig. 27**B).

So the use of recombinant *Drosophila* or yeast octamers did not improve the system for both promoters, neither in the quality or reliability of the closed pattern nor in the extent of Pho4-induced chromatin remodeling.

3.2.6 Summary of *in vitro* chromatin remodeling results

In order to compare the different *in vitro* chromatin patterns at the *PHO5* and the *PHO8* promoter, representative samples of each state were loaded onto the same gel (**Fig. 28**). Each state was generated from the same preparation of salt gradient dialysis chromatin. Most samples loaded onto this summary gel correspond to lanes of *in vitro* shifting and remodeling reactions discussed in paragraphs 3.1.3-3.2.5.
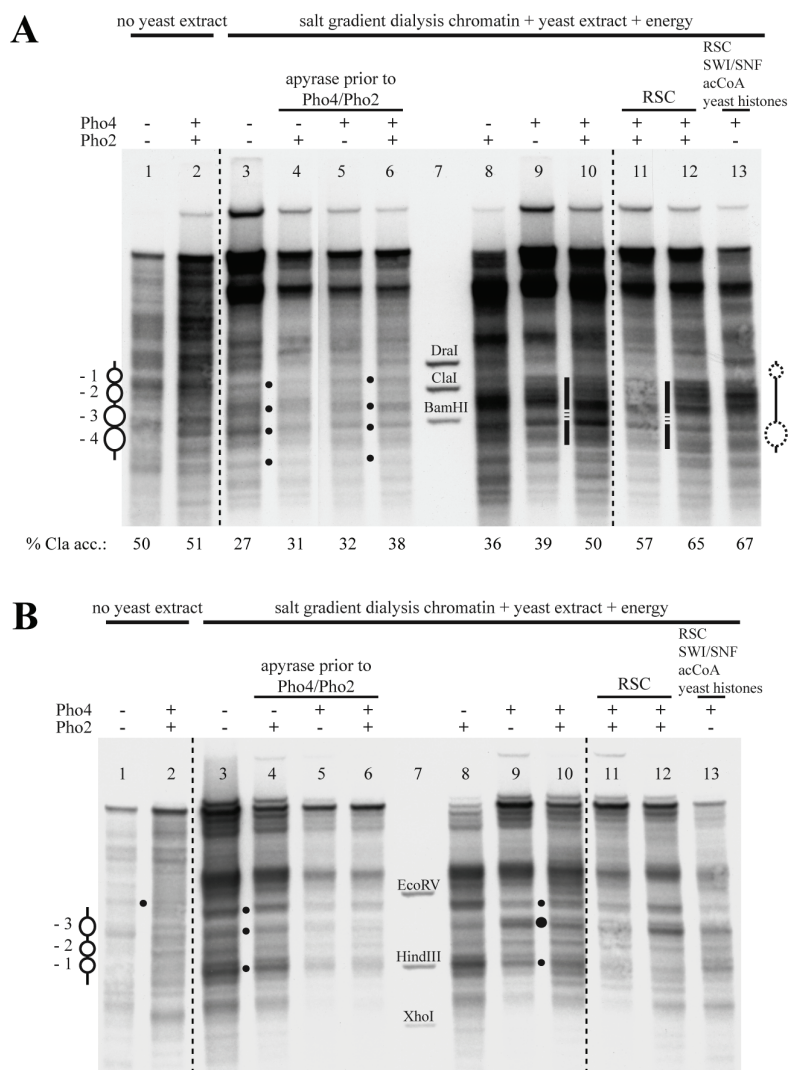
Fig. 28 *In vitro* **chromatin reconstitution and remodeling reactions: Remodeling of *PHO5* promoter nucleosomes into a hypersensitive site *in vitro*. No extensive remodeling at the *PHO8* promoter.** (A) DNaseI indirect end-labeling analysis of the *PHO5* promoter region in chromatin treated as indicated on top of the lanes after pre-assembly by salt gradient dialysis and incubation with yeast extract in the presence of energy. Lane 11: Pho4 and Pho2 were added after the salt gradient dialysis chromatin was incubated with yeast extract, lane 12: Pho4 and Pho2 were added together with the yeast extract. In all DNaseI mapping experiments a range of DNaseI concentrations was used, but due to space limitations only one representative concentration is shown for each condition. See **Fig. 17**A for description of dots, ramps, marker bands and ClaI-accessibility values. (B) Same blot as in panel A but re-hybridized for the *PHO8* promoter region. See **Fig. 17**B for description of dots and ramps. Marker fragments were generated by double digests of EcoRV, HindIII and XhoI each with BglII.

The DNaseI pattern of salt gradient dialysis chromatin (**Fig. 28**, lane 1) was unchanged by the addition of both transcription factors (lane 2), so their mere binding did not change the DNA accessi-

bility. The characteristic closed *PHO5* promoter chromatin pattern was generated by incubation of the salt gradient dialysis chromatin with yeast extract and energy (lane 3). This closed pattern did not change much when the system was depleted of energy by addition of apyrase prior to supplementation with Pho2, or Pho4, or both (lanes 4-6). Importantly, a hypersensitive site was generated in the presence of energy and Pho2, or Pho4, or both (lanes 8-10), although Pho2 alone had less of an effect and resulted only in increased hypersensitivity of the linker region between nucleosome -2 and -3 (lane 8). The remodeled pattern differed clearly from the closed promoter chromatin pattern (compare lane 6 and 10). Addition of RSC to the standard remodeling reaction failed to change the pattern (lane 11). Pre-incubation of chromatin together with extract, energy and Pho4/Pho2 and a subsequent addition of RSC could not increase the hypersensitive site any further (lane 12). Chromatin generated with yeast histones, shifted with extract and energy to the closed pattern, and then remodeled by addition of Pho4 with acetyl CoA, RSC and SWI/SNF (**Fig. 28**A, lane 13) also showed a similar hypersensitive site.

Hybridization of the same summary blot for the *PHO8* promoter showed analogous results regarding the closed pattern, but no extensive hypersensitivity in the presence of Pho4. The salt dialysis pattern without extract (**Fig. 28**, lane 1) again did not change upon addition of Pho4 and Pho2 only (lane 2), but was clearly different from chromatin treated with extract and energy (lane 3), representing repressed state *PHO8* promoter chromatin. The removal of energy prior to transcription factor addition did not change the pattern (lanes 4-6). The standard remodeling reaction led to a more pronounced hypersensitive site due to binding of Pho4 to UASp2 (lanes 9, 10) whereas addition of Pho2 alone showed the closed *PHO8* pattern (lane 8). Addition of RSC (lanes 11-12) or usage of yeast histones in chromatin assembly and supplementing the reaction with acetyl CoA, RSC and SWI/SNF (lane 13), as described for *PHO5*, did not change the pattern.

ClaI-accessibilities of chromatin states described in **Fig. 28** and above are summarized in **Fig. 29**. The salt gradient dialysis chromatin started with an accessibility of about 50%, independent of Pho4/Pho2 addition (**Fig. 29**, columns 1 and 2). In this experiment chromatin treated with yeast extract and energy (column 3) had about 30% ClaI-accessibility, but experiments shown in **Fig. 17** and **Fig. 18** showed even lower values of 19-23%. These values suggested that factors in the yeast extract use ATP to reposition a nucleosome over the ClaI site, pretty much as it probably happens *in vivo*. Addition of Pho2, or Pho4, or both transcription factors led to an increased ClaI-accessibility of 40-50% (columns 7-9). The respective ClaI-accessibilities of reactions depleted of energy before addition of Pho2 and/or Pho4 (columns 4-6) were always lower (compare columns 4 to 7, 5 to 8, and 6 to 9). Further addition of SWI/SNF, or RSC, or both remodelers (columns 10-12) led to a minor increase to 55%. Whereas pre-incubation of the chromatin with yeast extract and energy and both transcription factors led already to 60-65% accessibility, this was not further enhanced upon addition of acetyl CoA, or RSC, or SWI/SNF (columns 13-16). Chromatin assembled with yeast histones and treated with

extract and energy started already with higher ClaI-accessibilities of 41% (compare columns 17 to 3) that increased to 70% upon addition of Pho4, or Pho4 and acetyl CoA (columns 18, 19).
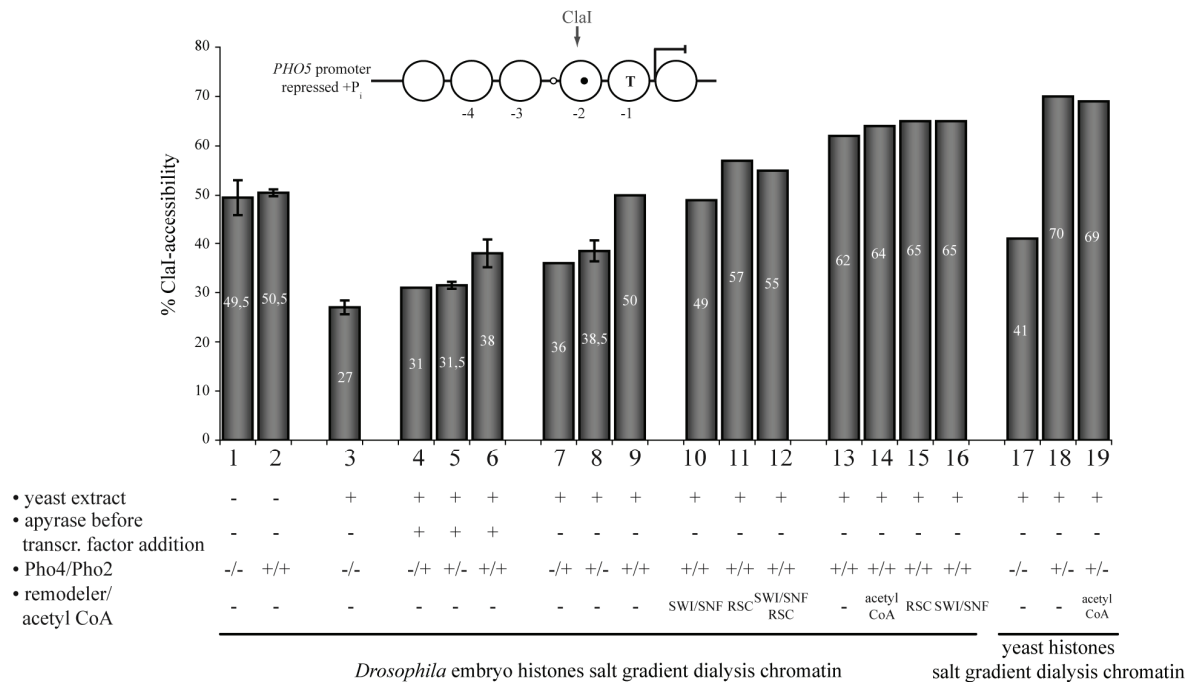
Fig. 29 Pho4-induced remodeling at the *PHO5* promoter leads to an enhanced accessibility of the ClaI restriction site that is protected by a nucleosome in the repressed state. Accessibility values for ClaI restriction enzyme digestion of *in vitro* assembled chromatin treated as indicated. Columns 1 to 16 represent experiments with *Drosophila* embryo octamers and columns 17 to 19 using recombinant yeast octamers. For columns 4 to 12 and 17 to 19 Pho4 and/or Pho2 were added after the salt gradient dialysis chromatin was incubated with yeast extract. For columns 13 to 16 Pho4 and Pho2 were added together with the yeast extract. Error bars show the variation of two to three independent experiments starting from the same salt gradient dialysis chromatin preparation.

In summary, we see an energy- and Pho4-dependent remodeling of *PHO5* promoter chromatin as demonstrated by the generation of a hypersensitive region in DNaseI patterns and by increased ClaI-accessibility. Still, the *in vitro* accessibilities did not reach *in vivo* values. In contrast, the *PHO8* promoter chromatin showed very little remodeling seen only as an accentuated hypersensitivity at the UASp2 site. None of the factors that yielded remodeling at the *PHO5* promoter had a similar effect on the *PHO8* promoter. Furthermore, *PHO5* promoter chromatin is not so reliable in *in vitro* reconstitution, shifting and remodeling reactions, especially the closed pattern was often unclear.

3.2.7 Purification of chromatin subpopulations

As we were not able to achieve the *in vivo* extent of remodeling by ClaI digestion but strong hypersensitivity by DNaseI indirect end-labeling, we wondered if our chromatin contained a mixture of subpopulations that behaved differently, e.g., were more and less remodeled. One further argument for the presence of chromatin subpopulations was that the remodeled *in vitro* pattern of the DNaseI digests was generally more structured, i.e. it contained more distinct bands in comparison to the rather smeared hypersensitive site of the induced state *in vivo* (see **Fig. 18**). The chromatin populations could

involve, for example, more or less supercoiled plasmids, plasmids covered with a variety of factors from the extract, leading to plasmids where the promoter could not be opened at all by the addition of Pho4 in contrast to plasmids with maybe fully remodeled promoter chromatin. We tried different approaches to separate such putative subpopulations: first on the level of salt gradient dialysis chromatin and second on the level of remodeled chromatin.

The first approach involved centrifugation of salt gradient dialysis chromatin through a sucrose gradient that should lead to the separation of different *PHO5* and *PHO8* chromatin populations along the gradient (see schematic **Fig. 30**A) according to their contributions of mass and structure. After sucrose gradient separation, fractions were removed and analyzed for the DNA content to estimate the distribution of chromatin along the gradient (**Fig. 30**B). Chromatin was enriched in the lower half of the gradient and was found in 12 of 23 fractions. In almost all chromatin fractions analyzed for their DNA content the nicked form of the plasmids (upper arrow) and the supercoiled form of the plasmids (lower arrow) could be distinguished and always appeared as a double band due to the different sizes of the used *PHO5* and *PHO8* plasmids. The nicked form was always enriched, which happens typically by shearing if salt gradient dialysis chromatin with plasmids larger than 2 kb is pipetted (Gernot Längst, personal communication). Chromatin fractions highlighted with an asterisk (fraction 15, 18, 20, 22) were treated with yeast extract and energy to analyze if they gave a clearer closed pattern for the *PHO5* and the *PHO8* promoter chromatin (**Fig. 30**C and D), which may indicate a more homogeneous population of chromatin templates which in turn may be remodeled to a more homogeneous state. The chromatin used as starting material gave a more or less typical closed promoter pattern upon addition of extract and energy (**Fig. 30**C, input 1, lane 1). This had to be concentrated in order to get a better resolution in sucrose gradient centrifugation and was therefore dialyzed against concentrated PEG to reduce the volume. The pattern of this more highly concentrated chromatin upon treatment with extract and energy was maybe a little bit more smeared, but mostly unchanged (input 2, lane 2). Shifting the fractions 15, 18, 20 and 22 did not result in a clearer pattern of the closed *PHO5* and *PHO8* promoter chromatin but rather weakened the quality in a way that now additional bands appeared that were not *in vivo*-like for both promoters (**Fig. 30**C and D, lanes 4-12).

A second approach to separate subpopulations made use of differential $MgCl_2$-precipitation. Adding rising concentrations of $MgCl_2$ to chromatin results in self-association and precipitation of chromatin populations whereas unbound proteins, free DNA, plasmids with only few nucleosomes or RNA will remain soluble (Schwarz et al. 1996). Using this method, chromatin could be purified to remove excess proteins from the extract that were not or weakly bound to chromatin. Salt gradient dialysis chromatin was treated with yeast extract and energy with or without Pho4. Both preparations were treated with the lowest $MgCl_2$ concentration, incubated on ice and centrifuged. The resulting pellet contained the chromatin fraction that aggregated at the lowest $MgCl_2$ concentration.
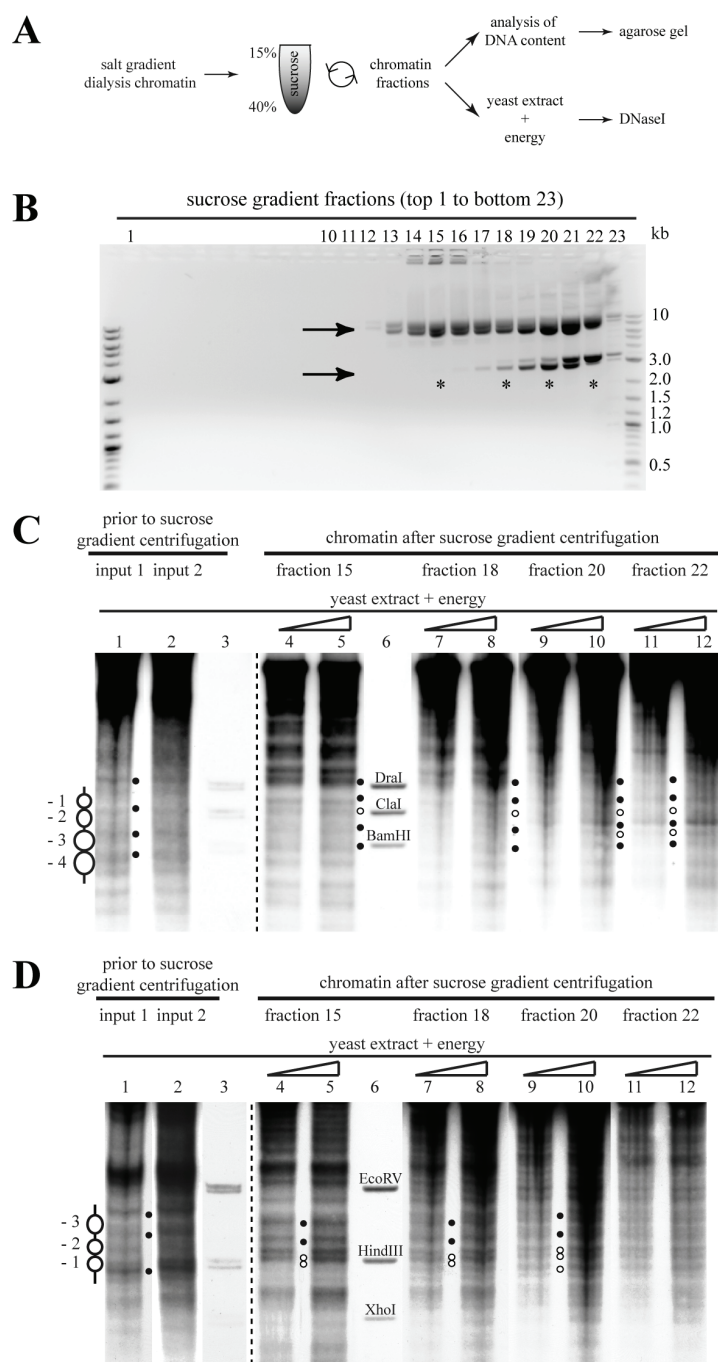
Fig. 30 Sucrose gradient centrifugation of salt gradient dialysis chromatin and subsequent nucleosome repositioning ("shifting") to the repressed state by yeast extract *in vitro* did not result in a subpopulation with a more uniform pattern. (A) Experimental scheme: salt gradient dialysis chromatin was centrifuged through a sucrose gradient to separate potentially different assembly states. Fractions were collected and the distribution of the DNA content along the gradient was analyzed. Some chromatin fractions were shifted to the closed nucleosomal pattern by incubation with yeast extract and energy. (B) Distribution of salt gradient dialysis chromatin after sucrose gradient fractionation. Inverse color image of agarose gel electrophoresis of proteinase K-, RNase A-digested and ethanol-precipitated salt gradient dialysis chromatin fractions after centrifugation through a sucrose gradient. Upper arrow points to the nicked, lower arrow points to the supercoiled form of the plasmids. Double bands occur due to a difference in size of the *PHO5* and *PHO8* plasmid. Asterisks highlight the chromatin samples (fractions 15, 18, 20, 22) that were processed further. (C) DNaseI indirect end-labeling analysis of the *PHO5* promoter region in chromatin treated as indicated on top of the lanes after pre-assembly by salt gradient dialysis and fractionation via sucrose gradient centrifugation. Input 1 refers to salt gradient dialysis chromatin; chromatin from input 2 was treated with PEG to reduce the volume before centrifugation. Black dots mark bands corresponding to the linker regions between *in vivo* nucleosome positions. White dots mark bands that do not correspond to *in vivo* linker regions. See **Fig. 17**A for description of ramps and marker bands. (D)

Same blot as in panel B but re-hybridized for the *PHO8* promoter region. See **Fig. 17**B for description of dots and ramps. Marker fragments were generated by double digests of EcoRV, HindIII and XhoI each with BglII.

The supernatant contained the remaining chromatin and other factors and was treated with the next higher $MgCl_2$ concentration, put on ice and centrifuged. This procedure was repeated for several concentrations (1, 2.5, 6, 8, 10, 15 mM $MgCl_2$). Each precipitated chromatin pellet was analyzed for its DNA content and in parallel subjected to DNaseI indirect end-labeling as well as ClaI-accessibility assays (see schematic, **Fig. 31**A). **Fig. 31**B shows the DNA concentration of the differential $MgCl_2$ precipitated chromatin fractions, the remaining supernatant (SN), the input material (input) and the first chromatin fraction that was pelleted due to background $MgCl_2$ concentration (4.5 mM) in the buffer (in) for both chromatin preparations without (**Fig. 31**B, left) and with Pho4 (**Fig. 31**B, right). There were again the nicked (upper arrow) and the supercoiled form (lower arrow) of the plasmid, which both migrated at different positions compared to the pUC plasmid. This may hint at incomplete removal of proteins or a different degree of superhelicity. The nicked form was depleted relative to the supercoiled form during the serial precipitation steps, no matter if Pho4 was present or not. With Pho4 the chromatin was depleted more completely at lower $MgCl_2$ concentrations. Additionally, there was a third distinct band that ran below the supercoiled plasmid and became enriched in the final fractions, i.e. could hardly be precipitated by $MgCl_2$. As this band migrated at the same position as the untreated supercoiled pUC *PHO5* plasmid, it may represent a maximally supercoiled form that was never assembled into chromatin. Most of the nucleic acid material, i.e. mostly RNA (bracket region in the gel) remained in the last supernatant. These differential behaviors confirmed that different chromatin and nucleic acid populations were effectively separated. Nonetheless, DNaseI digestion and indirect end-labeling of the chromatin without Pho4 that represented the closed *PHO5* promoter pattern showed the clearest pattern in the input material (**Fig. 31**C, lane1) and all other sequentially precipitated fractions showed a fuzzier pattern where the locations of the nucleosomes could not be distinguished very well (lanes 2-13). Surprisingly, there was a rather distinct pattern of the final supernatant fraction. However, if this pattern corresponds to the closed *PHO5* promoter pattern remains to be assessed. The ClaI-accessibilities of all fractions of chromatin not treated with Pho4 were rather close to 24% of the input material (**Fig. 31**C, below the blot). A different result was observed for the chromatin that was treated with Pho4 (**Fig. 31**D). Here, ClaI-accessibilities showed an increase from 36% of the mixed chromatin population (input material) to 48% of fractions that were precipitated (lanes 6-10). This could point either to more remodeled subpopulations or to histones that were stripped away during the process. However, the effect was not large enough to follow this up.

A variation of this approach addressed the separation of subpopulations in chromatin of different assembly degrees. For this under-assembled (relative histone to DNA ratio: 0.8:1) or fully-assembled (relative histone DNA to ratio: 1.0:1) (see also 2.8.2) chromatin was subjected to differential $MgCl_2$ precipitation (as described for **Fig. 31** and **Supp. Fig. 1**A). Analysis of the DNA content of the fractions showed a preferential precipitation at 6 mM $MgCl_2$ (**Supp. Fig. 1**B).
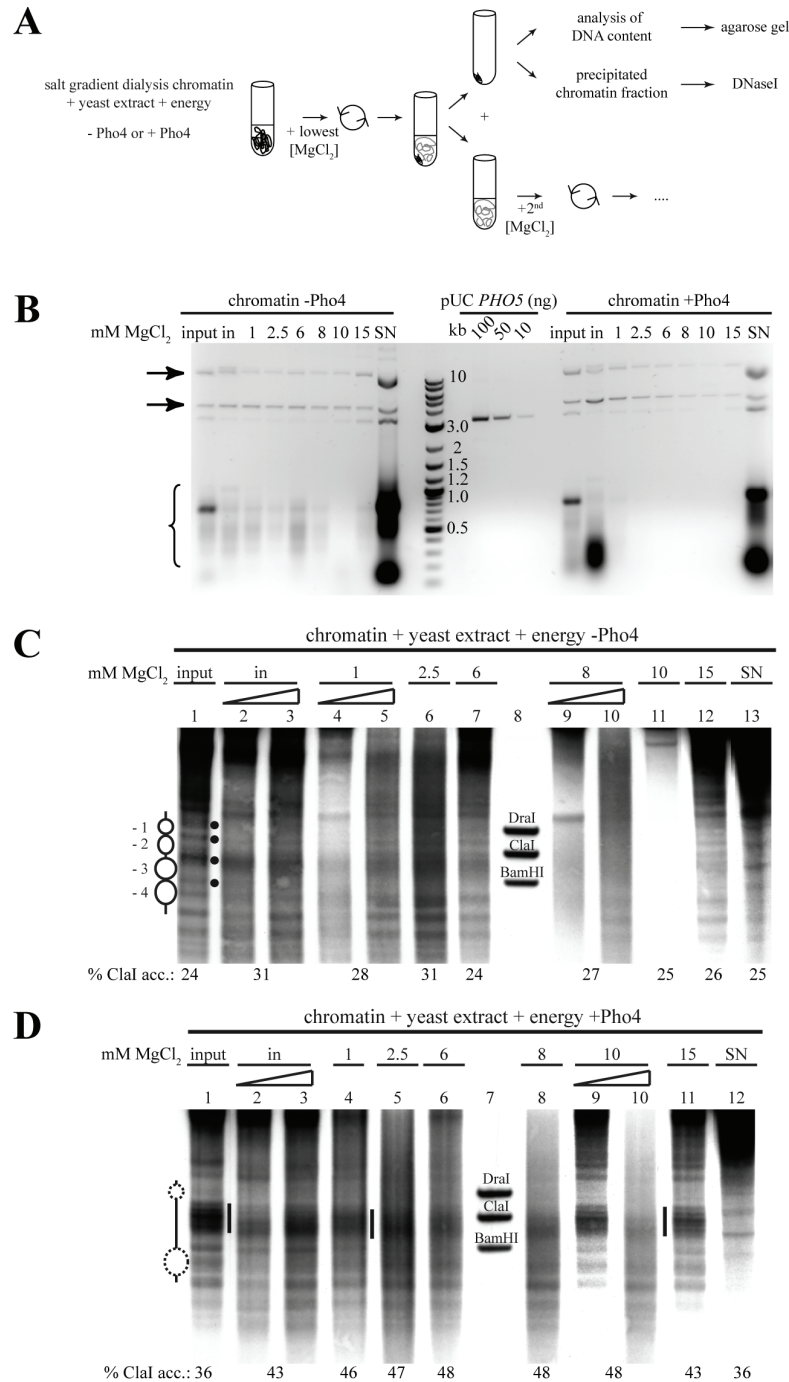
Fig. 31 Differential MgCl₂-precipitation of extract-treated chromatin with or without the addition of Pho4 did not separate subpopulations that showed a clearer closed or remodeled nucleosomal pattern. (A) Experimental scheme: extract- and energy-treated salt gradient dialysis chromatin with or without Pho4 was precipitated with the lowest MgCl₂ concentration, incubated on ice and centrifuged. This resulted in a chromatin pellet and non-precipitated chromatin in the supernatant. The supernatant was transferred into a new tube and treated with the next higher MgCl₂ concentration. The procedure was repeated with increasing concentrations of MgCl₂. The DNA content and the nucleosomal pattern of each precipitated chromatin were analyzed. (B) Analysis of the distribution of extract-treated chromatin with or without Pho4 and subsequent differential MgCl₂ precipitation using the concentrations indicated on top of the gel. Inverse color image of agarose gel electrophoresis of proteinase K-, RNase A-digested and ethanol-precipitated chromatin. Upper arrow points to the nicked form of the plasmid. Lower arrow points to the supercoiled plasmid. Brackets indicate region with RNA. Defined amounts of untreated supercoiled pUC *PHO5* plasmid serve for quantification. (C) DNaseI indirect end-labeling analysis of the *PHO5* promoter region in extract- and energy-treated chromatin without Pho4 after pre-assembly by salt gradient dialysis and subsequent MgCl₂ precipitation. Input (lane1) refers to the starting material, in (lanes 2-3) corresponds to chromatin precipitated due to MgCl₂ in the shifting buffer. See **Fig. 17**A for description of dots

and ramps and marker bands. (D) Same analysis as in panel C but with Pho4 and subsequent MgCl₂ precipitation.

Addition of yeast extract and energy to the precipitated fractions and subsequent DNaseI indirect end-labeling showed the closed nucleosomal patterns generated with each precipitate. The closed pattern of the under-assembled input chromatin (**Supp. Fig. 1**C, lane 1) was not much different from any of the precipitated chromatin fractions, for both the *PHO5* as well as for the *PHO8* promoter (lanes 3-15). The same result was observed for fully-assembled chromatin (**Supp. Fig. 1**D). So even if the generation of different chromatin subpopulations was fostered by competition for limiting histones, this approach could not distinguish subpopulations that differed in nucleosome positioning upon incubation with yeast extract and energy.

Collectively, our attempts to separate chromatin subpopulations of *in vitro* chromatin with or without yeast extract and energy and with or without Pho4 using sucrose gradient ultracentrifugation or differential MgCl₂-precipitation failed. None of the subpopulations of chromatin showed a clearer closed nucleosomal pattern in the case of chromatin without Pho4 or was remodeled to a much higher extent in chromatin treated with Pho4.

3.2.8 Further variables that did not increase chromatin remodeling *in vitro*

As we wanted to get closer to the extent of *in vivo* promoter chromatin remodeling, we prepared extracts from phosphate-starved yeast cells. These cells were induced and contained unphosphorylated Pho4 and potentially other factors that should help in remodeling at the *PHO* promoters. Using this extract in the *in vitro* assay could not further enhance the extent of the hypersensitive site at the *PHO5* promoter (not shown). Another idea was the use of topoisomerase I in the *in vitro* reaction. Topoisomerase I creates a single-stranded DNA backbone break by passing the intact DNA strand through the break and re-ligating the broken strand (Osheroff 1989) This could lead to relaxation of the supercoiled template and may allow more space for the moving and remodeling nucleosomes. If superhelical strain in the chromatin template was a problem the use of a restriction enzyme on the chromatin template before shifting may make the circular chromatinized plasmid linear and relaxed and maybe more amenable to remodeling events. However, remodeling was not improved by either method (not shown). A further thought referred to the methylation pattern of DNA. As the plasmids in the lab were isolated from *E.coli* strains that carry the DNA methyltransferases Dam and Dcm, some sites might be more resistant for restriction with endonucleases in the context of chromatin because methylase recognition sites overlap the endonuclease recognition site. We prepared plasmids from *dam dcm-E.coli* strains that were free of dam and dcm methylation, assembled the DNA with histones into salt gradient dialysis chromatin and shifted the chromatin with yeast extract and energy and incubated with Pho4 in the presence of energy. Still, these un-methylated chromatinized plasmids were no better substrate for remodeling (not shown).

3.3   The influence of assembly degree on remodeling chromatin *in vitro*

The *in vitro* assays were always performed with a salt gradient dialysis chromatin preparation where the ratio of histones to DNA was thoroughly titrated to give a clear closed nucleosomal pattern of the *PHO5* promoter after shifting the nucleosomes with extract and energy. This was never an easy task as the closed *PHO5* promoter pattern was hard to obtain: a too low histone to DNA ratio led to a nucleosomal structure that looked under-assembled with hypersensitive bands that did not correspond to the *in vivo* pattern, while too high histone to DNA ratios resulted in precipitation of the chromatin.
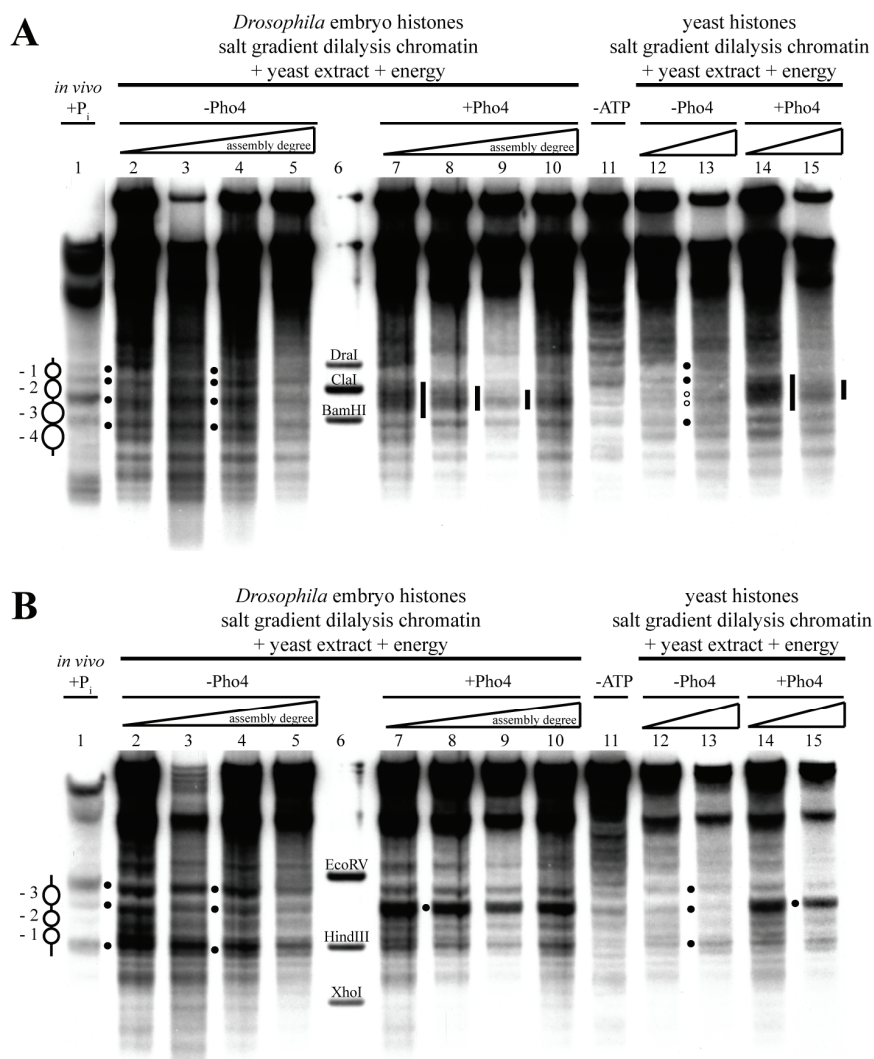
Fig. 32 Higher chromatin assembly degrees inhibit the remodeling potential at the *PHO5* promoter. (A) DNaseI indirect end-labeling analysis of the *PHO5* promoter region in chromatin treated as indicated on top of the lanes after pre-assembly by salt gradient dialysis and incubation with yeast extract in the presence of energy. Ramps on top of the gel indicate the increasing assembly degree from low assembled chromatin to fully assembled chromatin. In all DNaseI mapping experiments a range of DNaseI concentrations was used, but due to space limitations only one representative concentration is shown for each condition. Experiments were performed using *Drosophila* embryo histones (lanes 2-11) or recombinant yeast octamers (lanes 12-15) for salt dialysis chromatin. See **Fig. 17**A for description of dots, bars and marker bands. (B) Same blot as in panel A but rehybridized for the *PHO8* promoter region. See **Fig. 17**B for description of dots. Marker fragments were generated by double digests of EcoRV, HindIII and XhoI each with BglII.

We recognized that in-between these states of too low and too high chromatin assembly states the promoter nucleosomes showed some potential to be remodeled more extensively when the assembly degree was at the lower end of histone to DNA ratios that still yielded the proper closed pattern. In comparison to the *PHO5* promoter the *PHO8* promoter did not turn out to be such a delicate system and showed reliably a closed promoter pattern even with lower assembly degrees (Hertel et al. 2005).

We used four different assembly degrees (relative amount histones to DNA: 0.9/1.0/1.1/1.2:1, see also 2.8.2) from middle to high histone to DNA assemblies and shifted the nucleosomes with yeast extract and energy and with or without the transactivator Pho4 (**Fig. 32**). In comparison to the uninduced *in vivo* pattern (**Fig. 32**A, lane 1), the differently assembled chromatin preparations showed a very similar and uniform closed nucleosomal pattern (lanes 2-5). Pho4 addition generated a hypersensitive site that was more prominent in the less assembled (lanes 7-8) than in the higher assembled (lanes 9-10) chromatin preparations. In fact, the hypersensitivity was rather limited to the UASp2 region with the highest assembly degree chromatin. In any case, the most extensive remodeling was seen with the lowest assembled chromatin. As shown before, both the closed and the remodeled patterns differed clearly from chromatin treated without ATP (lane 11).

The same approach but now with yeast histones yielded again a less clear closed nucleosomal pattern with bands that did not belong to the typical *PHO5* promoter structure (lanes 12-13, white dots). Nonetheless also with these chromatin preparations there was the same trend, i.e. more remodeling of lower assembled chromatin (lanes 14-15).

As expected, the *PHO8* promoter chromatin showed not much difference with changing chromatin assembly degrees (**Fig. 32**B).

We concluded that the extent of *PHO5* promoter chromatin remodeling *in vitro* is significantly affected by the assembly degree, i.e. too high histone to DNA ratios will inhibit remodeling.

3.4 Pho4-induced chromatin remodeling at the *PHO84* promoter is impaired *in vitro*

In addition to the *PHO5* and the *PHO8* promoters, our laboratory was able to assemble chromatin with *in vivo*-like nucleosome positioning at the *PHO84* promoter *in vitro* by using the described system with yeast extract and energy (Wippo et al. 2009). The *PHO84* promoter is co-regulated by Pho4 with the *PHO5* and *PHO8* promoters *in vivo*. As described above we observed a remarkable discrepancy of *in vitro* remodeling efficiency at the *PHO5* promoter and at the *PHO8* promoter. That is why we wanted to check *in vitro* remodeling of *PHO84* promoter chromatin.

As in the case of the *PHO8* promoter, we did not observe Pho4-induced remodeling of *PHO84* promoter chromatin that was assembled by salt gradient dialysis (**Fig. 33**). The upstream and downstream nucleosomes of the *PHO84* promoter protected the region from DNaseI digestion and the short hypersensitive site (sHS) in-between the nucleosomes was accessible. Similar to the observed increase

of the *PHO8* promoter UASp2 there was some broadening of the linker region at the *PHO84* promoter that contains UASpC and UASpD (**Fig. 33**, right arrow), the two high-affinity Pho4 binding sites of the *PHO84* promoter (**Fig. 7**C).
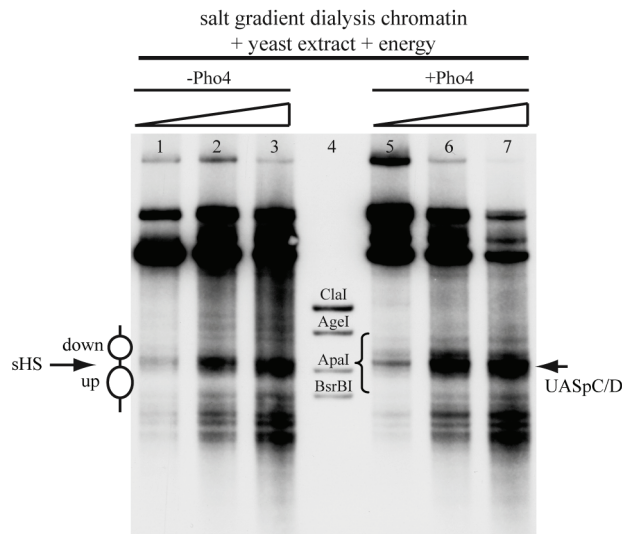
Fig. 33 Hardly any Pho4-induced chromatin remodeling at the *PHO84* promoter *in vitro*. DNaseI indirect end-labeling analysis of the *PHO84* promoter region in chromatin pre-assembled by salt gradient dialysis, incubated with yeast extract in the presence of energy and then treated or not treated with Pho4 as indicated. Schematic on the left corresponds to positioned nucleosomes as in **Fig. 7**C. Bracket shows the region that becomes hypersensitive upon induction *in vivo*. Marker fragments were generated by double digests of ClaI, AgeI, ApaI and BsrBI each with SspI. Ramps on top of the lanes denote increasing DNaseI concentrations.

These results were obtained using chromatin preparations of a thoroughly titrated assembly degree that was used in standard *in vitro* remodeling reactions for the *PHO5* and the *PHO8* promoter. The question arose if the *PHO84* promoter could be remodeled to a higher extent with lower chromatin assembly degrees (see 3.3) and would therefore rather resemble the *PHO5* promoter or if it would be resistant to remodeling as in the case of the *PHO8* promoter. Preliminary results hinted at more remodeling of *PHO84* promoter chromatin with lower chromatin assembly degrees (not shown).

3.5   The activation domain of the transcription factor Pho4 was dispensable for chromatin remodeling *in vitro*

Pho4 consists of a DNA binding domain and an activation domain (**Fig. 5**). Experiments *in vivo* using a truncated form of Pho4 that carried only the DNA binding domain could show that this domain alone is not sufficient to cause nucleosome -2 disruption at the *PHO5* promoter, even if the protein was overexpressed (Svaren et al. 1994). The activation domain probably recruits remodelers and cofactors (Neely et al. 1999; Neely et al. 2002; Morse 2007). We asked if this *in vivo* effect would also prove true in our *in vitro* assay. For this we used a standard shifting reaction and added Pho4 wild type (Pho4 wt), or Pho4 without an activation domain (Pho4ΔAD), or no Pho4 (**Fig. 34**).

The nucleosome structure of the *PHO5* promoter was equally remodeled into the hypersensitive site upon addition of both wild type and truncated Pho4 (**Fig. 34**A, compare lanes 1-2 and 3-4). The remodeling extent was the same as judged by DNaseI digestion and ClaI-accessibility. Binding of both Pho4 preparations at the *PHO8* promoter revealed the same nucleosomal pattern as described before (**Fig. 34**B).

A

salt gradient dialysis chromatin
+ yeast extract + energy

+Pho4 wt   +Pho4 ΔAD   -

1   2   3   4   5   6   7

DraI
ClaI
BamHI

% Cla acc.: 47   46   30
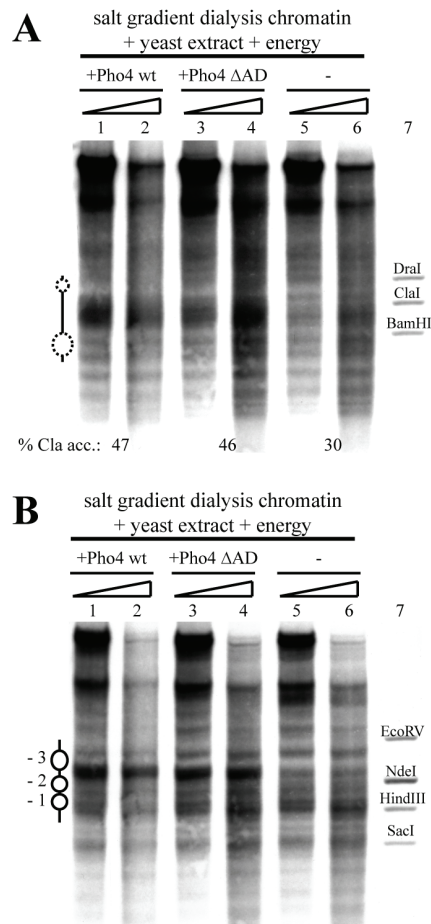
Fig. 34 Pho4 without activation domain did lead to the same extent of remodeling as wild type Pho4 in an *in vitro* remodeling reaction. (A) DNaseI indirect end-labeling analysis of the *PHO5* promoter region in chromatin after pre-assembly by salt gradient dialysis and incubation with yeast extract in the presence of energy. Pho4 wt (lanes 1-2), Pho4 without activation domain (ΔAD) (lanes 3-4) or no Pho4 (lanes 5-6) was added to the reaction. See **Fig. 17**A for description of ramps, bars, marker bands and ClaI-accessibility values. (B) Same blot as in panel A but re-hybridized for the *PHO8* promoter region. See **Fig. 17**B for description of dots and ramps. Marker fragments were generated by double digests of EcoRV, HindIII and XhoI each with BglII.

B

salt gradient dialysis chromatin
+ yeast extract + energy

+Pho4 wt   +Pho4 ΔAD   -

1   2   3   4   5   6   7

EcoRV
NdeI
HindIII
SacI

- 3
- 2
- 1

Summarizing all previous experiments, we observed extensive remodeling *in vitro* only at the *PHO5* promoter. The chromatin structures at the *PHO8* and *PHO84* promoters could not be remodeled to a similar extent. We addressed the reason for this discrepancy with the following *in vivo* experiments.

3.6   The intranucleosomal location of a UASp element has an auxiliary role in opening *PHO5* promoter chromatin *in vivo*

One possible explanation for the different behavior of the three promoters in the *in vitro* remodeling assay was the difference in nucleosome stability. The Korber lab already showed that nucleosomes of the *PHO5* promoter are intrinsically less stable than those of the co-regulated *PHO8* promoter (Hertel et al. 2005). Additionally, the *PHO84* promoter turned out to be kind of a mixture of both promoters with a rather stable nucleosome upstream of the short hypersensitive site resembling the *PHO8* promoter nucleosomes in stability and a less stable nucleosome downstream of UASpC/D similar to the *PHO5* promoter nucleosomes (**Fig. 7**C) (Wippo et al. 2009). Nonetheless, as the downstream nucleosome of the *PHO84* promoter was almost not remodeled *in vitro*, too, the difference in nucleosome stability could not be the complete answer (**Fig. 33**).

The *PHO5* promoter chromatin represented the only nucleosomal structure that could be remodeled in our *in vitro* system with a measurable increase in hypersensitivity whereas the *PHO8* and the *PHO84* promoters behaved rather refractive to all remodeling attempts. We concluded that the remodeling power of the extract system *in vitro* was lower than that observed *in vivo*. This made us compare the features of the three promoters (**Fig. 7**) and prompted us to the fact, that only the *PHO5* promoter harbors a high-affinity intranucleosomal UASp element (**Fig. 7**A). The *PHO8* promoter con-

tains a high- and a low-affinity site each in linker regions (**Fig. 7**B) and the *PHO84* promoter has two high-affinity sites in the linker region framed by two low-affinity sites covered by one nucleosome each (within the up and down nucleosomes, respectively) (**Fig. 7**C). Thus the main difference is that only at the *PHO5* promoter there is a high-affinity Pho4 binding site occluded by a nucleosome. This suggested a possible contribution of a competition between formation of nucleosome -2 and transcription factor binding to the high-affinity UASp2 site at the *PHO5* promoter upon remodeling. Maybe this mechanistic contribution of the high-affinity intranucleosomal UASp element was a crucial factor for remodeling to take place under the suboptimal *in vitro* conditions. Till now such a role for a UASp site was not investigated for *PHO5* promoter chromatin opening *in vivo*, although it would have important implications for the mechanism of promoter chromatin remodeling.

3.6.1 UASp mutants of the *PHO5* promoter

We pursued this interesting but yet unrecognized role of the intranucleosomal location of a high-affinity site at the *PHO5* promoter with *PHO5* promoter mutants *in vivo*.

The *PHO5* wild type promoter harbors the low-affinity site UASp1 in the linker region between nucleosome -2 and -3 and the high-affinity UASp2 element covered by nucleosome -2 (**Fig. 7**A, **Fig. 35**). Importantly, Pho4 is a basic helix-loop-helix protein, so the affinity of a UASp element mainly depends on the sequence of the core E box ((Ogawa and Oshima 1990; Lam et al. 2008)). Nonetheless, as discussed below, the Pho4-DMS footprint comprises about 20 bases and the flanking sequence also influences UASp affinity.
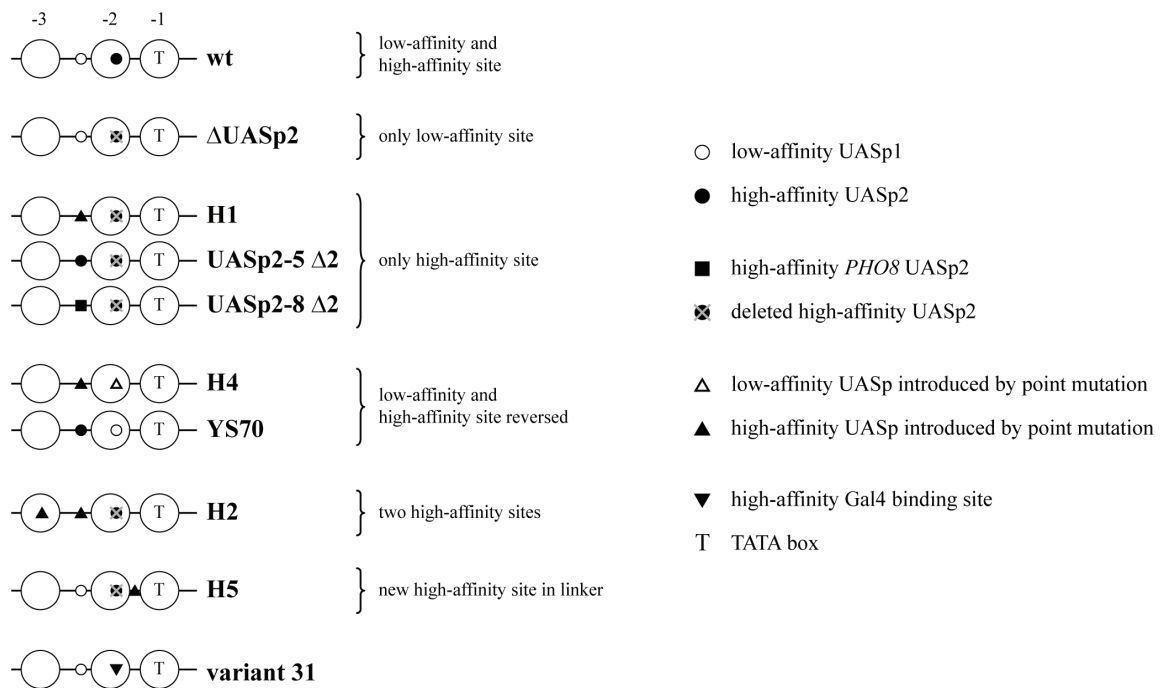
Fig. 35 Schematic of *PHO5* UASp mutants. Large open circles illustrate nucleosomes -3 to -1. Symbols denote promoter DNA elements as explained on the right.

The mutant promoter ΔUASp2 had only the wild type low-affinity UASp1 site left, whereas in the H1 mutant, the low-affinity UASp1 element was turned into a high-affinity UASp site by point mutation of the core E box motif. Replacement of the low-affinity UASp1 wild type site with the complete Pho4 footprint regions of the UASp2 elements of *PHO5* and *PHO8*, resulted in the mutants UASp2-5 Δ2 and UASp2-8 Δ2, respectively. Mutant H4 resembled the H1 mutant but here the wild type UASp2 element was turned into a low-affinity UASp site by point mutation. H4 therefore was reminiscent to the earlier constructed strain YS70, where the UASp1 and UASp2 sites were interchanged for each other (Venter et al. 1994). Nonetheless, for the generation of strain YS70 the UASp sites were swapped including the surrounding sequences of the whole Pho4 footprint (**Fig. 36**). Mutant H2 was again derivated from H1 with an additional high-affinity E box introduced by point mutation in the region of the -3 nucleosome. The integration plasmids with the mutant *PHO5* promoters H1, H2 and H4 were generated in the O´Shea lab (Lam et al. 2008). The construct H5 was generated by us and derived from the ΔUASp2. It harbored an additional high-affinity UASp introduced by point mutation in the smaller linker region between nucleosome -2 and -1 near the BstEII restriction site. We also made use of the variant 31 *PHO5* promoter (Ertinger 1998) that can be viewed as a derivative of ΔUASp2 with a high-affinity Gal4 binding site instead of the deleted high-affinity UASp2 site. A schematic of all constructs is given in **Fig. 35** and the exact sequences are shown in **Fig. 36**.
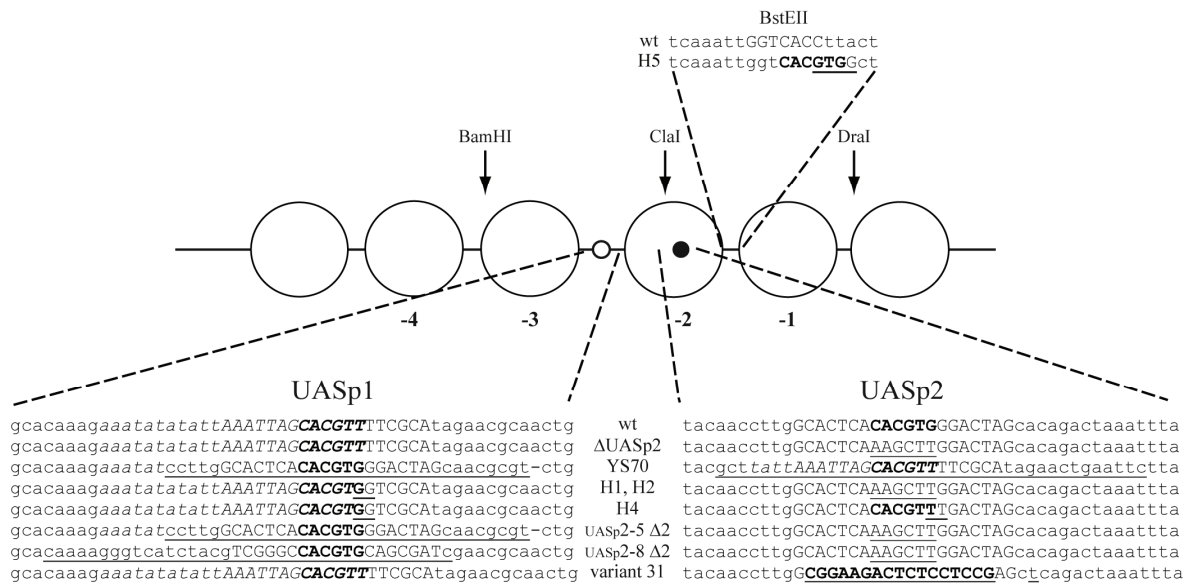
Fig. 36 Sequence comparison of *PHO5* UASp mutants. Schematic of the *PHO5* wild type promoter and sequence alignments of the *PHO5* promoters with altered UASp elements compared to the wild type sequence. The UASp2 E-box was deleted by conversion to a HindIII site. In bold: bases of the core hexanucleotide E-box of the UASp elements. Underlined: mutated DNA regions. Uppercase bases: Pho4 DMS footprint regions. Italic bases: Pho2 DMS footprint region (Vogel et al. 1989; Barbaric et al. 1992; Barbaric et al. 1996). The H2 mutant contains additionally (not shown) a high-affinity UASp element at position 418 in the -3 nucleosome by mutation of ct**tatgtg**cgc to ct*cacgtg*ggc (Lam et al. 2008). Underlined bases at UASp1 of construct UASp2-8 Δ2 derive from UASp2 region of the *PHO8* promoter. Bold underlined upper case bases at UASp2 in variant 31: Gal4 binding site. Underlined point mutation next to it (a to t): introduced SacI site.

3.6.2   The position of the UASp element at the *PHO5* promoter is important for chromatin remodeling *in vivo*

To ensure a properly closed *PHO5* promoter pattern of these constructs, nucleosome positions under high phosphate conditions were analyzed. Proper nucleosome positions were confirmed for ΔUASp2, H1, UASp2-5/8 Δ2 and H5 by DNaseI indirect end-labeling. This could also be seen by the mostly low ClaI-accessibilities around 17-18%, although the high-affinity sites introduced into the linker in H1 and UASp2-5/8 Δ2 led to a somewhat increased hypersensitivity at the sHS of 20-28% ClaI-accessibility (**Fig. 37**, below the blot and **Table 2**). YS70 and variant 31 were previously shown to have a properly closed *PHO5* promoter pattern (Venter et al. 1994; Ertinger 1998). So all these mutant *PHO5* promoters were assembled into properly positioned nucleosomes under repressive conditions *in vivo*. However, and in contrast to previous reports (Lam et al. 2008), the H4 and H2 mutants were already partly induced under high phosphate conditions and showed a slightly remodeled DNaseI pattern and higher ClaI-accessibilities of 45-48%, respectively (**Supp. Fig. 2**A and **Table 2**). So Pho4-induced remodeling at these promoter mutants started from a different pattern.

The deletion of the intranucleosomal UASp2 site at the *PHO5* promoter, in mutant ΔUASp2, hindered full chromatin remodeling *in vivo* as analyzed by DNaseI digestion and indirect end-labeling of nuclei prepared from cells under standard inducing conditions (overnight incubation in phosphate-free medium). The hypersensitive site at the ΔUASp2 promoter was shorter compared to the wild type pattern as it did not exceed beyond the ClaI marker band, i.e. it did not extent so much into the region of nucleosome -2 as in the wild type pattern (**Fig. 38**A, compare wild type and ΔUASp2). This lack of remodeling was reflected in a ClaI-accessibility of only 44% (**Table 2**) compared to induced wild type ClaI-accessibilities of 70-90%. Consequently, the ΔUASp2 mutant *PHO5* promoter showed remodeling mostly of nucleosomes -3 and -4 and less remodeling in the downstream half, i.e. of nucleosomes -2 and -1. Even inducing two times overnight in phosphate-free medium could not enhance much promoter opening (48% ClaI-accessibility).

However, deleting the only intranucleosomal high-affinity site is not conclusive to show the importance of the intranucleosomal location of this site as the promoter was not only deleted for its intranucleosomal, but also for its only high-affinity site and left with just the low-affinity UASp1. Consequently we turned to *PHO5* promoter mutants with a high-affinity UASp site in a linker region.

All such UASp mutants were induced overnight and chromatin opening was analyzed. DNaseI indirect end-labeling resulted in rather similar patterns for the H1, UASp2-5 Δ2, H4, H2 and H5 mutant (**Fig. 38**, **Supp. Fig. 2**B). These mutants resembled the induced promoter pattern of ΔUASp2, i.e. there was only partial spreading of the hypersensitive site into nucleosome -2. Interestingly, the DNaseI pattern of H1 was the most similar to the pattern of ΔUASp2 (**Fig. 38**A and B) with a hypersensitive site that did not pass beyond the ClaI marker band and left the downstream promoter region undisturbed. UASp2-5 Δ2 looked even less remodeled. The upstream region with nucleosomes -3 and -4 showed reduced hypersensitivity with an outstanding sHS linker region (**Fig. 38**C). The ClaI-

accessibility of both, the H1 and UASp2-5 Δ2 mutant, was 41% and 37% (**Fig. 38**B and C), respectively and therefore similar to ΔUASp2. Accordingly, a high-affinity linker binding site is not sufficient to trigger full chromatin remodeling under standard induction conditions.
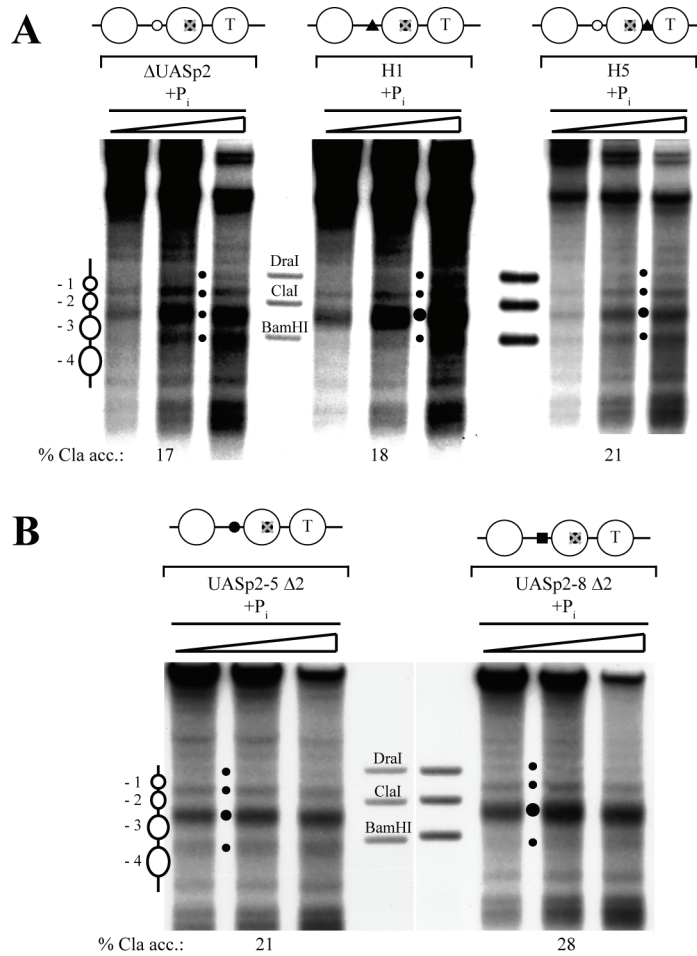
Fig. 37 *PHO5* **promoter UASp mutants showed mostly unaltered chromatin structures of the repressed state** *in vivo*. DNaseI indirect end-labeling analysis of the *PHO5* promoter region in strains with the following *PHO5* promoter configurations: (A) ΔUASp2 (CY341), H1 (CY337 EB1615) and H5 (CY337 FE1600) and (B) UASp2-5 Δ2 (CY339 *ura3* pCB-UASp2-5 Δ2) and UASp2-8 Δ2 (CY339 *ura3* pCB-UASp2-8 Δ2) of logarithmically growing cells in phosphate-rich (+P$_i$) medium. See **Fig. 38** for description of dots, stippled vertical lines and schematics of UASp configuration and **Fig. 17**A for ramps, marker bands and schematics next to the gels.

The mutants H2 and H4 also did not show full remodeling after overnight induction in phosphate-free medium (**Supp. Fig. 2**B, **Table 2**). Both displayed slightly higher induced ClaI-accessibilities of 44% and 46%, respectively (**Table 2**), compared to the before mentioned constructs. H4 addressed the importance of a low-affinity intranucleosomal binding site in nucleosome -2 generated by point mutation and H2 offered insight into the impact an additional high-affinity intranucleosomal binding site in nucleosome -3 can have. The observed effect could therefore be due to the additional high-affinity site in nucleosome -3 in the case of H2 and the low-affinity site in nucleosome -2 for H4 compared to ΔUASp2. Nonetheless, the difference was very weak and could equally well be due to the already partially remodeled chromatin structure under repressed conditions (**Supp. Fig. 2**A and **Table 2**).
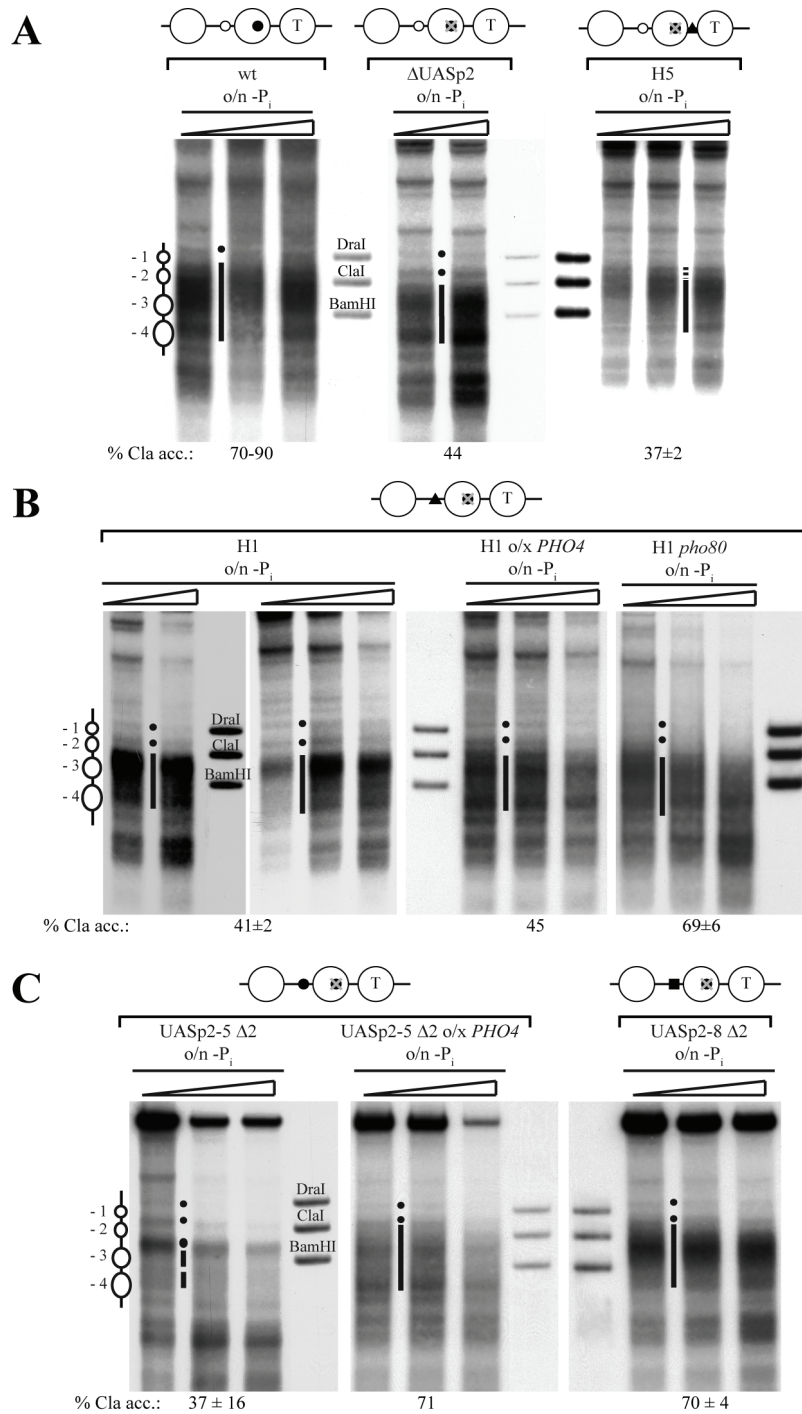
Fig. 38 The intranucleosomal location of a UASp element in the -2 nucleosome is important but not essential for *PHO5* promoter chromatin opening *in vivo*. DNaseI indirect end-labeling analysis of the *PHO5* promoter region in strains with the following *PHO5* promoter configurations: (A) wt (CY337), ΔUASp2 (CY341) and H5 (CY337 FE1600), (B) H1 (CY337 EB1615) and (C) UASp2-5 Δ2 (CY339 ura3 pCB-UASp2-5 Δ2) and UASp2-8 Δ2 (CY339 ura3 pCB-UASp2-8 Δ2) after overnight (o/n) incubation in phosphate-free (-P$_i$) medium. For the H1 mutant experiments with incubation in phosphate-free medium with overexpression (o/x) of *PHO4* and deletion of *PHO80* (*pho80*) are shown. For the UASp2-5 Δ2 mutant an experiment with incubation in phosphate-free medium for 40 h and one experiment with overexpression (o/x) of *PHO4* are shown. Small dots in-between lanes mark the bands corresponding to the linker regions flanking the positioned nucleosome -1 as shown in the schematic on the left and vertical bars in-between the lanes highlight the extent of a hypersensitive region. For UASp2-5 Δ2 the stippled vertical line denotes less pronounced hypersensitivity in the region of the -3 and -4 nucleosomes. The large dot marks the increased hypersensitivity of the linker between the -2 and -3 nucleosomes. Samples from the same chromatin preparation but from two different gels are shown for the H1 mutant promoter o/n -P$_i$. Schematics on top of the panels show the UASp configuration at the *PHO5* promoter
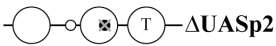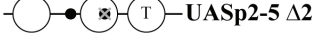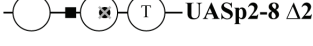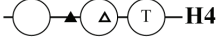
(see also **Fig. 35**). The three large circles stand for nucleosomes -3, -2, -1 (from left to right) and small symbols for different types of UASp elements: wt *PHO5* UASp1 (open circle), wt *PHO5* UASp2 (closed circle), wt *PHO8* UASp2 (closed square), high-affinity UASp by point mutation (closed triangle), deleted *PHO5* UASp2 (crossed out closed circle). Markers, ramps, and schematics next to the gels are as in **Fig. 17**A.

The partial opening of the H4 mutant stands in contrast to the complete promoter chromatin remodeling in strain YS70 (Venter et al. 1994), although both promoter mutants should have a high-affinity UASp element in the linker and a low-affinity UASp element in nucleosome -2 (**Fig. 35**). Analyzing the H5 mutant by DNaseI indirect end-labeling after overnight induction, we observed a more extensive hypersensitive region compared to ΔUASp2. Nonetheless, ClaI-accessibility was still similarly low at 37% (**Fig. 38**A and below the blot). Therefore, also an additional high-affinity Pho4 site in the linker region between nucleosome -1 and -2 is not able to trigger complete remodeling of nucleosome -2. Such a discrepancy between similar ClaI-accessibilities but different DNaseI indirect end-labeling patterns is not necessarily contradictory as digestion with ClaI is extensive and covers all chromatin templates whereas DNaseI indirect end-labeling uses limited digestion degrees and probes preferentially the most sensitive chromatin subpopulations. Therefore DNaseI digestion does not always mirror the average chromatin state. Further, a smeared DNaseI pattern can reflect repositioning as well as eviction of nucleosomes.

Distinct from all analyzed constructs was the mutant UASp2-8 Δ2 that showed full promoter remodeling after overnight induction (ClaI-accessibility 70%, **Fig. 38**C, **Table 2**) and apparently displayed therefore the most potent UASp site.

Under high phosphate conditions all mutants showed low phosphatase activity (not more than 22 units, **Table 2**) confirming the uninduced state. In general, transcriptional output depends both on the extent of promoter chromatin remodeling and on the total number, affinity and distance to the transcription start of Pho4 binding sites. So the resulting phosphatase levels of the different promoter mutants under inducing conditions may be viewed as a measure that integrates over these properties. After overnight induction in phosphate-free medium the ΔUASp2 mutant had an impaired transcriptional output as measured by the acid phosphatase assay (**Table 2**, 37 units compared to > 400 units for wild type) that confirmed the partial remodeling seen by DNaseI indirect end-labeling and ClaI-accessibility. The mutant UASp2-5 Δ2 gave similarly low phosphatase levels as ΔUASp2 (40 vs. 37 units). Interestingly, the mutant UASp2-8 Δ2 showed only moderate phosphatase levels of 125 units (**Table 2**), whereas H1 produced more acid phosphatase (166 units). Also the H5 mutant exhibited much higher phosphatase levels (223 units, **Table 2**) after overnight induction, similar to activity of the H2 and H4 mutants (308 and 189 units, **Table 2**). For unknown reasons the mutant UASp2-5 Δ2 showed relatively low phosphatase values compared to the other UASp mutants that harbored a high-affinity site in the linker region. We conclude that phosphatase values might be a helpful control but do not have to be conclusive.

We controlled complete induction by checking in parallel HpaI-accessibilities at the *PHO8* promoter. Accessibility to HpaI at the *PHO8* promoter increases upon phosphate starvation to more than 60%, usually 70-90%, which depends on the strain background and induction conditions (Barbaric et al. 1992; Korber et al. 2006; Barbaric et al. 2007). As the *PHO* promoters are a co-regulated system, induction should also affect the *PHO8* promoter and monitoring accessibility to the HpaI restriction site gives therefore information about the overall degree of induction in the cell. Using this internal control we confirmed for all UASp mutants a good induction (**Table 2**) although H1 and H5 were at the lower limit of complete induction.

	+phosphate		-phosphate							
			o/n[b]		2x o/n		o/n o/x *PHO4*[c]		o/n *pho80*	
	ClaI (HpaI)[a] acc.	Pase Units	ClaI (HpaI) acc.	Pase Units	ClaI (HpaI) acc.	Pase Units	ClaI (HpaI) acc.	Pase Units	ClaI (HpaI) acc.	Pase Units
ΔUASp2	17% (n.d.[e])	22±5	44±0%[d] (66±4%)	37±8	48% (64%)	33	n.d.	49±10	n.d.	n.d.
H1	18% (n.d.)	14	41±2% (60±6%)	166±16	n.d.	n.d.	45% (73%)	181	69±6% (81±2%)	215±83
UASp2-5 Δ2	21% (26%)	18±3	37±16% (65±8%)	40±4	41% (74%)	41	71% (81%)	117	n.d.	n.d.
UASp2-8 Δ2	28% (30%)	17±4	70±5% (n.d.)	125±17	n.d.	n.d.	83% (n.d.)	222	n.d.	n.d.
H4	48±4% (60%)	9±0	46% (69%)	189	n.d.	n.d.	n.d.	n.d.	n.d.	n.d.
H2	45±1% (48%)	4	44±8% (70±4%)	308	n.d.	n.d.	66% (79%)	355	n.d.	n.d.
H5	21% (28%)	11	37±2% (53±3%)	223±4	57% (64%)	336	n.d.	n.d.	n.d.	n.d.
variant 31[f]										
-Gal4 (1-147)	n.d.	n.d.	41% (67%)	49	79%	107	n.d.	n.d.	n.d.	n.d.
+Gal4 (1-147)	ca. 20%[g]	n.d.	59% (74%)	63	87%	115	n.d.	n.d.	n.d.	n.d.

[a] Accessibility of the HpaI site at the *PHO8* promoter is given in brackets as internal control for induction.

[b] overnight (o/n) induction in phosphate free medium

[c] overexpression (o/x) of *PHO4*

[d] Errors show the variation of two to three biologically independent experiments.

[e] not determined (n.d.)

[f] strain AH2341 grown in YNB 2% raffinose, 2% galactose

[g] value not determined by PhosphorImager analysis but estimated from gel picture

○ low affinity UASp1   ■ high affinity *PHO8* UASp2   △ low affinity UASp by point mutation   ▼ high affinity Gal4 binding site
● high affinity UASp2   ⊠ deleted high affinity UASp2   ▲ high affinity UASp by point mutation   T   TATA box

Table 2 ClaI-accessibility values and acid phosphatase units of UASp mutants.

As both the ClaI- and the HpaI-accessibilities were sometimes quite low, we applied stronger induction conditions using prolonged incubation without phosphate two times overnight, or overexpression of *PHO4*, or deletion of *PHO80* in connection to phosphate-free medium to eventually open the

UASp mutants (**Table 2**). Inducing the ΔUASp2 and UASp2-5 Δ2 mutants two times overnight did not lead to an increase in ClaI-accessibility (48% and 41%, respectively, **Table 2**), whereas prolonged induction of H5 in phosphate-free medium did (57%, **Table 2**). Overexpression of *PHO4* in the H1 mutant could not enhance promoter opening as seen by the still partially remodeled DNaseI pattern and an unchanged ClaI-accessibility of 45% (**Fig. 38**B, **Table 2**), but the same approach with the mutant UASp2-5 Δ2 resulted in remodeling observed by a considerable increase of DNaseI hypersensitivity and an elevated ClaI-accessibility of 71% (**Fig. 38**C, **Table 2**). Both mutants showed upon *PHO4* overexpression more HpaI-accessibility speaking for more remodeling also at the *PHO8* promoter (**Table 2**). Eventually the H1 mutant promoter showed successful remodeling upon induction by overnight phosphate depletion and *pho80* deletion (**Fig. 38**B and **Table 2**). Also for the H2 mutant we additionally strengthened the induction conditions by overexpression of *PHO4* and observed substantially more chromatin opening of the DNaseI pattern as well as ClaI-accessibility (66%, **Supp. Fig. 2**B, **Table 2**). Even UASp2-8 Δ2 could be further remodeled as observed by the increased ClaI-accessibility of 83% (**Table 2**).

Six of the seven mutant *PHO5* promoters without an intranucleosomal high-affinity Pho4 binding site showed a defect in chromatin opening after overnight induction in phosphate-free medium, i.e. under standard induction conditions. Not even a high-affinity site in a linker region could compensate for the loss of UASp2 as shown in the mutants H1, UASp2-5 Δ2 and H5. We conclude that placing the high-affinity site out of nucleosome -2 into a linker region, regardless on which side of the nucleosome, inhibited complete remodeling of *PHO5* promoter chromatin. Therefore we propose that the intranucleosomal position of the high-affinity Pho4 binding site in nucleosome -2 has an important role. Still, given the complete remodeling of the UASp2-8 Δ2 mutant using standard induction conditions this role was not essential. Furthermore, forced induction conditions were also able to move the UASp2-5 Δ2 and H1 mutants, and to some extent the H5 mutant, towards complete remodeling. The quality of the UASp elements seems to play a crucial part as high-affinity linker binding sites used in UASp2-5 Δ2, H1, H2, H4 and H5 mutants did not have the same effect on remodeling as the high-affinity site in UASp2-8 Δ2, still all could remodel under forced conditions. Additionally, the interchanged UASp sites leading to a high-affinity binding site in the linker and a low-affinity intranucleosomal site as in the H4 mutant could not achieve the same remodeling degree as the previously published construct in the YS70 strain. Obviously, UASp elements exhibit more potential remodeling power if they contain the surrounding sequences of the whole Pho4 footprint (YS70) than if they were introduced by point mutations generating a palindromic E-box (H4).

3.6.3 Increase of Pho4-dependent remodeling starting from UASp1 by mere binding competition at nucleosome -2

As described before in chapter 3.5, Pho4 has two functional domains: the DNA binding domain and the activation domain (Svaren et al. 1994). Given the results described in 3.6.2, i.e. the position of

an intranucleosomal binding site in nucleosome -2 of the *PHO5* promoter is important for the remodeling mechanism, we wondered if we could pinpoint more precisely the role of Pho4 in this process. On the one hand the Pho4 activation domain could target and recruit cofactors to this UASp. On the other hand a binding competition between the Pho4 DNA binding domain and the formation of the nucleosome may be sufficient. To address this question we made use of the *PHO5* promoter variant 31 (Ertinger 1998). The yeast strain AH2341 contains this construct with a strong consensus Gal4 binding site instead of UASp2 (**Fig. 35**, **Fig. 36**). This mutant is effectively a ΔUASp2 construct with respect to Pho4 binding sites (**Fig. 35**). We checked for chromatin opening after overnight induction in phosphate-free medium and observed again, similar to the earlier analyzed ΔUASp2 mutant, incomplete remodeling shown by a ClaI-accessibility of 41% (**Table 2**). Strain growth was slower under the used conditions of raffinose and galactose as carbon source instead of glucose. These conditions had to be applied as experiments described below included galactose induction and we needed a direct comparison of growth conditions. Slower growth and therefore delayed depletion of intracellular phosphate pools made overnight induction less effective. Such weaker induction conditions could be the reason for incomplete remodeling which led us to analyze chromatin opening after two times overnight induction. Here, the variant 31 *PHO5* promoter showed full chromatin remodeling with an accessibility value of 79% (**Table 2**). This result contradicted our previous finding that the construct ΔUASp2 in strain CY341 could only be induced partially and never showed complete promoter remodeling even after prolonged induction two times overnight (**Table 2**) whereas variant 31 in strain AH2341 could be fully remodeled. It has been observed before that such conflicting results could be obtained in different strain backgrounds. For unknown reasons the AH background is more potent than the CY background with regard to *PHO5* promoter opening (after overnight induction in phosphate-free medium: 100% ClaI-accessibility vs. 70% ClaI-accessibility, respectively at the wild type *PHO5* promoter).

Nonetheless, we could still use strain AH2341 as a reference point for incomplete promoter opening under suboptimal induction conditions (overnight induction). In order to directly address the effect of mere DNA binding competition we used the same strain AH2341, which is deleted in *gal4*, i.e. harbors no endogenous Gal4, and expressed the Gal4 DNA binding domain from a plasmid. Both the *GAL* and the *PHO* system were induced by addition of galactose and removal of phosphate overnight, respectively. The induction conditions were the same as before using AH2341 without the Gal4 plasmid. Nonetheless, we controlled again for the internal degree of *PHO* induction by monitoring HpaI-accessibility, which was very similar in both cases (67% vs. 74%, **Table 2**). Expressing the DNA binding domain of the Gal4 construct led to an increased ClaI-accessibility of 59% (**Table 2**) after overnight induction and consequently to more remodeling than without the Gal4 DNA binding domain. Importantly, expression of the Gal4 DNA binding domain under high phosphate conditions in the presence of galactose was not enough to remodel nucleosome -2 as it resulted in low ClaI-accessibility of 20% (**Table 2**) (Ertinger 1998).

Consequently, extensive remodeling of nucleosome -2 depended on an activation domain, in this case from Pho4 and could start from the UASp1 site. This remodeling was enhanced in the presence of the Gal4 DNA binding domain by mere binding competition with nucleosome -2.

3.7   Remodeling UASp-mutated *PHO8 and PHO84* promoters *in vitro*
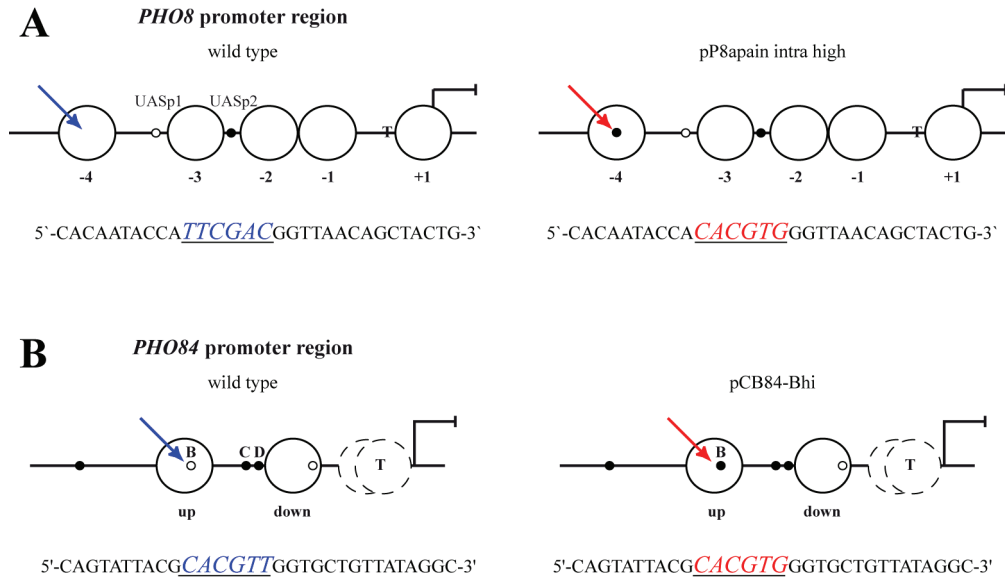
Fig. 39 UASp mutations at the *PHO8* and *PHO84* promoter. (A) Left: *PHO8* wild type promoter with a central region of DNA sequence occupied by nucleosome -4. Right: The mutated *PHO8* promoter in plasmid pP8apain intra high with an additional high-affinity UASp site in nucleosome -4. Underlined DNA sequence shows the mutation to a high-affinity site. (B) Left: *PHO84* wild type promoter. Right: The mutated *PHO84* promoter in plasmid pCB84-Bhi with low-affinity UASpB site changed into a high-affinity UASpB site (underlined). Arrows point to the position of mutation in the schematics.

We went back to the *in vitro* system and asked if *PHO8* and *PHO84* promoter plasmids with artificially introduced high-affinity intranucleosomal binding sites would show the generation of extensive hypersensitive sites also at these promoters similar to *in vitro* remodeling at the *PHO5* promoter. So we generated new plasmids containing the *PHO8* and *PHO84* promoter sequences with an artificially introduced high-affinity UASp: pP8apain intra high and pCB84-Bhi, respectively. The plasmid pP8apain intra high harbored a new high-affinity site in nucleosome -4 and pCB84-Bhi had the low-affinity site UASpB mutated to high-affinity, both via point mutations (**Fig. 39**A and B).

pP8apain intra high exhibited the same nucleosomal promoter pattern in a standard shifting and remodeling reaction as seen before (compare **Fig. 40** with **Fig. 28**B). We repeated the same remodeling reaction using a lower assembly degree and included pCB84-Bhi in our analysis. We observed again the same lack in chromatin remodeling at the pP8apain intra high promoter (**Fig. 41** lanes 9-10). Surprisingly, we saw extensive remodeling at the pCB84-Bhi promoter with the high-affinity intranucleosomal UASpB site upon addition of yeast extract, energy and Pho4 (**Fig. 41** lanes 4-5). This enlargement of the hypersensitive site was not present in earlier *PHO84 in vitro* remodeling experiments

salt gradient dialysis chromatin using
pP8apain intra high

+ yeast extract + energy

-Pho4   +Pho4

1   2   3   4   5

EcoRV

NdeI

- 3
- 2
- 1

HindIII

SacI
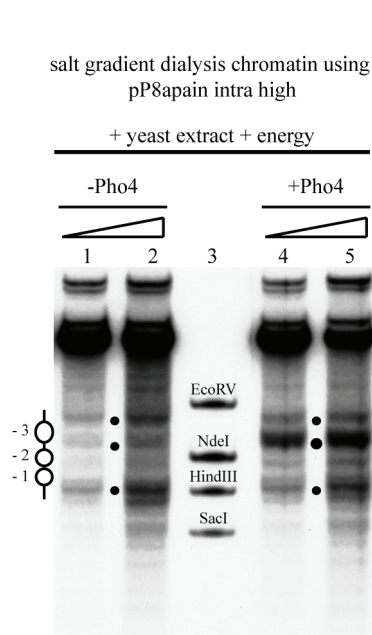
(**Fig. 33**), maybe because the previously used assembly degree ratio of histones to DNA was higher. This called for a control of the wild type *PHO84* plasmid assembled into chromatin with the same low assembly degree as applied for *in vitro* remodeling in **Fig. 41**. Preliminary results suggested a Pho4- and energy-dependent remodeling of the lower assembled wild type *PHO84* promoter as well (not shown).

Fig. 40 No Pho4-induced remodeling of pP8apain promoter chromatin using chromatin of standard assembly degree. DNaseI indirect end-labeling analysis of the pP8apain promoter region in chromatin pre-assembled by salt gradient dialysis using standard histone to DNA ratio, incubated with yeast extract in the presence of energy and then treated or not treated with Pho4 as indicated. See **Fig. 17**B for description of dots, ramps and marker bands.

In summary, the mutated *PHO8* promoter (pP8apain intra high) did not show Pho4-induced remodeling even not at low chromatin assembly degrees. Maybe the introduced site was not strong enough. The mutated *PHO84* promoter (pCB84-Bhi) showed extensive remodeling upon Pho4 addition using lower assembly degrees. But preliminary experiments suggested that also wild type *PHO84* promoter chromatin could be remodeled using these conditions, modifying the conclusion from earlier experiments with highly assembled chromatin. So in summary, the insertion of artificial high-affinity intranucleosomal sites into the *PHO8* and *PHO84* promoters could so far not conclusively answer the question why the *in vitro* remodeling was successful at the *PHO5* but not at the *PHO8* and *PHO84* promoter. To be sure, this approach could not address why the remodeling potential of the *in vitro* system was suboptimal, as remodeling *in vivo* occurs without the high-affinity intranucleosomal binding sites at the *PHO8* and *PHO84* promoters anyway.

salt gradient dialysis chromatin + yeast extract + energy

pCB84-Bhi   pP8apain intra high

-Pho4   +Pho4   -Pho4   +Pho4

1   2   3   4   5   6   7   8   9   10

AgeI
SpeI

ApaI

BsrBI

down
sHS →
up

EcoRV

NdeI

- 3
- 2
- 1

HindIII

SacI
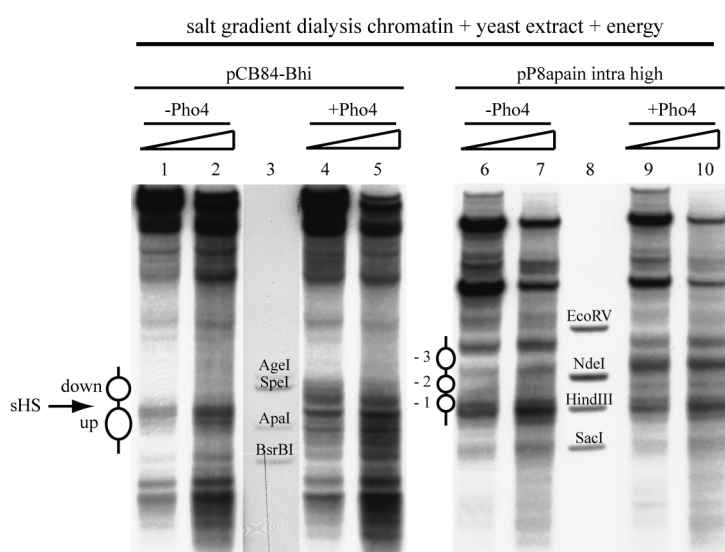
Fig. 41 No Pho4-induced chromatin remodeling at the pP8apain intra high and extensive remodeling at the pCB84-Bhi promoter chromatin *in vitro* using chromatin of lower assembly degrees. DNaseI indirect end-labeling analysis of pP8apain intra high and pCB84-Bhi promoter regions pre-assembled into chromatin by salt gradient dialysis using lower histone to DNA ratios (0.8:1) incubated with yeast extract in the presence of energy and then treated or not treated with Pho4 as indicated. See **Fig. 17**B for description of dots, ramps and marker bands.

3.8 Cofactor requirement for the co-regulated *PHO84* promoter *in vivo*

The *PHO84* promoter is also co-regulated by Pho4 and is even stronger than the *PHO5* promoter as it exhibits higher transcriptional activity (Ogawa et al. 1995). Genome-wide expression analysis showed that the promoter is down regulated in *gcn5* or *snf2* strains (Lee et al. 2000). In the absence of the HAT Gcn5 less histone H3 acetylation and impaired TBP and polymerase II recruitment to the promoter region was observed (Shukla et al. 2006a; Shukla et al. 2006b). The induced *PHO84* promoter is occupied by at least two remodelers, Snf2 and Ino80 (Steger et al. 2003; Jonsson et al. 2004). Furthermore, also the importance of the five characteristic Pho4 binding sites and their distribution relative to the promoter nucleosomes (**Fig. 7**C) was part of a study and was correlated to the lower threshold for *PHO84* induction. It was also shown that induction leads to *PHO84* promoter chromatin remodeling (Lam et al. 2008) but the mechanistic function and the role of chromatin cofactors were unknown.

Fig. 42 Histone loss kinetics from the *PHO84* promoter region upon induction in wt, *snf2* and *gcn5* strains. ChIP kinetics using anti-histone H3 antibody and the *PHO84* promoter amplicon in wt (CY337), *snf2* (CY407) and *gcn5* (CY53379) strains after transfer of the yeast strains to phosphate-free medium. o/n, overnight induction. ChIP data were normalized to input DNA and to the *ACT1* amplicon. Error bars show the standard deviations of three biological replicates.
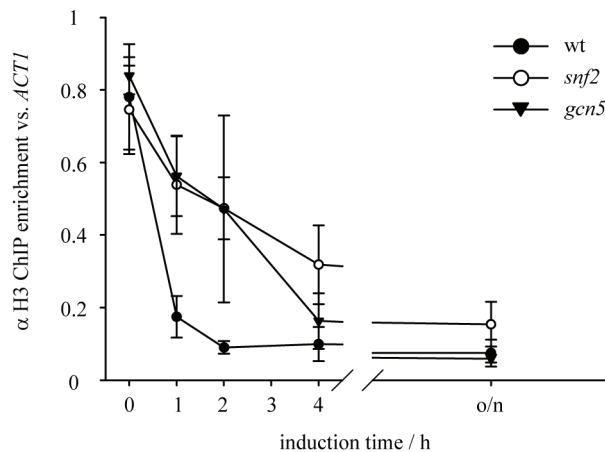
Building on studies started in the Hörz group, the Korber lab studied the *PHO84* promoter further, continuing the collaboration with the Barbaric group. We showed that the *PHO84* promoter nucleosomes undergo extensive remodeling upon induction, exposing a large hypersensitive site (**Fig. 7**C) similar to remodeling at the *PHO5* promoter. In order to analyze the cofactor requirements for remodeling at the *PHO84* promoter, we measured histone loss kinetics of wild type, *snf2* and *gcn5* strains. Wild type cells showed a fast decrease in histone H3 ChIP signal and reached maximal *PHO84* promoter chromatin opening after 2 h. Histone eviction was slower in *snf2* cells. Furthermore, *PHO84* promoter chromatin of *snf2* cells could not be remodeled completely, the H3 ChIP signal did not decrease to wild type levels after overnight induction (**Fig. 42**) which was confirmed by restriction accessibilities (not shown, (Wippo et al. 2009)). *gcn5* cells also exhibited a strong delay in histone eviction kinetics but reached in the end full opening similar to wild type levels (**Fig. 42**).

As the chaperone Asf1 was found to be important for induction of the *PHO5* and *PHO8* promoters (Adkins et al. 2004; Korber et al. 2006) and recent reports described the dependency of the HAT Rtt109 on Asf1 (Tsubota et al. 2007), we wanted to test both cofactors for their role in *PHO84* remodeling. Indeed, *PHO84* promoter chromatin remodeling was delayed in the *rtt109* strain but showed only a minor delay in the *asf1* strain compared to wild type cells in histone loss kinetics (**Fig. 43**). Both these effects were less pronounced than for the kinetics of *snf2* and *gcn5* mutants.
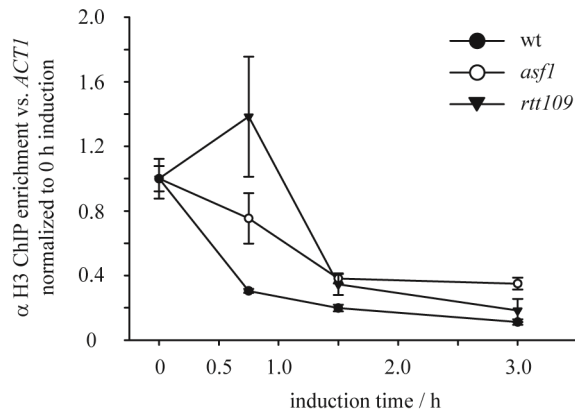
Fig. 43 Histone loss kinetics from the *PHO84* promoter region upon induction in wt, *asf1* and *rtt109* strains. ChIP kinetics using anti-histone H3 antibody and the *PHO84* promoter amplicon with wt (W303a), *asf1* (W303a *asf1*) and *gcn5* (PKY4170) strains after transfer of the yeast strains to phosphate-free medium. ChIP data were normalized to input DNA, to the *ACT1* amplicon and to 0 h time point. Error bars show the variations of two biological replicates.

The nucleosome transition upon induction was dependent on Snf2 and Gcn5, and weakly dependent on Rtt109 and even less dependent on Asf1. From these data and other experiments described in Wippo et al. 2009 we concluded that the *PHO84* promoter is a hybrid of the *PHO5* and the *PHO8* promoter that harbors a stable, Snf2-dependent nucleosome and a less stable nucleosome that can be remodeled with redundant cofactor requirements.

3.9   Replication and its impact on *PHO5* and *PHO8* promoter opening *in vivo*

The Hörz lab showed that the *PHO5* promoter can be opened and closed in the absence of replication (Schmid et al. 1992). As this study compared the end point of induction of replicating and non-replicating yeast cells, it addressed rather if replication was essential but not if it had a role at all during opening of *PHO5* promoter chromatin, e.g., if it affected opening kinetics.

As mentioned above, under standard induction conditions the cells undergo at least two rounds of replication while the internal phosphate pools are depleted. Therefore establishment of full induction for the *PHO* promoters usually happens during ongoing replication. Our new findings about the importance of a high-affinity intranucleosomal binding site (paragraph 3.6) encouraged us to have a closer look at the impact replication had on remodeling *PHO5* promoter chromatin. A possible scenario during *PHO5* induction is that replication could lead to the displacement of nucleosomes from the promoter and thereby help transcription factor binding. Replication could also reassemble repressive chromatin along the promoter region. In the first case, replication would help promoter opening (**Fig. 44** left), and in the second case replication would be a hindrance as it would lead to a resetting of the

closed promoter state (**Fig. 44** right). Both possibilities involve a binding competition between Pho4 and a nucleosome to the region of UASp2 at the *PHO5* promoter.
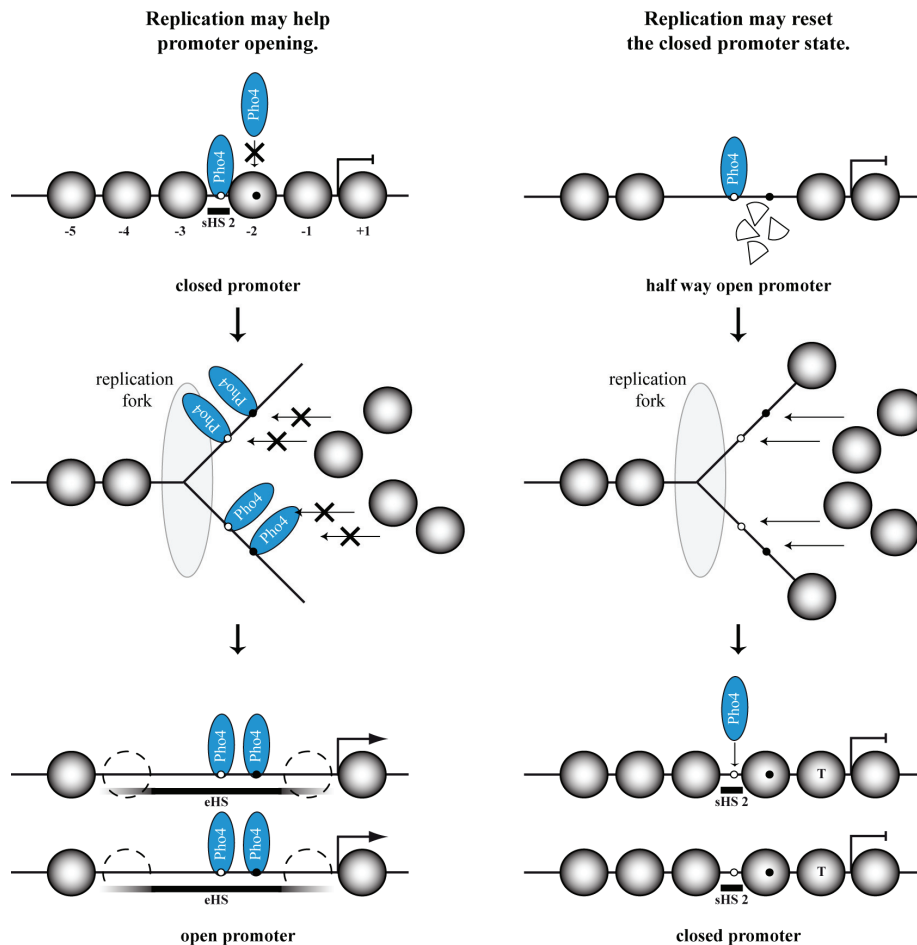
Fig. 44 Possible roles of replication during *PHO5* promoter induction. Left: replication aids in promoter opening. As the replication fork proceeds along the template DNA, histone octamers loose contact to the DNA facilitating access of the transcription factor Pho4 to its UASp binding sites. Right: replication hinders chromatin opening. Pho4 binding is disrupted by the moving replication fork which enables histones to form octamers along the DNA before the transcription factor can re-associate to its recognition site.

3.9.1   Replication hinders chromatin opening

We addressed the question of the role of replication using a temperature sensitive *pho80* allele (Schmid et al. 1992). With this mutation it is possible to induce the *PHO* genes by a temperature up-shift to 37°C and circumvent the necessity of replication to deplete intracellular phosphate.

We compared histone loss kinetics at the promoter as a measure of chromatin opening at the *PHO5* and *PHO8* promoter using chromatin immunoprecipitation (ChIP). H3 ChIP samples were collected and analyzed from logarithmically growing or uracil starved stationary yeast cultures representing replicating and non-replicating cells, respectively. Cultures of both conditions were induced by the temperature up-shift which triggered histone eviction. DNA prepared from the chromatin immunoprecipitated samples was analyzed with Real Time PCR (regions detected by probes are shown in **Fig. 45**B). The kinetics showed a reproducibly faster histone loss at the *PHO5* and *PHO8*

promoter region in cells without replication (**Fig. 45**, **Supp. Fig. 3**), speaking for replication being rather a hindrance during *PHO5* and *PHO8* promoter opening. The major difference in histone loss at both *PHO* promoters between replicating and non-replicating cells was observed half an hour after induction. Later induction time points still showed a decrease of the histone ChIP signal that resulted in equal histone loss after 2 h induction for both promoters irrespective of the replication status. There are no good negative controls for changes in histone occupancy under replicating and non-replicating conditions as the whole genome is replicated. We used two control loci, telomere and actin, as it was less likely that both showed parallel effects in our assay. Both the telomere and the actin locus did not respond much to the applied induction conditions and showed not much difference between replicating and non-replicating cells. We used the telomere locus as negative control and the actin locus for normalization of the ChIP signal.
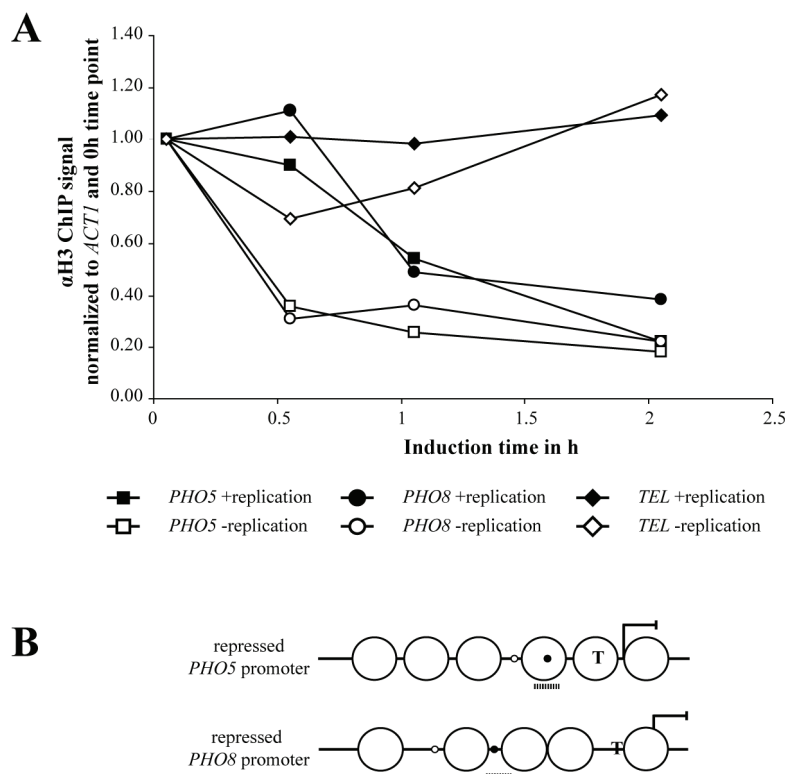
Fig. 45 Histones were depleted faster from the *PHO5* and *PHO8* promoters in non-replicating than in replicating cells. (A) ChIP kinetics of histone loss upon induction by temperature up-shift from 24°C to 37°C in a *pho80* temperature sensitive yeast strain (YS44). ChIP was done using a histone H3 C-terminal antibody and amplicons at the *PHO5* and *PHO8* promoters, the telomere (*TEL*) and the actin open reading frame (*ACT1*). The H3 ChIP signal was normalized to input DNA, to the *ACT1* amplicon, and to the 0 h time point of induction. Legend under the graph shows the analyzed loci: *PHO5* UASp2 (squares), *PHO8* (circles), *TEL* (diamonds). Closed symbols represent replicating conditions (+ uracil medium), open symbols represent non-replicating conditions (- uracil starvation). (B) Scheme is analogous to **Fig. 7**A and B and shows the position of the TaqMan amplicons as stippled bars.

3.9.2   Histone reassembly during replication (hydroxyurea synchronization)

Apparently replication imposes an obstacle for *PHO* promoter chromatin remodeling. We set out to substantiate this interpretation by testing the according mechanistic prediction that replication resets

a nucleosomal structure at the *PHO5* promoter even if it was already partially or fully open. We used yeast strains mutated in *pho80* that showed a constitutively induced *PHO5* promoter structure and synchronized the cells. We wanted to know what happens with regard to histone occupancy at the promoter after release into the cell cycle. Would we see promoter chromatin resetting during or after replication in S phase? Would the promoter structure change to the closed nucleosomal pattern or would it stay open? Importantly, answers to these questions could tell us how an open promoter structure is inherited or re-established upon passage through S phase.

Logarithmically growing *pho80* cells were synchronized with hydroxyurea which arrested the cells in G1/S phase. Hydroxyurea affects DNA synthesis by reducing the production of deoxyribonucleotides by inhibiting the ribonucleotide reductase (Alvino et al. 2007). Washing the cells in water and resuspending them into fresh medium released the synchronized population collectively into the cell cycle. Samples were taken every 15 min to monitor synchrony by FACS analysis and histone occupancy by H3 ChIP (**Fig. 46**A). To directly compare any changes at the histone level that occurred during the passage through the cell cycle we used *pho80* and wild type cells, which represented induced and repressed *PHO* chromatin states, respectively. Both strains showed a characteristic FACS profile of cycling cells with a G1 (1n DNA content) and a G2 (2n DNA content) peak framing the cells of the S phase plateau. *pho80* cells were exposed longer to hydroxyurea than wild type cells due to a slower growth rate. As *pho80* cells had a longer generation time it took longer till the whole cell population arrived at the cell cycle block. Both showed G1 arrested cells after hydroxyurea arrest of 4 h and 3 h, respectively. Upon release into the cell cycle the cell population represented by the G1 peak in the FACS profiles moved on to S phase. *pho80* cells entered S phase after 30 min and wild type cells after 45 min release (**Fig. 46**B). FACS analysis of subsequent time points showed a prominent G2 peak and soon afterwards the profile of cycling cells (**Fig. 46**B). Parallel sample preparation for FACS analysis and ChIP ensured good correlation of the observed stages of the cell cycle with the histone occupancy signals. The H3 ChIP corresponding to the described FACS analysis showed a very prominent signal of histone reassembly at the *PHO5* and *PHO8* promoters at the time point of S phase after 30 min release (**Fig. 46**C) for *pho80* cells. This increase was more than fourfold in the case of the *PHO5* promoter and more than threefold at the *PHO8* promoter compared to the point of release. Time points before and after S phase did not show any increase in histone signal speaking for an otherwise constitutively open promoter chromatin structure.

The telomere (*TEL*) control locus showed no histone reassembly during the analysis and served as control region that is not regulated by the phosphate signaling pathway (**Fig. 46**).We observed this transient peak of histone H3 during S phase repeatedly. One more example is given in **Supp. Fig. 4**. A comparable H3 ChIP analysis with wild type cells did not lead to a histone peak in S phase after 45 min (**Fig. 46**). For unknown reasons this population started with a higher ChIP signal of cycling cells. The larger graphs represent H3 ChIP signals that were normalized to the input DNA, to the control locus actin (*ACT1*) and to the time point of release.
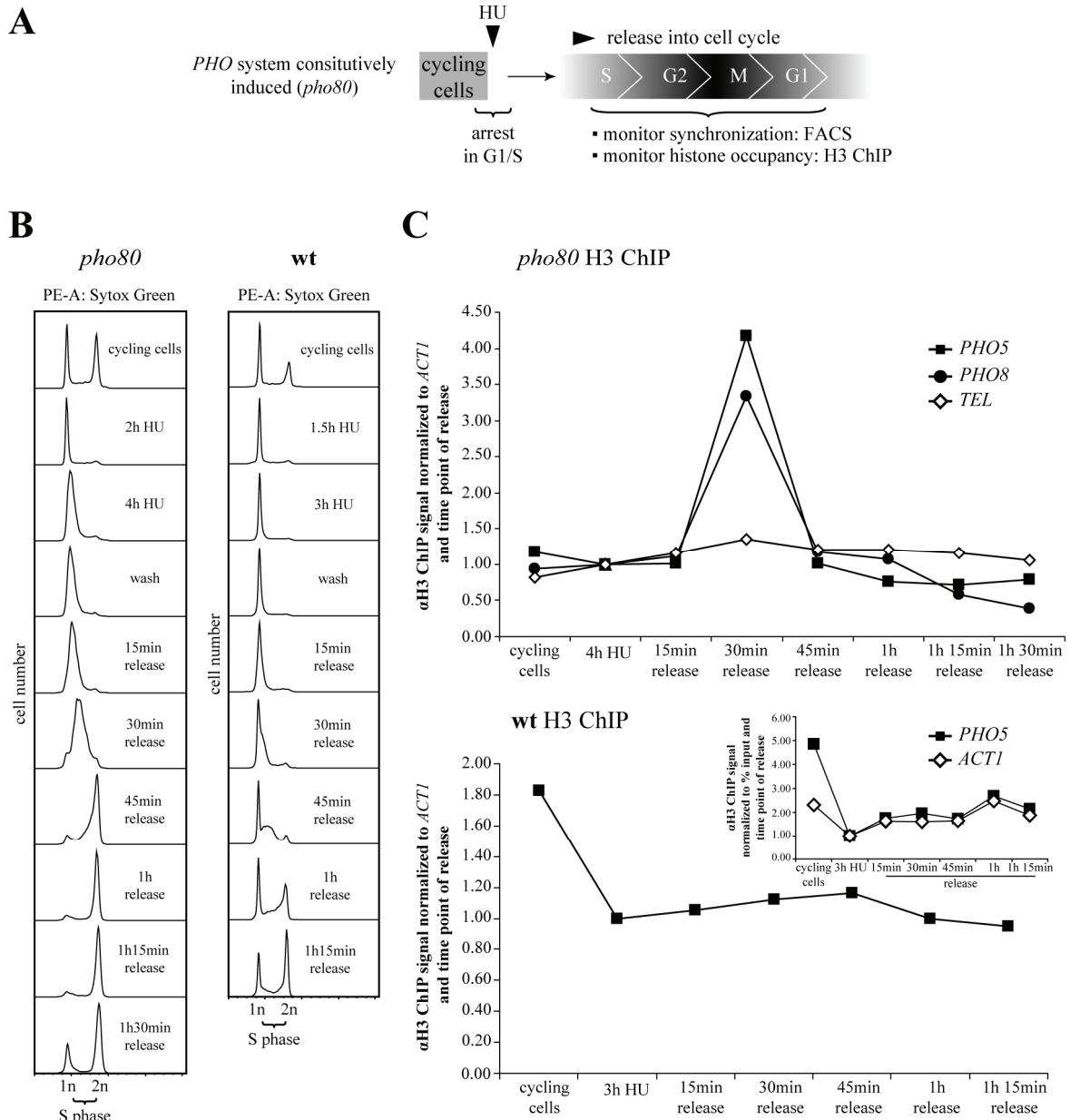
Fig. 46 Hydroxyurea synchronized *pho80* cells showed histone reassembly during replication, in contrast to wild type cells. (A) Experimental scheme: logarithmically growing cells were arrested with hydroxyurea (HU) in G1/S phase. Arrest and release into the cell cycle was monitored by FACS and H3 ChIP in 15 min intervals. (B) FACS analysis of the DNA content of cycling *pho80* and wt cells, cells that were arrested with HU and cells that were released into the cell cycle after HU arrest. (C) Histone H3 ChIP kinetics of histone occupancy of HU synchronized *pho80* cells (upper ChIP profile) and wt cells (lower ChIP profile). The H3 ChIP signal was normalized to input DNA, to the control locus *ACT1* and the time point of release. The inset shows an alternative analysis plotting the ChIP signal normalized to % input and the time point of release for wt cells. Legend in the graph shows analyzed loci: *PHO5* (closed squares), *PHO8* (closed circles), *TEL* (open diamonds).

The inset in **Fig. 46**C represents an alternative analysis normalizing the ChIP signal only to % input and to the time point of release. In the following ChIP experiments we switched to this kind of normalization as it included the individual input DNA of every sample. To have a second negative control in addition to wild type cells we also made use of a *pho4* strain. This mutant is not able to induce *PHO5* as it lacks the transcription factor Pho4. Here we observed a slight increase in the ChIP

signal during S phase, which was apparently due to the normalization to the control locus actin that showed rather low levels of histone occupancy. Anyhow, this slight increase was not significant as the parallel analysis using the normalization to % input did not display a histone peak in S phase (compare larger graph vs. inset **Supp. Fig. 4**).

In summary, we observed a transient peak of histone H3 occupancy during S phase at the *PHO5* and *PHO8* promoters in *pho80* cells that were synchronized by hydroxyurea. Wild type cells or *pho4* cells did not show histone reassembly during any cell cycle stage. This argues for promoter chromatin resetting during replication and against a continuously open promoter. However, a drawback in this system is the use of hydroxyurea as cell cycle arresting drug as it only slows progression through S phase and does not arrest the cells in a defined G1/S block (Santocanale and Diffley 1998). Hydroxyurea-induced dNTP depletion affects probably only one type of replication origin. Early firing origins of replication will therefore be activated while the replication forks continue to move very slowly during hydroxyurea arrest in early S phase and only late replicating origins will be stalled and await reactivation upon release (Santocanale and Diffley 1998). Analyzing the proximity of our regions of interest to origins of replication showed that both promoters could be part of early replication events (Saccharomyces Genome Database, http://www.yeastgenome.org/ (25.03.2010), www.oridb.org). A different group even suggested hydroxyurea had the same effect on all active origins and does not differentiate between early and late firing but results in overall progression in slow motion through S phase (Alvino et al. 2007). Therefore we were not sure if the *PHO5* and the *PHO8* promoters were already replicated during hydroxyurea treatment starting from nearby origins of replication. We decided to verify our preliminary observations of histone reassembly during S phase using a different approach to synchronize the cells.

3.9.3 Histone reassembly during replication ($cdc7^{ts}$ synchronization)

For this alternative analysis we made use of the *cdc7-4* allele, which confers temperature sensitivity to Cdc7. Cdc7 is a serine/threonine protein kinase that gets activated upon binding to Dbf4, which is required for entry into S phase (Bousset and Diffley 1998; DePamphilis 2006). Therefore inactivation of $cdc7^{ts}$ by a temperature up-shift will result in inhibition of S phase initiation. As Cdc7 is required for origin firing, we had to make sure that all origins were not fired yet. For this we applied a serial approach of synchronizing the yeast cells to make sure that all origin were fired and awaited reactivation. We performed again ChIP and FACS analysis following histone occupancy at the *PHO5* and the *PHO8* promoter at defined cell cycle stages.

We began by arresting cycling cells with nocodazole in G2/M phase, which hinders microtubule polymerization. After washing the cells to get rid of the nocodazole the temperature was raised from 24°C to restrictive conditions of 38°C to arrest the cells in late G1 by inactivation of Cdc7. Release into the cell cycle was accomplished by a shift to the permissive temperature of 24°C (**Fig. 47**A). We compared the $cdc7^{ts}$ *pho80* strain (**Fig. 47**) with a constitutively induced *PHO* system with the corres-

ponding *cdc7ts PHO80* (**Fig. 48**) that represented the uninduced status of the *PHO* promoters to control for unspecific effects. The FACS profile of cycling *cdc7ts pho80* cells (**Fig. 47**B) was different from the previously analyzed *CDC7 pho80* cells (**Fig. 46**B before "*pho80*") as it showed a higher G2 peak. Nocodazole arrested the cells completely in G2. The subsequent shift to the restrictive temperature yielded most of the cell population at the G1/S boundary. Upon shift to the permissive temperature the cells began to proceed towards S phase. Synchronized *cdc7ts pho80* cells were clearly in S phase between 15 to 30 min after release, and in G2 phase after 45 min. Soon afterwards they adopted again the profile of logarithmically growing cells (**Fig. 47**B).
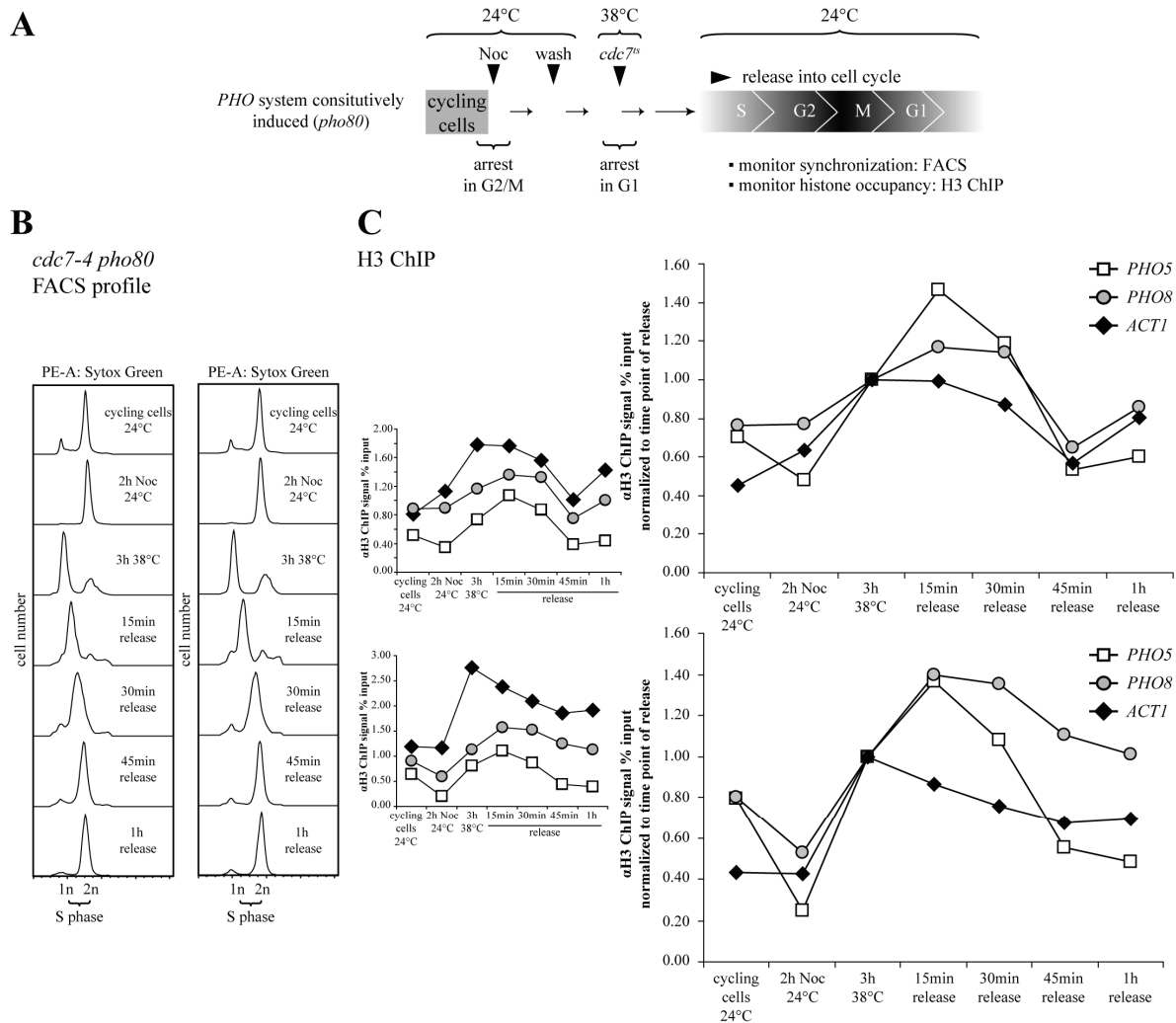
Fig. 47 Synchronization of *pho80* cells using sequential arrest by nocodazole and via *cdc7ts* resulted in a transient peak of histone occupancy in S phase. (A) Experimental scheme: logarithmically growing *cdc7tsph80* cells were arrested first with nocodazole (Noc) in G2/M phase, washed and released into G1 and afterwards arrested by a temperature up-shift to 38°C at G1/S phase. Release into the cell cycle was monitored by FACS and H3 ChIP in 15 min intervals. (B) FACS analysis of the DNA content of cycling *cdc7tsph80* cells. Cell stages as in (A). FACS profiles of *cdc7tsph80* cells from two independent experiments are shown. (C) Histone H3 ChIP kinetics of Noc and *cdc7ts* synchronized *pho80* cells. The H3 ChIP signals normalized to % input (smaller graphs, left) or to % input and to the time point of release (larger graphs, right) for *cdc7tsph80* cells from two independent experiments are shown. Left and right FACS profile in B correspond to upper and lower graph in C, respectively. Legend in the graph shows analyzed loci: *PHO5* (open squares), *PHO8* (grey circles), *ACT1* (closed diamonds).

The corresponding H3 ChIP analysis of the *cdc7^{ts} pho80* cells confirmed our previous results. In two biologically independent experiments we observed a transient H3 peak during S phase at both promoters with about 1.4 fold enrichment of the signal relative to the G1/S arrest (3 h) (**Fig. 47**C). The signal decreased very fast after passage through S phase. In contrast to the transient histone occupancy at the promoter regions we did not see a similar increase at the control locus actin. Interestingly, we observed a higher H3 ChIP signal for all loci directly after 3 h of 38°C, representing the restrictive temperature arrest, compared to earlier time points. This effect is probably due to better cross-linking efficiency at the elevated temperature.

A

cdc7-4
FACS profile

B

H3 ChIP
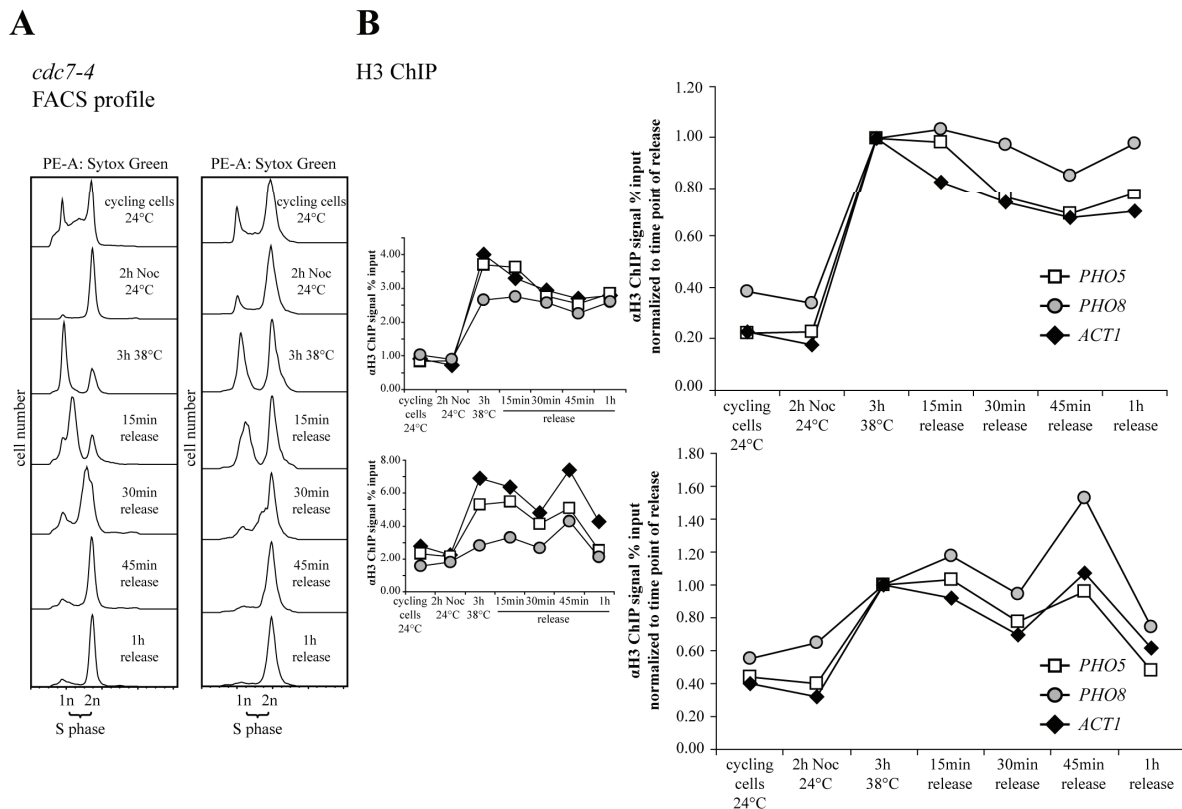
Fig. 48 Synchronization of *PHO80* cells using nocodazole and *cdc7^{ts}* did not result in a change of histone occupancy during replication. Experimental set up as in **Fig. 47** but using *cdc7-4 PHO80* cells (*cdc7-4*). (A) FACS analysis of the DNA content of cycling *cdc7-4 PHO80* cells. Cell stages as in **Fig. 47**A. FACS profiles of *cdc7-4 PHO80 cells* from two independent experiments are shown. (B) Histone H3 ChIP kinetics of histone occupancy of Noc and *cdc7^{ts}* synchronized *PHO80* cells. The H3 ChIP signal as % input (smaller graphs, left) or as % input normalized to the time point of release (larger graphs, right) for *cdc7^{ts} PHO80* cells from two independent experiments are shown. Left and right FACS profile in A correspond to upper and lower graph in B, respectively. Legend in the graph shows analyzed loci: *PHO5* (open squares), *PHO8* (grey circles), *ACT1* (closed diamonds).

We controlled the results using the corresponding *cdc7^{ts} PHO80*. The experiment was performed as described for the *cdc7^{ts} pho80* strain (**Fig. 47**A). The FACS profiles of two independent experiments showed the typical stages we observed before with a prominent G2 peak of logarithmically growing cells, an arrest in G2/M phase after nocodazole treatment, an almost complete arrest in late G1 phase at the restrictive temperature and the release into the cell cycle at the permissive temperature with a more or less uniform peak of S phase cells between 15 to 30 min after release (**Fig. 48**A). Syn-

chronized release of *cdc7^{ts} PHO80* cells did not lead to a transient reassembly of histones along the *PHO5* and *PHO8* promoter during the time of S phase 15 min to 30 min after release (**Fig. 48**B). We could observe again an increase in H3 ChIP signal after arrest at the restrictive temperature as already mentioned above for ChIP analysis of *cdc7^{ts} pho80* cells, again probably due to higher cross-linking efficiency. All analyzed loci, the actin control and both *PHO* promoters, behaved similar in the first ChIP experiment (**Fig. 48**B upper graph). For unknown reasons, in the second ChIP experiment all loci showed a peak in H3 ChIP signal at 45 min. As this happened also at the control locus *ACT1*, it was probably not biologically meaningful but due to technical issues, e.g., recovery efficiency of IP-DNA.

We conclude that we were able to monitor a transient histone reassembly at the *PHO5* and the *PHO8* promoters that occurred during replication in S phase. We could confirm our previous results of a histone peak only during S phase that we saw in hydroxyurea synchronized *pho80* cells also in cells synchronized with a combinatorial approach of nocodazole and Cdc7 inactivation. There was a similar signal of histone reassembly over both promoters during replication. This finding of a replication dependent transient histone reassembly correlates nicely with our result that replication hinders chromatin opening (3.9.1) and represents an obstacle for chromatin remodeling. Follow up experiments could include the search for cofactors that are necessary to keep the chromatin open or to re-open it again.

4   Discussion

In yeast, and probably also in other organisms, there appear to be two general strategies of promoter chromatin architecture (Tirosh and Barkai 2008; Cairns 2009). The chromatin structure at open promoters is preset for constitutive transcription as binding sites for regulatory factors are located in linker regions and therefore freely accessible. In contrast, covered promoters, like the *PHO5* promoter, often depend more on chromatin remodeling for induction as functional elements (e.g., UAS or TATA) are intranucleosomal, i.e. less accessible and need to be "freed up" (1.1.5, **Fig. 49**) (Rando and Chang 2009). The covered promoters are especially interesting, as they comprise the inducible promoters. So in order to understand the basis for switching genes on and off we need to study the mechanism of chromatin remodeling upon induction of such a covered promoter.
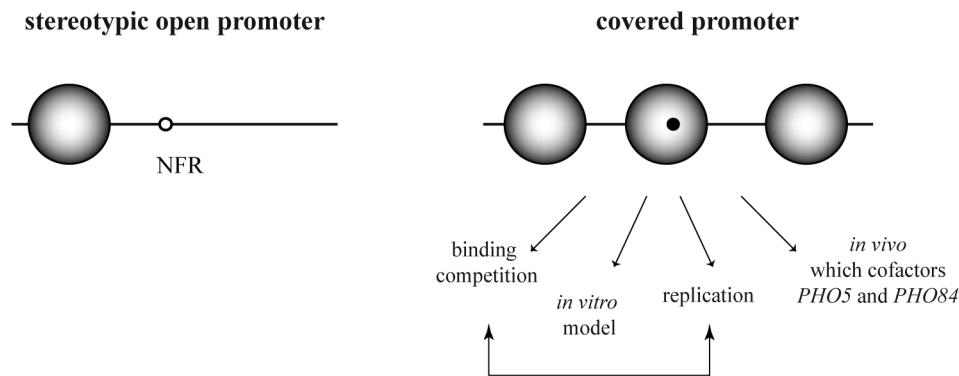
Fig. 49 Open and covered promoter structure. Open promoter: housekeeping genes with TATA-less promoters that are characterized by a canonical NFR (nucleosome free region) upstream of their TSS (transcriptional start site). Covered promoter: stress-responsive, TATA-containing genes that are noisily expressed and regulated by chromatin remodeling factors. Promoters are often occupied by nucleosomes (Rando and Chang 2009). Large circles denote nucleosomes, small circles functional DNA elements.

4.1   Methodological approach: Is it possible to reconstitute *PHO5* and *PHO8* promoter chromatin remodeling *in vitro*?

4.1.1   Need for a tool that biochemically dissects the chromatin remodeling mechanism *in vitro*

After a long series of *in vivo* studies there are still open questions regarding chromatin remodeling at the *PHO5* promoter upon induction. The redundancy of remodeling cofactors especially at this promoter makes it difficult to dissect the mechanism *in vivo* (Barbaric et al. 2007). *In vivo* deletion studies can hardly affect sufficiently many cofactors in order to dissect their roles at the *PHO5* promoter without severely compromising cell viability at the same time leading to multiple side effects. In

contrast, an *in vitro* remodeling system that recapitulates promoter chromatin remodeling is promising as effects of titrated purified cofactors could be determined directly.

4.1.2 First success: Generation of a hypersensitive site is Pho4- and ATP-dependent

We used chromatin reconstitution by salt gradient dialysis and initiated shifting of nucleosomes to their *in vivo* position by addition of energy, yeast extract and remodeling cofactors. As the standard shifting reaction led to the repressed nucleosomal pattern of both promoters it showed that the yeast extract contained factors to position the nucleosomes along the DNA but that it could not initiate remodeling to hypersensitive sites that are typical for the induced promoter states. Therefore this *in vitro* system offered the advantage to add individual components into the system and to observe directly their influence on remodeling.

Using a careful titration of chromatin, energy, yeast extract and the essential transcription factor Pho4, also in combination with Pho2, we saw the generation of a DNaseI hypersensitive site and an increase in ClaI-accessibility at the *PHO5* promoter. Both methods confirmed that this remodeling was Pho4- and energy-dependent. The essential role of energy points to a role for at least one ATP-dependent chromatin remodeler in this process. *In vivo* data already suggested the remodeling complexes Snf2 and Ino80 (Neef and Kladde 2003; Dhasarathy and Kladde 2005; Barbaric et al. 2007). Therefore, this *in vitro* system principally provides the opportunity to recapitulate the mechanism of the transition from the positioned to the remodeled *PHO5* promoter nucleosomes.

We tried to study explicitly the effect of the chromatin remodeling complexes RSC, SWI/SNF and Ino80 on *PHO5* promoter chromatin opening in this *in vitro* system. There was a moderate increase in remodeling *in vitro* upon addition of RSC and SWI/SNF, but the effects were too small to allow robust mechanistic conclusions. This may be due to the use of a whole cell yeast extract that is full with activating as well as inhibiting factors that could occlude the substrate or a special binding site. Further the temporal or spatial order of cofactors as it may exist in the nucleus is not given, the factors are "turned loose". Future experiments involving fractionation of the extract and use of more purified components should help to directly assess the mechanistic contribution of cofactors. This may also increase the remodeling potential of the *in vitro* system, which was so far suboptimal as chromatin at the *PHO5* promoter could not be remodeled as completely as *in vivo* and chromatin at the *PHO8* and *PHO84* promoters hardly at all.

4.1.3 Suboptimal remodeling conditions *in vitro* cannot completely recapitulate remodeling *in vivo*

So up to now, there are still some drawbacks and limitations to the *in vitro* system. The *PHO5* promoter chromatin pattern *in vitro* was very similar to *in vivo*-like promoter nucleosome positions in the repressed as well as in the remodeled state. But the *in vivo* pattern of nuclei from induced cells showed a broader and more homogeneous distribution of hypersensitivity along the region of interest

whereas chromatin remodeled *in vitro* displayed more distinct bands and was overall less accessible. Even more strikingly, this lower extent of remodeling at *PHO5* could not be observed at the *PHO8* and *PHO84* promoters; both showed hardly any Pho4-dependent remodeling *in vitro*. These limitations could so far not be overcome, despite a wide range of approaches to increase the remodeling potential in the *in vitro* system.

Even though the *PHO5* and *PHO8* promoters establish a transient hyperacetylation during chromatin opening *in vivo* (Reinke et al. 2001; Reinke and Horz 2003) and strongly depend on the HAT Gcn5 (Gregory et al. 1998b; Barbaric et al. 2001), we were not able to recapitulate the acetyl CoA-dependency of chromatin remodeling *in vitro*. Treatment with acetyl CoA and Gcn5 did modify the chromatin substrates *in vitro* but did not increase remodeling. Maybe this is related to the finding that Gcn5 is not absolutely necessary for opening of the *PHO5* promoter also *in vivo* (Barbaric et al. 2001)? Or the transient hyperacetylation is part of a more complex temporal order of events that was not recapitulated in the extract system. Further, we wondered if the Gcn5 independency was the result of the heterologous source of histones, i.e. the use of *Drosophila* embryo histones. Nonetheless, we reconstituted chromatin with *Drosophila* embryo histones, recombinant *Drosophila* histones and recombinant yeast histones. The repressed nucleosomal pattern could be established with all three histone preparations *in vitro* although yeast histones gave the most unclear pattern. This indicates that pre-existing modifications of *Drosophila* embryo histones do not inhibit the system and that these modifications are not needed as the pattern is generated also with recombinant histones from two different species. The same is true for comparing the remodeling degree upon addition of Pho4 *in vitro*. All tested histones permitted remodeling to a similar degree. In the future it may be worthwhile to also test purified endogenous yeast histones which may carry modifications that are important for remodeling and could not be set properly by the yeast extract *in vitro*.

Chromatin remodeling upon induction of the *PHO5* promoter proceeds via complete unfolding of nucleosomes and subsequent loss of histones from the promoter region by an eviction in *trans* (Boeger et al. 2003; Reinke and Horz 2003; Boeger et al. 2004; Korber et al. 2004). This eviction is rather complete, on average only one nucleosome remains at the promoter (Jessen et al. 2006). It remains to be elucidated if remodeling in our *in vitro* assay also led to histone-free regions, or to persistently altered nucleosomes or nucleosome sliding. In this context, we tested nonspecific competitor DNA as possible histone acceptor, which was suggested by previous *in vitro* remodeling studies (Workman and Kingston 1992), but found only minor effects. This was not necessarily expected as nonspecific DNA could not only capture evicted histones, but also compete away remodeling factors or Pho4 and thereby inhibit remodeling. Further, the yeast whole cell extract contains already large amounts of RNA, e.g., tRNA (**Fig. 31**B), which may already provide unspecific histone acceptor function. The actual histone acceptor *in vivo* is not known yet, although it seems likely that histone chaperones are involved. At the *PHO5* promoter the H3/H4 chaperone Asf1 is involved in induction kinetics (Adkins et al. 2004; Korber et al. 2006). However, this role is confounded by the essential dependency of the

HAT Rtt109 on Asf1 and its role in *PHO5* promoter activation (Williams et al. 2008; Wippo et al. 2009). Supplementation of the *in vitro* system with purified histone chaperones could help to identify dedicated chaperones.

One further interesting aspect was the difference in remodeling extent of *in vitro* chromatin templates with varying assembly degrees. Maximally assembled chromatin (further increase of histone concentration would result in chromatin aggregation) was refractory to Pho4-induced remodeling even at the *PHO5* promoter, whereas less tightly assembled chromatin responded more readily. As the templates are circular plasmids, nucleosome movement upon remodeling would be more restricted with tightly assembled chromatin whereas more loosely assembled nucleosomes would be conducive to remodeling. A similar observation was made before in the group of Gernot Längst, such that not the highest assembly degrees of salt gradient dialysis chromatin, but a bit less assembled templates are used routinely for *in vitro* remodeling assays (personal communication Gernot Längst (University Regensburg, Germany)). The reason for the inhibition by too highly assembled chromatin could involve unspecific binding of excess histones to the highly assembled template, superhelicity of the DNA distorting the double helix which may prevent a potential remodeling enzyme to bind or generate its required conformation for binding, and possibly the formation of some sort of repressive higher order structure of chromatinized plasmids. Preliminary *in vitro* results with the *PHO84* promoter already suggested the importance of an optimal assembly degree as there was chromatin remodeling with rather low assembly degrees in contrast to the lack of remodeling at standard assembly degrees. This aspect will be followed up in the future.

While successful chromatin remodeling at the *PHO5* promoter upon addition of energy, yeast extract and transcription factor was relatively straightforward to achieve, it proved much more difficult to enhance this remodeling at the *PHO5* promoter or induce it at all at the *PHO8* promoter. It is striking how stable and robust the nucleosomes in these chromatin templates were if one considers that nucleosomes are highly dynamic *in vivo*. For example, G1-arrested yeast cells exhibit a high H3 turnover at promoter regions of active genes, which transiently exposes nucleosome-covered binding sites or erases posttranslational histone marks (Dion et al. 2007). Also histone H2B is constantly reassembled at promoters and at coding regions independent of replication (Jamai et al. 2007). Truncated proteins of H2A and H3 without the N-terminal tail behave similar and imply that replication-independent histone incorporation functions without the histone tail (Jamai et al. 2007). Further, not only *in vivo*, but also *in vitro* remodeling is usually readily achieved, even regardless of the template. A recent publication characterized *in vitro* assembled nucleosomes at four different sequences, the synthetic strong positioning sequences 601 and TPT and the naturally occurring 5S and ARB (arbitrary bacterial plasmid) sequences. All assemblies were easily remodeled by different chromatin remodeling enzymes regardless of the intrinsic stability of nucleosomes assembled at the high- or low-affinity positioning sequences (Partensky and Narlikar 2009). What prevents remodeling of the *PHO8* promoter nucleosomes in our *in vitro* system, even though the extract is rich in remodeling activities (Korber and Horz

2004) and was even supplemented with purified remodelers? Apparently, some factors in the yeast extract could occlude binding sites and thereby inhibit effective remodeling or induce the generation of aggregates. Or maybe nucleosomes, especially at the *PHO8* promoter, are too stable and need a specific activity that is missing in the *in vitro* system.

4.1.4   Surprising at first: A hypersensitive site at the *PHO5* promoter is observed also without the activation domain of Pho4

Using the truncated version of the transcription factor Pho4 without the activation domain in our *in vitro* remodeling assay led to the generation of a hypersensitive site at the *PHO5* promoter very much as observed with wild type Pho4. This contradicted *in vivo* studies on the strict dependency of promoter remodeling on the activation domain (Svaren et al. 1994; McAndrew et al. 1998), which possibly recruits chromatin remodeling activities to the promoter region. Genome-wide microarray gene expression analysis showed a down-regulation of *PHO* responsive genes in a yeast strain lacking SWI/SNF activity (Sudarsanam et al. 2000). Indeed, several subunits of the SWI/SNF complex interact with transcriptional activators. Each of the subunits Snf5, Swi1 and Swi2 (=Snf2) directly binds to the activation domain of Pho4 (Neely et al. 2002). Concomitantly, the yeast HAT complexes SAGA and NuA4 also interact with acidic activation domains (Utley et al. 1998; Brown et al. 2001). HAT activity of Gcn5 contributes to the rate of *PHO5* and *PHO84* induction but has no influence on the final level of expression (Barbaric et al. 2001; Wippo et al. 2009). SAGA recruitment to the *PHO5* promoter was directly demonstrated and depends on induction conditions and Pho4 (Barbaric et al. 2003). *In vitro* reconstitution strongly suggested that SWI/SNF and SAGA, once recruited by transcriptional activators, can occupy a locus independently of transcription factors but via bromodomains of their subunits binding acetylated histones (Hassan et al. 2002). So it seems that the function of the activation domain is mainly required to initiate the increase of local concentration of cofactors at the promoter. It may well be that our extract system provided sufficiently high bulk concentration of cofactors so that the recruitment function of the activation domain was not required. However, this interpretation remains speculative at the moment until careful titration studies may clarify this point. In this view it is especially unresolved why an unphysiological high bulk concentration of remodelers could still not remodel *PHO8* and *PHO84* promoter chromatin. In any case, the *in vitro* system has to be developed further to not only recapitulate the basics of chromatin remodeling but also the complexities that involve transactivation domain dependency, histone dynamics, histone modifications - especially acetylation of histones - that play a main part in remodeling *in vivo*. To refine the *in vitro* system in order to get the whole picture with all involved cofactors of *PHO5* and *PHO8* promoter chromatin remodeling is a future challenge.

4.2   What is the consequence of the intranucleosomal location of an UAS element?

PHO5 promoter chromatin remodeling *in vitro* was not dependent on the activation domain. This suggested that maybe the mere binding of Pho4 to UASp2 could trigger remodeling of nucleosome -2 provided that the bulk concentration of remodelers was sufficiently high. So we wondered if binding competition between Pho4 and histones was mechanistically important. In this context it was striking that *PHO5* promoter chromatin could be remodeled quite effectively *in vitro* whereas *PHO8* and *PHO84* promoter chromatin did not respond to the same treatment. One major aspect that differentiates the *PHO5* promoter from the *PHO8* and *PHO84* promoters is the intranucleosomal location of a high-affinity UASp element. An *in vivo* approach addressed the specific mechanistic question of the consequence of the intranucleosomal location of an UAS element.

4.2.1   Thy hybrid *PHO84* promoter

During this thesis, we established also the *PHO84* promoter as another example of a covered promoter with two intranucleosomal UASp elements (UASpB and UASpE). Accordingly, *PHO84* promoter chromatin remodeling was dependent on chromatin cofactors, i.e. on Snf2, Ino80, Gcn5 and to a smaller degree on Asf1 (this thesis and Wippo et al. 2009). Interestingly, the *PHO84* promoter harbors two positioned nucleosomes flanking the short hypersensitive site that were differentially dependent on these cofactors. The upstream nucleosome showed a strong dependency on Snf2, whereas the downstream nucleosome could be completely remodeled in the absence of Snf2. A similar effect was observed for Ino80 (Wippo et al. 2009). This differential dependency of neighboring nucleosomes on the same remodeling cofactor is a novelty in the field and was not observed *in vivo* so far. We think that the *PHO84* promoter resembles a hybrid of the *PHO5* and the *PHO8* promoter, consisting of a redundantly remodeled downstream nucleosome as in *PHO5* and a Snf2-dependent upstream nucleosome as in *PHO8*.

Regarding the role for the intranucleosomal UASp elements, *PHO84* promoter chromatin remodeling is not essentially dependent on the UASpB and UASpE elements. Deletion of the intranucleosomal UASpB site had no effect at all, and deletion of UASpE delayed remodeling and decreased somewhat the extent of the hypersensitive site upon induction. Therefore, complete remodeling of both the upstream and the downstream nucleosomes that harbor the UASpB and UASpE elements, respectively, was possible in the absence of these elements (Wippo et al. 2009).

4.2.2   The intranucleosomal UASp element is not just a "problem" to overcome, but also part of the "solution"

UASp sites are DNA elements that are bound specifically by transactivator proteins that mediate further activation processes; so far the role of their location relative to nucleosomes in promoter chromatin remodeling was not fully elucidated.

4.2.2.1 An old discussion

There are many examples of *in vitro* studies exploiting nucleosome remodeling and disassembly by binding competition to intranucleosomal UAS sites. *In vitro* studies using reconstituted mononucleosomes with five intranucleosomal Gal4 binding sites demonstrated that binding of the transcriptional activator protein Gal4 resulted in an unstable ternary complex of Gal4, histone proteins and DNA. Histones in this complex could be transferred onto competitor DNA resulting in disassembled nucleosomes and DNA bound Gal4 (Workman and Kingston 1992). An *in vivo* analysis made use of plasmids containing a stable positioned nucleosome with one central Gal4 binding site. This nucleosome was disrupted upon Gal4 expression, again independent of the activation domain (Morse 1993). Both studies revealed a complete disruption of the nucleosome triggered by binding of Gal4. It was also observed that Gal4 binding was enhanced if multiple Gal4 binding sites were present on the template whereas heat shock factor (HSF) bound to its nucleosomal template only in the presence of TFIID, the TATA binding protein (Taylor et al. 1991). Nucleosome disassembly was enhanced by the addition of the histone chaperone nucleoplasmin that removes H2A-H2B upon Gal4 binding and increases the transfer of H3-H4 onto competitor DNA (Chen et al. 1994). Importantly, this kind of "remodeling" did not involve any remodeling activity and was not dependent on an activation domain. So all in all, these studies suggested a mere binding competition between a DNA binding factor and a nucleosome as the basis for nucleosome remodeling *in vivo*.

Nonetheless, there is no evidence for a role of binding competition in a truly physiological *in vivo* system so far. In contrast, there is ample evidence for the requirement of activation domains and for ATP-dependent remodelers. The major view on the function of activation domains in chromatin remodeling implicates the recruitment of chromatin remodelers and modifiers (Neely et al. 1999; Neely et al. 2002; Morse 2007). This concept is currently the key to explain chromatin remodeling, in contrast to simple DNA binding competition.

The Pho4 activation domain is essential for remodeling at the *PHO5* promoter as the DNA binding domain alone could not bind to intranucleosomal UASp2 or trigger remodeling (Svaren et al. 1994; Venter et al. 1994). Even overexpression of the truncated Pho4 was not able to trigger chromatin disruption, but interestingly overexpression of the full length protein could overcome the difficulties of remodeling *PHO5* without the linker binding site UASp1 (Venter et al. 1994). Therefore, we do not exclude that transient binding of Pho4 to UASp2 within nucleosome -2 may happen, possibly in an altered, transiently accessible nucleosomal state. Recently, an intermediate state of Pho4 occupying

the nucleosome-bound UASp2 element was trapped by slowing down the process of initiation using an *asf1* yeast strain defective in chromatin disassembly (Adkins et al. 2004; Ransom et al. 2009). Maybe such transient binding is part of the remodeling mechanism and even an important part?

There was a recent study on the location and strength of UASp elements. Lam et al (Lam et al. 2008) addressed the location of UASp elements at almost all *PHO* promoters with regard to threshold (onset of induction during kinetics) and promoter strength (maximal transcriptional output). The authors differentiated between Pho4 binding to exposed linker sites of different strength and found that the affinity of linker binding sites determines the threshold, whereas the total number and affinity of accessible sites after full induction correlates with promoter strength. A shortcoming of this analysis was that chromatin remodeling was not sufficiently analyzed. So there were no data to indicate if location and strength of UASp elements affected remodeling extent or efficiency. In fact, the authors missed that remodeling in some of their mutants was incomplete (see below).

4.2.2.2 Our new data

We present evidence for the critical importance of the intranucleosomal location of a transactivator binding site *in vivo*, using different *PHO5* promoter UASp mutants. Our data underline the significance of the intranucleosomal location of the UASp2 site within nucleosome -2 and demonstrate impaired remodeling if there is no intranucleosomal UASp element. Four UASp mutants (ΔUASp2, UASp2-5 Δ2, H1 and H5) were severely affected by the deletion of the intranucleosomal UASp and in the case of the UASp2-5 Δ2, H1 and H5 mutants not even the additional new high-affinity UASp elements in the linker region could compensate. The ΔUASp2 promoter mutant and the H1 mutant were almost not remodeled upon induction. Interestingly, upon induction of the mutant promoters individual nucleosomes showed different degrees of remodeling, uncoupled from the neighboring nucleosomes. Nucleosomes -3 and -4 of the ΔUASp2 and H1 mutant were fully remodeled whereas nucleosomes -1 and -2 hardly at all. This uncoupling of nucleosome remodeling could not always be compensated for by a low-affinity UASp site in the -2 nucleosome (H4 mutant), or by an additional intranucleosomal high-affinity UASp site in the -3 nucleosome (H2 mutant). This observation is made for the first time, as the *PHO5* promoter nucleosomes were thought to become remodeled upon induction in an all or nothing fashion and were therefore also described as a "chromatin microdomain" (Venter et al. 1994; Svaren and Horz 1997). In contrast, our results suggest that nucleosomes -3 and -4 are remodeled more easily from the neighboring UASp1 site, whereas nucleosome -2 requires an internal site for efficient remodeling.

Furthermore we saw clear evidence for the different strengths of engineered UASp elements as the yeast strain YS70 with interchanged UASp elements (natural Pho4 footprint sequence) was able to completely open the promoter (Venter et al. 1994) whereas the analogous swap mutant H4 (point mutated UASp elements) was not remodeled to the same extent. Similarly, the mutant UASp2-5 Δ2

(high-affinity linker UASp by introduced Pho4 footprint) was somewhat more conducive to remodeling than the H1 mutant (high-affinity linker UASp by point mutation).

Importantly, we saw increased remodeling by binding of a truncated Gal4 activator, i.e. only with the DNA binding domain, to an intranucleosomal Gal4 binding site in nucleosome -2 (strain AH2341, plasmid YCpGal4 (1-147)). This clearly demonstrates that this site need not participate in the recruitment of remodeling cofactors. So we propose that mere binding competition between retention of the nucleosome and stable binding of the activator to its cognate site importantly facilitates remodeling of nucleosome -2. The intranucleosomal site need not be high-affinity as complete remodeling was observed in strain YS70 with swapped UASp elements, i.e. the low affinity UASp1 was intranucleosomal.

Our analysis of the *PHO5* promoter probably represents the first *in vivo* evidence for the contribution of transcription factor-nucleosome binding competition in nucleosome remodeling. This hypothesis does not restrict chromatin remodeling to this mechanism alone but is an additional aspect in addition to the classic view of remodeling by cofactor, especially remodeler, recruitment.

Reminiscent of wild type *PHO8* promoter chromatin remodeling *in vivo* that is accomplished with only one high-affinity binding site in the linker region (Munsterkotter et al. 2000) we also obtained a *PHO5* promoter mutant (UASp2-8 Δ2) that was readily remodeled with an insertion of the strong *PHO8* UASp element in the linker between nucleosomes -2 and -3. Further, forced induction conditions (two times overnight incubation, overexpression of *PHO4*, or *pho80* deletion) eventually remodeled even the promoter mutants H1, H2, and UASp2-5 Δ2. Surprisingly, a change in the yeast strain background (from CY to AH) could even remodel the ΔUASp2 mutant. After all, we agree with previous opinions that the observed binding competition is not essential for promoter nucleosome remodeling at the *PHO5* promoter, but consider it to be nonetheless a crucial aspect of the wild type remodeling mechanism *in vivo*.

Genome-wide analysis of RSC localization revealed the association of RSC with RNA Pol II promoters and Pol III genes leading to the hypothesis that this remodeler induces changes in chromatin structure to help transcription (Ng et al. 2002). This picture was strengthened by results demonstrating the involvement of RSC in the process of transcription *in vivo* (Parnell et al. 2008). Cryo-EM analysis discovered that RSC, when associated to chromatin, exists as RSC-nucleosome complex with a nucleosome bound in the central cavity of the remodeler. Interestingly, the RSC-nucleosome complex seems to have only one H2A-H2B dimer left (Chaban et al. 2008). Very recently a mechanism for RSC remodeling has been proposed that described the binding of RSC to the nucleosome and a subsequent release of the DNA from the histone surface as initial event for DNA translocation. The deep cavity of the remodeler encloses the nucleosome and it was suggested that entry into the cavity promotes unwrapping of the nucleosomal DNA (Lorch et al. 2010). The Kornberg lab offered the hypothesis that the removal of nucleosomes at the *PHO5* promoter could involve sliding-mediated histone disassembly (Boeger et al. 2008). They combined biochemical analyses with modeling based on basic

assumptions and propose that a remodeler like RSC might bind one nucleosome and slide along the promoter during association with the nucleosome thereby displacing adjacent nucleosomes. This sliding-mediated nucleosome disassembly would result in one nucleosome remaining bound by the remodeler on the promoter. Previous studies showing on average one nucleosome left on the fully induced promoter region support this model (Boeger et al. 2003; Boeger et al. 2004; Korber et al. 2004; Boeger et al. 2008). Nonetheless, our results suggest that nucleosome -2 is less efficiently remodeled if the intranucleosomal UASp element is missing, which would amount to an obstacle for the sliding RSC-nucleosome complex. Therefore, we consider especially for nucleosome -2 a remodeling mechanism that entails binding competition of nucleosome and Pho4, which is not part of the hypothesis of sliding-mediated nucleosome disassembly and may call for a modified model.

4.2.3   So maybe a window of opportunity for Pho4 binding to UASp2 could help during replication?

As our new data suggested the importance of a high-affinity intranucleosomal binding site, we considered the impact of replication on promoter chromatin remodeling. Replication could help chromatin remodeling by displacing nucleosomes from the promoter region thereby, maybe through a window of opportunity, enabling binding of Pho4 to UASp2.

4.2.3.1 No! Replication is rather a hindrance

The Hörz lab discovered that nucleosome remodeling at the *PHO5* promoter could be uncoupled from the process of DNA replication (Schmid et al. 1992). In our experiments using H3 ChIP analysis early induction time points showed a faster histone loss of *PHO5* and *PHO8* promoter nucleosomes in non-replicating compared to replicating yeast cells. We therefore suggest that replication imposes a hindrance for chromatin remodeling that resets nucleosomes, at least in part, to the closed state (**Fig. 50**).
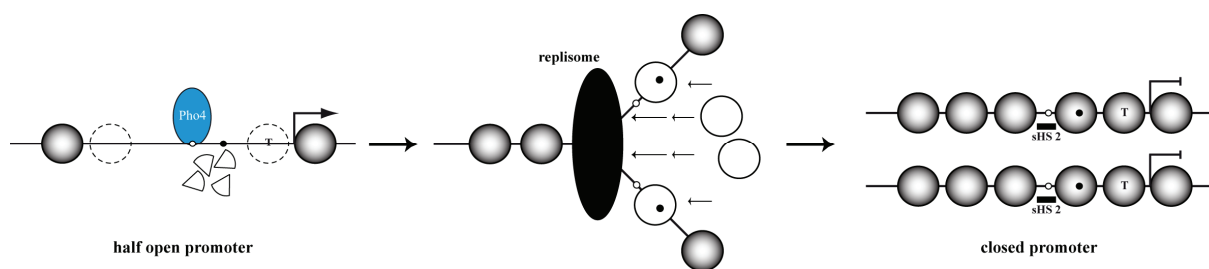
Fig. 50 Replication resets promoter chromatin structure. Upon replication fork passage promoter chromatin gets disturbed and active processes leading to promoter opening are interrupted. After DNA replication the chromatin structure is reset to its initial state.

By analyzing synchronized yeast cells we observed a transient peak of histone H3 reassembly during the time of replication in S phase at constitutively open *PHO5* and *PHO8* promoters (*pho80* background). The replication-dependent transient histone reassembly and our result that replication

hinders chromatin opening complement each other and identify the process of replication as an obstacle for chromatin remodeling.

4.2.3.2 Open questions

So called "kinetic effect" mutants that cause a kinetic delay in chromatin opening at the *PHO5* and *PHO8* promoters could be the result of this replication hindrance. This raised the question if these mutants would catch up on the rate of chromatin opening, resembling wild type induction kinetics, if replication was blocked. If this turned out to be true the task of the cofactor would be rather specific to antagonize or even overcome the replication-coupled re-setting of promoter chromatin. Cofactor candidates are Ino80 and Snf2. Mutation of either factor resulted in a kinetic delay of *PHO5* induction (Barbaric et al. 2007). Furthermore, Ino80 was found to be involved in progression of replication forks and replisome stability which could explain *PHO5* induction defects in *ino80* strains (Papamichos-Chronakis and Peterson 2008).

A lot of data has been collected on the mechanism of replication, but recent studies particularly address the inheritance of epigenetic information during S phase. Upon passage of the replication fork, parental histones and newly synthesized histones have to be re-assembled into chromatin on the sister chromatids. This assembly meets two demands: inheritance of epigenetic information in daughter cells and maintenance of genome integrity (Groth et al. 2007b). Replication-coupled memory is now thought to happen via PCNA as central anchor point that forms the bridge between replication (DNA polymerase processivity factor) and chromatin restoration (epigenetic inheritance). PCNA interacts with several chromatin modifiers (CAF1, DNMT1, HDACs and WSTF-SNF2h) and recruits them to replication sites (Groth et al. 2007b, Probst et al. 2009 and references therein). Additionally, all of these factors have the potential to recruit further enzymes involved in chromatin maturation. PCNA and CAF1 persist on replicated DNA for 20 min and possibly enable during this time window the re-setting of posttranslational modifications onto the newly synthesized histones. This is an important aspect during epigenetic inheritance. It is thought that marks on neighboring parental histones represent a template for this purpose (Groth 2009; Probst et al. 2009). Follow up experiments of the replication-dependent transient histone reassembly could include the search for cofactors that are necessary to keep the chromatin open or to re-open it again which would also touch on the subject of chromatin inheritance at the *PHO* promoters. Analyzing a potential difference of re-assembled histones after replication, either after the promoter was open or not prior to replication, may enhance the understanding of "epigenetic memory" in yeast.

Additionally we should think about a mechanistic differentiation of remodeling the *PHO5* promoter in different stages of the cell cycle. *PHO5* activation during mitosis was shown to be dependent on SWI/SNF and Gcn5 (Krebs et al. 2000; Neef and Kladde 2003). Considering the condensed state of mitotic chromatin it was shown that SWI/SNF and Gcn5 are a critical part of gene expression during this stage of the cell cycle (Krebs et al. 2000). Recently, studies on the mechanism that mediates the

mitotic induction of *PHO5* found further activators to bind at the *PHO5* promoter, namely Mcm1, Fkh1 and Fkh2. Mcm1 is part of a network of proteins controlling the cell cycle and gene activation in G2/M phase and is essential for *PHO5* induction with Pho4 and Pho2 and either of the Fkh proteins in late M/G1 (Pondugula et al. 2009).

After all these years of *PHO5* research it is amazing how novel aspects of the mechanisms of chromatin remodeling and *PHO5* induction, like the role of the intranucleosomal location of an UASp element or the new factors Mcm1 and Fkh1/2, keep coming up.

5   Supplementary material

A

B

C

D
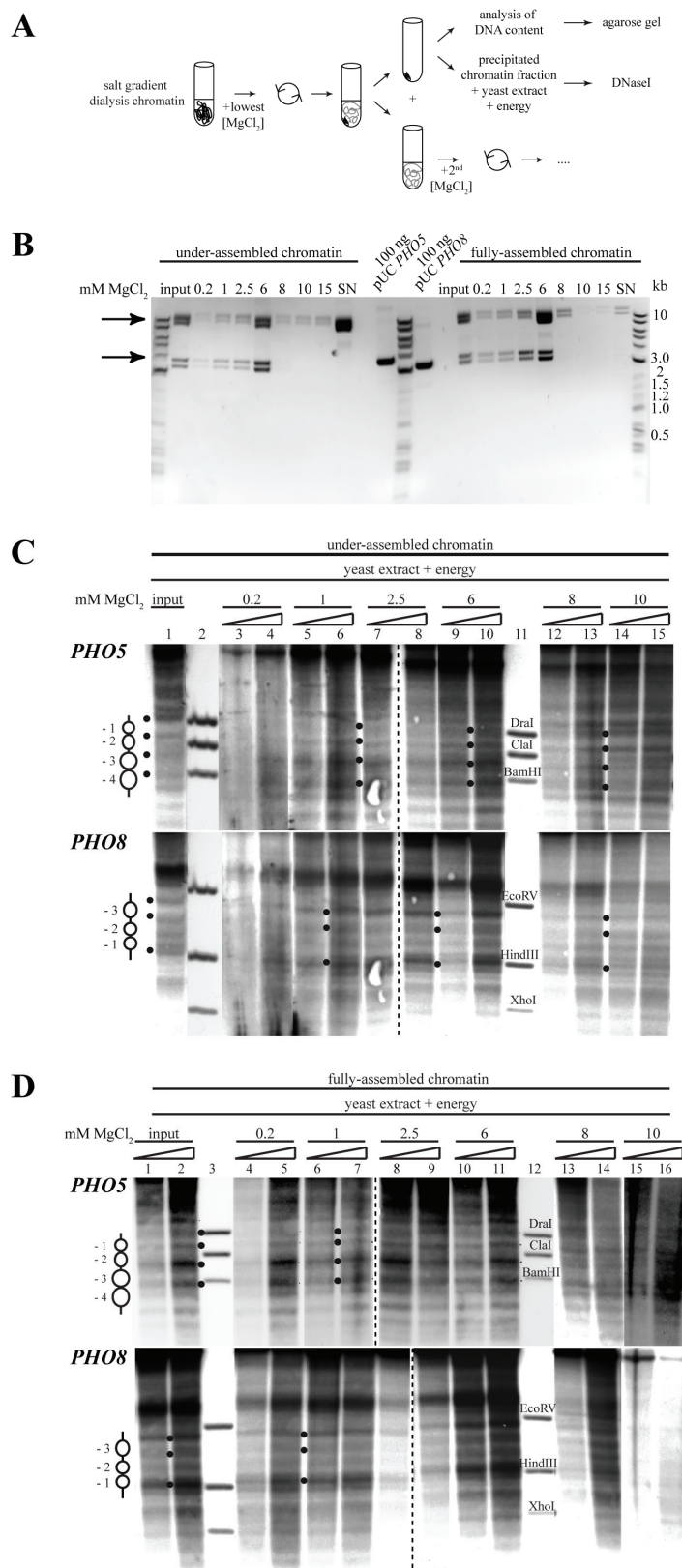
Supp. Fig. 1 Differential MgCl$_2$ precipitation of under- or fully-assembled salt gradient dialysis chromatin and subsequent shifting to the repressed state *in vitro* did not increase the quality of the nucleosomal pattern. (A) Experimental scheme: salt gradient dialysis chromatin (under- or fully-assembled) was precipitated with the lowest MgCl$_2$ concentration, incubated on ice and centrifuged. This resulted in a chromatin pellet and non-precipitated chromatin in the supernatant. The supernatant was transferred into a new tube and treated with the next higher MgCl$_2$ concentration. The procedure was repeated with increasing concentrations of MgCl$_2$. The DNA content was analyzed on an agarose gel and the precipitated chromatin was shifted to the closed nucleosomal pattern by incubation with yeast extract and energy. (B) Analysis of the distribution of salt gradient dialysis chromatin after differential MgCl$_2$ precipitation. Agarose gel electrophoresis of proteinase K-, RNase A-digested and ethanol-precipitated salt gradient dialysis chromatin that was precipitated with indicated MgCl$_2$ concentrations on top of the gel. Upper arrow points to the nicked form of the plasmids. Lower arrow points to the supercoiled plasmids. For each form double bands occur due to a difference in size of the *PHO5* and *PHO8* plasmid. (C) DNaseI indirect end-labeling analysis of the *PHO5* and *PHO8* promoter regions in under-assembled chromatin treated as indicated on top of the lanes after pre-assembly by salt gradient dialysis and differential MgCl$_2$ precipitation. The blot showing the *PHO8* promoter is the same as the *PHO5* blot but re-hybridized for the *PHO8* promoter region. See **Fig. 17**A and B for description of dots, ramps and marker bands. (D) Same analysis as in panel C but with fully-assembled chromatin.
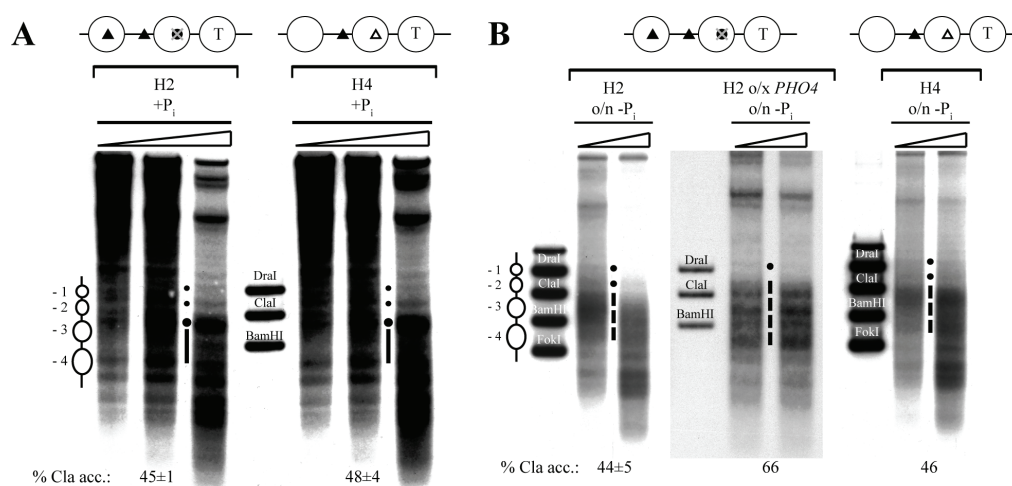
Supp. Fig. 2 The intranucleosomal location of a UASp element in the -2 nucleosome is important but not essential for *PHO5* promoter chromatin opening *in vivo*. DNaseI indirect end-labeling analysis of the *PHO5* promoter region in strains with the following *PHO5* promoter configuration: H2 (CY337 EB1500) and H4 (CY337 EB1626). (A) Logarithmically growing cells in phosphate-rich (+P$_i$) medium. (B) After overnight (o/n) incubation in phosphate-free (-P$_i$) medium and for H2 one experiment with overexpression (o/x) of *PHO4* is shown. See **Fig. 35** for explanation of schematics and **Fig. 38** for description of dots and stippled vertical lines and **Fig. 17**A for ramps, marker bands and schematics next to the gels.
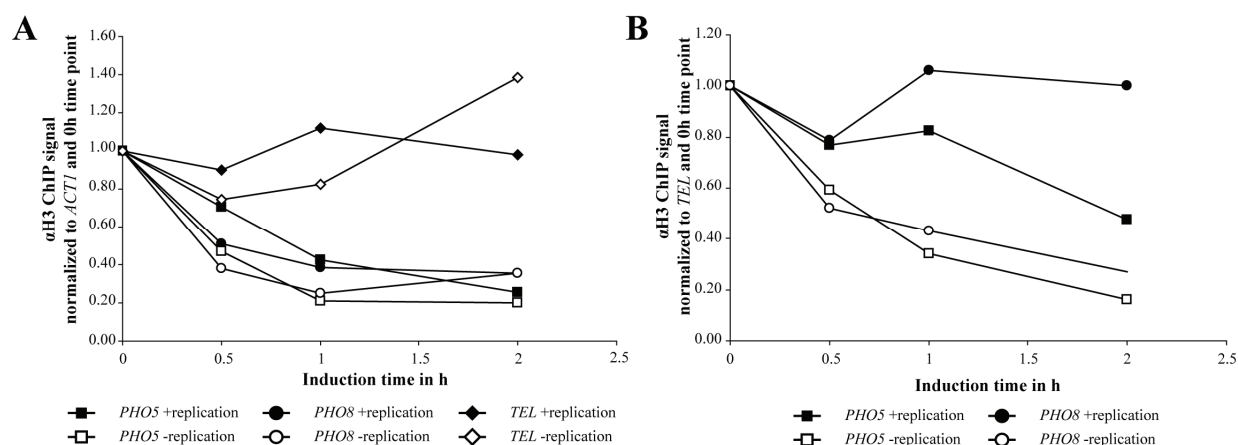
Supp. Fig. 3 Histones were depleted faster from the *PHO5* and *PHO8* promoters in non-replicating cells than in replicating cells *in vivo*. Histone H3 ChIP kinetics are as in **Fig. 45**. Shown are two biologically independent experiments (A) and (B). The H3 ChIP signal was normalized to input DNA and 0 h time point of induction and to the *ACT1* amplicon (A) or to the *TEL* amplicon (B).

A

pho80   *pho4*

PE-A: Sytox Green   PE-A: Sytox Green

cycling cells   cycling cells
2h HU   1.5h HU
4h HU   3h HU
wash   wash
15min release   15min release
30min release   30min release
45min release   45min release
1h release   1h release
1h15min release   1h15min release
1h30min release

cell number

1n 2n   1n 2n
S phase   S phase

B

pho80 H3 ChIP

pho4 H3 ChIP
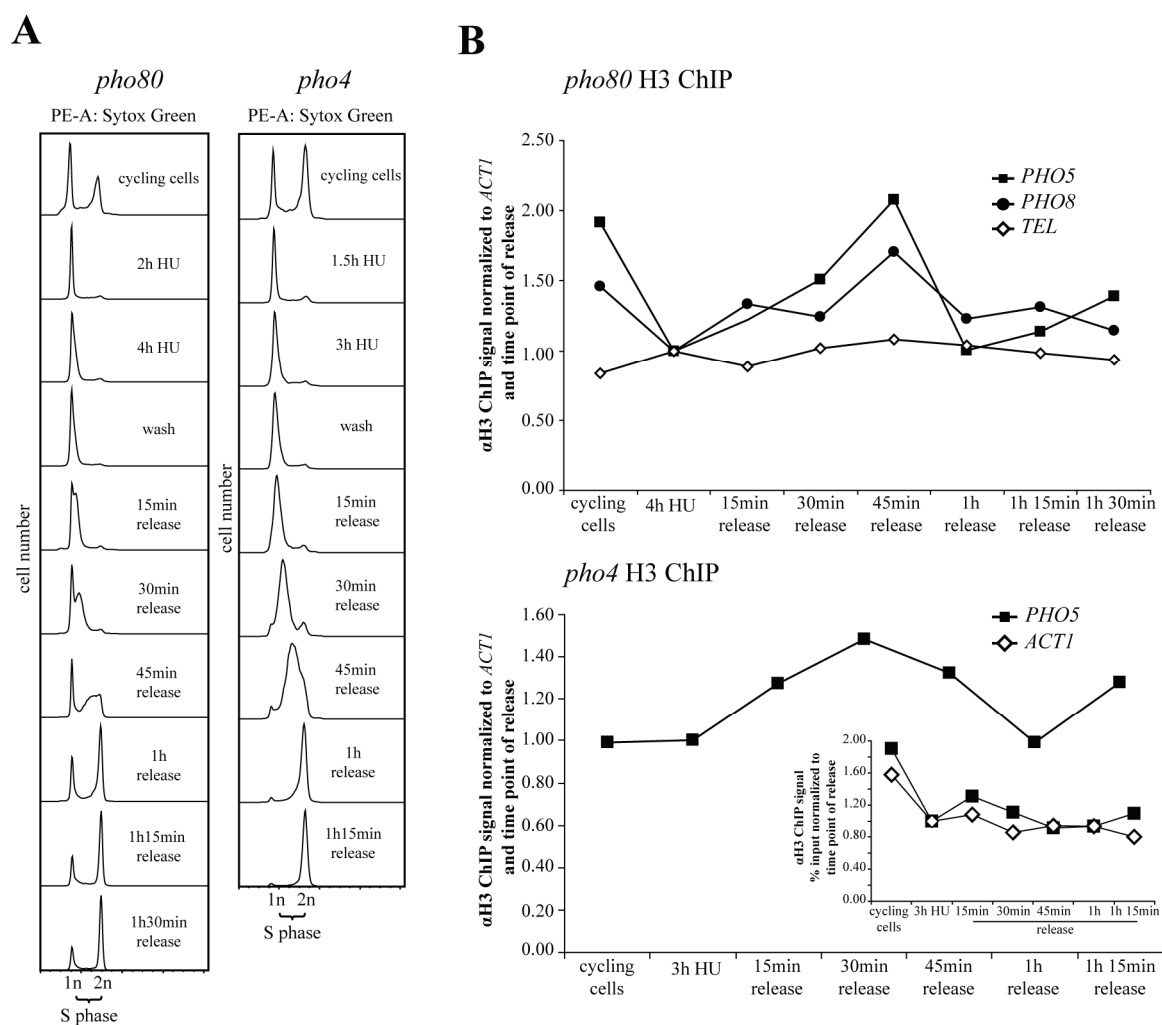
Supp. Fig. 4 Histone reassembly during replication in hydroxyurea synchronized *pho80* but not *pho4* cells. Experimental set up as in **Fig. 46**. (A) FACS analysis of the DNA content of cycling *pho80* and *pho4* cells, cells that were arrested with HU and cells that were released into the cell cycle after HU arrest. (B) Histone H3 ChIP kinetics of histone occupancy of HU synchronized *pho80* cells (upper ChIP profile) and *pho4* cells (lower ChIP profile). The H3 ChIP signal was normalized to input DNA, the actin control locus and the time point of release. The inset shows an alternative analysis plotting the ChIP signal normalized to % input and the time point of release for *pho4* cells. Legend in the graph shows analyzed loci: *PHO5* (closed squares), *PHO8* (closed circles), *TEL* or *ACT1* (open diamonds).

6   References

Adkins, M. W., S. R. Howar and J. K. Tyler. 2004. "Chromatin disassembly mediated by the histone chaperone Asf1 is essential for transcriptional activation of the yeast PHO5 and PHO8 genes." Mol Cell 14(5): 657-666.

Adkins, M. W. and J. K. Tyler. 2006. "Transcriptional activators are dispensable for transcription in the absence of Spt6-mediated chromatin reassembly of promoter regions." Mol Cell 21(3): 405-416.

Akhtar, A., D. Zink and P. B. Becker. 2000. "Chromodomains are protein-RNA interaction modules." Nature 407(6802): 405-409.

Albert, I., T. N. Mavrich, L. P. Tomsho, J. Qi, S. J. Zanton, S. C. Schuster and B. F. Pugh. 2007. "Translational and rotational settings of H2A.Z nucleosomes across the Saccharomyces cerevisiae genome." Nature 446(7135): 572-576.

Almer, A., H. Rudolph, A. Hinnen and W. Horz. 1986. "Removal of positioned nucleosomes from the yeast PHO5 promoter upon PHO5 induction releases additional upstream activating DNA elements." EMBO J 5(10): 2689-2696.

Alvino, G. M., D. Collingwood, J. M. Murphy, J. Delrow, B. J. Brewer and M. K. Raghuraman. 2007. "Replication in hydroxyurea: it's a matter of time." Mol Cell Biol 27(18): 6396-6406.

Babu, M. M., S. C. Janga, I. de Santiago and A. Pombo. 2008. "Eukaryotic gene regulation in three dimensions and its impact on genome evolution." Curr Opin Genet Dev 18(6): 571-582.

Bao, Y. and X. Shen. 2007. "INO80 subfamily of chromatin remodeling complexes." Mutat Res 618(1-2): 18-29.

Barbaric, S., K. D. Fascher and W. Horz. 1992. "Activation of the weakly regulated PHO8 promoter in S. cerevisiae: chromatin transition and binding sites for the positive regulatory protein PHO4." Nucleic Acids Res 20(5): 1031-1038.

Barbaric, S., T. Luckenbach, A. Schmid, D. Blaschke, W. Horz and P. Korber. 2007. "Redundancy of chromatin remodeling pathways for the induction of the yeast PHO5 promoter in vivo." J Biol Chem 282(38): 27610-27621.

Barbaric, S., M. Munsterkotter, C. Goding and W. Horz. 1998. "Cooperative Pho2-Pho4 interactions at the PHO5 promoter are critical for binding of Pho4 to UASp1 and for efficient transactivation by Pho4 at UASp2." Mol Cell Biol 18(5): 2629-2639.

Barbaric, S., M. Munsterkotter, J. Svaren and W. Horz. 1996. "The homeodomain protein Pho2 and the basic-helix-loop-helix protein Pho4 bind DNA cooperatively at the yeast PHO5 promoter." Nucleic Acids Res 24(22): 4479-4486.

Barbaric, S., H. Reinke and W. Horz. 2003. "Multiple mechanistically distinct functions of SAGA at the PHO5 promoter." Mol Cell Biol 23(10): 3468-3476.

Barbaric, S., J. Walker, A. Schmid, J. Q. Svejstrup and W. Horz. 2001. "Increasing the rate of chromatin remodeling and gene activation--a novel role for the histone acetyltransferase Gcn5." EMBO J 20(17): 4944-4951.

Bassett, A., S. Cooper, C. Wu and A. Travers. 2009. "The folding and unfolding of eukaryotic chromatin." Curr Opin Genet Dev 19(2): 159-165.

Becker, P. B. and W. Horz. 2002. "ATP-dependent nucleosome remodeling." Annu Rev Biochem 71: 247-273.

Boeger, H., D. A. Bushnell, R. Davis, J. Griesenbeck, Y. Lorch, J. S. Strattan, K. D. Westover and R. D. Kornberg. 2005. "Structural basis of eukaryotic gene transcription." FEBS Lett 579(4): 899-903.

Boeger, H., J. Griesenbeck and R. D. Kornberg. 2008. "Nucleosome retention and the stochastic nature of promoter chromatin remodeling for transcription." Cell 133(4): 716-726.

Boeger, H., J. Griesenbeck, J. S. Strattan and R. D. Kornberg. 2003. "Nucleosomes unfold completely at a transcriptionally active promoter." Mol Cell 11(6): 1587-1598.

Boeger, H., J. Griesenbeck, J. S. Strattan and R. D. Kornberg. 2004. "Removal of promoter nucleosomes by disassembly rather than sliding in vivo." Mol Cell 14(5): 667-673.

Bonaldi, T., A. Imhof and J. T. Regula. 2004. "A combination of different mass spectroscopic techniques for the analysis of dynamic changes of histone modifications." Proteomics 4(5): 1382-1396.

Bonisch, C., S. M. Nieratschker, N. K. Orfanos and S. B. Hake. 2008. "Chromatin proteomics and epigenetic regulatory circuits." Expert Rev Proteomics 5(1): 105-119.

Bouazoune, K., A. Mitterweger, G. Langst, A. Imhof, A. Akhtar, P. B. Becker and A. Brehm. 2002. "The dMi-2 chromodomains are DNA binding modules important for ATP-dependent nucleosome mobilization." EMBO J 21(10): 2430-2440.

Bousset, K. and J. F. Diffley. 1998. "The Cdc7 protein kinase is required for origin firing during S phase." Genes Dev 12(4): 480-490.

Brachmann, C. B., A. Davies, G. J. Cost, E. Caputo, J. Li, P. Hieter and J. D. Boeke. 1998. "Designer deletion strains derived from Saccharomyces cerevisiae S288C: a useful set of strains and plasmids for PCR-mediated gene disruption and other applications." Yeast 14(2): 115-132.

Brown, C. E., L. Howe, K. Sousa, S. C. Alley, M. J. Carrozza, S. Tan and J. L. Workman. 2001. "Recruitment of HAT complexes by direct activator interactions with the ATM-related Tra1 subunit." Science 292(5525): 2333-2337.

Cairns, B. R. 2007. "Chromatin remodeling: insights and intrigue from single-molecule studies." Nat Struct Mol Biol 14(11): 989-996.

Cairns, B. R. 2009. "The logic of chromatin architecture and remodelling at promoters." Nature 461(7261): 193-198.

Cairns, B. R., Y. Lorch, Y. Li, M. Zhang, L. Lacomis, H. Erdjument-Bromage, P. Tempst, J. Du, B. Laurent and R. D. Kornberg. 1996. "RSC, an essential, abundant chromatin-remodeling complex." Cell 87(7): 1249-1260.

Chaban, Y., C. Ezeokonkwo, W. H. Chung, F. Zhang, R. D. Kornberg, B. Maier-Davis, Y. Lorch and F. J. Asturias. 2008. "Structure of a RSC-nucleosome complex and insights into chromatin remodeling." Nat Struct Mol Biol 15(12): 1272-1277.

Chen, H., B. Li and J. L. Workman. 1994. "A histone-binding protein, nucleoplasmin, stimulates transcription factor binding to nucleosomes and factor-induced nucleosome disassembly." EMBO J 13(2): 380-390.

Clapier, C. R. and B. R. Cairns. 2009. "The biology of chromatin remodeling complexes." Annu Rev Biochem 78: 273-304.

Corona, D. F., G. Langst, C. R. Clapier, E. J. Bonte, S. Ferrari, J. W. Tamkun and P. B. Becker. 1999. "ISWI is an ATP-dependent nucleosome remodeling factor." Mol Cell 3(2): 239-245.

Corpet, A. and G. Almouzni. 2009. "Making copies of chromatin: the challenge of nucleosomal organization and epigenetic information." Trends Cell Biol 19(1): 29-41.

Cremer, T. and C. Cremer. 2001. "Chromosome territories, nuclear architecture and gene regulation in mammalian cells." Nat Rev Genet 2(4): 292-301.

Cremer, T. and M. Cremer. 2010. "Chromosome territories." Cold Spring Harb Perspect Biol 2(3): a003889.

Cremer, T., M. Cremer, S. Dietzel, S. Muller, I. Solovei and S. Fakan. 2006. "Chromosome territories--a functional nuclear landscape." Curr Opin Cell Biol 18(3): 307-316.

Davis, J. L., R. Kunisawa and J. Thorner. 1992. "A presumptive helicase (MOT1 gene product) affects gene expression and is required for viability in the yeast Saccharomyces cerevisiae." Mol Cell Biol 12(4): 1879-1892.

De Koning, L., A. Corpet, J. E. Haber and G. Almouzni. 2007. "Histone chaperones: an escort network regulating histone traffic." Nat Struct Mol Biol 14(11): 997-1007.

Del Rosario, B. C. and L. F. Pemberton. 2008. "Nap1 links transcription elongation, chromatin assembly, and messenger RNP complex biogenesis." Mol Cell Biol 28(7): 2113-2124.

DePamphilis, M. 2006. "DNA Replication and Human Disease." CSHL Press.

Dhasarathy, A. and M. P. Kladde. 2005. "Promoter occupancy is a major determinant of chromatin remodeling enzyme requirements." Mol Cell Biol 25(7): 2698-2707.

Dion, M. F., T. Kaplan, M. Kim, S. Buratowski, N. Friedman and O. J. Rando. 2007. "Dynamics of replication-independent histone turnover in budding yeast." Science 315(5817): 1405-1408.

Eberharter, A. and P. B. Becker. 2004. "ATP-dependent nucleosome remodelling: factors and functions." J Cell Sci 117(Pt 17): 3707-3711.

Eberharter, A., S. Ferrari, G. Langst, T. Straub, A. Imhof, P. Varga-Weisz, M. Wilm and P. B. Becker. 2001. "Acf1, the largest subunit of CHRAC, regulates ISWI-induced nucleosome remodelling." EMBO J 20(14): 3781-3788.

Eberharter, A., S. John, P. A. Grant, R. T. Utley and J. L. Workman. 1998. "Identification and analysis of yeast nucleosomal histone acetyltransferase complexes." Methods 15(4): 315-321.

Ehrenhofer-Murray, A. E. 2004. "Chromatin dynamics at DNA replication, transcription and repair." Eur J Biochem 271(12): 2335-2349.

English, C. M., M. W. Adkins, J. J. Carson, M. E. Churchill and J. K. Tyler. 2006. "Structural basis for the histone chaperone activity of Asf1." Cell 127(3): 495-508.

Ertinger, G. 1998. "Rolle der Transkriptionsfaktoren bei der Öffnung der Chromatinstruktur am *PHO5*-Promoter in *Saccharomyces cerevisiae*." PhD Thesis, Universität München.

Falbo, K. B. and X. Shen. 2006. "Chromatin remodeling in DNA replication." J Cell Biochem 97(4): 684-689.

Fascher, K. D., J. Schmitz and W. Horz. 1990. "Role of trans-activating proteins in the generation of active chromatin at the PHO5 promoter in S. cerevisiae." EMBO J 9(8): 2523-2528.

Fascher, K. D., J. Schmitz and W. Horz. 1993. "Structural and functional requirements for the chromatin transition at the PHO5 promoter in Saccharomyces cerevisiae upon PHO5 activation." J Mol Biol 231(3): 658-667.

Felsenfeld, G. and M. Groudine. 2003. "Controlling the double helix." Nature 421(6921): 448-453.

Flaus, A., D. M. Martin, G. J. Barton and T. Owen-Hughes. 2006. "Identification of multiple distinct Snf2 subfamilies with conserved structural motifs." Nucleic Acids Res 34(10): 2887-2905.

Fletcher, T. M., B. W. Ryu, C. T. Baumann, B. S. Warren, G. Fragoso, S. John and G. L. Hager. 2000. "Structure and dynamic properties of a glucocorticoid receptor-induced chromatin transition." Mol Cell Biol 20(17): 6466-6475.

Fletcher, T. M., N. Xiao, G. Mautino, C. T. Baumann, R. Wolford, B. S. Warren and G. L. Hager. 2002. "ATP-dependent mobilization of the glucocorticoid receptor during chromatin remodeling." Mol Cell Biol 22(10): 3255-3263.

Francis, N. J. 2009. "Does maintenance of polycomb group proteins through DNA replication contribute to epigenetic inheritance?" Epigenetics 4(6): 370-373.

Gaillard, P. H., E. M. Martini, P. D. Kaufman, B. Stillman, E. Moustacchi and G. Almouzni. 1996. "Chromatin assembly coupled to DNA repair: a new role for chromatin assembly factor I." Cell 86(6): 887-896.

Gangaraju, V. K. and B. Bartholomew. 2007. "Mechanisms of ATP dependent chromatin remodeling." Mutat Res 618(1-2): 3-17.

Garcia, B. A., S. B. Hake, R. L. Diaz, M. Kauer, S. A. Morris, J. Recht, J. Shabanowitz, N. Mishra, B. D. Strahl, C. D. Allis and D. F. Hunt. 2007. "Organismal differences in post-translational modifications in histones H3 and H4." J Biol Chem 282(10): 7641-7655.

Gaudreau, L., A. Schmid, D. Blaschke, M. Ptashne and W. Horz. 1997. "RNA polymerase II holoenzyme recruitment is sufficient to remodel chromatin at the yeast PHO5 promoter." Cell 89(1): 55-62.

Grant, P. A., L. Duggan, J. Cote, S. M. Roberts, J. E. Brownell, R. Candau, R. Ohba, T. Owen-Hughes, C. D. Allis, F. Winston, S. L. Berger and J. L. Workman. 1997. "Yeast Gcn5 functions in two multisubunit complexes to acetylate nucleosomal histones: characterization of an Ada complex and the SAGA (Spt/Ada) complex." Genes Dev 11(13): 1640-1650.

Gregory, P. D., S. Barbaric and W. Horz. 1998a. "Analyzing chromatin structure and transcription factor binding in yeast." Methods 15(4): 295-302.

Gregory, P. D., S. Barbaric and W. Horz. 1999a. "Restriction nucleases as probes for chromatin structure." Methods Mol Biol 119: 417-425.

Gregory, P. D., A. Schmid, M. Zavari, L. Lui, S. L. Berger and W. Horz. 1998b. "Absence of Gcn5 HAT activity defines a novel state in the opening of chromatin at the PHO5 promoter in yeast." Mol Cell 1(4): 495-505.

Gregory, P. D., A. Schmid, M. Zavari, M. Munsterkotter and W. Horz. 1999b. "Chromatin remodelling at the PHO8 promoter requires SWI-SNF and SAGA at a step subsequent to activator binding." EMBO J 18(22): 6407-6414.

Griesenbeck, J., H. Boeger, J. S. Strattan and R. D. Kornberg. 2003. "Affinity purification of specific chromatin segments from chromosomal loci in yeast." Mol Cell Biol 23(24): 9275-9282.

Groth, A. 2009. "Replicating chromatin: a tale of histones." Biochem Cell Biol 87(1): 51-63.

Groth, A., A. Corpet, A. J. Cook, D. Roche, J. Bartek, J. Lukas and G. Almouzni. 2007a. "Regulation of replication fork progression through histone supply and demand." Science 318(5858): 1928-1931.

Groth, A., W. Rocha, A. Verreault and G. Almouzni. 2007b. "Chromatin challenges during DNA replication and repair." Cell 128(4): 721-733.

Haase, S. B. and S. I. Reed. 2002. "Improved flow cytometric analysis of the budding yeast cell cycle." Cell Cycle 1(2): 132-136.

Haguenauer-Tsapis, R. and A. Hinnen. 1984. "A deletion that includes the signal peptidase cleavage site impairs processing, glycosylation, and secretion of cell surface yeast acid phosphatase." Mol Cell Biol 4(12): 2668-2675.

Hake, S. B. and C. D. Allis. 2006. "Histone H3 variants and their potential role in indexing mammalian genomes: the "H3 barcode hypothesis"." Proc Natl Acad Sci U S A 103(17): 6428-6435.

Hassan, A. H., P. Prochasson, K. E. Neely, S. C. Galasinski, M. Chandy, M. J. Carrozza and J. L. Workman. 2002. "Function and selectivity of bromodomains in anchoring chromatin-modifying complexes to promoter nucleosomes." Cell 111(3): 369-379.

Haswell, E. S. and E. K. O'Shea. 1999. "An in vitro system recapitulates chromatin remodeling at the PHO5 promoter." Mol Cell Biol 19(4): 2817-2827.

Hecht, A. and M. Grunstein. 1999. "Mapping DNA interaction sites of chromosomal proteins using immunoprecipitation and polymerase chain reaction." Methods Enzymol 304: 399-414.

Hertel, C. B., G. Langst, W. Horz and P. Korber. 2005. "Nucleosome stability at the yeast PHO5 and PHO8 promoters correlates with differential cofactor requirements for chromatin opening." Mol Cell Biol 25(24): 10755-10767.

Horn, P. J. and C. L. Peterson. 2002. "Molecular biology. Chromatin higher order folding--wrapping up transcription." Science 297(5588): 1824-1827.

Imhof, A. and A. P. Wolffe. 1999. "Purification and properties of the Xenopus Hat1 acetyltransferase: association with the 14-3-3 proteins in the oocyte nucleus." Biochemistry 38(40): 13085-13093.

Ito, T., M. Bulger, R. Kobayashi and J. T. Kadonaga. 1996. "Drosophila NAP-1 is a core histone chaperone that functions in ATP-facilitated assembly of regularly spaced nucleosomal arrays." Mol Cell Biol 16(6): 3112-3124.

Jamai, A., R. M. Imoberdorf and M. Strubin. 2007. "Continuous histone H2B and transcription-dependent histone H3 exchange in yeast cells outside of replication." Mol Cell 25(3): 345-355.

Jenuwein, T. and C. D. Allis. 2001. "Translating the histone code." Science 293(5532): 1074-1080.

Jessen, W. J., S. A. Hoose, J. A. Kilgore and M. P. Kladde. 2006. "Active PHO5 chromatin encompasses variable numbers of nucleosomes at individual promoters." Nat Struct Mol Biol 13(3): 256-263.

Jonsson, Z. O., S. Jha, J. A. Wohlschlegel and A. Dutta. 2004. "Rvb1p/Rvb2p recruit Arp5p and assemble a functional Ino80 chromatin remodeling complex." Mol Cell 16(3): 465-477.

Kaffman, A., I. Herskowitz, R. Tjian and E. K. O'Shea. 1994. "Phosphorylation of the transcription factor PHO4 by a cyclin-CDK complex, PHO80-PHO85." Science 263(5150): 1153-1156.

Kaffman, A., N. M. Rank, E. M. O'Neill, L. S. Huang and E. K. O'Shea. 1998a. "The receptor Msn5 exports the phosphorylated transcription factor Pho4 out of the nucleus." Nature 396(6710): 482-486.

Kaffman, A., N. M. Rank and E. K. O'Shea. 1998b. "Phosphorylation regulates association of the transcription factor Pho4 with its import receptor Pse1/Kap121." Genes Dev 12(17): 2673-2683.

Komeili, A. and E. K. O'Shea. 1999. "Roles of phosphorylation sites in regulating activity of the transcription factor Pho4." Science 284(5416): 977-980.

Korber, P., S. Barbaric, T. Luckenbach, A. Schmid, U. J. Schermer, D. Blaschke and W. Horz. 2006. "The histone chaperone Asf1 increases the rate of histone eviction at the yeast PHO5 and PHO8 promoters." J Biol Chem 281(9): 5539-5545.

Korber, P. and W. Horz. 2004. "In vitro assembly of the characteristic chromatin organization at the yeast PHO5 promoter by a replication-independent extract system." J Biol Chem 279(33): 35113-35120.

Korber, P., T. Luckenbach, D. Blaschke and W. Horz. 2004. "Evidence for histone eviction in trans upon induction of the yeast PHO5 promoter." Mol Cell Biol 24(24): 10965-10974.

Kouzarides, T. 2007. "Chromatin modifications and their function." Cell 128(4): 693-705.

Krebs, J. E., C. J. Fry, M. L. Samuels and C. L. Peterson. 2000. "Global role for chromatin remodeling enzymes in mitotic gene expression." Cell 102(5): 587-598.

Kurdistani, S. K. and M. Grunstein. 2003. "Histone acetylation and deacetylation in yeast." Nat Rev Mol Cell Biol 4(4): 276-284.

Lam, F. H., D. J. Steger and E. K. O'Shea. 2008. "Chromatin decouples promoter threshold from dynamic range." Nature 453(7192): 246-250.

Langst, G. and P. B. Becker. 2001. "ISWI induces nucleosome sliding on nicked DNA." Mol Cell 8(5): 1085-1092.

Langst, G., E. J. Bonte, D. F. Corona and P. B. Becker. 1999. "Nucleosome movement by CHRAC and ISWI without disruption or trans-displacement of the histone octamer." Cell 97(7): 843-852.

Lee, T. I., H. C. Causton, F. C. Holstege, W. C. Shen, N. Hannett, E. G. Jennings, F. Winston, M. R. Green and R. A. Young. 2000. "Redundant roles for the TFIID and SAGA complexes in global transcription." Nature 405(6787): 701-704.

Lee, Y. S., K. Huang, F. A. Quiocho and E. K. O'Shea. 2008. "Molecular basis of cyclin-CDK-CKI regulation by reversible binding of an inositol pyrophosphate." Nat Chem Biol 4(1): 25-32.

Levine, M. and R. Tjian. 2003. "Transcription regulation and animal diversity." Nature 424(6945): 147-151.

Li, G., R. Margueron, G. Hu, D. Stokes, Y. H. Wang and D. Reinberg. 2010. "Highly compacted chromatin formed in vitro reflects the dynamics of transcription activation in vivo." Mol Cell 38(1): 41-53.

Lorch, Y., B. Maier-Davis and R. D. Kornberg. 2006. "Chromatin remodeling by nucleosome disassembly in vitro." Proc Natl Acad Sci U S A 103(9): 3090-3093.

Lorch, Y., B. Maier-Davis and R. D. Kornberg. 2010. "Mechanism of chromatin remodeling." Proc Natl Acad Sci U S A 107(8): 3458-3462.

Lorch, Y., M. Zhang and R. D. Kornberg. 1999. "Histone octamer transfer by a chromatin-remodeling complex." Cell 96(3): 389-392.

Lowary, P. T. and J. Widom. 1998. "New DNA sequence rules for high affinity binding to histone octamer and sequence-directed nucleosome positioning." J Mol Biol 276(1): 19-42.

Luger, K. and J. C. Hansen. 2005. "Nucleosome and chromatin fiber dynamics." Curr Opin Struct Biol 15(2): 188-196.

Luger, K., A. W. Mader, R. K. Richmond, D. F. Sargent and T. J. Richmond. 1997. "Crystal structure of the nucleosome core particle at 2.8 A resolution." Nature 389(6648): 251-260.

Luger, K., T. J. Rechsteiner and T. J. Richmond. 1999. "Expression and purification of recombinant histones and nucleosome reconstitution." Methods Mol Biol 119: 1-16.

Luk, E., N. D. Vu, K. Patteson, G. Mizuguchi, W. H. Wu, A. Ranjan, J. Backus, S. Sen, M. Lewis, Y. Bai and C. Wu. 2007. "Chz1, a nuclear chaperone for histone H2AZ." Mol Cell 25(3): 357-368.

Maier, V. K., M. Chioda, D. Rhodes and P. B. Becker. 2008. "ACF catalyses chromatosome movements in chromatin fibres." EMBO J 27(6): 817-826.

Marfella, C. G. and A. N. Imbalzano. 2007. "The Chd family of chromatin remodelers." Mutat Res 618(1-2): 30-40.

McAndrew, P. C., J. Svaren, S. R. Martin, W. Horz and C. R. Goding. 1998. "Requirements for chromatin modulation and transcription activation by the Pho4 acidic activation domain." Mol Cell Biol 18(10): 5818-5827.

Mellor, J., W. Jiang, M. Funk, J. Rathjen, C. A. Barnes, T. Hinz, J. H. Hegemann and P. Philippsen. 1990. "CPF1, a yeast protein which functions in centromeres and promoters." EMBO J 9(12): 4017-4026.

Morse, R. H. 1993. "Nucleosome disruption by transcription factor binding in yeast." Science 262(5139): 1563-1566.

Morse, R. H. 2007. "Transcription factor access to promoter elements." J Cell Biochem 102(3): 560-570.

Mousson, F., F. Ochsenbein and C. Mann. 2007. "The histone chaperone Asf1 at the crossroads of chromatin and DNA checkpoint pathways." Chromosoma 116(2): 79-93.

Munsterkotter, M., S. Barbaric and W. Horz. 2000. "Transcriptional regulation of the yeast PHO8 promoter in comparison to the coregulated PHO5 promoter." J Biol Chem 275(30): 22678-22685.

Neef, D. W. and M. P. Kladde. 2003. "Polyphosphate loss promotes SNF/SWI- and Gcn5-dependent mitotic induction of PHO5." Mol Cell Biol 23(11): 3788-3797.

Neely, K. E., A. H. Hassan, C. E. Brown, L. Howe and J. L. Workman. 2002. "Transcription activator interactions with multiple SWI/SNF subunits." Mol Cell Biol 22(6): 1615-1625.

Neely, K. E., A. H. Hassan, A. E. Wallberg, D. J. Steger, B. R. Cairns, A. P. Wright and J. L. Workman. 1999. "Activation domain-mediated targeting of the SWI/SNF complex to promoters stimulates transcription from nucleosome arrays." Mol Cell 4(4): 649-655.

Nemeth, A. and G. Langst. 2004. "Chromatin higher order structure: opening up chromatin for transcription." Brief Funct Genomic Proteomic 2(4): 334-343.

Ng, H. H., F. Robert, R. A. Young and K. Struhl. 2002. "Genome-wide location and regulated recruitment of the RSC nucleosome-remodeling complex." Genes Dev 16(7): 806-819.

Nourani, A., R. T. Utley, S. Allard and J. Cote. 2004. "Recruitment of the NuA4 complex poises the PHO5 promoter for chromatin remodeling and activation." EMBO J 23(13): 2597-2607.

Ogawa, N. and Y. Oshima. 1990. "Functional domains of a positive regulatory protein, PHO4, for transcriptional control of the phosphatase regulon in Saccharomyces cerevisiae." Mol Cell Biol 10(5): 2224-2236.

Ogawa, N., H. Saitoh, K. Miura, J. P. Magbanua, M. Bun-ya, S. Harashima and Y. Oshima. 1995. "Structure and distribution of specific cis-elements for transcriptional regulation of PHO84 in Saccharomyces cerevisiae." Mol Gen Genet 249(4): 406-416.

Olins, D. E. and A. L. Olins. 2003. "Chromatin history: our view from the bridge." Nat Rev Mol Cell Biol 4(10): 809-814.

Osheroff, N. 1989. "Biochemical basis for the interactions of type I and type II topoisomerases with DNA." Pharmacol Ther 41(1-2): 223-241.

Papamichos-Chronakis, M. and C. L. Peterson. 2008. "The Ino80 chromatin-remodeling enzyme regulates replisome function and stability." Nat Struct Mol Biol 15(4): 338-345.

Parnell, T. J., J. T. Huff and B. R. Cairns. 2008. "RSC regulates nucleosome positioning at Pol II genes and density at Pol III genes." EMBO J 27(1): 100-110.

Partensky, P. D. and G. J. Narlikar. 2009. "Chromatin remodelers act globally, sequence positions nucleosomes locally." J Mol Biol 391(1): 12-25.

Pazin, M. J., P. L. Sheridan, K. Cannon, Z. Cao, J. G. Keck, J. T. Kadonaga and K. A. Jones. 1996. "NF-kappa B-mediated chromatin reconfiguration and transcriptional activation of the HIV-1 enhancer in vitro." Genes Dev 10(1): 37-49.

Peterson, C. L. and I. Herskowitz. 1992. "Characterization of the yeast SWI1, SWI2, and SWI3 genes, which encode a global activator of transcription." Cell 68(3): 573-583.

Pondugula, S., D. W. Neef, W. P. Voth, R. P. Darst, A. Dhasarathy, M. M. Reynolds, S. Takahata, D. J. Stillman and M. P. Kladde. 2009. "Coupling phosphate homeostasis to cell cycle-specific transcription: mitotic activation of Saccharomyces cerevisiae PHO5 by Mcm1 and Forkhead proteins." Mol Cell Biol 29(18): 4891-4905.

Poot, R. A., L. Bozhenok, D. L. van den Berg, N. Hawkes and P. D. Varga-Weisz. 2005. "Chromatin remodeling by WSTF-ISWI at the replication site: opening a window of opportunity for epigenetic inheritance?" Cell Cycle 4(4): 543-546.

Pray-Grant, M. G., J. A. Daniel, D. Schieltz, J. R. Yates, 3rd and P. A. Grant. 2005. "Chd1 chromodomain links histone H3 methylation with SAGA- and SLIK-dependent acetylation." Nature 433(7024): 434-438.

Probst, A. V., E. Dunleavy and G. Almouzni. 2009. "Epigenetic inheritance during the cell cycle." Nat Rev Mol Cell Biol 10(3): 192-206.

Racki, L. R., J. G. Yang, N. Naber, P. D. Partensky, A. Acevedo, T. J. Purcell, R. Cooke, Y. Cheng and G. J. Narlikar. 2009. "The chromatin remodeller ACF acts as a dimeric motor to space nucleosomes." Nature 462(7276): 1016-1021.

Raisner, R. M., P. D. Hartley, M. D. Meneghini, M. Z. Bao, C. L. Liu, S. L. Schreiber, O. J. Rando and H. D. Madhani. 2005. "Histone variant H2A.Z marks the 5' ends of both active and inactive genes in euchromatin." Cell 123(2): 233-248.

Rando, O. J. and H. Y. Chang. 2009. "Genome-wide views of chromatin structure." Annu Rev Biochem 78: 245-271.

Ransom, M., B. K. Dennehey and J. K. Tyler. 2010. "Chaperoning histones during DNA replication and repair." Cell 140(2): 183-195.

Ransom, M., S. K. Williams, M. L. Dechassa, C. Das, J. Linger, M. Adkins, C. Liu, B. Bartholomew and J. K. Tyler. 2009. "FACT and the proteasome promote promoter chromatin disassembly and transcriptional initiation." J Biol Chem 284(35): 23461-23471.

Rayasam, G. V., C. Elbi, D. A. Walker, R. Wolford, T. M. Fletcher, D. P. Edwards and G. L. Hager. 2005. "Ligand-specific dynamics of the progesterone receptor in living cells and during chromatin remodeling in vitro." Mol Cell Biol 25(6): 2406-2418.

Reinke, H., P. D. Gregory and W. Horz. 2001. "A transient histone hyperacetylation signal marks nucleosomes for remodeling at the PHO8 promoter in vivo." Mol Cell 7(3): 529-538.

Reinke, H. and W. Horz. 2003. "Histones are first hyperacetylated and then lose contact with the activated PHO5 promoter." Mol Cell 11(6): 1599-1607.

Reinke, H. and W. Horz. 2004. "Anatomy of a hypersensitive site." Biochim Biophys Acta 1677(1-3): 24-29.

Robinson, P. J., L. Fairall, V. A. Huynh and D. Rhodes. 2006. "EM measurements define the dimensions of the "30-nm" chromatin fiber: evidence for a compact, interdigitated structure." Proc Natl Acad Sci U S A 103(17): 6506-6511.

Robinson, P. J. and D. Rhodes. 2006. "Structure of the '30 nm' chromatin fibre: a key role for the linker histone." Curr Opin Struct Biol 16(3): 336-343.

Rufiange, A., P. E. Jacques, W. Bhat, F. Robert and A. Nourani. 2007. "Genome-wide replication-independent histone H3 exchange occurs predominantly at promoters and implicates H3 K56 acetylation and Asf1." Mol Cell 27(3): 393-405.

Sambrook, J., E. F. Fritsch and T. Maniatis. 1989. "Molecular Cloning: A Laboratory Manual." Cold Spring Harbor, NY: Cold Spring Harbor Laboratory Press 2nd edition.

Sandaltzopoulos, R., C. Mitchelmore, E. Bonte, G. Wall and P. B. Becker. 1995. "Dual regulation of the Drosophila hsp26 promoter in vitro." Nucleic Acids Res 23(13): 2479-2487.

Santocanale, C. and J. F. Diffley. 1998. "A Mec1- and Rad53-dependent checkpoint controls late-firing origins of DNA replication." Nature 395(6702): 615-618.

Schalch, T., S. Duda, D. F. Sargent and T. J. Richmond. 2005. "X-ray structure of a tetranucleosome and its implications for the chromatin fibre." Nature 436(7047): 138-141.

Schmid, A., K. D. Fascher and W. Horz. 1992. "Nucleosome disruption at the yeast PHO5 promoter upon PHO5 induction occurs in the absence of DNA replication." Cell 71(5): 853-864.

Schwarz, P. M., A. Felthauser, T. M. Fletcher and J. C. Hansen. 1996. "Reversible oligonucleosome self-association: dependence on divalent cations and core histone tail domains." Biochemistry 35(13): 4009-4015.

Segal, E. and J. Widom. 2009. "Poly(dA:dT) tracts: major determinants of nucleosome organization." Curr Opin Struct Biol 19(1): 65-71.

Sengstag, C. and A. Hinnen. 1987. "The sequence of the Saccharomyces cerevisiae gene PHO2 codes for a regulatory protein with unusual aminoacid composition." Nucleic Acids Res 15(1): 233-246.

Sengstag, C. and A. Hinnen. 1988. "A 28-bp segment of the Saccharomyces cerevisiae PHO5 upstream activator sequence confers phosphate control to the CYC1-lacZ gene fusion." Gene 67(2): 223-228.

Shahbazian, M. D. and M. Grunstein. 2007. "Functions of site-specific histone acetylation and deacetylation." Annu Rev Biochem 76: 75-100.

Sheridan, P. L., C. T. Sheline, K. Cannon, M. L. Voz, M. J. Pazin, J. T. Kadonaga and K. A. Jones. 1995. "Activation of the HIV-1 enhancer by the LEF-1 HMG protein on nucleosome-assembled DNA in vitro." Genes Dev 9(17): 2090-2104.

Shimamura, A., D. Tremethick and A. Worcel. 1988. "Characterization of the repressed 5S DNA minichromosomes assembled in vitro with a high-speed supernatant of Xenopus laevis oocytes." Mol Cell Biol 8(10): 4257-4269.

Shukla, A., P. Bajwa and S. R. Bhaumik. 2006a. "SAGA-associated Sgf73p facilitates formation of the preinitiation complex assembly at the promoters either in a HAT-dependent or independent manner in vivo." Nucleic Acids Res 34(21): 6225-6232.

Shukla, A., N. Stanojevic, Z. Duan, P. Sen and S. R. Bhaumik. 2006b. "Ubp8p, a histone deubiquitinase whose association with SAGA is mediated by Sgf11p, differentially regulates lysine 4 methylation of histone H3 in vivo." Mol Cell Biol 26(9): 3339-3352.

Simon, R. H. and G. Felsenfeld. 1979. "A new procedure for purifying histone pairs H2A + H2B and H3 + H4 from chromatin using hydroxylapatite." Nucleic Acids Res 6(2): 689-696.

Simpson, R. T. 1990. "Nucleosome positioning can affect the function of a cis-acting DNA element in vivo." Nature 343(6256): 387-389.

Smale, S. T. and J. T. Kadonaga. 2003. "The RNA polymerase II core promoter." Annu Rev Biochem 72: 449-479.

Springer, M., D. D. Wykoff, N. Miller and E. K. O'Shea. 2003. "Partially phosphorylated Pho4 activates transcription of a subset of phosphate-responsive genes." PLoS Biol 1(2): E28.

Steger, D. J., E. S. Haswell, A. L. Miller, S. R. Wente and E. K. O'Shea. 2003. "Regulation of chromatin remodeling by inositol polyphosphates." Science 299(5603): 114-116.

Sudarsanam, P., V. R. Iyer, P. O. Brown and F. Winston. 2000. "Whole-genome expression analysis of snf/swi mutants of Saccharomyces cerevisiae." Proc Natl Acad Sci U S A 97(7): 3364-3369.

Sudarsanam, P. and F. Winston. 2000. "The Swi/Snf family nucleosome-remodeling complexes and transcriptional control." Trends Genet 16(8): 345-351.

Sutton, A., J. Bucaria, M. A. Osley and R. Sternglanz. 2001. "Yeast ASF1 protein is required for cell cycle regulation of histone gene transcription." Genetics 158(2): 587-596.

Svaren, J. and W. Horz. 1997. "Transcription factors vs nucleosomes: regulation of the PHO5 promoter in yeast." Trends Biochem Sci 22(3): 93-97.

Svaren, J., J. Schmitz and W. Horz. 1994. "The transactivation domain of Pho4 is required for nucleosome disruption at the PHO5 promoter." EMBO J 13(20): 4856-4862.

Tan, B. C., C. T. Chien, S. Hirose and S. C. Lee. 2006. "Functional cooperation between FACT and MCM helicase facilitates initiation of chromatin DNA replication." EMBO J 25(17): 3975-3985.

Taylor, I. C., J. L. Workman, T. J. Schuetz and R. E. Kingston. 1991. "Facilitated binding of GAL4 and heat shock factor to nucleosomal templates: differential function of DNA-binding domains." Genes Dev 5(7): 1285-1298.

Terrell, A. R., S. Wongwisansri, J. L. Pilon and P. J. Laybourn. 2002. "Reconstitution of nucleosome positioning, remodeling, histone acetylation, and transcriptional activation on the PHO5 promoter." J Biol Chem 277(34): 31038-31047.

Tirosh, I. and N. Barkai. 2008. "Two strategies for gene regulation by promoter nucleosomes." Genome Res 18(7): 1084-1091.

Tremethick, D. J. 2007. "Higher-order structures of chromatin: the elusive 30 nm fiber." Cell 128(4): 651-654.

Truss, M., J. Bartsch, A. Schelbert, R. J. Hache and M. Beato. 1995. "Hormone induces binding of receptors and transcription factors to a rearranged nucleosome on the MMTV promoter in vivo." EMBO J 14(8): 1737-1751.

Tsubota, T., C. E. Berndsen, J. A. Erkmann, C. L. Smith, L. Yang, M. A. Freitas, J. M. Denu and P. D. Kaufman. 2007. "Histone H3-K56 acetylation is catalyzed by histone chaperone-dependent complexes." Mol Cell 25(5): 703-712.

Tsukiyama, T. and C. Wu. 1995. "Purification and properties of an ATP-dependent nucleosome remodeling factor." Cell 83(6): 1011-1020.

Turner, B. M. 2002. "Cellular memory and the histone code." Cell 111(3): 285-291.

Uhler, J. P., C. Hertel and J. Q. Svejstrup. 2007. "A role for noncoding transcription in activation of the yeast PHO5 gene." Proc Natl Acad Sci U S A 104(19): 8011-8016.

Utley, R. T., K. Ikeda, P. A. Grant, J. Cote, D. J. Steger, A. Eberharter, S. John and J. L. Workman. 1998. "Transcriptional activators direct histone acetyltransferase complexes to nucleosomes." Nature 394(6692): 498-502.

Varga-Weisz, P. D., M. Wilm, E. Bonte, K. Dumas, M. Mann and P. B. Becker. 1997. "Chromatin-remodelling factor CHRAC contains the ATPases ISWI and topoisomerase II." Nature 388(6642): 598-602.

Venter, U., J. Svaren, J. Schmitz, A. Schmid and W. Horz. 1994. "A nucleosome precludes binding of the transcription factor Pho4 in vivo to a critical target site in the PHO5 promoter." EMBO J 13(20): 4848-4855.

Verreault, A., P. D. Kaufman, R. Kobayashi and B. Stillman. 1996. "Nucleosome assembly by a complex of CAF-1 and acetylated histones H3/H4." Cell 87(1): 95-104.

Vicent, G. P., R. Zaurin, A. S. Nacht, J. Font-Mateu, F. Le Dily and M. Beato. 2010. "Nuclear factor 1 synergizes with progesterone receptor on the mouse mammary tumor virus promoter wrapped around a histone H3/H4 tetramer by facilitating access to the central hormone-responsive elements." J Biol Chem 285(4): 2622-2631.

Vogel, K., W. Horz and A. Hinnen. 1989. "The two positively acting regulatory proteins PHO2 and PHO4 physically interact with PHO5 upstream activation regions." Mol Cell Biol 9(5): 2050-2057.

Vogelauer, M., J. Wu, N. Suka and M. Grunstein. 2000. "Global histone acetylation and deacetylation in yeast." Nature 408(6811): 495-498.

Wall, G., P. D. Varga-Weisz, R. Sandaltzopoulos and P. B. Becker. 1995. "Chromatin remodeling by GAGA factor and heat shock factor at the hypersensitive Drosophila hsp26 promoter in vitro." EMBO J 14(8): 1727-1736.

Williams, S. K., D. Truong and J. K. Tyler. 2008. "Acetylation in the globular core of histone H3 on lysine-56 promotes chromatin disassembly during transcriptional activation." Proc Natl Acad Sci U S A 105(26): 9000-9005.

Wippo, C. J., B. S. Krstulovic, F. Ertel, S. Musladin, D. Blaschke, S. Sturzl, G. C. Yuan, W. Horz, P. Korber and S. Barbaric. 2009. "Differential cofactor requirements for histone eviction from two nucleosomes at the yeast PHO84 promoter are determined by intrinsic nucleosome stability." Mol Cell Biol 29(11): 2960-2981.

Wittmeyer, J. and T. Formosa. 1997. "The Saccharomyces cerevisiae DNA polymerase alpha catalytic subunit interacts with Cdc68/Spt16 and with Pob3, a protein similar to an HMG1-like protein." Mol Cell Biol 17(7): 4178-4190.

Workman, J. L. and R. E. Kingston. 1992. "Nucleosome core displacement in vitro via a metastable transcription factor-nucleosome complex." Science 258(5089): 1780-1784.

Wykoff, D. D., A. H. Rizvi, J. M. Raser, B. Margolin and E. K. O'Shea. 2007. "Positive feedback regulates switching of phosphate transporters in S. cerevisiae." Mol Cell 27(6): 1005-1013.

Abbreviations

A	Absorption
Ac	Acetylation
acetyl CoA	Acetyl CoenzymeA
ACF	ATP-utilizing chromatin assembly and remodeling factor
ADP	Adenosindiphosphate
ARB	Arbitrary bacterial plasmid
ASF1	Antisilencing function 1
ATP	Adenosintriphosphate
bp	Base pairs
BSA	Bovine serum albumin
CAF1	Chromatin assembly factor 1
CENP-A	Centromer protein A
CDK	Cyclin dependent kinase
CHD	Chromodomain-helicase-DNA-binding
ChIP	Chromatin immunoprecipitation
CK	Creatine kinase
CP	Creatine phosphate
DMSO	Dimethylsulfoxide
DNA	Desoxyribonucleic acid
DNaseI	Bovine deoxyribonucleaseI
DNMT	DNA methyltransferase
dNTP	Desoxyribonucleotidetriphosphate
Drosophila	*Drosophila melanogaster*
DTT	Dithiothreitrol
E.coli	*Escherichia coli*
EDTA	Ethylendiamintetraacetate
EGTA	Ethylenglycol-bis(2-aminoethyl)-N,N,N´,N`-tetraacetic acid
EM	Electron microscopy
EtBr	Ethidiumbromide
EtOH	Ethanol
FACS	Fluorescence activated cell sorting
FACT	Facilitates chromatin transcription
fwd	Forward
Gcn5	General control non-derepressible
GR	Glucocorticoid receptor
h	hour(s)
H2A, H2B, H3, H4	Histones
HAT	Histone acetyltransferase
HDAC	Histone deacetylase
HDM	Histone demethylase
Hepes	(N-(2-Hydroxyethyl)piperazine-H´-(2-ethanesulfonic acid)
HMT	Histone methyltransferases
HRE	Hormone response element
HSF	Heat shock factor
IAC	Isoamylalcohol/chloroform
INO80	Inositol requiring
IP_7	Inositol heptakisposphate
IPTG	1-isopropyl-s-D-1-thiogalacto-pyranoside
ISWI	Imitation switch
K	Lysine
kb	Kilobase
l	Liter
M	Molar
MCM	Mini-Chromosome Maintenance
Me	Methylation
min	Minute(s)

ml	Milliliter
mM	Milli molar
MMTV	Mouse mammary tumor virus
MNase	Micrococcal nuclease
MW	Molecular weight
MWCO	Molecular weight cut off
NaBu	Sodium butyrate
NaClO$_4$	Sodium perchlorate
NAP-1	Nucleosome assembly protein 1
NDR	Nucleosome depleted region
NF-1	Nuclear factor 1
NFR	Nucleosome free region
NPP	4-Nitrophenyl phosphate Disodium Salt Hexahydrate
NuA4	Nucleosome acetyltransferase of histone H4
OD	Optical density
o/n	Overnight
ORC	Origin recognition complex
ORF	Open reading frame
P	Phosphorylation
PAGE	Polyacrylamide gel electrophoresis
PCNA	Proliferating cell nuclear antigen
PCR	Polymerase chain reaction
PEG	Polyethylene glycol
PEPCK	Phosphoenolpyruvate carboxykinase
PHD	Plant homeodomain
PHO	Phosphatase
PMSF	Phenylmethanesulfonyl fluoride
PR	Progesterone receptor
pre-RC	Pre-replicative complex
PTM	Posttranslational modification
rDNA	Repetitive ribosomal DNA
RFC	Replication factor C
rev	Reverse
RNA	Ribonucleic acid
rpm	Revoltations per minute
RSC	Remodels the structure of chromatin
RT	Room temperature
Rtt109	Regulation of Ty1 transposition
S	Serine
SAGA	Spt-Ada-Gcn5-acetyltransferase
SANT	SWI3, ADA2, N-CoR and TFIIIB B"
S. cerevisiae	*Saccharomyces cerevisiae*
SDS	Sodiumdodecylsulfate
Sir2	Silent information regulator
SNF2	Sucrose non-fermenting protein 2 homolog
Sth1	Snf two homologous 1
SWI/SNF	Switch/sucrose non-fermenting
SWR1	Swi2/Snf2-related 1
TEMED	N,N,N',N'-Tetramethylethylenediamine
Tris	Tris(hydroxymethyl)aminomethane
TSA	Trichostatin A
TSS	Transcriptional start site
UAS	Upstream activating sequence
v/v	Volume per volume
w/v	Weight per volume
WSTF	Williams syndrome transcription factor
wt	Wild type
α	Anti, alpha

Curriculum Vitae

Franziska Ertel

Date of birth: August 20th 1980

Place of birth: Dresden

Education

01/2006 – present	**PhD thesis at the Ludwig-Maximilians-University of Munich, Prof. Peter Becker, supervisor: Dr. Philipp Korber**

Project: *In vitro* chromatin remodeling of the *PHO5* and *PHO8* promoters in *Saccharomyces cerevisiae*

PhD program: "Protein Dynamics in Health and Disease" sponsored by the Elite Network of Bavaria

01/2005 – 10/2005	**Diploma thesis at the Ludwig-Maximilians-University of Munich, Prof. Charles David, supervisor: PD Dr. Enrico Schleiff**

Project: Biochemical comparison of the ß-barrel polypeptide transporters psToc75 und Ana69

10/2000 – 10/2005	**Studies of Biology at the Ludwig-Maximilians-University of Munich**
1996 – 2000	**Gymnasium, Munich**
1993 – 1996	**Gymnasium, Berlin**
1987 – 1993	**Elementary school, Berlin**

Publications

Ertel F, Dirac-Svejstrup AB, Bech Hertel C, Blaschke D, Svejstrup JQ, Korber P. *In vitro* reconstitution of *PHO5* promoter chromatin remodeling points to a role for activator-nucleosome competition *in vivo*. In press.

Wippo CJ, Krstulovic BS, **Ertel F**, Musladin S, Blaschke D, Stürzl S, Yuan GC, Hörz W, Korber P, Barbaric S. Differential cofactor requirements for histone eviction from two nucleosomes at the yeast *PHO84* promoter are determined by intrinsic nucleosome stability. 2009, MCB 11, 2960-2981.

Bredemeier R, Schlegel T, **Ertel F**, Vojta A, Borissenko L, Bohnsack MT, Groll M, von Haeseler A, Schleiff E. Functional and phylogenetic properties of the pore-forming beta-barrel transporters of the Omp85 family. 2007, JBC 3, 1882-1890.

Bredemeier R, **Ertel F** und Schleiff E. Die Grenze zwischen Prokaryont und Eukaryont. 2005, BIOforum.

Ertel F, Mirus O, Bredemeier R, Moslavac S, Becker T and Schleiff E. The Evolutionary Related ß-Barrel Polypeptide Transporters from Pisum sativum and Nostoc PCC7120 Contain Two Distinct Functional Domains. 2005, JBC 31, 28281-28289.